Microfossil and isotopic evidence for Holocene sea-level change in the Mersey Estuary

Graham Paul Wilson

Thesis submitted in fulfilment of the requirements of Liverpool John Moores University for the degree of Doctor of Philosophy

October 2004

Abstract

The reconstruction of Holocene coastal environments, and ultimately relative sea-level changes, normally utilises a range of microfossil proxies, such as diatoms, foraminifera and pollen. As microfossils are sometimes poorly preserved, sparse or absent from coastal sediments, this thesis assesses the potential of using $\delta^{13}C$ and C/N analysis of sedimentary organic material as a possible alternative. Modern high inter-tidal and sub-tidal surface sediments of the Inner Mersey Estuary, UK, reveal distinctly different $\delta^{13}C$ values, with variation in C/N ratios also evident, reflecting changes in the dominant source of organic matter in relation to ground elevation within the tidal frame. Despite decomposition effects, the relationship between ground elevation, $\delta^{13}C$ and C/N, is preserved in the sediment record, with a gradual increase in $\delta^{13}C$ and a decrease in C/N from supra-tidal, through to inter-tidal and to sub-tidal environments. Holocene variations in $\delta^{13}C$ and C/N are compared with coastal palaeoenvironmental changes inferred from microfossil evidence and show a good correspondence. Although $\delta^{13}C$ and C/N are not as accurate as microfossil indicators in terms of coastal palaeoenvironmental reconstruction, they may be applied successfully in the field of relative sea-level reconstruction by helping to verify sea-level index points when microfossils are absent. This is demonstrated by employing $\delta^{13}C$ and C/N analysis as part of a multi-proxy investigation into the Holocene evolution of the Inner Mersey Estuary, which was found to follow the tripartite model of estuarine evolution common to other UK estuaries. Early Holocene expansion and Mid Holocene contraction of the coastal zone was driven by changes in the rate of regional RSL rise, and a possible increase in terrigenous sediment flux in the Late Holocene may have allowed the re-establishment of lower inter-tidal conditions. These processes resulted in the observed minerogenic-organic-minerogenic sediment structures, which is the characteristic sediment-stacking pattern of estuarine deposits associated with the tripartite model of evolution.

Acknowledgments

This work was completed whilst I was in receipt of a Liverpool John Moores studentship, for which financial support is gratefully acknowledged. Carbon isotope and C/N analysis was funded by a generous grant from the NERC Isotope Geoscience Facilities Steering Committee (NIGFSC grant no. IP/708/0901).

Many thanks go firstly to my supervisor, Dr Angela Lamb. She has been a constant source of expertise, help, support and encouragement, and has allowed me considerable freedom to investigate the potential of isotopes in coastal palaeoenvironmental research. Professor Dave Huddart and Dr Silvia Gonzalez have also provided helpful advice throughout. It is a pleasure to acknowledge the help and support of Dr Melanie Leng of the NERC Isotope Geoscience Facility at the British Geological Survey, Keyworth. She has taken an enthusiastic interest in this research from the start, and has been generous with her time, knowledge and experience. Also at the NERC Isotope Geoscience Facility, I would like to thank Carol Arrowsmith and Joanne Green, who carried out the isotope and C/N measurements.

The staff of the Coastal Geosciences & Global Change Programme at the British Geological Survey, Dr John Ridgway and Dr Gareth Jenkins in particular, are thanked for providing access to the Helsby and Ince Marshes sediment cores, which were taken as part of a larger investigation into the palaeoenvironmental evolution of the Mersey Estuary (project code: ESB85900074), and for providing the funds for six radiocarbon dates. This research has benefited from the constructive comments of Dr Jerry Lloyd at the Department of Geography, the University of Durham, for which I am very grateful. I owe a debt of gratitude to Dr Andy Plater of the Department of Geography, the University of Liverpool, not least for allowing me to use the Coulter Laser particle sizer. His enthusiasm for, and interest in, Holocene environmental change, and the eloquent and inspiring lectures he delivered on coastal evolution whilst I was a student at Liverpool University, provided the motivation to pursue research in this area. He has remained a reliable source of help and advice throughout.

I am indebted to my parents for their unending support, encouragement and generosity. This thesis is dedicated to my fiancée, Lesley Fletcher, for her unselfish sacrifices, patience, love and support.

Contents

List of Figures

List of Tables

MISSING PAGES REMOVED ON INSTRUCTION FROM THE UNIVERSITY

Chapter 1

Introduction

1.1 Scientific background and justification

Holocene coastal sediment deposits contain an array of valuable information regarding both natural and human-induced changes in the marine, riverine and terrestrial environment. These, often lengthy, unconsolidated sequences of intercalated minerogenic and organic sediments may provide information regarding the height of Holocene relative sea-levels (RSL)[1] and their rates of change (e.g. Long *et al.*, 1998). This information has been used to improve the accuracy of postglacial isostatic adjustment models (e.g. Peltier *et al.*, 2002) and is also pertinent to elucidating the response of present day coastlines to current and future climate changes (Shennan, 1995). In addition, Holocene coastal deposits have been utilised in sediment provenance studies (e.g. Plater *et al.*, 2000a) and to reconstruct changes in the volume of palaeoriver discharge (e.g. Byrne *et al.*, 2001). This spectrum of valuable information contained in the sediments of Holocene coastal deposits may remain unobtainable if microfossils, the cornerstone of most coastal palaeoenvironmental investigations, are poorly preserved, or even absent in the sediments.

Diatoms, foraminifera and pollen are the most commonly used microfossils in coastal palaeoenvironmental reconstructions (e.g. Denys & De Wolf, 1999; Lloyd *et al.*, 1999; Waller *et al.*, 1999). In particular, diatoms and foraminifera are used to reconstruct RSL change as their distribution in the contemporary inter-tidal zone is related to ground elevation within the tidal frame (Gehrels *et al.*, 2001). Microfossils are, however, susceptible to chemical and mechanical damage (e.g. Ryves *et al.*, 2001). Further, each of these microfossils is only abundant in certain sediment deposits: pollen is generally confined to organic rich sediments, and diatoms and foraminifera largely to minerogenic deposits. As a result, it is not uncommon to encounter sediment deposits containing a discontinuous microfossil record that is in various stages of preservation, severely restricting coastal palaeoenvironmental reconstructions.

---

[1] Relative sea-level change refers to a change in sea-level relative to the land. This may occur due to ocean level changes (eustatic) and/or land level changes over shorter (isostatic) or longer (tectonic) timescales.

Carbon isotope ratios ($^{13}C/^{12}C$, expressed as $\delta^{13}C$) and organic carbon to nitrogen ratios (C/N) measurements in bulk sedimentary organic matter have become successful tools for palaeoenvironmental reconstruction in lacustrine deposits (e.g. Lamb *et al.*, 2004; Street-Perrott *et al.*, 2004), despite the fact that some diagenetic alteration of organic matter inevitably occurs in the early stages of decomposition (Meyers & Eadie, 1993). $\delta^{13}C$ and C/N values provide information about the source and amount of organic matter entering a lake system and thus vegetation changes through time (Meyers & Teranes, 2001). $\delta^{13}C$ analysis has been used effectively in some coastal palaeoenvironmental investigations, where vegetation dominating the saltmarshes utilises the C_4 photosynthetic pathway ($\delta^{13}C$ range of –15.0‰ to –9.0‰) and vegetation on the fresh water marshes, the C_3 pathway ($\delta^{13}C$ range of –33.0‰ to –23.0‰) (Deines, 1980). The large variation in $\delta^{13}C$ between these two groups allows their host palaeoenvironment to be distinguished from the sedimentary deposits (e.g. Chmura & Aharon, 1995).

C_4 vegetation has either been introduced or is rare on UK saltmarshes (Rackham, 1986; Crawford, 1989; Preston *et al.*, 2002), thus greatly restricting the range of organic $\delta^{13}C$ values. Despite this, some studies have been able to distinguish between organic matter sources in the modern coastal environment using a combination of $\delta^{13}C$ and C/N ratios (Thornton & McManus, 1994; Andrews *et al.*, 1998; Middelburg & Nieuwenhuize, 1998). The ability of $\delta^{13}C$ and C/N to detect changes in the source of organic matter in C_3 dominated systems has resulted in their application to isolation basin sediments as a proxy of shoreline displacement during the Holocene (Westman & Hedenström, 2002), and to lagoonal deposits to detect palaeoenvironmental changes as a result of Holocene sea-level change (Müller & Mathesius, 1999; Müller & Voss, 1999). Andrews *et al.* (2000) were the first to analyse $\delta^{13}C$ and C/N in estuarine deposits from a C_3 vegetated catchment. They used $\delta^{13}C$ and C/N values, together with additional geochemical proxies, to identify environmental facies in Humber Estuary deposits in order to calculate estuarine storage changes of carbon and nitrogen in the Holocene. However, they gave no consideration to decompositional impacts on bulk sediment $\delta^{13}C$ and C/N values, which may be of sufficient magnitude to complicate the use of $\delta^{13}C$ and C/N as geochemical 'signatures' of environmental facies. In addition, the coarse sampling resolution (approximately 1 measurement per metre of sediment), although sufficient for the aims of their study, means that the potential of $\delta^{13}C$ and C/N analysis in

detecting smaller scale environmental changes in estuarine deposits within C_3 vegetated catchments is yet to be fully explored. $\delta^{13}C$ and C/N analysis may also be used effectively in sea-level reconstruction studies. Hitherto in estuarine deposits, changes in RSL are identified by changes in the microfossil assemblages. $\delta^{13}C$ and C/N analysis may potentially represent a viable alternative for identifying RSL changes if microfossils are absent or poorly preserved in the estuarine sediment record.

This thesis explores the potential of $\delta^{13}C$ and C/N analysis of organic matter as an alternative tool for reconstructing RSL and associated coastal palaeoenvironmental change in a UK estuary within a C_3 vegetated catchment. This is achieved by comparing the $\delta^{13}C$ and C/N record with, principally, the diatom record, but also the pollen record, both of which are established coastal palaeoenvironmental indicators (e.g. Denys & De Wolf, 1999; Waller *et al.*, 1999). Comparing high-resolution diatom records with high-resolution $\delta^{13}C$ and C/N records will allow an assessment of the degree of sensitivity of $\delta^{13}C$ and C/N analysis in detecting small scale, as well as large scale, diatom-inferred palaeoenvironmental changes. This thesis also addresses the issue of decompositional-induced changes in $\delta^{13}C$ and C/N values, and explores the viability of using $\delta^{13}C$ and C/N as RSL indicators. A comprehensive $\delta^{13}C$ and C/N survey of a modern saltmarsh and estuarine environment is also an important component of this thesis. This is essential, in the first instance, to determine if any relationship exists between coastal environments and $\delta^{13}C$ and C/N values, knowledge of which will be invaluable for interpreting the Holocene $\delta^{13}C$ and C/N record. Furthermore, due to the range in saltmarsh morphology and estuarine hydrology, a modern, site-specific, saltmarsh and estuarine $\delta^{13}C$ and C/N survey should be a prerequisite to any coastal palaeoenvironmental reconstruction utilising $\delta^{13}C$ and C/N analysis.

Organic $\delta^{13}C$ and C/N analysis has the potential of becoming an important tool in coastal palaeoenvironmental research, as organic matter is present, in variable degrees, in all coastal sediments, ensuring a continuous palaeoenvironmental record. Furthermore, sediment $\delta^{13}C$ potentially remains unchanged over multi-million year time periods (Meyers, 1994) and analysis of organic matter is free from some of the inherent difficulties associated with microfossil analysis, such as poor preservation.

The availability of a suite of sediment cores taken by the British Geological Survey (BGS) from Helsby and Ince Marshes, located in the Inner Mersey Estuary (Figure 1.1), provides an opportunity to test the application of $\delta^{13}C$ and C/N in the field of coastal palaeoenvironmental reconstruction. It also offers an opportunity to reconstruct the Holocene evolution of the Inner Mersey Estuary. Many detailed investigations into Holocene RSL change have been conducted in the region to the north and to the south of the Mersey Estuary (Tooley, 1974; 1978a; 1978b; 1985; Kenna, 1986; Innes *et al.*, 1990; Huddart, 1992; Pye & Neal, 1993a; 1993b; Neal, 1993; Bedlington, 1994; Gonzalez *et al.*, 1996; Huddart *et al.*, 1999a; 1999b). However, it is apparent through efforts of correlation (Bedlington, 1994), and uncertainties regarding the degree of control of site-specific factors on coastal sequences, that these studies can be site-specific. Therefore, a detailed local study is needed to elucidate the Holocene evolution of the Inner Mersey Estuary in the context of regional changes in RSL.

Few investigations have been carried out into the Holocene evolution of the Mersey Estuary. Tooley (1978a) obtained two radiocarbon dates from Helsby Marsh: a transgressive overlap date of 5,470 ± 155 ^{14}C yr BP; and a regressive overlap date of 5,250 ± 385 ^{14}C yr BP (see Section 2.1.3.1 for information on terminology). Through microfossil analysis, he was able to establish the height of RSL at 5,470 ± 155 ^{14}C yr BP and at 5,250 ± 385 ^{14}C yr BP, and he incorporated this information into his regional RSL curve. The extensive intercalated peats, silts and clays of Helsby and Ince Marshes offer a valuable opportunity to investigate, in more detail, the Holocene evolution of the Inner Mersey Estuary in relation to isostatic and regional eustatic sea-level change, as well as to pursue the application of carbon isotope and C/N analysis for the elucidation of past coastal environments.

1.2 Specific aims and objectives

The specific objectives of this research revolve around two overall aims: firstly, to investigate the potential of $\delta^{13}C$ and C/N analysis as coastal palaeoenvironmental and sea-level indicators and secondly, to reconstruct the Holocene evolution of the Inner Mersey Estuary. The specific objectives are:

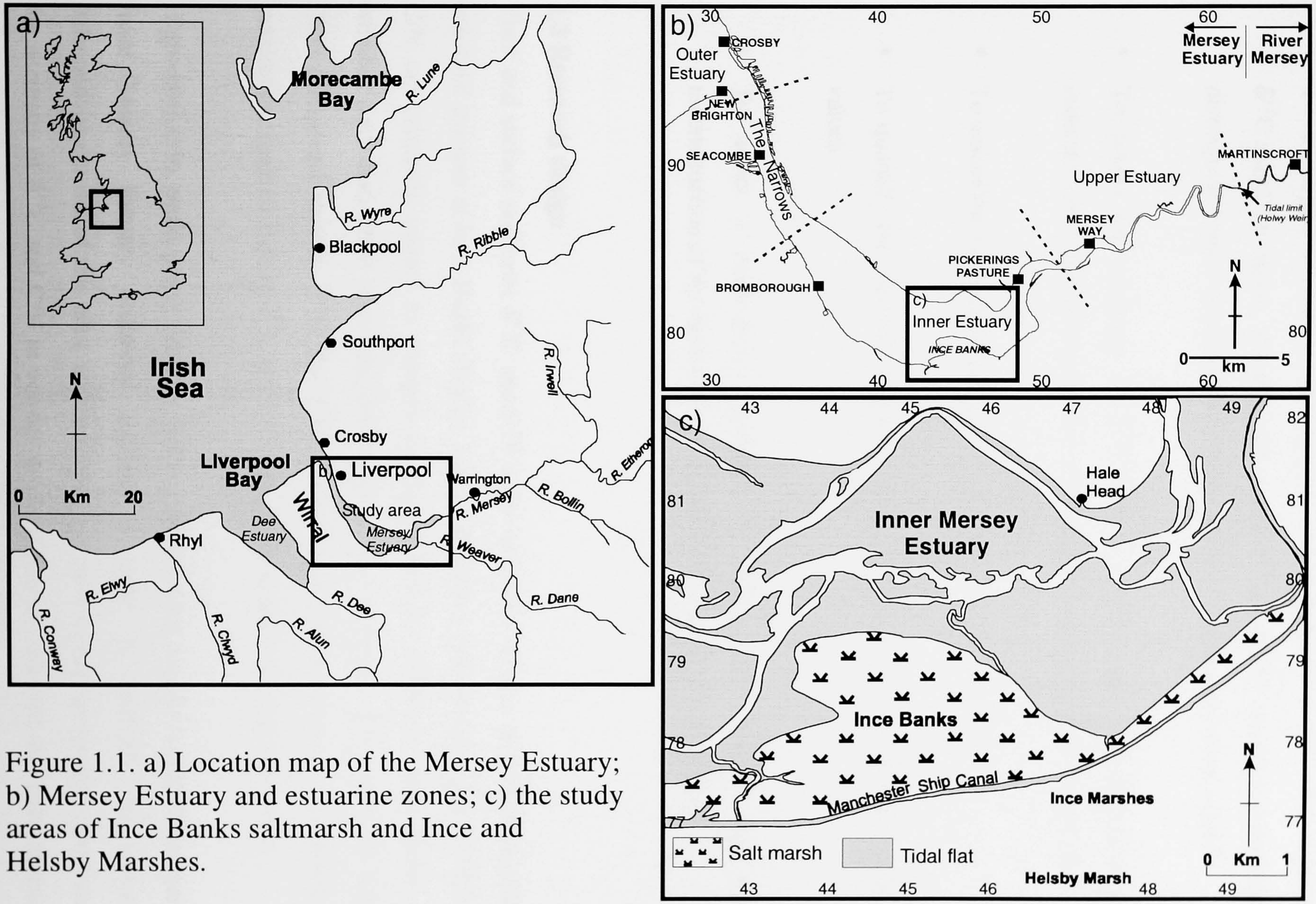

Figure 1.1. a) Location map of the Mersey Estuary; b) Mersey Estuary and estuarine zones; c) the study areas of Ince Banks saltmarsh and Ince and Helsby Marshes.

- To determine if any relationship exists between $\delta^{13}C$, C/N and ground altitude within the tidal frame.

- To investigate whether specific coastal environments have distinctive 'signature' $\delta^{13}C$ and C/N values, allowing the use of $\delta^{13}C$ and C/N analysis in isolation to distinguish coastal palaeoenvironments in the Holocene sediment record.

- To assess the accuracy of $\delta^{13}C$ and C/N as coastal palaeoenvironmental indicators by comparison with the established technique of diatom analysis.

- To assess the viability of using $\delta^{13}C$ and C/N as RSL indicators

- To quantify the effects of organic matter decomposition on bulk $\delta^{13}C$ and C/N values.

- To adopt a multi-proxy approach to achieve an accurate and robust reconstruction of the Holocene evolution of the Inner Mersey Estuary.

1.3 Research design

Plant and surface sediment $\delta^{13}C$ and C/N were measured along a modern inter-tidal to sub-tidal transect at Ince Banks (Figure 1.1) to determine whether changes in $\delta^{13}C$ and C/N are primarily related to changes in ground altitude within the tidal frame, and whether each distinctive inter-tidal environment has 'signature' $\delta^{13}C$ and C/N values. Plant compound specific $\delta^{13}C$ and C/N analysis was also undertaken to quantify the maximum expected shift in $\delta^{13}C$ and C/N values associated with decomposition.

High-resolution, multi-proxy (diatom, pollen, particle size, organic content) analysis of Inner Mersey Estuary sediment deposits is used to establish the Holocene palaeoenvironments of this area, and to serve as a basis to assess, through comparison, the accuracy of $\delta^{13}C$ and C/N as coastal palaeoenvironmental and sea-level indicators. Two sediment cores have been analysed. One contains a tripartite peat sequence, with intercalated sand, silt, clay and organic clay sediments. The second core investigated is from a more seaward site. Clays, silts and sands dominate the deposits, with only a

single muddy peat horizon. These two contrasting cores were purposefully selected for analysis in order to test the accuracy of $\delta^{13}C$ and C/N in a range of coastal environmental deposits. Chronological control for the two cores is provided by six radiocarbon dates.

1.4 Study location and site description

The Mersey Estuary in north west England occupies one of several Pleistocene river valleys cut into a basement of Carboniferous and Triassic rocks (Howell, 1973; Bathurst & Brenchley 1975). The estuary extends from Warrington, where it receives freshwater from the River Mersey, to Liverpool Bay, 47km to the west (Figure 1.1), and is divided into four zones: the Upper Estuary, the Inner Estuary, the Narrows, and the Outer Estuary. The Upper Estuary extends from the tidal limit at Howley Weir, Warrington, to the Runcorn bridge, approximately 17km down stream. The Inner Estuary occurs between the Runcorn bridge and Bebington. The Estuary reaches 5km in width here, and this large, shallow basin dries out at low tide. Ince Banks, an extensive saltmarsh, is found on the southern shore of the Inner Estuary (Figure 1.1). The width of the Estuary decreases to around 1km along the Narrows, a 10km stretch of water between Bebington and New Brighton. The Narrows opens to the Outer Estuary at the Rock Lighthouse at New Brighton and this merges with Liverpool Bay. The Mersey Estuary is unusual in the sense that it does not conform to the open funnel shape that is characteristic of drowned macro-tidal estuaries (Hayes, 1975).

The majority of the freshwater entering the estuary is from the Rivers Mersey and Weaver, which drain a catchment area of approximately 4,600km^2 (Shaw, 1975). The Mersey Estuary is strongly tidal, and has a spring tidal range of 8.4m (Admiralty Tide Tables, 2003). Consequently, the volume of water at high tide (35×10^4 Ml) is fifty times that at low tide (0.7×10^4 Ml) (WPRL, 1974), resulting in a pronounced marine influence in the estuary. Land reclamation between 1800 and 1900 has resulted in the loss of approximately 490ha of inter-tidal area in the Mersey Estuary (Davidson *et al.*, 1991). Ince Banks remains the only extensive area of saltmarsh in the Mersey Estuary. Even so, parts of the upper saltmarsh have been destroyed by the construction of the Manchester Ship Canal between 1887 and 1893, which isolates the saltmarsh from the mainland. Tidal heights on the saltmarsh have been inferred from those recorded at

Hale Head (Table 1.1). Only high tide levels are available as large areas of the Inner Estuary dry out at lower tides.

Table 1.1. Tidal data at Hale Head, Inner Mersey Estuary.

HAT†	MHWS*	MHWN*	MLWN	MLWS	LAT
6.1m OD	4.9m OD	2.9m OD	Dries out	Dries out	Dries out

†Interpolated (David Blackman, Proudman Oceanographic Laboratories, pers. com.)
*Admiralty Tide Tables (2003)

Thick accumulations of unconsolidated Holocene sediments are preserved in lowlands flanking the southern banks of the Inner Mersey Estuary (Tooley, 1978a). As a result, this area has been selected for coring by the BGS as part of a large investigation into the environmental evolution of the Mersey Estuary (BGS project title: Coastal and Estuarine Evolution; project code: ESB85900074). Cores were taken from Helsby Marsh and the more seaward Ince Marshes in summer 2000. Additional cores were taken by the BGS in summer 2003 from Ince Banks.

1.5 Thesis structure

Chapter 2 outlines the developments in RSL reconstruction methodology and reviews the advantages and disadvantages of diatom analysis, which is the principal microfossil indicator used in the current study. The second part of Chapter 2 focuses on previous $\delta^{13}C$ and C/N work. Chapter 3 provides an overview of global sea-level change since the Last Glacial Maximum, the principal driving mechanism of coastal evolution up to the Mid Holocene, together with empirical evidence of RSL change and associated coastal evolution of north west England coastlines. Chapter 4 details the field and laboratory methods employed in this study. Results and interpretation of the modern Ince Banks and Mersey Estuary $\delta^{13}C$ and C/N survey are given in Chapter 5, whilst the results of the multi-proxy analysis of the sediment cores from Helsby Marsh and Ince Marshes are presented in Chapter 6 and the interpretation in Chapter 7. Chapter 8 assesses the potential of $\delta^{13}C$ and C/N analysis as coastal palaeoenvironmental indicators and evaluates the Holocene evolution of the Inner Mersey Estuary in the context of regional driving mechanisms. The chapter ends with concluding remarks.

Chapter 2

Coastal Reconstruction Methodology and Techniques

2.1 Coastal Reconstruction Methodology

2.1.1 Introduction

The methodology of reconstructing Holocene RSL and associated coastal palaeoenvironmental change has been subject to significant refinement during the previous two decades. Workers employing disparate reconstruction methods, a limited consideration of the sources of error, and use of conflicting terminology played no small part in the failure to attain the goals of International Geological Correlation Programme (IGCP) Project 61, the principal aim of which was to construct a graph of 'eustatic' sea-level change during the last 15,000 years. The deficiencies in the methodology of sea-level reconstruction, highlighted during IGCP Project 61, has since been addressed. The subsequent emplacement of a fundamental methodological framework has facilitated comparison of sea-level records from different areas, leading to a greater appreciation of differing rates of Holocene isostatic recovery between sites. Further, with a sound and universally accepted methodology and the increasing refinement of research techniques, it is now becoming possible to apply the science of coastal environmental reconstruction to help resolve some of the most pressing and challenging issues regarding the possible impacts of our presently changing climate.

2.1.2 Modern coastal environments and sediment deposits

Holocene sediment deposits are often well preserved in sheltered, low-energy and tide dominated coastal environments, where they may be protected from high-energy waves, commonly experienced by environments at the open coast. Therefore, sediment accumulations in estuaries, lagoons, bays, inlets, rias, and isolation basins offer the greatest opportunity to investigate climate, sea-level and land-level changes, as well as more local scale changes throughout the Holocene. The sediment characteristics of tide dominated environments, such as organic content (Long *et al.*, 1999b), particle size (Tanner, 1991), architecture (Stupples, 2002), geochemistry (Freitas *et al*, 2003), isotope geochemistry (Malamud-Roam & Ingram, 2001), luminescence properties (Plater & Poolton, 1992) and biotic content, for example pollen (Innes *et al.*, 1996),

diatoms (Zong & Horton, 1998), foraminifera (Horton, 1999), testate amoeba (Charman *et al.*, 2002), ostracods (Peypouquet, 1979-80) and plant remains (Bhiry *et al.*, 2000) are often significantly related to altitude within and above the tidal frame.

Supra-tidal zone deposits, defined as freshwater organic or minerogenic sediments deposited in an environment influenced by tidal movement (Hageman, 1969), are characterised by fluvial deposits flanking the lower tidal reaches of rivers, freshwater mud deposits from ponded freshwater, and topogenous peat deposits from fen, fen carr and bog communities (Godwin, 1940). Changes in RSL may affect the water table, nutrient status and pH of the environment, thus significantly influencing vegetation species assemblages. By identifying the supra-tidal zone in the sediment record from the occurrence of freshwater fen or acidic bog pollen assemblages and freshwater diatoms species, conclusions may be drawn on the approximate position of RSL. However, other allogenic factors, such as climate and land use, as well as autogenic succession, which would also lead to changes in nutrient status, pH status and exposure to freshwater, exert equal authority over the spatial and temporal development of supra-tidal vegetation communities (Waller *et al.*, 1999). Nevertheless, analysis of supra-tidal sediments has contributed greatly to the elucidation of RSL movement (e.g. Hageman, 1969; Godwin, 1978).

Mudflats and saltmarshes inhabit the inter-tidal zone of sheltered, low-energy coastal environments in the temperate and high latitudes (Chapman, 1977; Eisma, 1998). The formation and characteristics of individual mudflats and saltmarshes, for example vertical range, grain size, organic content and vegetation species and patterns, is site specific, but a generalized overview of mudflat and saltmarsh formation is possible for most parts of Britain (Allen & Pye, 1992). Minerogenic sediments are principally received from the semi-diurnal tide. Fine sand and silt particles are deposited on the mudflats and sandflats, whilst flocculated clay particles are deposited on the landward reaches of the mudflat during slack high water. The increase in deposition rates on the landward reaches of the mudflat, an outcome of low velocities coupled with the process of settling lag (Postma, 1967), result in its elevation within the tidal frame and consequent reduction in tidal flooding duration and frequency. Colonisation by halophytes, species of *Salicornia* or *Spartina* for example, further encourages sedimentation. Progressive elevation of the saltmarsh and consequent further reductions

in flooding duration and frequency result in a succession to middle marsh species, such as *Festuca rubra* and *Juncus gerardii*, and then to higher marsh species, such as *Rumex crispus* and *Triglochin palustre* (Gray, 1992).

Elevation within the tidal frame is therefore a significant controlling factor of vegetation type, giving rise to a zonation of vegetation species from salt tolerant species on the low saltmarsh to progressively more salt intolerant species on the upper saltmarsh. This zonation applies also to diatoms (Oppenheim, 1988; Nelson & Kashima, 1993; Hemphill-Haley, 1995; Zong & Horton, 1998), foraminifera (Scott & Medioli, 1978; 1980; Jennings *et al.*, 1995; Horton, 1999; Horton *et al.*, 1999) and testate amoebae (Charman *et al.*, 1998; 2002), where certain species assemblages are found in each zone.

2.1.3 Relative sea-level and coastal reconstruction methodology

The identification of sub-tidal, inter-tidal and supra-tidal deposits in the Holocene coastal sediment record using macro- and microfossils contained within the sediments is fundamental to the elucidation of Holocene coastal palaeoenvironments and associated RSL. However, during a large international scientific collaboration programme, International Geological Correlation Programme (IGCP) Project 61, it became apparent that the field of RSL reconstruction lacked a robust, unified methodology.

IGCP Project 61 'Sea-level movements during the last deglacial hemicycle (about 15,000 years)' ran from 1974 to 1982. Its principal aim was to construct a global sea-level (eustatic) curve from approximately 15,000 years to the present by compiling RSL data from sites around the world (Tooley, 1982a). It was anticipated that comparison of RSL records would allow an insight into isostatic variations and the relationship between climate change, global ice-budget fluctuations and the response of sea-level. Bloom (1977) compiled and published RSL curves from sites around the world. However, with an inconsistent methodology of RSL reconstruction adopted by workers, comparison of RSL curves for different sites was difficult. Furthermore, an inconsistent terminology for describing changes in lithostratigraphy and RSL also impeded between-site correlation, and a limited consideration of the sources of error resulted in Holocene RSL curves of varying accuracy. Such problems were subsequently addressed (Section 2.1.3.1) but it was the realisation of differences in the geodetic sea-level over geological

time (Mörner, 1976) that essentially ended efforts to construct a globally valid eustatic sea-level curve (Section 3.1).

2.1.3.1 Methodological improvements generated by Project 61

Terminology

In an effort to introduce a formally accepted terminology, Tooley (1982b) proposed the use of the terms 'transgressive overlap' and 'regressive overlap' to describe lithostratigraphic changes. He suggested that a transgressive overlap should refer to a change in sedimentation from terrestrial facies to littoral facies and then successively to inner, middle and outer neritic facies, whilst a regressive overlap should refer to the successive replacement of outer, middle and inner neritic facies by littoral and terrestrial facies.

Sea-level index age, altitude, and indicative meaning

Errors in determining the altitude of a sea-level index (SLI) point may be introduced during several stages of measurement. The accuracy of measurement of depth in a borehole, for example, may be compromised by its angle and also by sediment compaction induced through coring (Shennan, 1982). Further, a single borehole may or may not reflect accurately the altitude of underlying former surfaces, which will inherently depend on the terrain roughness of such surfaces. The accurate determination of altitude of the former terrain surface will be influenced, therefore, by terrain roughness and borehole density (Shennan, 1982). Errors may also be introduced when levelling. Indeed, aside from errors incurred from levelling the borehole site to a local benchmark, differences in height between local benchmarks and the national geodetic datum in Newlyn may be ±0.15m for England and Wales (Eady, 1976). Tooley (1978a) recommended that radiocarbon dates should be independently corroborated by pollen analyses. Comparison of the local pollen assemblage of the sample to a radiocarbon dated, regional pollen assemblage record will in many cases determine if a radiocarbon date should be accepted or rejected.

The indicative meaning of a SLI point is the relationship between the environment in which it accumulated and a reference water level, whilst the altitudinal range that this indicator may have occupied, either above or below the reference water level, is known as the indicative range (van de Plassche, 1986). The indicative meaning and indicative

range of sediments and flora and fauna are known for tidalflats and saltmarshes from modern surveys (Section 2.2.3). However, reclamation of parts of the high saltmarsh and modification of the supra-tidal zone in most coastal areas of Europe (Ranwell, 1974) greatly limits the opportunity to investigate the relationships between the flora and fauna of these environments, their sediments and associated tidal parameters. Nevertheless, based on published research, Shennan (1980; 1982) has related commonly dated SLI point material to reference tide levels, together with its indicative range. By dating the level at which a change in the sedimentary environment occurs, apparent by changes in microfossils assemblages (Long, 1992) and/or stratigraphy, the indicative range may be reduced. More recently, research into the ecology and environmental associations of biota in the inter-tidal zone has enabled quantitative relationships between flora and fauna assemblages and tidal levels to be established. The greater accuracy of the indicative meaning of several sea-level indicators (Horton, 1999; Zong & Horton, 1999; Charman *et al.*, 2002) has allowed the reconstruction of palaeotidal levels with increased precision (e.g. Zong & Horton, 1999).

Correlation

SLI points from a single site will record local, site-specific processes such as changes in the availability of sediment and autocompaction, as well as registering larger scale processes such as RSL change. Coupled with consideration of the inherent errors discussed above, SLIs from a single site will be unable to distinguish between locally induced and regionally induced palaeoenvironmental change. Intra-regional correlation and comparison of SLIs is necessary before a positive or negative tendency of sea-level movement, that is, an increase or decrease in marine influence (Shennan, 1983), may become apparent (Shennan *et al.*, 1983). Only then can hypotheses, such as evidence of a regional change in the altitude of RSL, be tested.

A consequence of the allowance for altitude and dating errors in an effort to generate more robust and realistic time/altitude graphs (e.g. Heyworth & Kidson, 1982) is that the resultant broad sea-level envelope renders the correlation of time/altitude graphs to identify regional-scale processes impractical. Correlation of RSL records based on the tendency concept allows a more precise and robust alternative (Shennan *et al.*, 1983). This involves combining and plotting the radiocarbon dated SLIs from all sites within a region, after distinguishing between transgressive and regressive overlap SLIs. The

clustering of SLIs indicates a region-wide sea-level tendency, with the date of the regional tendency constrained by the oldest and youngest SLIs (e.g. Tooley, 1982b). The great advantage of this approach to intra-regional correlation is that it is dependent entirely on chronostratigraphic correlation, and is therefore free of the errors associated with altitude (for example, compaction, indicative range, errors in measuring altitude), which prevents time/altitude graph comparisons. In addition, the registration of positive tendencies at similar times in areas with opposing isostatic recovery, for example, may indicate changes in sea-level of wider significance (Shennan *et al.*, 1983). There are some disadvantages of this technique, however. For example, Long (1992) found that the lithological registration of a positive sea-level tendency may lag the associated change in microfossil assemblages by around 400 ^{14}C years. This has implications for constraining the onset of a sea-level tendency.

2.1.4 Remaining challenges

Irrespective of the advances in methodology outlined above, the fundamental problems of sediment autocompaction and a general lack of information about palaeotidal range changes during the Holocene, limit the accuracy of RSL reconstructions.

Autocompaction

The degree of autocompaction, a process in which the vertical thickness of unconsolidated sediments is reduced under self-weight (Allen, 1999), is largely dependent on the sediment characteristics and thickness (Greensmith & Tucker, 1986) and is extremely difficult to quantify (e.g. Paul & Barras, 1998; Allen, 1999). For this reason, the inevitable distortion of the original altitude of SLIs due to autocompaction is acknowledged but not corrected for in many Holocene sea-level studies. Moreover, not only does autocompaction introduce significant errors into the altitude component of time/altitude graphs constructed using intercalated organic sequences (e.g. intercalated SLIs were displaced by up to 1m in a study by Gehrels (1999)), but it may greatly inhibit the accurate calculation of the rates of RSL change (Allen, 1999). The construction of time/altitude graphs based solely on the analysis of basal peats (e.g. Jelgersma, 1961; Törnqvist *et al.*, 1998; Gehrels, 1999), which are independent of autocompaction, offer the best solution in accurately determining the former altitude of RSL.

Palaeotidal range

Time/altitude graphs usually depict the trend of MHWS (e.g. Long *et al.*, 1998), with the onset of organic sedimentation and significant changes in the microfossil assemblages associated with this tidal level, allowing its perception in the sediment record (Tooley, 1969). Local sea-level reconstructions, which, in reality are often MHWS reconstructions, may only be directly comparable if changes in the palaeotidal range are accounted for. Until relatively recently, the lack of adequate techniques to identify and quantify Holocene palaeotidal range changes have necessitated the assumption of a constant tidal range when attempting to interpolate MSL (e.g. Tooley, 1974).

The elucidation of palaeotidal range based on sedimentological and numerical modeling is now possible. For example, Roep & Beets (1988) reconstructed Mid and Late Holocene palaeotidal range using the difference between MHW and MLW sediment indicators from shoreline pit exposures in the western Netherlands. Additionally, Holocene palaeotidal range has been computed using sophisticated models (e.g. Gehrels *et al.*, 1995; Shennan *et al.*, 2000b), which require detailed knowledge of the changes in coastal geometry. All of these studies have shown that palaeotidal range has not remained constant throughout the Holocene. Unfortunately, MLW sediment indicators are not always well preserved or apparent in the sediment record, therefore preventing sediment-based palaeotidal reconstructions for many coastlines. Moreover, the detailed knowledge of changes in coastal geometry required for numerical model-based palaeotidal range reconstructions is only possible from comprehensive palaeogeographical reconstructions (e.g. Shennan *et al.*, 2000b), which is beyond the scope of many local sea-level studies. Nevertheless, the elucidation of palaeotidal range remains essential to facilitate Holocene sea-level record comparisons and to better constrain glacio-hydro-isostatic models (Shennan *et al.*, 2000b).

2.2 Diatom analysis

2.2.1 Introduction

Diatoms are microscopic, unicellular plants belonging to the algal class *Bacillariophyceae* that secrete a silicious shell, or frustule, composed of two valves held together by girdle bands (Round *et al.*, 1990). They are abundant in all aquatic

environments that have sufficient light (Dixit *et al.*, 1992) and range in size from less than 1μm to up to 2mm (Denys, 1984). It is the characteristic size and frustule ornamentation of diatoms that aids their identification, usually to species level. Within the field of palaeoenvironmental reconstruction, diatom analysis has assumed a prominent position. Diatoms respond rapidly to environmental change because they migrate and replicate rapidly (Dixit *et al.*, 1992). Further, many species are sensitive to environmental conditions and have narrow optima and tolerances for a range of environmental variables, including salinity, pH and temperature. Consequently, diatom analysis has been successfully applied to elucidate coastal palaeoenvironments and RSL changes (Denys & De Wolf, 1999), lake acidification (Birks *et al.*, 1990) and past ocean surface water temperatures (Sancetta, 1999). A further advantage is the high preservation potential of diatoms in the sediment record, due to their opaline, silicious, cell walls which are relatively resistant to chemical alterations after burial (Palmer & Abbott, 1986). Together with their occurrence in high numbers, these factors mean that quantitative environmental reconstructions to a high degree of certainty are often possible (Dixit *et al.*, 1992).

2.2.2 Life form

Diatoms may be subdivided into planktonic and benthic groups. Planktonic diatoms metabolise and reproduce in the water column, whilst benthic diatoms undergo all, or most, of their life cycle associated with sediments (Round, 1971). Diatoms may be further subdivided into different habitats, which describe the spectra of diatom life forms (Table 2.1).

2.2.3 Modern coastal zonation

Hendey (1964) recognises three main diatom zones from studies around the British coastline: the sub-littoral; littoral and supra-littoral, in which many diatom species are sensitive to particular environmental conditions, including salinity and duration of inundation. Diatom sensitivity to salinity has long been documented (Kolbe, 1927) and several salinity classification systems have been proposed (e.g. Kolbe, 1927; Hustedt, 1953; 1957; Van der Werff & Huls, 1957-1974). Indeed, the salinity gradient apparent along the main axis of an estuary is often the most influential environmental variable affecting diatom assemblage distribution in estuarine environments (Amspoker & McIntire, 1978; Juggins, 1992). Admaraal (1977), however, demonstrated that unialgal

diatom cultures and mixed populations from inter-tidal flats were highly tolerant when exposed to extreme salinity ranges of between 4‰ and 60‰. Consequently, the euryhaline behaviour displayed by these diatoms questions the accuracy of salinity classifications systems. In the field, competition for resources between species may be compounded by physio-chemical conditions, such as salinity. Isolating just one environmental variable, therefore, is perhaps unrepresentative of a more complex reality. Moreover, although the limitations of such salinity classifications are acknowledged, Petersen (1943) found Kolbe's (1927) halobian system to be a fairly accurate estimate of salinity when applied to water of known salinity.

Table 2.1. Principal habitat of diatoms (adapted from Round (1971) and Vos & De Wolf (1993a)).

Life form		Description of habitat
Planktonic	Plankton *sensu stricto*	live in the water column
	Tychoplankton	occur frequently in water column but also related to other habitats
Epiphytic		growing attached to other plants
Benthic	Epipelon	growing on mud (sediments)
	Endopelon	growing within the sediment
	Epipsammon	growing attached to sand grains
	Epilithon	growing attached to rock surfaces
	Endolithon	growing within cavities of rock
	Epizoon	growing attached to animals
	Aerophilous	live in irregular flooded areas

In the inter-tidal zone, diatom species assemblage is principally controlled by ground elevation within the tidal frame (Zong & Horton, 1998). Varying frequency and duration of tidal inundation as a consequence of ground elevation results in sediment physio-chemical gradients of desiccation, particle size, organic content, water content, pH, salinity and illumination, all of which have varying degrees of influence on diatom species and result in characteristic assemblages. Indeed, contemporary diatom surveys

along transects from tidalflats to high saltmarshes at various locations in the US (Nelson & Kashima, 1993; Hemphill-Haley, 1995; Shennan *et al.*, 1996; Patterson, *et al.*, 2000), Japan (Sawai, 2001) and the UK (Oppenheim, 1988; Zong, 1997; Zong & Horton, 1998; 1999) distinguish tidalflat, low saltmarsh and high saltmarsh zones. In general, the tidalflat zone is characterised by marine brackish epipsammon and epipelon diatom communities that dominate the sandflats and mudflats respectively (Vos & De Wolf, 1993a), together with marine planktonic and tychoplanktonic forms brought in from the tide, which may cover this part of the inter-tidal area daily. The low saltmarsh area, with its sparse vegetation and frequent periods of exposure, is characterised by epipelic species, with some epiphytes (Zong & Horton, 1998). Tidal inundation is infrequent and of short duration in the high saltmarsh environment. Here, long periods of exposure make high saltmarsh environments prone to desiccation, which explains the high occurrence of marine brackish and brackish freshwater aerophilous forms found in this environment (Vos & De Wolf, 1993a). With dense vascular plant cover and fine particle sizes, epiphyte and epipelon life forms are also abundant (e.g. Zong & Horton, 1998).

2.2.4 Autochthonous and allochthonous diatoms

Large volumes of water are frequently displaced at the coastline under tidal and riverine influence. The capacity for the introduction of allochthonous (transported) diatom cells and frustules is therefore significant. Riverine and marine-derived plankton and tychoplankton diatoms may be washed into an estuary and deposited in inter-tidal areas. A diatom assemblage therefore reflects autochthonous (benthic), as well as allochthonous (planktonic and tychoplanktonic) environmental conditions. Sawai (2001) compared living and dead diatom assemblages for several marsh inter-tidal areas and found that whilst the upper saltmarsh contained few allochthonous valves, the low saltmarsh contained many and essentially represented a mixed assemblage of allochthonous and autochthonous forms. This was attributed to higher frequencies of tidal processes experienced at this elevation. Indeed, a high abundance of planktonic and tychoplanktonic diatom frustules is a common component of low saltmarsh and tidalflat areas (Hemphill-Haley, 1995). The presence of allochthonous diatom valves and frustules has obvious implications. Failure to distinguish allochthonous from autochthonous forms may compromise the accuracy of subsequent palaeoenvironmental interpretations (Section 2.2.6).

2.2.5 Application to Holocene coastal palaeoenvironmental reconstruction

In the coastal environment, substrate and salinity constitute two of the most influential variables with regard to diatom species distribution (Kosugi, 1987). Based on extensive literature surveys and supplemented by research carried out on the coastal deposits of the Netherlands, De Wolf (1982) assigned an 'ecological code' to many commonly occurring coastal diatom species. The code for each individual species contained information on life form (Table 2.1) as well as salinity (Table 2.2), pH, nutrient status, temperature, tides and current velocity that characterise the environment in which the diatom species is often found. Similarly, ecological codes were presented for freshwater diatoms from the Netherlands (Van Dam *et al.*, 1994) and for diatoms commonly encountered in the coastal deposits of Belgium (Denys, 1991-2).

Table 2.2. Salinity classification used in coding diatoms (De Wolf, 1982) based on the halobian system of Hustedt (1957).

Salinity classification	Salinity boundaries
Polyhalobous	>30 ‰
Mesohalobous	0.2‰ to 30 ‰
Oligohalobous halophilous	Optimum in slightly brackish water
Oligohalobous indifferent	Optimum in freshwater but tolerant of slightly brackish water
Halophobous	Exclusively freshwater

Based on life form and salinity, Vos & De Wolf (1988) combined diatom species into ecological groups. The relative abundance (%) of ecological groups represented in a fossilised diatom assemblage is related to specific coastal sedimentary environments (Table 2.3). This method was further developed and refined by Vos & De Wolf (1993a) who named the ecological groups after the basal factors of life form and salinity, for example, freshwater epiphytes. This method allows a more complete coastal palaeoenvironmental reconstruction (e.g. Plater & Shennan, 1992; Vos & De Wolf, 1993b; Zong, 1997; Spencer *et al.*, 1998) than would otherwise have been the case based on salinity alone.

Table 2.3. Relationship between the relative abundance (%) of the ecological groups and sedimentary environments (from Vos & De Wolf, 1988; 1993a).

Ecological groups	Macro- and mesotidal environments							Microtidal and non-tidal environments		
	Subtidal area		Intertidal area		Supratidal area			Marine/brackish		non-marine (fresh)
	open marine tidal channels	estuarine tidal channels	sand-flats	mud-flats	salt-marshes, around MHW	salt-marshes, above MHW	pools in the salt-marshes	tidal lagoons, small tidal range	lagoons, no tides	rivers, ditches and lakes
Marine plankton	10-80	10-60	1-25	10-70	10-70	10-70	10-50	10-60	0-10	0-5
Marine tychoplankton	20-90	15-60	1-25	10-70	10-70	10-70	10-50	10-60	0-10	0-5
Brackish plankton	1-10	20-70	1-10	1-30	1-30	1-30	1-15	1-15	0-10	0-5
Marine brackish epipsammon	1-40	1-45	50-95	1-45	0-15	0-15	0-15	0-25	0-5	0-1
Marine brackish epipelon	0-5	0-5	1-30	15-50	1-40	0-5	5-30	5-50	5-60	0-1
Marine brackish aerophilous	0-1	0-1	0-1	0-1	10-40	15-95	10-40	0-1	0-1	0-1
Brackish freshwater aerophilous	0-1	0-1	0-1	0-1	10-40	15-95	10-40	0-1	0-1	0-10
Marine brackish epiphytes	0-1	0-1	0-5	0-5	0-5	0-5	10-60	10-75	10-90	0-5
Brackish freshwater plankton	0-1	0-25	0-1	0-1	0-1	0-1	0-1	0-20	0-25	0-5
Brackish freshwater tychoplankton	0-1	0-1	0-5	0-5	0-5	0-5	5-50	5-50	5-80	0-10
Brackish freshwater epiphytes	0-1	0-1	0-5	0-5	0-5	0-5	1-50	1-50	1-80	0-10
Freshwater epiphytes	0-1	0-1	0-1	0-1	0-5	0-5	0-10	0-10	0-10	1-75
Freshwater epipelon	0-1	0-1	0-1	0-1	0-1	0-1	0-10	0-5	0-10	1-75
Freshwater plankton	0-1	0-1	0-1	0-1	0-1	0-1	0-5	0-15	0-20	10-95

This method, however, has been developed based on the relationships between diatom ecological groups and associated palaeoenvironments for the Netherlands coastal zone. The tidal range of much of the Netherlands coastline is thought to have evolved from a microtidal range (<2m according to Davies, 1964) during the Early and Mid Holocene, to the present mesotidal range (2m to 4m according to Davies, 1964) (Vos & van Kesteren, 2000). Today, the coastal environments of the Mersey Basin are associated with a macrotidal range (>4m according to Davies, 1964). Changes in the Holocene tidal range of most coastlines, including those of north west England, are largely unresolved. Consequently, RSL reconstructions are often forced to assume a constant tidal range. In reality, this may not be the case and Plater *et al.* (1999) have suggested, although tentatively, that coastal sediment deposits of the Mersey Basin may have formed under mesotidal range conditions at some time during the last 6,000 ^{14}C yrs BP. Caution must be exercised, therefore, when using the diatom ecological groups of Vos & De Wolf (1988; 1993a), which relate characteristic diatom assemblages to palaeosedimentary environments formed under microtidal and mesotidal range conditions, to infer palaeosedimentary environments formed under macrotidal range conditions.

Zong & Horton (1999) have successfully reconstructed Late Holocene palaeotidal heights of greater accuracy by developing a diatom-based, tidal-level transfer function, which statistically relates contemporary diatom assemblages to tidal levels. The increasing accuracy of palaeotidal-level reconstructions using diatoms is necessary to quantify small-scale changes in RSL during the Late Holocene, where there are no significant changes in lithology such as those witnessed during the Early Holocene (Tooley, 1974). Investigation of Late Holocene coastal deposits may provide important information regarding the relationships between climate, RSL and coastline response, with important implications for coastal zone management. Increasing reliance is therefore placed on analysis of microfossils that must be sensitive to subtle changes in elevation (Zong, 1997). Indeed, it has been demonstrated that diatoms are the most sensitive proxy indicator of elevation change in the inter-tidal zone (Gehrels *et al.*, 2001).

2.2.6 Taphonomic considerations

The death assemblage of diatoms will contain information about the environment in which it was deposited, which may be derived from the autochthonous assemblage, as well as details of the surrounding environment, derived from the allochthonous assemblage (Section 2.2.4). Vertical transport of diatom valves within the sediment column may also introduce an allochthonous component to an assemblage. Although details of vertical transport are poorly understood (Beyens & Denys, 1982), it is believed that percolation of precipitation, especially in coarse sediments, may displace valves in the sediment record. Reworking due to water currents or bioturbation may also disturb recently deposited valves.

Identification of the autochthonous component of an assemblage is one of the most important aspects of any microfossil palaeoenvironmental reconstruction (Vos & De Wolf, 1988) as only the autochthonous assemblage provides information about the local palaeoenvironment of interest. Several procedures have been introduced to aid identification of allochthonous valves. By definition, the benthic diatom assemblage should represent the autochthonous component (Vos & De Wolf, 1988) and Simonsen (1969) argued that benthic species only should be used to derive palaeoenvironmental information. The allochthonous component in a sediment sample, however, may provide valuable information on the physical and hydrographical palaeoenvironment (Beyens & Denys, 1982). Beyens & Denys (1982) argued that identification of the 'optimal group' based on the dominant salinity group of the benthic diatom assemblage, together with its 'nearest neighbour' salinity groups, constitutes the autochthonous component. Such an approach disregards the euryhaline taxa, which may form an important component of the diatom assemblage (Juggins, 1992). High fragmentation of diatom valves in a sample is also an unreliable approach to identifying the allochthonous component. Breakage of diatom valves may indeed result from transport (Vos & De Wolf, 1988; 1993a), but may also result from sediment compaction and predation (Beyens & Denys, 1982) and even careless slide preparation (Flower, 1993), all of which may have a greater effect on larger, less silicified valves.

Vos & De Wolf's (1988; 1993a) classification of ecological groups (Section 2.2.5) can help to distinguish the autochthonous component. For example, if both marine and freshwater ecological groups are represented in a single assemblage, then one of the

ecological groups must be allochthonous. Further, the sedimentary sequence should exhibit a succession of the ecological groups. As Shennan (1986, p. 157) states, 'Sequences which occur comformably in a stratigraphic section reflect a change in environments which are spatially adjacent'. Vos & De Wolf (1988; 1993a) also suggest several non-diatom related criteria that may be useful in distinguishing the allochthonous component. In terms of sediment composition, for example, the presence of epipsammic species in heavy clays will represent the allochthonous component due to the absence of a sand substrate (Vos & De Wolf, 1988; 1993a).

Dissolution of diatom valves is a further problem that may jeopardise the quality of palaeoenvironmental inferences. Diatom dissolution rates, which may be enhanced by the presence of iron oxides in the sediments, for example, (Mayer *et al.*, 1991), have seldom been quantified for different species (*cf.* Ryves *et al*, 2001). Preferential dissolution of certain species may seriously bias subsequent palaeoenvironmental interpretations (Hemphill-Haley, 1995; Innes *et al.*, 1996; Kato *et al.*, 2003) and so more research into this area is needed. In a sediment trap and surface sediment study in Omura Bay, Japan, a severe loss of planktonic diatom frustules was found to occur at the sediment-water interface because of dissolution and fragmentation (Kato *et al.*, 2003). Comparison of the planktonic diatom assemblage in the water column with the newly fossilised assemblage revealed the fossilised assemblage to be a biased reflection of the living diatom flora (Kato *et al.*, 2003).

Finally, the adoption of a uniformitarianism approach, in which modern diatom assemblages are used as an analogue to reconstruct past environments (e.g. Plater *et al.*, 2000b), may be complicated by restricted modern analogues, as well as by taphonomic processes. Zong (1997) found some degree of lack of comparability between modern diatom assemblages and fossil assemblages at Roundsea Marsh, north west England. He attributed this to changes in sediment type, water salinity and acidity between the Mid Holocene and the contemporary marsh environment, but suggested that a consideration of diatom analogues from other sites may overcome such problems. Innes *et al.* (1996) found that many of the most common diatoms species of Kentra Bay, Scotland, were of a very small size, unlike the larger valves that dominate the fossil assemblage. They suggest that post-depositional processes may have destroyed smaller and weaker valves preferentially. Further, Hemphill-Haley (1995) found that many

abundant diatom valves in the contemporary marsh environment have little chance of surviving in the fossil record, either due to their delicate nature or poor preservation potential, and that some of the more rare contemporary diatoms may appear to be an important component of the fossil assemblage due to their robust nature.

2.3 Carbon Isotope Analysis

2.3.1 Introduction

Estuarine saltmarshes and tidalflats receive sediment from several different sources, including riverine- and marine-derived minerogenic sediment and particulate organic matter, organic matter from saltmarsh plants and other biota (Luternauer, *et al.*, 1995). These sediment sources may be distinguished using their carbon isotope ratios ($^{13}C/^{12}C$, expressed as $\delta^{13}C$), as the isotopic composition of the organic carbon associated with each of these sediments varies between sources (Megens *et al.*, 2002). This has resulted in the use of $\delta^{13}C$ analysis in saltmarsh sediment provenance studies (e.g. Haines, 1976; Ember *et al.*, 1987; Chmura & Aharon, 1995) and carbon budget determinations (e.g. Middelburg *et al.*, 1997; Andrews *et al.*, 2000).

Saltmarsh sediments may be divided into autochthonous (sediments derived from the saltmarsh) and allochthonous (sediments brought in from elsewhere) components. The dominant autochthonous saltmarsh sediment component is derived from plant material. At the most landward limit of saltmarshes, infrequent tidal inundation allows extensive vegetation cover, resulting in highly organic surface sediments. In contrast, tidalflats are frequently inundated for lengthy periods, vascular vegetation is absent, and allochthonous, tidal-derived minerogenic and particulate organic matter, dominate the surface sediments (Figure 2.1). The sediment composition of saltmarsh surfaces is therefore related to elevation within the tidal frame (Allen, 1990). These two contrasting sources of organic matter (vascular vegetation *vs.* tidal-derived particulate organic matter) have distinctly different $\delta^{13}C$ compositions (Sections 2.3.3 and 2.3.4). Measurement of $\delta^{13}C$ in bulk sediments should, theoretically, directly reflect the relative amounts of the two sources (Fry & Sherr, 1989). Consequently, $\delta^{13}C$ analysis of organic matter may be applicable to Holocene coastal deposits to determine changes in the dominant organic sediment source over time, which will vary as a function of RSL change, for example.

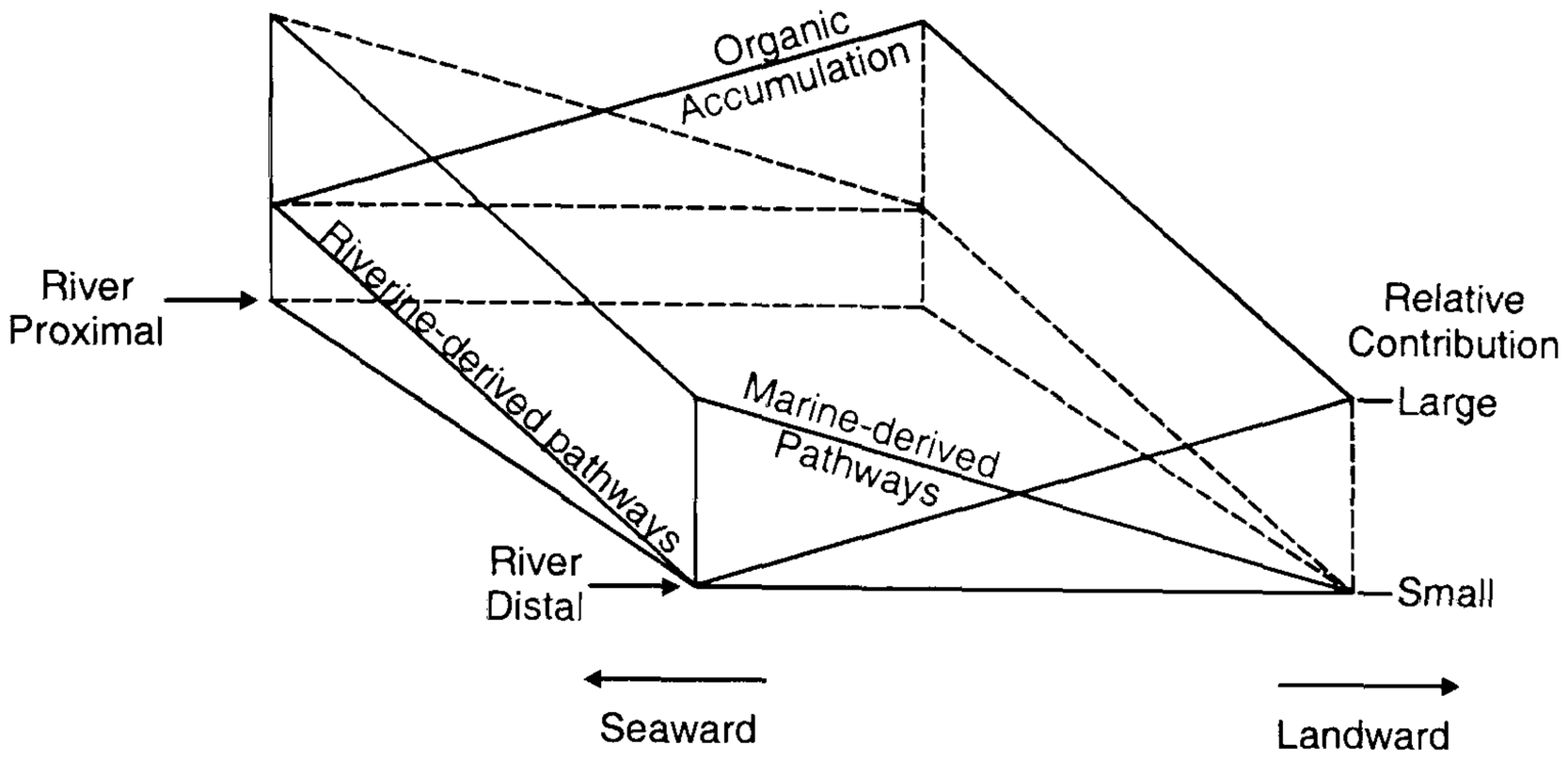

Figure 2.1. Relative contributions and provenance of sediments on an estuarine saltmarsh (from Luternauer *et al.*, 1995).

Hitherto, $\delta^{13}C$ analysis has been used successfully as a coastal palaeoenvironmental indicator in estuarine deposits that have a mixture of C_3 and C_4 vegetation in their catchments (e.g. Delaune, 1986). In estuaries with C_3 vegetated catchments, the study by Andrews *et al.* (2000) is the only one to utilise $\delta^{13}C$ analysis as a coastal palaeoenvironmental indicator, although this study is geared towards the calculation of carbon and nitrogen storage rather than an evaluation of $\delta^{13}C$ analysis as an accurate coastal environmental proxy. Consequently, in estuarine deposits in C_3 vegetated catchments, there remains much to be learnt about the potential of $\delta^{13}C$ as a coastal environmental indicator. Specifically; the sensitivity of $\delta^{13}C$ in detecting small scale coastal palaeoenvironmental changes, the accuracy of $\delta^{13}C$ values as coastal environmental indicators, the suitability of using $\delta^{13}C$ values as geochemical 'signatures' of environmental facies in light of decompositional effects, a factor not considered in the study by Andrews *et al.* (2000), and the viability of employing $\delta^{13}C$ as an alternative RSL indicator to microfossils.

2.3.2 $\delta^{13}C$ measurement and notation

There are two stable isotopes of carbon. Carbon-12 (^{12}C) is the most abundant (98.89%) with carbon-13 (^{13}C) present only in small amounts (1.11%) (Nier, 1950). Organic material is converted into CO_2 prior to measurement in a mass spectrometer. The ratio (R) of $^{13}CO_2/^{12}CO_2$ in a sample is then measured and expressed relative to a standard, 'PDB', which is derived from a fossil belemnite from the Pee Dee Formation

in South Carolina (Craig, 1957) (expressed as V-PDB when using protocol devised by the IAEA at Vienna). The carbon isotope composition of the sample is expressed in δ notation:

$$\delta^{13}C = \left[\left(R_{sample} / R_{standard}\right) - 1\right] \times 1000 \qquad \text{(Equation 2.1)}$$

where $\delta^{13}C$ is the carbon isotope ratio of the sample relative to the standard in delta units, and $R_{(Sample)}$ and $R_{(Standard)}$ are the absolute carbon isotope ratios of the sample and standard respectively. Multiplying by 1000 and expressing the values as ‰ ('per mil') overcomes the small differences in absolute values.

2.3.3 Autochthonous saltmarsh organic carbon sources

2.3.3.1 Saltmarsh vegetation

Saltmarsh vegetation is the most dominant source of autochthonous organic carbon to the underlying sediments. In general, plants exhibit a range of $\delta^{13}C$ values as a consequence of both endogenous (internal) and exogenous (external) factors. Endogenous $\delta^{13}C$ variation arises as a consequence of photosynthesis. Plants fractionate carbon isotopes during photosynthesis and the magnitude of this ultimately varies according to the photosynthetic pathway utilised by the plant. Plant species that follow the C_3 photosynthetic pathway, which constitutes about 90% of all plants (Hoefs, 1997), have $\delta^{13}C$ values that generally range between –32.0‰ and –21.0‰ (Deines, 1980). The negative $\delta^{13}C$ values of plants indicate that they discriminate against ^{13}C, preferentially using the ^{12}C isotope. The degree of this discrimination in plants may be quantified as the difference between the $\delta^{13}C$ composition of source and product (O'Leary *et al.*, 1992):

$$\Delta^{13}C = \delta^{13}C_s - \delta^{13}C_p \qquad \text{(Equation 2.2)}$$

where $\delta^{13}C_s$ is the source (atmospheric CO_2: $\delta^{13}C$ = –8.0‰, Keeling *et al.*, 1995) and $\delta^{13}C_p$ is the product, (C_3 plant, using $\delta^{13}C$ average of –25.0‰). Therefore:

$$\Delta^{13}C = -8.0‰ - - 25.0‰ = 17.0‰ \qquad \text{(Equation 2.3)}$$

The positive discrimination against ^{13}C is largely due to the enzyme Ribulose 1.5-bisphosphate carboxylase/oxygenase (RuBisCO). This enzyme is the first step in CO_2

fixation (Park & Epstein, 1960) and causes a carbon isotope fractionation of 30.0‰ (e.g. Roeske & O'Leary, 1984), although the availability of inorganic carbon to the C_3 plant will ultimately determine if this degree of fractionation is expressed (*cf.* Equation 2.3). Plant species following the C_4 photosynthetic pathway have much higher $\delta^{13}C$ values and range between –15.0‰ and –9.0‰ (Deines, 1980). These higher values are caused by a much smaller fractionation (5.7‰) associated with CO_2 fixation by the enzyme phosphoenol pyruvate carboxylase (PEP) (e.g. O'Leary *et al.*, 1992). Plants that exhibit crassulacean acid metabolism (CAM) are able to incorporate inorganic carbon using both the C_3 and C_4 photosynthetic pathways, resulting in intermediate $\delta^{13}C$ values (Osmond *et al.*, 1973). In addition to photosynthetic pathway, it is apparent that intra-species genetic diversity may also cause $\delta^{13}C$ variation in plants. Kohorn *et al.* (1994), for example, found a 5.1‰ range in $\delta^{13}C$ values in a natural population of the desert shrub *Simmondsia chinensis*, which they attributed to genotype diversity.

The two distinct $\delta^{13}C$ ranges associated with C_3 and C_4 plants have been used as a basis to reconstruct palaeovegetation, as the $\delta^{13}C$ composition in sediments remains unchanged over multi-million year time periods (Meyers, 1994). $\delta^{13}C$ of soil and sediment organic matter reflect the relative contributions of C_3 and C_4 plant species over time (e.g. Stout *et al.*, 1975; McPherson *et al.*, 1993; Boutton *et al.*, 1998). In the coastal environment, work in the US has focussed on characterising the $\delta^{13}C$ values of modern C_4 saltmarsh and C_3 freshwater marsh plants and surface sediments (Ember *et al.*, 1987; Craft *et al.*, 1988; Cloern *et al.*, 2002) and applying these data to aid marsh palaeovegetation and associated palaeosalinity reconstructions (DeLaune, 1986; Byrne *et al.*, 2001). Further, mixing models have been developed in an attempt to predict surface sediment $\delta^{13}C$ values, based on the relative abundance and $\delta^{13}C$ values of the overlying marsh vegetation, in order to achieve more accurate coastal palaeovegetation reconstructions (Chmura *et al.*, 1987; Chmura & Aharon, 1995; Malamud-Roam & Ingram, 2001). In all of the above cases, the soil or sediment $\delta^{13}C$ value proved to be a faithful recorder of the overlying vegetation, despite some diagenetic effects (Section 2.3.6).

Use of distinct $\delta^{13}C$ values to reconstruct palaeosalinity is restricted to areas in which plants species exhibiting C_3 and C_4 photosynthetic pathways have been present for the duration of the time period being studied. Although several C_4 saltmarsh plant species

are currently present in many British saltmarshes, for example *Spartina alterniflora*, *S. anglica*, *S. maritima*, *S. townsendii*, *Atriplex laciniata*, *Cynodon dactylon*, *Cyperus longus* (Crawford, 1989), they have either been introduced in the nineteenth century (e.g. *S. alterniflora*) or are hybrids of introduced species (e.g. *S. townsendii* and *S. anglica*) (Rackham, 1986), or are otherwise rare or absent along the north west England coastline (Preston *et al.*, 2002). Consequently, remnants of C_4 plants will be particularly rare in north west England Holocene coastal deposits.

In terms of exogenous factors, environmental conditions can also affect plant $\delta^{13}C$ values. During plant fixation of atmospheric CO_2, carbon isotope fractionation occurs during two stages (Park & Epstein, 1960): the carboxylation reaction already discussed, and the diffusion of CO_2 by the plant stomata to the site of carboxylation. The resulting plant $\delta^{13}C$ value can, therefore, vary with stomatal aperture, as the plant stomata modulate the uptake and associated internal concentration of CO_2 (Farquhar *et al.*, 1982a):

$$\Delta = a + (b - a) \times c_i/c_a \qquad \text{(Equation 2.4)}$$

where Δ is the total fractionation, a is 4.4‰, which is the fractionation caused by the slower diffusion of $^{13}CO_2$ relative to $^{12}CO_2$ into cell environments (O'Leary & Osmond, 1980), b is the fractionation due to carboxylation (in C_3 plants = 30.0‰) and c_a and c_i are the external and internal partial pressures of CO_2 respectively.

Changes in the ratio c_i/c_a will cause considerable variation in Δ (and therefore $\delta^{13}C$) of C_3 plants in particular (Figure 2.2). This is because fractionation associated with diffusion, a (4.4‰), and carboxylation, b (30.0‰), are significantly different from each other. The ratio of c_i/c_a may theoretically vary between 0 and 1 and changes as a function of stomatal conductance (Farquhar *et al.*, 1982a). For example, a reduction in the stomata aperture will limit conductance of CO_2 and, consequently, the internal CO_2 pool (c_i) will be small (c_i approaching 0). Therefore, the carboxylation isotope fractionation (30.0‰) is not expressed, as all of the internal CO_2 is utilised. The resulting $\delta^{13}C$ value of a C_3 plant will reflect the $\delta^{13}C$ value of source CO_2 (–8.0‰) and diffusion (–4.4‰), giving a $\delta^{13}C$ value of –12.4‰ (Schleser, 1995). Alternatively, the diffusion value will not be expressed when the stomata are open to the extent that

internal CO_2 concentration approaches external CO_2 concentration (c_i approaches 1). The resulting $\delta^{13}C$ value for a C_3 plant will then reflect the $\delta^{13}C$ value of source CO_2 (−8.0‰) and carboxylation (−30.0‰), giving a $\delta^{13}C$ value of −38.0‰ (Schleser, 1995).

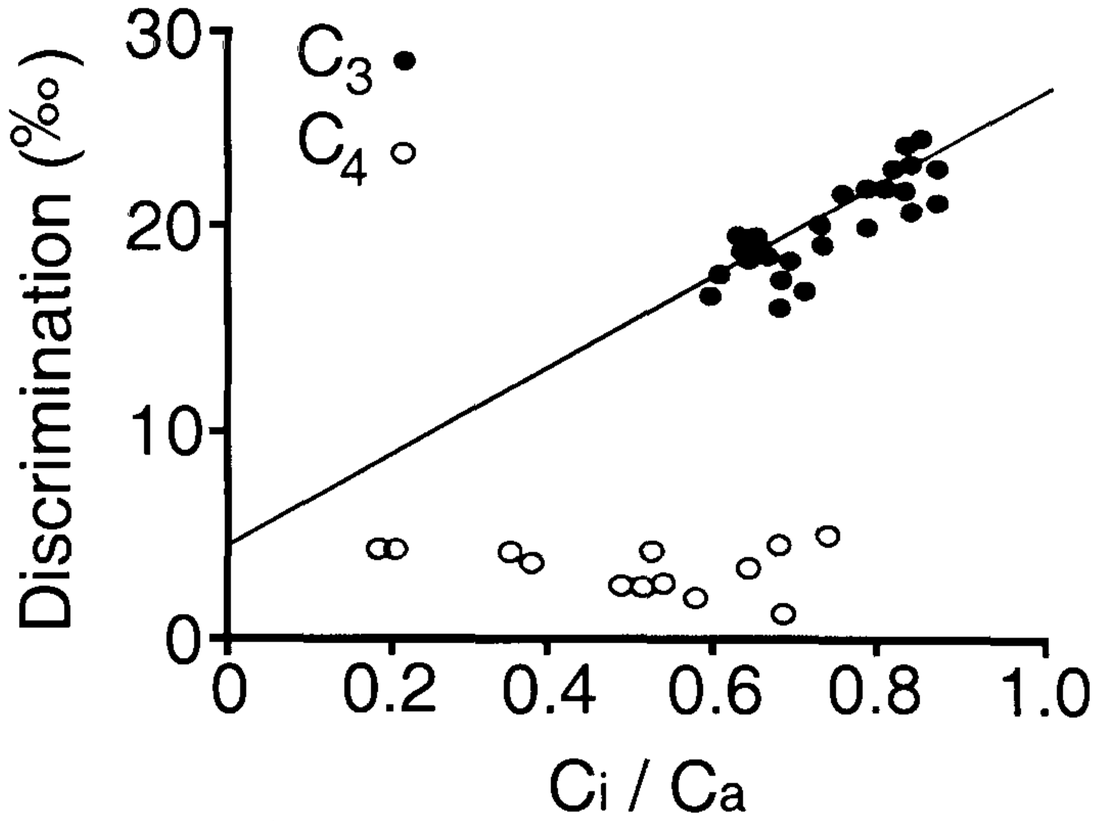

Figure 2.2. Relationship between carbon isotope discrimination (Δ) and the ratio of intercellular and ambient CO_2 partial pressures (C_i/C_a) (from Farquhar *et al.*, 1989a).

The large range in $\delta^{13}C$ values of C_3 plants (>10.0‰) may therefore be explained by variations in stomatal mediated CO_2 diffusion. Consequently, exogenous factors that cause changes in stomatal aperture may influence $\delta^{13}C$ values of C_3 plants. In view of this phenomenon, $\delta^{13}C$ analysis has been applied to investigate the effects on C_3 plants of, for example, drought stress (Farquhar *et al.*, 1989b), salinity stress (Seemann & Critchley, 1985), vapour pressure deficit (Turney *et al.*, 1999) and fluctuations in ambient CO_2 concentrations (Schleser, 1995). Many of the established relationships between C_3 plant $\delta^{13}C$ and exogenous factors have direct application to palaeoenvironmental and palaeoclimatic reconstructions (e.g. Krishnamurthy & Epstein, 1990; Turney *et al.*, 1999).

A significant relationship between soil salinity and C_3 halophyte $\delta^{13}C$ has been observed both in the field and under laboratory conditions. For example, for a Canadian inland saline area, Guy *et al.* (1980) measured a +5.8‰ shift in the $\delta^{13}C$ values of *Salicornia europaea* ssp. *rubra* as soil water potential decreased along a 5.55m transect from -25×10^2 kPa to -73×10^2 kPa. Further, in growth chamber experiments, *Puccinellia*

nuttalliana $\delta^{13}C$ values changed by approximately 11.0‰, from around –36.0‰ to –25.0‰, as the solute potential of the nutrient solution was reduced from -0.25×10^2 kPa to -40.25×10^2 kPa. Neales *et al.* (1983) found a maximum shift in $\delta^{13}C$ values from –26.1‰ to –20.0‰ in the leaves of *Disphyma clavellatum*, a succulent halophyte endemic to southern Australia, as the salinity of the root environment was increased from 0 to 500 mol m^{-3} NaCl.

A clearly defined vegetation zonation is often apparent in saltmarshes (Gray, 1992). Saltmarsh species vary with elevation within the tidal frame as a function of their salinity tolerance, with salt tolerant species, such as *Puccinellia maritima* and *Salicornia europaea,* present on the low saltmarsh, and less salt tolerant species, such as *Phragmites australis* and *Agrostis stolonifera,* often present on marsh areas above high water. Such a salinity gradient may be expected to cause a systematic reduction of $\delta^{13}C$ values in C_3 plants with increasing elevation within the tidal frame. However, an investigation into the $\delta^{13}C$ composition of saltmarsh vegetation zones at Kentra Bay, Scotland, found no such relationship between $\delta^{13}C$ of C_3 saltmarsh species and salinity (Twiddy, 1996). Further, a large variation in $\delta^{13}C$ values between species was observed (up to 4.0‰) in the same saltmarsh zones, together with significant seasonal variations in individual species. This disparity is most probably a reflection of the degree of exposure to salinity, with plants in inland saline areas subject to continued exposure, whilst saltmarsh plants are subject only to periodic fluctuations in salinity. Indeed, Twiddy (1996) explained the absence of a relationship between C_3 plant $\delta^{13}C$ and salinity in the saltmarsh he studied as a result of the plants restricting photosynthesis to periods when precipitation had reduced the content of marine-derived salts in the sediment.

A fundamental prerequisite for the successful application of $\delta^{13}C$ analysis to coastal palaeoenvironmental reconstruction in the present study is that autochthonous (terrestrial C_3 plant matter) and allochthonous (tidal-derived organic matter) organic carbon sources are isotopically distinct (see Figure 2.3). Contrasting evidence of the behaviour of plants, manifest in their $\delta^{13}C$ values, under conditions of fluctuating salinity appears to be site or area specific. It is important, therefore, to investigate the relationship between plant $\delta^{13}C$ values and altitude within the tidal frame at Ince Banks, as this is a potential source of large variation in plant $\delta^{13}C$. Indeed, if plant $\delta^{13}C$ values

are observed to increase with decreasing altitude on Ince Banks, then this may 'bridge the gap' between the otherwise distinct $\delta^{13}C$ values of autochthonous and allochthonous organic carbon. Nevertheless, although this may complicate organic carbon source determination in bulk surface sediments, the trend of increasing $\delta^{13}C$ values with proximity to the lower saltmarsh will remain.

External (atmospheric), as well as internal (stomata mediated), CO_2 concentrations are subject to change. Atmospheric CO_2 concentrations have fluctuated throughout the Holocene in response to changes in the terrestrial biosphere and sea-surface temperatures (Indermühle *et al.*, 1998). From 10,500 ^{14}C yr BP to 8,300 ^{14}C yr BP, CO_2 concentrations decreased from 268ppmv to 260ppmv, and then increased linearly to 285ppmv during the following 7,000 years (Indermühle *et al.*, 1998). Viewed in the context of this study, these changes in atmospheric CO_2 concentrations have led to fairly insignificant changes in atmospheric CO_2 $\delta^{13}C$ values. For example, between 11,000 ^{14}C yr BP and 6,600 ^{14}C yr BP, atmospheric CO_2 $\delta^{13}C$ values increased by 0.3‰ and then fell by 0.2‰ during the following 5,600 years (Indermühle *et al.*, 1998). Prior to major industrial development, the atmospheric CO_2 concentration was 280ppm and atmospheric CO_2 $\delta^{13}C$ values were around –6.5‰ (Friedli *et al.*, 1986). From around 1850, as a result of anthropogenic activities, atmospheric CO_2 concentrations have risen near exponentially to present (1995) levels of around 360ppm (Andrews *et al.*, 1996). Because fossil fuels have highly negative $\delta^{13}C$ values (–27.0‰) (Hoefs, 1997), atmospheric CO_2 $\delta^{13}C$ values have decreased to –8.0‰ (Keeling *et al.*, 1995). Clearly, when using $\delta^{13}C$ values to characterise modern organic carbon sources as analogous to Holocene sources, the significant decrease in atmospheric CO_2 $\delta^{13}C$ over the last two centuries will have to be taken into account.

2.3.3.2 Other autochthonous organic carbon sources

Although the incorporation of plant detritus into the sediment matrix appears to govern the $\delta^{13}C$ value of the saltmarsh sediment (e.g. Malamud-Roam & Ingram, 2001), nevertheless, many studies have questioned the degree to which other sources of autochthonous organic carbon, such as algae and bacteria, contribute to the observed bulk sediment $\delta^{13}C$ values (Table 2.4).

Table 2.4. Bacterial and algal $\delta^{13}C$ values from various studies (see also Figure 2.3).

Location	Autochthonous marsh material	$\delta^{13}C$ value (‰)
Georgia saltmarsh, USA[a] Bare creekbank	Benthic algae (mostly diatoms)	–16.2 to –17.9
North Carolina, USA[b] Lower saltmarsh	Benthic algae	–16.7
Kentra Bay, Scotland[c] Lower saltmarsh	Algae (*Pelvetica canaliculata*)	–17.0 to –21.0
Dorset, England[d] Mudflat	Unidentified filamentous algae	–18.9
San Francisco Bay estuary, USA[e] Surface marsh sediment	Cyanobacteria bloom	–26.6 to –28.0

[a]Haines (1976)
[b]Craft *et al.* (1988)
[c]Twiddy (1996)
[d]Bull *et al.* (1999)
[e]Cloern *et al.* (2002)

Peterson *et al.* (1980) argue that the different $\delta^{13}C$ values observed between living *Spartina alterniflora* (–11.0‰ to –13.0‰) and underlying surface sediments (–18.0‰ to –24.0‰) in some saltmarshes of the eastern USA may in fact be due to the presence of bacteria in the sediment which, when mixed with *S. alterniflora* detritus, would result in the observed bulk surface sediment $\delta^{13}C$ values. However, this study gave no indication of the amount of bacteria that would be needed to cause such a large deviation in sediment $\delta^{13}C$ values.

Saltmarsh vegetation is the dominant source of autochthonous organic carbon, the $\delta^{13}C$ value of which will remain relatively unaltered in the sediment record. In contrast, bacteria and algae contain more labile compounds, resulting in fairly rapid decomposition, and are therefore not expected to impact greatly on bulk sediment deposit $\delta^{13}C$ values. The $\delta^{13}C$ values of modern marsh bacteria and algae, however, may influence bulk surface sediment $\delta^{13}C$ values. As the range in $\delta^{13}C$ values between the two 'end-member' environments of autochthonous, terrestrial C_3 plant material and allochthonous, tidal-derived material is just a few per mil, slight differences in $\delta^{13}C$ values between surface sediment and vegetation as a result of the presence of bacteria

and algae may hamper efforts to establish a relationship between these two variables (surface sediment and vegetation). This has obvious implications for the subsequent integrity of $\delta^{13}C$ values in sediment deposits as indicators of organic carbon source, and ultimately as a coastal palaeoenvironmental reconstruction tool. Measurement of compound specific $\delta^{13}C$ in sediments may overcome this problem (e.g. Bull *et al.*, 1999). However, such an approach is unsuitable for multi-source studies such as this one. Instead, the ratio of organic carbon to total nitrogen (C/N) in the bulk sediment sample, which is measured alongside $\delta^{13}C$ analysis, is used. This provides an indication of the relative contributions of organic matter from contrasting sources, because bacteria and algae have C/N ratios that are distinct from terrestrial vegetation (Section 2.3.5).

2.3.4 Allochthonous saltmarsh organic carbon sources

2.3.4.1 Particulate organic carbon

Estuarine saltmarshes receive suspended particulate organic matter (POM) from estuarine, riverine and marine sources. POM is a broad term that encompasses the spectrum of plankton, in particular phytoplankton (e.g. diatoms, dinoflagellates, green algae, euglenoides), and to a lesser extent, zooplankton. This is mixed with terrestrial organic matter of both natural (e.g. plant detritus) and anthropogenic origin (e.g. sewage). Over 90% of the organic matter transported in streams is in particulate form (Tyson, 1995). The organic carbon contained in POM, or particulate organic carbon (POC), exhibit distinct $\delta^{13}C$ values, which are related to POM content and provenance (Figure 2.3). Typically, suspended POC $\delta^{13}C$ ($\delta^{13}C_{POC}$) values increase systematically towards the mouth of an estuary, resulting in two distinct riverine and marine 'end-member' values. For example, in the Schelde Estuary on the Netherlands-Belgium border, upper and lower estuarine $\delta^{13}C_{POC}$ values differ significantly (–28.9‰ and –20.1‰, respectively) (Middelburg & Nieuwenhuize, 1998). Similar values have been observed in the Great Ouse Estuary, UK (e.g. Fichez *et al.*, 1993) as well as other estuaries at various locations around the world, for example, in America (Sherr, 1982) and in Jamaica (Andrews *et al.*, 1998).

In general, riverine $\delta^{13}C_{POC}$ values are a reflection of the relative contributions from freshwater phytoplankton and terrestrial organic matter. Terrestrial organic matter entering an estuary usually has $\delta^{13}C_{POC}$ values of between –25.0‰ and –33.0‰ (e.g. Salomons & Mook, 1981; Barth *et al.*, 1998; Middelburg & Nieuwenhuize, 1998),

reflecting the prevalence of C_3 vegetation in the catchments studied. Sewage and industrial waste are the two dominant sources of anthropogenic organic carbon. The $\delta^{13}C$ values of industrial waste will vary according to the type of industry and will, therefore, be site specific (e.g. Rashid & Reinson, 1979; Andrews *et al.*, 1998). The study by Andrews *et al.* (1998) is one of few that incorporate sewage as an organic carbon source and they obtained $\delta^{13}C$ values for sewage of between –23.1‰ and –28.5‰.

Marine $\delta^{13}C_{POC}$ values will mainly be determined by the $\delta^{13}C$ value of phytoplankton, of which marine POC is mostly composed (Yamaguchi *et al.*, 2003). Indeed, the systematic shift in suspended $\delta^{13}C_{POC}$ values observed along the axis of many estuaries is principally a result of the changing relative abundance of riverine and marine phytoplankton, as marine $\delta^{13}C_{POC}$ values are often several per mil greater than riverine $\delta^{13}C_{POC}$: North Sea $\delta^{13}C_{POC}$ values are around –18.0‰ for example (Middelburg & Nieuwenhuize, 1998).

The degree of variation in $\delta^{13}C_{POC}$ between riverine (e.g. –26.0‰, Shultz & Calder, 1976) and marine waters (e.g.–20.4‰, Sherr, 1982) is mainly due to the different inorganic carbon source utilised by phytoplankton in these contrasting aquatic environments. Phytoplankton utilises dissolved inorganic carbon (DIC), of which two species (CO_2 and HCO_3^-) are important. These two species vary in abundance in accordance with water pH. For example, at pH 5.5, 80% of the DIC is as CO_2, whereas at pH 8.5, CO_2 comprises less than 1% of the DIC pool (Keeley & Sandquist, 1992). Therefore, CO_2 is primarily utilised by riverine phytoplankton, whilst the inorganic carbon source for marine phytoplankton is predominantly HCO_3^-. River water that is in equilibrium with atmospheric CO_2 will have a DIC $\delta^{13}C$ ($\delta^{13}C_{DIC}$) value of approximately –8.0‰, resulting in riverine phytoplankton with similar $\delta^{13}C$ values to terrestrial C_3 vegetation, as the C_3 photosynthetic pathway is prevalent also in phytoplankton (Schidlowski, 1987). In contrast, the $\delta^{13}C$ value of dissolved HCO_3^- is approximately 0‰ (Meyers, 1994), resulting in marine phytoplankton $\delta^{13}C$ values that are several per mil higher.

Riverine, estuarine and marine $\delta^{13}C_{DIC}$ is subject to large variations, with obvious implications for phytoplankton $\delta^{13}C$ values. For example, even fast flowing rivers may

not achieve isotopic equilibrium with atmospheric CO_2 (which would result in $\delta^{13}C_{DIC}$ values of approximately −8.0‰ (Keeling & Sandquist, 1992)). Further, in estuarine and nearshore environments, oxidation of organic matter may result in lower $\delta^{13}C_{DIC}$ values, whilst photosynthetic activity will lead to higher $\delta^{13}C_{DIC}$ values (Tan, 1989). In addition, variations in marine phytoplankton $\delta^{13}C$ also occur. For example, Wong & Sackett (1978) and Gearing *et al.* (1984) have shown that $\delta^{13}C$ values vary between phytoplankton classes, and also vary with temperature (e.g. Sackett *et al.*, 1965) and CO_2 concentration (Hinga *et al.*, 1994).

2.3.4.2 Dissolved organic carbon

Most of the carbon in the ocean occurs in the form of dissolved organic matter (DOM) (Hedges *et al.*, 1997). Further, in rivers and estuaries, on average, 60% of carbon transported is in the dissolved phase, whilst 40% is in the particulate phase (Raymond & Bauer, 2001). The axial estuary trend in $\delta^{13}C$ of dissolved organic carbon ($\delta^{13}C_{DOC}$) is extremely similar to that of $\delta^{13}C_{POC}$ (Figure 2.3), as dissolved organic carbon is principally derived from phytoplankton in the marine environment and a mixture of terrigenous organic matter and freshwater phytoplankton in the riverine environment (Rashid, 1985). For example, in a study of $\delta^{13}C_{DOC}$ in several estuaries in the U.S., Peterson *et al.* (1994) found that the marine end-members had $\delta^{13}C_{DOC}$ values of between –22.0‰ and –25.0‰ whereas the freshwater end-members had $\delta^{13}C_{DOC}$ values of between –26.0‰ and –28.0‰. This pattern of $\delta^{13}C_{DOC}$ in estuarine waters, reflecting riverine and marine source material, has been observed by other workers, for example, Van Heemst *et al.* (2000), Goñi *et al.* (2003) and Otero *et al.* (2003). Further, Otero *et al.* (2003) observed a seasonal shift in estuarine $\delta^{13}C_{DOC}$ in two estuaries of south eastern USA. They found estuarine waters enriched in ^{13}C by 2.0‰ from July to October.

Humic substances constitute a significant proportion of DOC. Otero *et al.* (2003) found that humic substances accounted for 50% to 80% of riverine DOC and 5% to 15% of marine DOC in the Altamaha and Satilla Estuaries in south eastern USA. Although the formation of humic and fulvic acids remains unresolved (Hatcher & Spiker, 1988; Hedges 1988), the provenance of humic substances may be determined by their $\delta^{13}C$ values. Terrigenous humic substances will retain $\delta^{13}C$ values in the C_3 plant range for C_3 plant dominated catchments, whilst the $\delta^{13}C$ value of marine humic substances will reflect their phytoplankton precursors (Harvey & Boran, 1985).

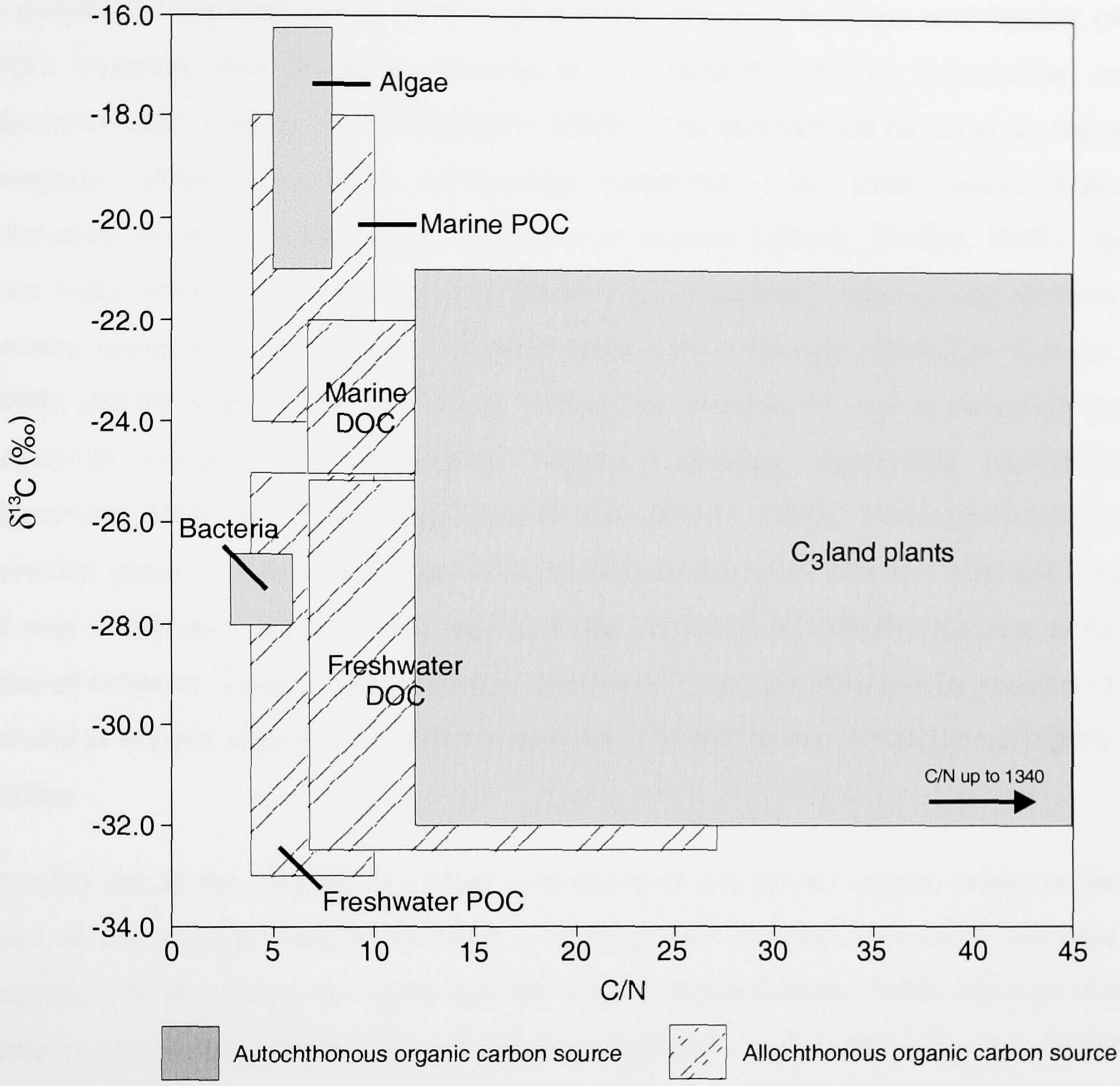

Figure 2.3. $\delta^{13}C$ and C/N ratios of autochthonous (C_3 vascular vegetation, algae and bacteria) and allochthonous (marine and freshwater POC and DOC) organic matter sources in saltmarsh sediments. Data is compiled from various sources (Haines, 1976; Deines, 1980 (and references therein); Salomons & Mook, 1981; Sherr, 1982; Peterson *et al.*, 1994; Tyson, 1995 (and references therein); Twiddy, 1996; Barth *et al.*, 1998; Middelburg & Nieuwenhuize, 1998; Raymond & Bauer, 2001 (and references therein); Cloern *et al.*, 2002; Goñi *et al.*, 2003).

2.3.4.3 Organo-clay complexes

The systematic increase in $\delta^{13}C_{DOC}$ with proximity to the ocean is indicative of conservative DOC mixing and this is related to the relatively short residence times (days to months) of estuarine waters (Raymond & Bauer, 2001). The humic acid fraction of DOC, however, may be partly removed in the estuarine zone by flocculation, or adsorption onto inorganic colloids (Mayer, 1985). Clay minerals are the most abundant inorganic colloids in estuarine environments (Andrews *et al.*, 1996), whilst humic substances represent a significant component of organic colloids (Rashid, 1985). In river water, which is a weak electrolyte, the net surface negative charge of clay minerals ensures suspension. In contrast, estuarine waters are a stronger electrolyte (Leeder, 1999), and the higher concentrations of cations (for example, N^+) act to neutralise the negatively charged clay and organic colloids, allowing organo-clay complexes (Stevenson, 1985) and organic aggregates to form (Mayer, 1985). Flocculation of clay particles, organic particles and organo-clay complexes can occur in water with salinities of only a few parts per thousand, leading to the formation of turbidity maxima at the head of estuaries (Leeder, 1999). Humic substances, either adsorbed to clay particles or present as organic aggregates, therefore represent a further source of terrigenous organic carbon.

Possibly due to the removal of a large component of terrigenous organic matter at the head of the estuary, there is evidence to suggest that colloidal material in estuaries appears to be dominated by marine-derived organic matter (Mayer, 1985), although this remains contentious. Other research has demonstrated a significant terrigenous DOM component in the marine environment (Lee & Wakeham, 1992). Apart from marine and riverine sources of DOM, *in situ* estuary DOM may be important in some estuaries. Estuarine DOM may originate from excretion by estuarine dwelling organisms, autolysis of dead organisms and microbial decomposers (Van Heemst *et al.*, 2000).

2.3.4.4 Estuarine surface sediment deposits

Bulk surface sediment $\delta^{13}C$ values along the axis of most estuaries mirror the systematic shift in suspended $\delta^{13}C_{POC}$ (Section 2.3.4.1). In a comprehensive study, Hunt (1970) measured the $\delta^{13}C$ values of surface sediment deposits in the rivers and estuaries along the entire Atlantic Coast of the United States. These samples were supplemented by measurement of near-shore and continental shelf surface sediments. He found that in most of the 32 rivers studied, river mouth sediments exhibited $\delta^{13}C$ values of around

–20.0‰, whilst sediments several kilometres upstream had $\delta^{13}C$ values of around –26.0‰. This progressive increase of $\delta^{13}C$ values with proximity to the coast was observed in all of the rivers studied, with the position and $\delta^{13}C$ values of the two 'end-members' in several rivers deviating as a function of geomorphology and hydrology. Short distances offshore, surface sediment $\delta^{13}C$ values of between –18.0‰ to –22.0‰ were observed, values typical of deep-sea sediments (e.g. Sackett, 1964). Therefore, along the US Atlantic Coast, terrestrial organic matter is only dominant in sediments up to the river mouth, beyond which marine phytoplankton become the dominant source of organic matter in sediments (Hunt, 1970).

The difference in $\delta^{13}C$ values between riverine and marine sediments is well established. For example, the range in surface sediment $\delta^{13}C$ values of rivers flowing into the Gulf of Mexico (–28.3‰ to –24.3‰) are significantly more negative than actual Gulf of Mexico surface sediments (–19.0‰ to –21.0‰) (Sackett & Thompson, 1963). Further, in two separate studies in North and South Carolina, surface sediment $\delta^{13}C$ values were shown to increase from –28.0‰ to –23.0‰ between the rivers and the mouths of the estuaries respectively (Brinson & Matson, 1983; Goñi *et al.*, 2003). Similar trends in surface sediment $\delta^{13}C$ values have also been observed in European estuaries. For example, upper and lower estuarine surface sediments in the Schelde Estuary at the Netherlands-Belgium border have $\delta^{13}C$ values of –26.3‰ and –23.5‰ respectively (Middelburg & Nieuwenhuize, 1998). Further, Salomons & Mook (1981) obtained a range in $\delta^{13}C$ values of between –28.0‰ and –25.0‰ for surface sediments from the Rhine, Meuse, Ems and Scheldt rivers, which were significantly different from the range in $\delta^{13}C$ values measured in surface sediments off the Belgium, Germany and Dutch coastlines (–20.1‰ to –25.3‰). Another example is the Tay Estuary, Scotland, where lower estuarine surface sediment $\delta^{13}C$ values were approximately 3.0‰ greater than upper estuarine surface sediment $\delta^{13}C$ values (Thornton & McManus, 1994).

It is apparent from the above discussion that the end-member $\delta^{13}C$ values in estuarine environments are subject to variation and, principally, this is a function of hydrology. For example, relatively uniform surface sediment $\delta^{13}C$ values of between –24.4‰ and –23.6‰ were observed throughout the Forth Estuary, Scotland (Graham *et al.*, 2001) reflecting efficient sediment mixing in this estuary. In addition, Shultz & Calder (1976) demonstrated that the reach of terrigenous organic carbon from the river mouth,

manifest in near-shore sediments in the form of lower $\delta^{13}C$ values, is correlated with the volume of river discharge.

In the present study, therefore, it is necessary to obtain River Mersey, Mersey Estuary and Liverpool Bay surface and suspended sediment $\delta^{13}C$ values, in order to determine the dominant source and $\delta^{13}C$ composition of allochthonous organic carbon on Ince Banks saltmarsh. With respect to the present study, the two end-member $\delta^{13}C$ values of Ince Banks is autochthonous terrestrial organic carbon derived principally from saltmarsh vegetation, and allochthonous POC introduced by the tide. Modern saltmarsh bulk sediment $\delta^{13}C$ analysis will differentiate between autochthonous organic carbon derived from vegetation ($\delta^{13}C$ values of approximately –27.0‰) and allochthonous organic carbon derived from marine POC ($\delta^{13}C$ values of approximately –20.0‰). $\delta^{13}C$ analysis, however, may not distinguish between autochthonous terrestrial plant carbon and allochthonous riverine POC (a mixture mostly of freshwater phytoplankton and terrigenous plant detritus), all of which will exhibit $\delta^{13}C$ values typical of C_3 plants. Use of $\delta^{13}C$ analysis alone is, therefore, inappropriate for multi-source organic carbon studies in which several sources have similar $\delta^{13}C$ values (Fry & Sherr, 1989; Cloern *et al.*, 2002), and must be used in combination with other techniques.

2.3.5. C/N ratios

The weight ratio of organic carbon to total nitrogen (C/N) provides a second way of discriminating the source of organic matter. Aquatic vegetation (including both marine and freshwater phytoplankton), bacteria and fungi, predominantly have C/N ratios of 4.0 to 10.0, whereas terrestrial plants generally have C/N ratios greater than 20.0 (Meyers, 1994) (Figure 2.3). Organic matter with C/N ratios of between 10.0 and 20.0 may represent a mixture of aquatic and terrestrial plant material, although some marginal macrophytes have intermediate ratios. The distinction arises because terrestrial plants are lignin and cellulose-rich, whereas aquatic plants are protein-rich, which gives them relatively high nitrogen levels (Meyers, 1994). Used in combination, C/N ratios and $\delta^{13}C$ analyses are effective indicators of organic carbon source in complex, multi-source, environments such as those found at the coast.

2.3.6 Organic matter degradation: implications for $\delta^{13}C$ and C/N ratios

2.3.6.1 Diagenesis

Since the work of Park & Epstein (1961), who were the first to demonstrate that lipids were up to 8.0‰ enriched in ^{12}C relative to the whole plant, several other plant compounds have been found to have different $\delta^{13}C$ values. For example, cellulose and hemi-cellulose, which make up between 57% and 77% of herbaceous and woody plant tissues respectively, are enriched in ^{13}C by 1.0‰ to 2.0‰ relative to the whole plant (Benner *et al.*, 1987). Lignin, which is only found in vascular plants, accounts for between 17% to 31% and 4% to 9% of woody and herbaceous plant tissues respectively, and is depleted in ^{13}C by 2.0‰ to 6.0‰ relative to the whole plant, and 4.0‰ to 7.0‰ relative to cellulose (Benner *et al.*, 1987).

Lignified macrophyte detritus is the single most refractory particulate organic component in sediments (Tyson, 1995). Incubation experiments and litter bag studies have demonstrated the preferential decay of hemi-cellulose and cellulose (e.g. Maccubbin & Hodson, 1980; Fogel *et al.*, 1989; Melillo *et al.*, 1989), with bulk $\delta^{13}C$ values of the whole plant approaching those of lignin over time (Ember *et al.*, 1987; Benner *et al.*, 1987; 1991). Similar results have been reported for degrading wood, where changes in $\delta^{13}C$ values of up to 2.0‰ have been measured and attributed to the relatively increasing residual lignin (Spiker & Hatcher, 1987). In addition, C/N ratios may progressively lower as diagenesis progresses, resulting from the preferential loss of carbon rich, labile material such as lipids (Meyers & Teranes, 2001).

Since up to 90% of plant material is composed of hemi-cellulose, cellulose and lignin, changes in the relative abundance of these plant compounds during decomposition in sediments will have important implications for bulk sediment $\delta^{13}C$ analysis. In several studies, for example, the selective preservation of lignin in surface saltmarsh sediments was thought to be responsible for the slightly lower $\delta^{13}C$ values of bulk sediments compared with the overlying vegetation (Ember *et al.*, 1987; Chmura & Aharon, 1995; Malamud-Roam & Ingram, 2001).

2.3.6.2 POC degradation

Estuarine POM is largely composed of a mixture of riverine and marine phytoplankton and terrigenous organic detritus (Section 2.3.4.1). Phytoplankton is susceptible to considerable degradation in the water column as easily degraded proteins and

carbohydrates account for between 63% and 93% of its biomass (Tyson, 1995). The lipid content of phytoplankton, which is more refractory, accounts for between 2% and 10% (Romankevich, 1984). The $\delta^{13}C$ composition of phytoplankton (e.g. $\delta^{13}C$ of −21.0‰) will change as degradation proceeds in the water column. This reflects the preferential degradation of the isotopically more positive carbohydrates and proteins (−20.0‰ and −18.0‰ respectively (Meyers, 1997)) and the subsequent relative increase in the concentration of the isotopically more negative lipid fraction (−23.0‰ to −26.0‰ (Deines, 1980)). However, changes in $\delta^{13}C$ values as a result of selective preservation of different compounds are usually small (2.0‰ or less (Meyers, 1997)). As a result of phytoplankton degradation in the water column, little further alteration of $\delta^{13}C$ values would be expected to occur in surface sediments. Evidence of the degradation of plankton material in estuarine waters prior to deposition is illustrated by comparison of atomic C/N ratios between the two phases (Cifuentes, 1991). Suspended POC in the Delaware Estuary, south eastern USA, exhibited C/N ratios of 6.4, compared with 11.1 for surficial sediment deposits. This is consistent with the breakdown of nitrogen-rich compounds of algal material in the water column prior to deposition.

2.3.7 Summary

Sediment delivery in estuarine saltmarshes may be partitioned into autochthonous material, namely *in situ* vegetation together with microbes, and allochthonous material of tidal origin. These contrasting sources may be distinguished using a combination of $\delta^{13}C$ and C/N ratio analysis (Figure 2.3). Once the relationship between the $\delta^{13}C$ and C/N ratio values of surface saltmarsh sediments and their sources have been established, measurement of these parameters in Holocene coastal sediment deposits may prove useful in determining past coastal changes in sediment delivery, which will vary as a function of RSL change, for example. Previous isotope-based coastal palaeoenvironmental research has largely been restricted to isolation basin and lagoon sediments (Müller & Mathesius, 1999; Müller & Voss, 1999; Westman & Hedenström, 2002), or otherwise to estuaries with a mixture of C_3 and C_4 vegetated catchments. This research is the first to specifically assess the accuracy of $\delta^{13}C$ and C/N as coastal palaeoenvironmental and RSL indicators in estuarine sediments within a C_3 vegetated catchment. In addition, this research will address the potential complication of the selective preservation of organic compounds during decomposition, which is inherent in

applying these techniques to elucidate palaeoenvironments, and which may result in a change in bulk sediment $\delta^{13}C$ values over time.

Chapter 3

Global and Regional Holocene Sea-Level Changes

3.1 Global sea-level changes since the Last Glacial Maximum

A significant outcome of IGCP Project 61 was the realisation that there can be no globally valid 'eustatic' sea-level curve (*cf.* Fairbridge, 1961). A compilation of published 'eustatic' sea-level curves by Mörner (1971) generated from different areas of the world, including the Netherlands (Jelgersma, 1961), Micronesia (Bloom, 1969), Bermuda (Neumann, 1969) and Florida (Scholl *et al.*, 1969), revealed that sea-level changes differed both in amplitude and timing. Mörner, (1976) argued that the lack of correspondence between age-altitude graphs of 'eustatic' sea-level curves is due to the spatially unevenness of the real ocean surface - the equipotential surface of the geoid set up by the opposing forces of gravity and the centrifugal force of the Earth's rotation - over geological timescales. The waxing and waning of the ice sheets during the Quaternary, and the resulting deformation of the Earth's surface and interiors, would have caused significant spatial and temporal variation in the geoid, as ocean water was continually redistributed in order to maintain a constant gravitational potential. Clark (1976) showed that changes in the geoid could have been of a similar magnitude as the 'glacio-eustatic' rise in sea-level. Indeed, the altimeter data from the 1978 NASA SEASAT mission showed that the 'topography' of the geoid ranges in altitude (in relation to the best-fitting ellipsoid) from +74m over Papua-New Guinea and Irian Jaya to –104m in southern India (Marsh & Martin, 1982).

Geoidal highs and lows are associated with positive and negative gravity anomalies (Lerch *et al.*, 1994), with positive gravity anomalies caused by the presence of dense Earth materials and negative gravity anomalies caused by the presence of less dense Earth materials. For example, as a result of a deficiency in mass caused by isostatic uplift, a negative gravity anomaly is currently found over the former glaciated areas of northern Canada and Fennoscandia. Not until the crust, mantle and asthenosphere return to their pre-glacial shape and density upon completion of uplift, will gravitational equilibrium be attained. In the meantime, the 100m of uplift left to occur before this equilibrium state is reached will affect the regional 'topography' of the geoid (Cazenave

et al., 2000). Consequently, the concept of eustasy according to Suess, (1906) – the global and simultaneously recorded vertical displacement of the sea-surface – is now redundant. 'Eustasy' is now defined as 'ocean level changes', in which no causal factor is implied (Mörner, 1976). A regional (north west European) eustatic sea-level curve has been presented by Mörner (1984), based on investigations along the Swedish west coast (Mörner, 1969) and is therefore valid for the UK (e.g. Shennan, 1989). Mörner (1980) argued that this area is small enough to have acted uniformly to changes in the geoid.

Late Quaternary RSL records represent an integrated signal of ocean water volume, the redistribution of water within the ocean basins, and vertical movements of the continental and oceanic crust. Therefore, the RSL record will differ significantly between regions that were once far removed from (far-field), peripheral to (intermediate-field), or located within (near-field) the former margins of the large Late Devensian ice sheets (Clark *et al.*, 1978). Glacio-isostatic effects dominate the near-field RSL records, which show significant lowering throughout the Late Quaternary (e.g. Greenland (Long *et al.*, 2003)). In intermediate-field regions, glacio-isostatic processes are reduced, but remain dominant. The Late Quaternary RSL records from these regions record a continued RSL rise (e.g. The Fenland; Shennan, 1986), which, in part, is caused by subsidence associated with the collapse of the proglacial forebulge, where displaced mantle material migrates back towards the formerly glaciated areas. Far-field regions are dominated by hydro-isostatic processes and contain a negligible glacio-isostatic signal. Consequently, once corrected for hydro-isostatic effects associated with the increasing meltwater load, and for gravitational changes associated with the redistribution of ocean waters (Peltier, 1998), far-field RSL records should be representative of globally averaged changes in eustatic sea-level (Lambeck & Chappell, 2001), which, in turn, will provide constraints on global ice volume estimates (Milne *et al.*, 2002) during the Last Glacial Maximum (LGM), 15,900 ^{14}C yr BP to 19,400 ^{14}C yr BP (Mix *et al.*, 2001).

Several RSL records from far-field sites, for example, Barbados (Fairbanks, 1989; Bard *et al.*, 1990a, 1990b), Tahiti (Bard *et al.*, 1996), Huon Peninsula (Chappell *et al.*, 1996), Sunda Shelf (Hanebuth *et al.*, 2000), and the Bonaparte Gulf (Yokoyama *et al.*, 2000), indicate that RSL was between 120m and 130m below present levels during the LGM.

An independent indicator of LGM sea-levels is contained in the deep-sea oxygen isotope record, which estimates similar values (Shackleton, 2000). Small differences do exist, however, between these far-field RSL records, although Peltier (2002) argues that these differences are based on incorrect assumptions regarding tectonic uplift rates (e.g. Chappell *et al.*, 1996), the indicative range of the RSL indicators (e.g. Chappell *et al.*, 1996; Bard *et al.*, 1996), as well as from adjustments of the observed data based on incorrect geophysical models (e.g. Yokoyama *et al.*, 2000). Lambeck *et al.* (2002) combined these far-field RSL records in order to try to comprehend the nature of Late Quaternary eustatic sea-level change. They concluded that sea-level rise was initially slow (approximately 3.3 mm/yr) between 15,900 ^{14}C yr BP to 13,300 ^{14}C yr BP, with rapid sea-level rise (approximately 16.6 mm/yr) occurring between 13,300 ^{14}C yr BP and 10,450 ^{14}C yr BP. Little change in sea-level is evident between 10,450 ^{14}C yr BP and 10,050 ^{14}C yr BP, corresponding to the Younger Dryas, but then sea-levels rose rapidly (approximately 15.2 mm/yr) until 7,725 ^{14}C yr BP. Ocean volumes were close to their present levels by 6,100 ^{14}C yr BP, with current levels being reached some time later.

Controversy surrounds the nature and timing of Late Holocene eustatic sea-level change, with Peltier (2002), for example, disputing any significant eustatic sea-level rise in the Late Holocene, contrary to the conclusions reached by Lambeck *et al.* (2002) above. A continued Late Holocene sea-level rise is clearly apparent in the eustatic model of Fleming *et al.* (1998), which is constructed from a combination of far-field and intermediate-field RSL records, and shows a continued increase in ocean volumes of between 3m to 5m from 6,100 ^{14}C yr BP to the present day. Near-field observational evidence also supports Late Holocene RSL rise (Shennan *et al.*, 2000a). However, Peltier (2002) argues that any significant rise in sea-level in the Late Holocene, such as that advocated by Fleming *et al*, 1998; Shennan *et al.*, 2000a and Lambeck *et al.*, 2002, is incompatible with the observed geomorphological evidence of a Mid Holocene RSL highstand and subsequent Late Holocene RSL fall in far-field regions (e.g. Nunn & Peltier, 2001), and that deglaciation was essentially complete by approximately 3,700 ^{14}C yr BP (Nunn & Peltier, 2001; Peltier, 2002). Clearly, more RSL reconstructions are needed in order to constrain the volume of glacial meltwater entering the oceans from the Mid Holocene and to reconcile the current disagreement concerning the nature of Mid and Late Holocene glacio-eustatic sea-level change.

3.2 General variability of Late Quaternary RSL change in the UK

Peltier (1998) believes Great Britain to be the most 'exotic' geographical region on Earth in terms of global isostatic adjustment and, consequently, of RSL change. This is attributed to the interaction of post glacial eustatic sea-level rise and isostatic recovery associated with both proglacial (Fennoscandia) forebulge collapse and the disintegration of the British and Irish Ice Sheet, which covered northern Britain at its maximum extent at around 18,500 ^{14}C yr BP (Bowen *et al.*, 2002). The interaction of eustatic and isostatic processes has produced a complex stratigraphy of intercalated peat, silt and clay deposits around the UK coastline. These deposits form the basis of RSL curves, which differ markedly between geographical regions as a function of distance from the center of the local ice sheet. For example, RSL records from Scotland are highly non-monotonic, showing a fall in RSL between 12,000 ^{14}C yr BP and 10,000 ^{14}C yr BP and after 5,000 ^{14}C yr BP, associated with glacio-isostatic uplift, interrupted by a period of RSL rise associated with the faster rate of eustatic sea-level rise (Shennan *et al.*, 1999). This is in contrast to the monotonic RSL records from southern England, which show continued submergence associated with eustatic sea-level rise and isostatic subsidence related to the collapse of the Fennoscandian forebulge and the disintegration of the British and Irish Ice Sheet to the north (e.g. Long *et al.*, 1996).

3.3 Late Quaternary RSL change in north west England

3.3.1 Late Devensian RSL change

Eyles & McCabe (1989) have identified what they believe to be raised marine deltas around the margin of the Irish Sea, the highest of which is in Wasdale, Cumbria, at 152m OD. They believe that around the LGM, the Irish Sea basin was isostatically depressed to such an extent that the ice margin came into contact with the eustatically lowered sea-level, causing rapid retreat. Eyles & McCabe (1989) argue that the existence of these raised marine deltas provides direct evidence of Late Devensian RSLs of up to 152m OD. The interpretation of these features as marine deltas is widely disputed (e.g. Huddart, 1993; Huddart & Clark, 1993; McCarroll, 2001). Indeed, the so-called glaciomarine model of Irish Sea deglaciation has been severely criticised (e.g. McCarroll & Harris, 1992; Austin & McCarroll, 1992; Huddart, 1994; Thomas *et al.*, 1998; McCarroll, 2001). In particular, glacio-hydroisostatic models of sea-level change predict that RSL did not reach above present levels at any time since the deglaciation of

the Irish Sea basin and that ice thickness over central and southern Ireland would have to reach 2000m to be compatible with the glaciomarine hypothesis of Eyles & McCabe (1989) (Lambeck & Purcell, 2001), which is over double the ice thickness estimates of 600m to 700m based on geomorphological evidence (Watts, 1977).

The change in altitude of RSL from the LGM to the present day has been predicted using glacial isostatic adjustment models (e.g. Peltier *et al.*, 2002; Shennan *et al.*, 2002). The absence of unequivocal observational evidence prevents the verification of Late Devensian RSL model predictions in north west England. Nevertheless, the good correspondence between model predictions and observational evidence extending to approximately 13,300 ^{14}C yr BP at a site in north west Scotland (Shennan *et al.*, 1999; Peltier *et al.*, 2002) indicates that the glacial isostatic adjustment model of Peltier *et al.* (2002) may provide a reasonable approximation of Late Devensian RSL change in north west England.

Figure 3.1 shows predicted RSL since the LGM for the area surrounding the Mersey Estuary using the most recent and refined glacial isostatic adjustment model (Peltier *et al.*, 2002). Empirical RSL data, which becomes available in the Holocene, is also shown for comparison with the model results (Peltier *et al.*, 2002). The model predicts a RSL fall of over 20m between approximately 15,500 ^{14}C yr BP to 12,450 ^{14}C yr BP (Figure 3.1), a result of isostatic uplift rates outstripping regional eustatic sea-level rise rates. A switch to a RSL rise occurs around 12,450 ^{14}C yr BP, and this inflection is observed in all RSL predictions for coastal sites in the UK (Shennan *et al.*, 2002) and represents the acceleration of global sea-level rise rates concomitant with the disintegration of the continental ice sheets (e.g. Bard *et al.*, 1996). The model shows a continuation of RSL rise, as global sea-level rise rates continue to outstrip isostatic uplift rates whereupon a Mid Holocene highstand is reached, the occurrence of which would produce raised beaches up to 3m above OD at around 3,700 ^{14}C yr BP (Peltier *et al.*, 2002; Shennan *et al.*, 2002). No empirical evidence exists to support a higher Mid Holocene RSL, however. This highlights the necessity of obtaining observational data to refine glacial isostatic adjustment models.

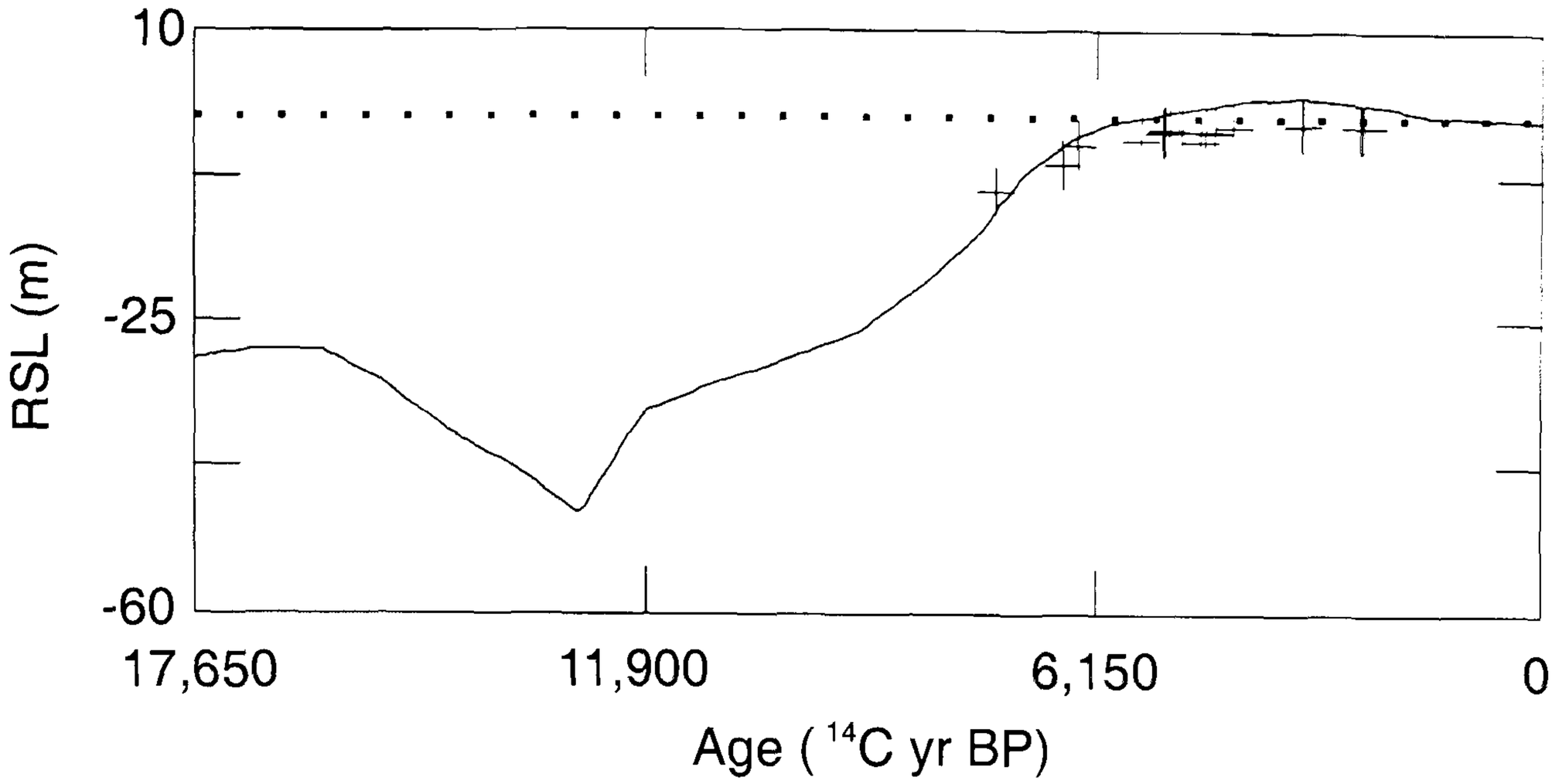

Figure 3.1. Predicted (solid line) and observed (+) RSL change for the area surrounding the Mersey Estuary. The dotted line denotes contemporary sea-level (from Peltier *et al.*, 2002).

3.3.2 Empirical evidence for north west England Holocene RSL change

The intercalated, unconsolidated, peats, silts and clays of the coastal strip between the River Ribble and the River Mersey, and along the north Wirral coastline, have been the focus of scientific enquiry for some time (e.g. Picton, 1849; Binney & Talbot, 1868 Reade, 1871, 1872). Early observations discussed the alternating peat and silty clay deposits in terms of land-level changes (e.g. Reade, 1871), although the possibility of barrier formation and collapse under a static sea-level was also considered (Binney & Talbot, 1868). Curiously, the phenomenon of absolute changes in sea-level was not considered, even though the idea of changes in sea-level as a consequence of the glacial theory had already been presented (MacLaren, 1842).

More recently, detailed litho-, bio- and chronostratigraphical investigations, principally by Tooley (e.g. 1978a), has enabled a detailed environmental reconstruction of these coastal deposits, revealing how the principal driving mechanisms of regional eustatic sea-level change and isostatic recovery have shaped the evolution of the coastline. Holocene sediment deposits are particularly well preserved in the lowlands fringing the Ribble Estuary, the Sefton coast and the north Wirral coast. These areas have been comprehensively investigated, the details of which are summarised in the following sections.

3.3.2.1 Ribble Estuary

Twelve positive tendencies and twelve negative tendencies of RSL have been identified in the Holocene sediment deposits along the coastline of north west England (Tooley, 1982b). These tendencies are show in Figure 3.2, along with tendencies inferred from other important UK sites to the north and south of north west England. Evidence of almost all of the RSL tendencies recorded in north west England have been derived from four sites flanking the Ribble Estuary (Figure 1.1): Nancy's Bay; Star Hills; Lytham Common and Lytham Hall Park (Tooley, 1978a), all of which lie within the former township of Lytham. This area has been used as the type-site of RSL change in north west England, forming the basis for inter-regional correlation (e.g. Tooley, 1978a), and is therefore one of the most important areas for Holocene RSL research (Huddart, 2002a).

An increase in marine conditions is recorded at Lytham on ten occasions (Tooley, 1978a), as indicated by changes in the lithology and in the microfossil assemblages of the sediment deposits in this area. Tooley (1978a) assigned the terms Lytham I to Lytham X to these 'transgressions', although this scheme has since been superseded (Tooley, 1982b). The onset and removal of the episodes of increased marine conditions, as recorded at Lytham, is summarised in Table 3.1.

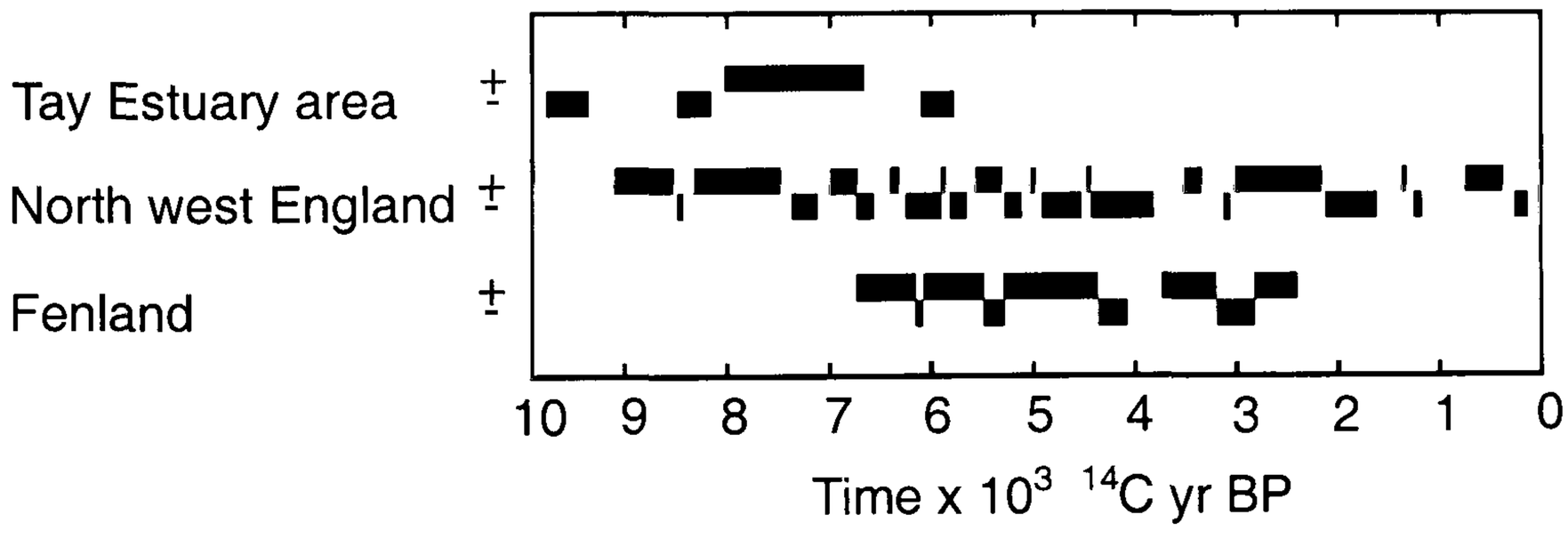

Figure 3.2. North west England Holocene RSL tendencies. Holocene RSL tendencies inferred from the Tay Estuary and the Fenland are also shown for comparison (from Shennan *et al.*, 1983).

Table 3.1. Chronology of transgressive and regressive overlaps recorded at Lytham (Tooley, 1978a; 1982b).

Chronology of transgressive overlaps (dates are in ^{14}C yrs BP)	Chronology of regressive overlaps (dates are in ^{14}C yrs BP)
Onset not recorded	8,575 ± 105
8,390 ± 105	7,800*
7,605 ± 85	7,200*
6,885 ± 80	Removal not dated
5,950 ± 85	5775 ± 85
5,570*	4,897†
3,700*	3,150 ± 150
3,090 ± 135	2,270 ± 65
Onset not dated	1,370 ± 85
830 to 805‡	

*Estimated age based on stratigraphical, pollen and altitudinal data

†Mean age based on several variants

‡Indirect evidence (date from dune slack peat)

3.3.2.2 Sefton coast

Holocene sediment accumulations along the Sefton Coast also contain a detailed record of RSL change. Downholland Moss is the classic site of Holocene RSL change in south west Lancashire (Huddart, 2002b), with three transgressive and regressive overlaps preserved in the deposits (Tooley, 1974; 1978a; 1978b; 1985; Huddart, 1992). The transgressive overlap associated with the onset of the earliest marine conditions in the area is recorded at Long Lane, Formby, at an altitude of –10.21m OD. This overlap has not been radiocarbon dated, but Tooley (1978a) estimated an age of around 8,000 ^{14}C yr BP based on between-site comparison of the altitude of this overlap with other dated sites to the north. Marine conditions culminated between 6,980 ± 55 ^{14}C yr BP and 6,760 ± 95 ^{14}C yr BP, with the associated marine deposits reaching approximately 8km inland of the present coastline. Tooley (1978a) states that the beginning of this marine episode may be correlated with the increase in marine conditions experienced at Lytham between 8,390 ± 105 ^{14}C yr BP and 7,800 ^{14}C yr BP (Table 3.1). There is no apparent evidence in south west Lancashire of the earliest marine episode experienced at Lytham,

which ended at 8,575 ± 105 ^{14}C yr BP. Two further transgressive overlaps, testifying to an increase in marine conditions, are recorded in the sediments of Downholland Moss. The ages of the two transgressive overlaps is equivocal due to radiocarbon dating errors, but the first of the two marine episodes culminated at 6,050 ± 65 ^{14}C yr BP, whilst the second ended at 5,615 ± 45 ^{14}C yr BP. An increase in marine conditions was also recorded at Lytham from 6,885 ± 80 ^{14}C yr BP and between 5,950 ± 85 ^{14}C yr BP and 5,775 ± 85 ^{14}C yr BP, and Tooley (1978a) concludes that these events may be related.

Sediment deposits in the east of Downholland Moss are capped by blown sand from 4,090 ± 170 ^{14}C yr BP (Tooley, 1978a), indicating the existence of sand dunes to the west. Tooley (1978a) presented evidence of two further episodes of increased marine conditions in this area, based on data from the Alt Mouth and from the Formby foreshore. Again, chronological control for the initial marine episode is lacking, although a date of 4,545 ± 90 ^{14}C yr BP has been secured for its termination. The final marine episode recorded at Downholland Moss is derived from a fossil dune slack peat and has been dated at 2,335 ± 120 ^{14}C yr BP. Tooley (1978a) has related these marine episodes with concurrent marine conditions at Lytham between approximately 5,570 ^{14}C yr BP and 4,897 ^{14}C yr BP, and between 3,090 ± 135 ^{14}C yr BP and 2,270 ± 65 ^{14}C yr BP.

Due in part to the diminishing number of transgressive overlaps recorded in the marshes to the north and south of Downholland Moss, Tooley (1978b) reasoned that the route of each marine inundation was to the west. However, after further stratigraphical and microfossil investigations, Huddart (1992) produced evidence of a south west route of marine inundation via the proto-Alt Estuary. This evidence came largely from foraminiferal analysis of Downholland Moss deposits, as well as analysis of deposits from new sites in the south of the area, which revealed an increasing presence of inner shelf foraminifera species in deposits with proximity to the proto-Alt Estuary. In addition, Huddart (1992) suggested that a barrier beach or sand barrier to the west of Downholland Moss must have been in existence from at least 8,400 ^{14}C yr BP. This theory was based around several main lines of evidence: the south west route of marine inundation; the change in orientation from east-west to north-south of Downholland Brook; the existence of low-energy environments (including lagoons); and the pattern of roddons (relic tidal creeks) which appear to feed towards the present-day Downholland

Brook to the north and to the River Alt to the south, indicating the presence of a barrier to the west.

If this hypothesis is correct, then the intercalated sediment deposits of Downholland Moss may represent a more complex, integrated record of regional RSL change and local changes in coastal morphology, making this an inappropriate representative site of RSL change in south west Lancashire. Direct evidence for the existence of a barrier to the west of Downholland Moss from 8,400 ^{14}C yr BP, as required by Huddart (1992), does not exist. Pye & Neal (1993a; 1993b) and Neal (1993) have demonstrated that inter-tidal and sub-tidal sand deposits were accumulating in the Formby area from at least 5,555 ± 110 ^{14}C yr BP and that, based on borehole evidence, this former environment was laterally extensive. They argue that this was the probable source of sediment for dune building, which may have commenced shortly afterwards. Indeed, a date obtained from a dune slack organic deposit between Formby and Ainsdale provides direct evidence of the existence of a dune barrier to the west of Downholland Moss from at least 5,110 ± 70 ^{14}C yr BP (Pye & Neal, 1993a; 1993b; Neal, 1993). Based on the pattern of roddons in the Formby area and, further north, in the Ainsdale, Birkdale and Southport area, Pye & Neal (1993a; 1993b) and Neal (1993) suggest that the dune barrier stretched from at least the position of the present day Ainsdale Nature Reserve in the north, to the Alt mouth in the south.

Based on this work, Pye & Neal (1993a; 1993b) invoke an alternative evolution model of Downholland Moss. They argue that the Downholland Moss deposits accumulated in the lee of an extensive sand barrier, which must have been in existence by about 5,500 ^{14}C yr BP. That the entire evolution of Downholland Moss from around 8,400 ^{14}C yr BP onwards occurred in the lee of an extensive sand barrier (Huddart, 1992) must remain equivocal. More robust evidence of deposition under back-barrier conditions in the Early Holocene is needed before this alternative evolution of the area can be fully accepted.

Pye & Neal (1993a; 1993b) and Neal (1993) have identified buried inter-tidal deposits that are periodically exposed on the present day Formby foreshore, which progressively thin in a landward direction and, consequently, are unrelated to the Downholland Moss sediment deposits. Although an *in situ Alnus* stem within this deposit has been dated at

3,230 ± 80 ^{14}C yr BP, the initiation and cessation of this deposit remains to be accurately dated. Further, the driving mechanism(s) behind the initiation of these inter-tidal deposits also remains unresolved. Pye & Neal (1993a; 1993b) present three, not necessarily mutually exclusive, mechanisms: a fall in RSL, a regional reduction in wave energy, or the presence of a second seaward sand barrier.

These sediments contain numerous prehistoric imprints, including human footprints. The imprints have been extensively catalogued and investigated within the context of their contemporaneous environment (Gonzalez *et al.*, 1996; Roberts *et al.*, 1996; Huddart *et al.*, 1999a; 1999b). Two, altitudinally distinct, sets of imprints are present on the Formby foreshore (Gonzalez *et al.*, 1996). The upper set was formed in a dune slack deposit, which has been dated to between 3,230 ± 80 ^{14}C yr BP (Pye & Neal, 1993a) and 3,649 ± 109 ^{14}C yr BP (Gonzalez *et al.*, 1996). The stratigraphic position of the lower set suggests a greater age, but this remains to be determined. Plater *et al.* (1999) pointed out that the imprint-bearing sediments are characteristic of a meso-tidal regime, in which spring tides ranged between 2m and 4m (Davies, 1964). Considering that the present coastline is characterised by a macro-tidal range of 8.4m (Admiralty Tide Tables, 2003), a significant change in palaeotidal range, perhaps by at least 4m, may have occurred along this coastline since the Mid Holocene (Plater *et al.*, 1999). If proven correct, then regional eustatic sea-level may have been higher in the Mid Holocene than previously thought, thus requiring a reappraisal of the local isostatic rebound models (e.g. Peltier *et al.*, 2002).

3.3.2.3 The Wirral

The coastal deposits of the north Wirral coastline also preserve important evidence of Holocene RSL change (Kenna, 1986; Innes *et al.*, 1990; Bedlington, 1994). Kenna (1986) presented an overview of the Holocene stratigraphy of the Wirral. This was based on exposed coastal sections and cores of Holocene sediments preserved in a series of pre-Holocene buried channels and depressions. He identified a tripartite peat sequence: a lower peat (6,460 ± 40 ^{14}C yr BP) containing *in situ Quercus* and *Betula* stumps and wood debris; a middle peat (5,550 ^{14}C yr BP to 3,500 ^{14}C yr BP) that contained *in situ* tree stumps and other wood and plant debris towards the top; and an upper peat, tentatively dated at 2,750 ± 55 ^{14}C yr BP. A clay and silt unit, equivalent to the 'Leasowe Marine Bed' of Reade (1871), intercalates the lower and middle peat, with

the presence of polyhalobous and mesohalobous diatom taxa confirming a marine origin (Kenna, 1986). A silty sand deposit intercalates the middle and upper peat and has a landward equivalent unit of silt and clay. Kenna (1986) suggests that these landward silt and clay deposits may reflect the presence of a lagoon, which was allowed to form due to the existence of a shallow coastal barrier seawards, as indicated by the silty sand deposits. Sediments associated with the presence of dunes (e.g. dune slack peats and dune sands) cap the Holocene sequence.

In north west Wirral, the pre-Holocene surface slopes seawards and forms a deep depression, which has been termed the 'western depression' by Kenna (1986). The sediment stratigraphy at Newton Carr, Hoylake, a site in the 'western depression', has been described by Innes *et al.* (1990). It shows evidence of a similar stratigraphy to that described by Kenna (1986). A tripartite peat sequence is again evident and, based on relative (pollen) dating, it is inferred that the lower peat was deposited around 7,200 ^{14}C yr BP, the middle peat sometime between 7,200 ^{14}C yr BP and 5,000 ^{14}C yr BP and the upper peat at around 5,000 ^{14}C yr BP. Three minerogenic units intersperse the peat deposits: the 'lower marine facies'; the 'middle marine facies'; and the 'upper marine facies' (Innes *et al.*, 1990).

Bedlington (1994) analysed the pollen and diatom assemblages of the sediments described by Innes *et al.* (1990) at Newton Carr. He obtained radiocarbon dates for the transgressive overlaps of the lower and middle peat, the regressive and transgressive overlaps of the upper peat, and the transgressive and regressive overlaps of the minerogenic unit that briefly interrupts the deposition of the upper peat. Bedlington (1994) correlated the chronology of regressive and transgressive overlaps at Newton Carr with sites in North Wales using the tendency technique (Section 2.1.3.1). Several sea-level tendencies of wider significance are recorded at Newton Carr (Table 3.2). Based on SLIs from North Wales and north Wirral, Bedlington (1994) calculated that rates of RSL rise were approximately 7mm per year between 8,000 ^{14}C yr BP and 7,000 ^{14}C yr BP and approximately 3mm to 4mm per year between 7,000 ^{14}C yr BP and 6,000 ^{14}C yr BP.

Table 3.2. Chronology of sea-level tendencies recorded at Newton Carr, north west Wirral (Bedlington, 1994).

Sea-level tendency	Radiocarbon date (^{14}C yr BP)
Positive	7,805 ± 70
Positive	6,680 ±75
Negative	5,465 ± 90
Positive	4,965 ± 40
Negative	4,525 ± 65
Positive	2,825 ± 40

3.3.2.4 Overview of Holocene RSL change in north west England

Based on his detailed investigations, Tooley (1974; 1978a) constructed a RSL curve to show the changing height of MHWS tides and mean tide level during the Holocene in north west England. In light of the refinements in the methodology of RSL reconstruction (Section 2.1.3.1), Tooley (1982b) has presented a refined, more geographically restricted, time-altitude graph of Holocene RSL change, which encompasses Liverpool Bay, south west Lancashire and the south Fylde (Figure 3.3).

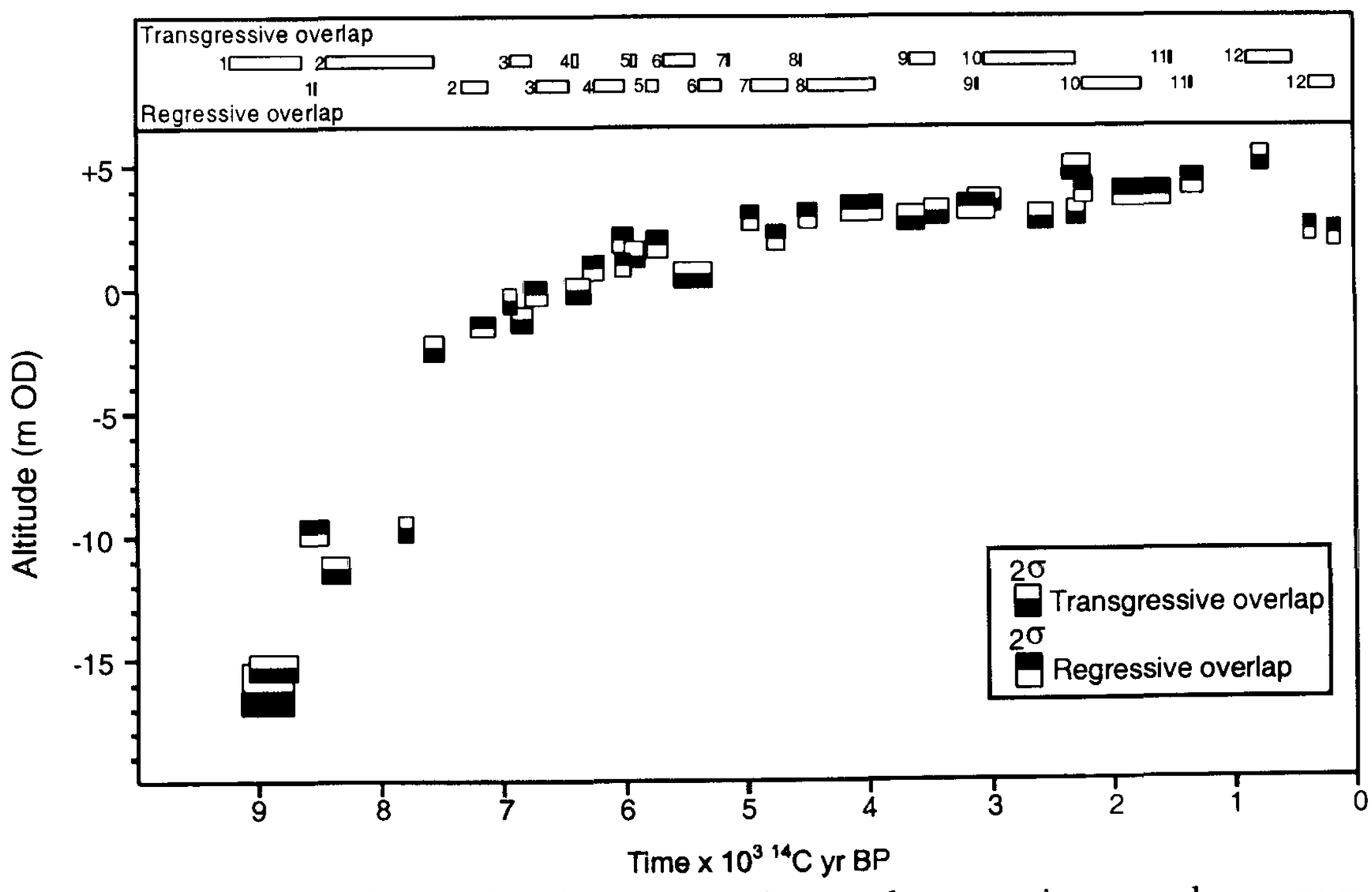

Figure 3.3. Time-altitude graph of transgressive and regressive overlaps recorded in coastal sediments from Liverpool Bay, south west Lancashire and the south Fylde (from Tooley, 1982b).

A prominent feature of the north west England time-altitude graphs is the rapid RSL rise between 8,000 ^{14}C yr BP and 7,600 ^{14}C yr BP, when RSL in Liverpool Bay, south west Lancashire and the south Fylde rose by around 7m. A positive sea-level tendency was also recorded around the same time in the Tay Estuary (Figure 3.2), as well as in other areas that were much closer to the centre of the former Scottish ice sheet (Shennan *et al.*, 1999). The widespread geographical registration of this positive sea-level tendency in areas undergoing continued isostatic uplift suggests a regional eustatic rise in sea-level. Blanchon & Shaw (1995) identified a c. 6m jump in eustatic sea-level at around 7,600 ^{14}C yr BP, possibly related to Antarctic ice-sheet instability. Recent research has constrained the timing of this event to around 7,500 ^{14}C yr BP (Blanchon *et al.*, 2002). In a more detailed analysis of Morecambe Bay Holocene RSL change, Zong & Tooley (1996) indicate that this 'catastrophic rise event' identified by Blanchon & Shaw (1995) may have resulted in the observed acceleration of RSL rise rates to over 30mm yr^{-1}.

Figure 3.3 demonstrates an overall upward trend in RSL in Liverpool Bay, south west Lancashire and the south Fylde throughout the Early Holocene, with RSL reaching contemporary levels at around 5,000 ^{14}C yr BP (Tooley, 1982b). This corroborates the geophysical model predictions of eustatic sea-level rise outstripping any isostatic rebound (Section 3.3.1). Shennan (1989) calculated isostatic rebound rates in South Lancashire of approximately 5mm per year at around 7,000 ^{14}C yr BP, which gradually diminished until 5,000 ^{14}C yr BP, when uplift was generally complete. Based on a larger SLI database, however, Shennan & Horton (2002) detected some isostatic adjustment after 3,700 ^{14}C yr BP in the area: uplift in south west Lancashire at a rate of 0.47mm per year, and subsidence in the areas surrounding the Mersey Estuary at a rate of 0.21mm per year.

Chapter 4

Methodology

4.1 Research approach

A fundamental requirement of a sea-level and coastal environment indicator is that it must possess an indicative meaning (Section 2.1.3), that is, a relationship between the environment in which it accumulated and a reference water level (van de Plassche, 1986). Contemporary saltmarsh and tidalflat surveys have revealed that diatoms, foraminifera and testate amoebae assemblages are principally controlled by ground elevation within the tidal frame (Section 2.2.3), with distinct assemblages relating to distinct coastal zones. To determine if any relationship exists between $\delta^{13}C$ and C/N of plants and surface sediments with ground elevation within the tidal frame, knowledge of the $\delta^{13}C$ and C/N of the plants and surface sediments in modern-day tidal zones is fundamental.

4.2 Modern survey

4.2.1 Ince Banks

Ince Banks is the only extensive saltmarsh that exists in the Mersey Estuary. It is a species poor saltmarsh located on the southern banks of the Inner Mersey Estuary (Figure 4.1). Fourteen sampling stations were established along a 1400 m transect (A–B) (Figure 4.1). The transect encompasses the entire width of Ince Banks, with sampling stations established on the tidalflats, lower saltmarsh and upper saltmarsh. Construction of the Manchester Ship Canal (1887-1893), however, has destroyed parts of the upper saltmarsh and separates Ince Banks from the mainland. One of the few accessible points onto the saltmarsh is a mooring site, reachable only by boat, on the south east corner of the saltmarsh (Figure 4.1). The saltmarsh contains numerous impassable creeks and therefore modern sampling was restricted to the east side of the saltmarsh. Each sampling station was levelled to OD using a Leica T600 Total Station. At each station, the plant species present, and their percentage cover, was estimated using a 50 cm^2 quadrat. Three specimens of each of the plant species present at each station were taken for $\delta^{13}C$ and C/N measurement. At the centre of each quadrat, a sample of the surface sediment (top 3 cm) was also taken for $\delta^{13}C$ and C/N measurement. A total of 88 plant and surface sediment

samples were collected. Preparation of samples and details of $\delta^{13}C$ and C/N analysis is outlined in Section 4.4.4.

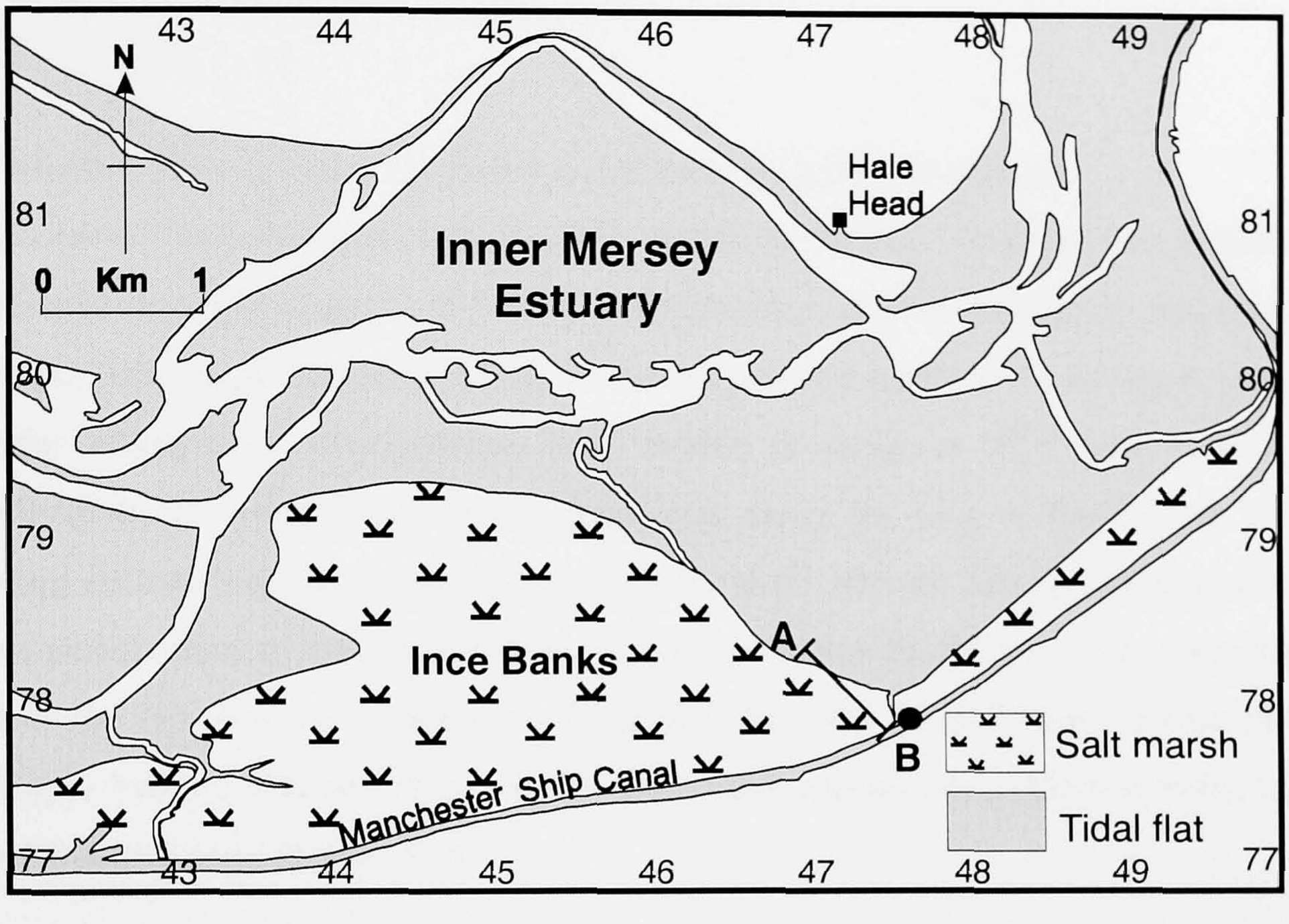

Figure 4.1. Location of modern transect A–B. The saltmarsh was accessed by boat at a mooring site (●).

Diagenetic alteration of organic matter inevitably occurs in the early stages of sediment deposition. The selective preservation of lignin in the sediment, which is the most refractory plant compound of vascular vegetation, will result in a shift in bulk sediment $\delta^{13}C$ values because the $\delta^{13}C$ composition of lignin differs from other plant compounds by several per mil (Section 2.3.6). In an attempt to quantify this change in $\delta^{13}C$ and C/N values over time, lignin was extracted from selected plant specimens and the $\delta^{13}C$ and C/N values compared to that of the whole plant.

Lignin was extracted from the plant material by a two-step procedure (TAPPI, 1988, 1997). A specimen of each plant species was shredded and placed in Whatman extraction thimbles. Initially, solvent soluble plant material (e.g. resin, fatty acids, waxes) was removed by cycling a 2:1 benzene/ethanol solvent through the soluble thimbles for 4 hours

in Soxhlet apparatus (TAPPI, 1997). The remaining carbohydrates were then removed by immersing the plant specimens in warm 72% H_2SO_4 for 2 hours and then boiling in 3% H_2SO_4 for 4 hours. The remaining acid-insoluble lignin was removed from the supernatant solution through a filtering crucible with a sintered glass disc of fine porosity (TAPPI, 1988).

4.2.2 Modern Mersey Estuary suspended and surficial sediment analysis

On account of fluctuations in Holocene RSL and River Mersey discharge, it is necessary to characterise the entire range in POC $\delta^{13}C$ and C/N (from riverine to marine) that may have potentially been deposited on a saltmarsh during tidal inundation. In addition, Holocene sub-tidal sedimentary environments may exhibit a range in $\delta^{13}C$ and C/N values, depending on the position of former deposition along the axis of the estuary. Seven sampling stations were established along the axis of the Mersey Estuary, ranging from the marine end-member of the Outer Estuary (Crosby and New Brighton), the brackish/marine water of the Narrows (Seacombe), the brackish/freshwater Inner Estuary (Bromborough) and Upper Estuary (Mersey Way), to the freshwater end-member (Martinscroft), located beyond the tidal limit (Figure 4.2).

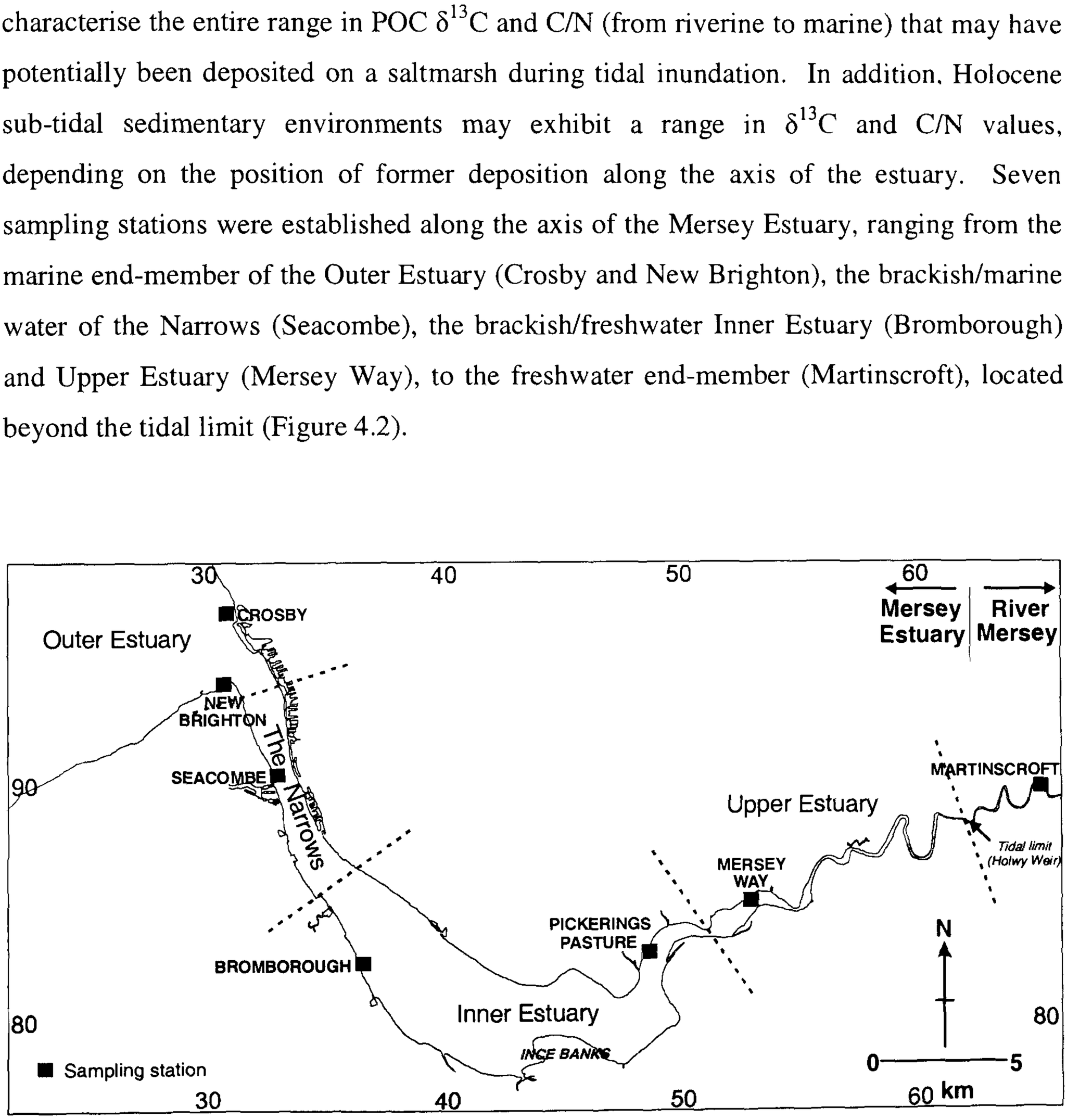

Figure 4.2. Location of sampling sites along the axis of the Mersey Estuary and the River Mersey.

At each station, water temperature, salinity, conductivity, and total dissolved solids were determined *in situ* using a Jenway 2000 Conductivity Meter, as well as pH using the electrometric method at both high tide and low tide. Suspended sediment was collected at high tide and, where possible, at low tide, in acid-rinsed 1L plastic Nalgene bottles for $\delta^{13}C$ and C/N analysis. High tide and low tide measurements were taken to determine the range in water salinity, conductivity and total dissolved solids at each station. Estuarine sub-tidal sediment (top 2 cm) was also collected at each station for $\delta^{13}C$ and C/N analysis, as this reflects seasonally integrated $\delta^{13}C$ and C/N values after organic matter degradation in suspension. In the laboratory, the suspended sediment samples were mixed with HCl to a concentration of 5% and left overnight to remove inorganic carbon. Suspended sediment was isolated by filtering the water samples through Whatman quartz micro-fibre filters, washed several times with deionised water, dried at 50°C and ground to a fine powder. The sub-tidal sediments were prepared and analysed for $\delta^{13}C$ and C/N following the procedures outlined in Section 4.4.4.

4.3 Holocene cores

Several marginal estuarine sediment cores were taken from Helsby and Ince Marshes by the British Geological Survey (BGS) in summer 2000 and 2003 (Figure 4.3 and Table 4.1). This area of the Estuary was chosen for coring by the BGS due to previous investigations showing extensive Holocene deposits existing here (Tooley, 1978a). Cores Ince 2 to Ince 5 form the basis of this investigation. The two contrasting cores of Ince 4 (containing intercalated organic and minerogenic sediments) and Ince 2 (containing mostly minerogenic sediments), from Helsby and Ince Marshes respectively, were selected for laboratory analysis in order to test the accuracy of $\delta^{13}C$ and C/N in a range of coastal environmental deposits. Cores Ince 6 to Ince 8, taken by the BGS at a later date (summer 2003), allow inferences to be made of associated environmental changes seawards of the study area. In addition, numerous commercial borehole logs, from various and sometimes undisclosed sources, collated by the BGS and made available through their Geoscience Data Index facility, have been used. Only significant changes in lithology are recorded in the commercial borehole logs, from peat to clay, for example. Coupled with the approximate measurement of the altitude of such changes, they are only used in the present

study to investigate the lateral extent of lithological units and in support of palaeoenvironmental interpretations.

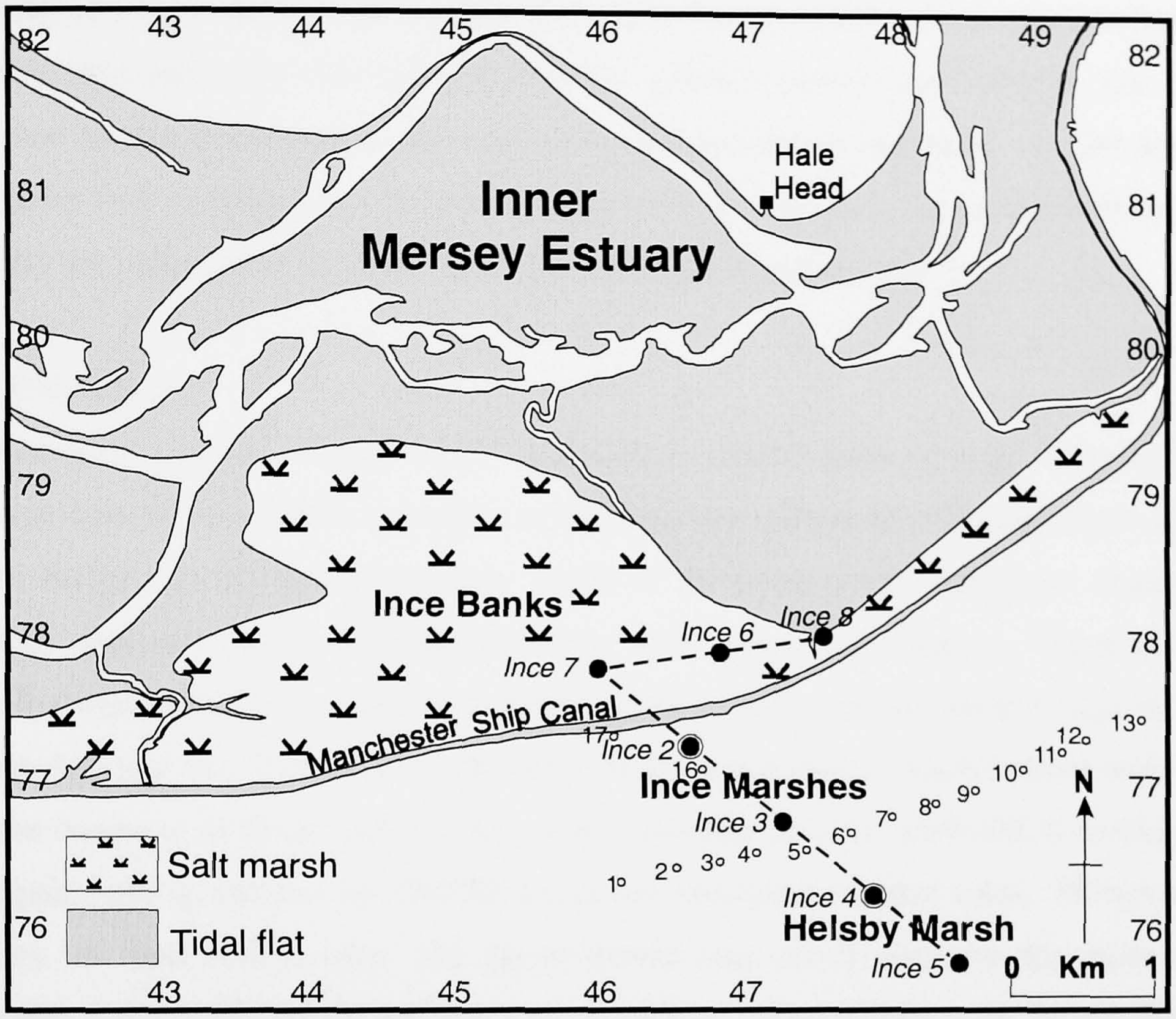

Figure 4.3. Location of BGS (●) and commercial (○) sediment cores. Cores Ince 2 and Ince 4, highlighted with an outer circle, were chosen for laboratory analysis.

Table 4.1. BGS borehole location, ground altitude and core depth.

Borehole	Location	Grid reference	Ground altitude (m OD)	Core depth (m)
Ince 8	Ince Banks	SJ 4756 7811	+5.11	9.00
Ince 6	Ince Banks	SJ 4668 7792	+5.29	8.30
Ince 7	Ince Banks	SJ 4590 7758	+5.36	6.80
Ince 2	Ince Marshes	SJ 4668 7730	+5.08	10.45
Ince 3	Ince Marshes	SJ 4702 7674	+5.24	8.21
Ince 4	Helsby Marsh	SJ 4792 7641	+5.42	7.07
Ince 5	Helsby Marsh	SJ 4862 7613	+4.33	6.60

4.4 Multi-proxy analysis

Samples for diatoms, loss on ignition, $\delta^{13}C$ and C/N analysis were taken at 8 cm intervals throughout cores Ince 2 and Ince 4, with higher resolution sampling across changes in sediment lithology. In addition, particle size analysis was carried out on core Ince 2 at 8cm intervals, this particular core being chosen for detailed particle size analysis due to the thick and largely uninterrupted accumulations of minerogenic sediments. Pollen analysis of organic- rich sediments at lithological boundaries in both cores was undertaken in order to verify the radiocarbon dates and to define the palaeoenvironments.

4.4.1 Chronology

Chronological control is based on six radiocarbon (AMS) dates on peat. Five of these dates are from Helsby Marsh (core Ince 4) and only one is from Ince Marshes (core Ince 2) due to the paucity of organic remains. Areas of the cores where significant changes in lithology and microfossil assemblages occur were selected for dating. Samples were visually inspected for root penetration before being sealed in plastic sample bags and sent to Beta Analytic Inc., Florida, for radiometric radiocarbon dating. Each sample underwent full pre-treatment at Beta Analytic Inc., which includes an acid wash (HCl) to eliminate carbonates, and an alkali wash (NaOH) to remove secondary organic acids. However, the quantity of final carbon after full pre-treatment was insufficient for the radiometric technique and so the AMS technique was necessary. The calibration of ^{14}C yrs BP into calendar years BP was performed using the INTCAL 98 dataset of Stuiver *et al.* (1998).

4.4.2 Lithology

Lithological descriptions of cores Ince 2 to Ince 5 was carried out by David Brew, and of cores Ince 6 to Ince 8 by Gareth Jenkins at the BGS, Keyworth. The lithological descriptions were checked before the cores were sampled.

4.4.2.1 Particle size analysis

Particle size parameters of minerogenic sediments are chiefly related to the mode of transport and the energy conditions of the transporting medium (Friedman, 1961). Investigating such textural characteristics of Mersey Estuary sediment deposits should, therefore, provide information on the mode and energy of transportation at the time of deposition. However, no universal solution exists to distinguish between depositional

environments in ancient deposits based on particle size criteria alone (McManus, 1988) and so this technique is primarily used to complement and verify the diatom-inferred palaeoenvironments of core Ince 2. Core Ince 2 alone was chosen for analysis due to the almost continuous minerogenic deposition at this site. For the purposes of this study, the particle size characteristics of mean, standard deviation and skewness of the sample population will be employed as these parameters are hydraulically controlled (Griffiths, 1967). The mean particle size parameter is an indication of the weight force that must be balanced by an applied fluid stress before transport is possible (Leeder, 1982) and is therefore a reflection of the energy of the transporting medium. The standard deviation of the particle size distribution is a measure of sorting, whilst skewness (the symmetry of the frequency curve) indicates whether the sample has an excess of coarse-grained particles (negatively skewed) or fine-grained particles (positively skewed) (Friedman & Sanders, 1978).

Particle size analysis was carried out in the Geography Department at the University of Liverpool using a Coulter Laser LS 130 particle sizer. Approximately 4g of sediment was placed in 20% H_2O_2 to remove organic matter. 1ml of calgon per gram of sediment was added to disperse the sediment and the samples were shaken overnight on an orbital shaker. The samples were washed through a 710μm sieve until a volume of 50ml was reached. After further dispersal in an ultrasonic bath for 1 minute the samples were transferred to a beaker with an electronic stirrer to ensure continuous sediment suspension and to prevent flocculation. The samples were then transferred to the Coulter Laser LS 130 particle sizer using a 2ml pipette. All data was converted from millimeters to the phi (ϕ) scale prior to statistical analysis (Equation 4.1). Using Folk & Ward (1957), the calculated percentiles of 5, 16, 25, 50, 75, 84 and 95 were used to calculate the mean, standard deviation and skewness of the sediment population (Equations 4.2 to 4.4).

$$\phi = -\log_2 D \qquad \text{(Equation 4.1)}$$

where D is grain diameter in mm

$$\text{Mean } (\phi) = \frac{(16\% + 50\% + 84\%)}{3} \qquad \text{(Equation 4.2)}$$

$$\text{Sorting } (\phi) = \frac{(84\% - 16\%)}{4} + \frac{(95\% - 5\%)}{6.6} \qquad \text{(Equation 4.3)}$$

$$\text{Skewness} = \frac{(16\% + 84\% - 2(50\%))}{2(84\% - 16\%)} + \frac{(5\% + 95\% - 2(50\%))}{2(95\% - 5\%)} \qquad \text{(Equation 4.4)}$$

The mean particle size for each sample was classified into gravel, sand, silt or clay, based on the Udden-Wentworth size classification for sediment grains, outlined in Leeder (1982), and the standard deviation and skewness values assigned a descriptive summary using Folk & Ward (1957). The interpretative model used in this study is based on the principles outlined in Friedman (1961).

4.4.2.2 Organic content

Loss on ignition determines the quantity of organic matter in sediments and is based on the principal that organic material combusts at high temperatures, with sample weight loss equating to organic matter content. The laboratory procedures for loss on ignition follows those outlined in Bengtsson & Enell (1986). Fresh sediment samples were added to crucibles of known weight. The samples were weighed before being oven dried overnight at 105°C and left to cool in a desiccator to prevent absorption of moisture before being re-weighed. This provides an estimation of the water content of the samples. Samples were then heated in a furnace at 550°C for two hours, allowed to cool in a desiccator and then weighed. The difference in weight between the oven dried samples and the ignited samples provides a measurement of the organic content of the samples (Equation 4.5), which have been converted into a percentage.

$$\text{Loss on ignition (g)} = \frac{C - D}{B - A} \qquad \text{(Equation 4.5)}$$

where C is the weight (g) of the oven dried sample and crucible, D is the weight (g) of the ignited sample and crucible, B is the weight (g) of the fresh sample and crucible, and A is the weight of the crucible.

4.4.3 Microfossil analysis

4.4.3.1 Pollen analysis

In this study, pollen analysis of the sediments at organic-rich, lithological boundaries, is primarily used to corroborate the radiocarbon dates (e.g. Tooley, 1978a; 1978b). This is achieved by identifying local pollen assemblage zones (LPAZs) and relating these zones to the radiocarbon-dated, regional pollen assemblage zones (RPAZs), at Red Moss, an upland site in Lancashire (Hibbert *et al.*, 1971). The radiocarbon dated RPAZs at Red Moss are in good agreement with comparable zones at Scaleby Moss, over 100 miles to the north (Hibbert *et al.*, 1971). Therefore, comparison of the LPAZs from the Inner Mersey Estuary with the RPAZs at Red Moss, approximately 40 miles to the east, appears justifiable, despite the differing environmental settings and altitudes of the two sites. This technique of corroborating radiocarbon dates using Red Moss has been employed routinely in other north west England Holocene coastal evolution studies (e.g. Tooley, 1978a; Zong & Tooley, 1996). The pollen assemblages at organic-rich, lithological boundaries have also been used to infer depositional environments.

Organic-rich sediments in coastal deposits generally indicate deposition high in the inter-tidal zone or in the supra-tidal zone where wetland vegetation communities are well established. Sequential pollen analysis of organic-rich sediments adjacent to transgressive or regressive overlaps may demonstrate a gradual transition of wetland communities, for example, from acidic bog, to fen carr and then to reedswamp, with the presence of pollen from saltmarsh vegetation indicating nearby marine conditions. Changes in coastal vegetation may be driven autogenically (internally), for example through vegetation succession (e.g. Godwin, 1940), or allogenically (externally), for example through changes in the elevation of the water table resulting from fluctuations in RSL or changes in effective precipitation (e.g. Waller *et al.*, 1999). A particular valuable application of pollen analysis in RSL reconstructions is for the validation of SLI points by demonstrating such a gradual transition of coastal vegetation communities prior to positive or negative tendencies in RSL (e.g. Shennan *et al.*, 2000a).

Like any other microfossil technique, variable preservation imposes limitations. Pollen grains may suffer mechanical or chemical damage in the sediment deposits or during preparation for analysis. Further, it is important to recognise that the pollen assemblages

may not be a faithful representation of the actual vegetation communities that once existed. For example, differences in the pollen production and dispersal of taxa may result in higher numbers of *Quercus*, *Betula*, *Alnus*, *Pinus* and *Corylus* pollen grains compared with *Ulmus* and *Tilia* grains in the regional pollen rain (Moore *et al.*, 1991). Although this effect has not been quantitatively corrected for, using 'R' values for example (Davies, 1963), it is nevertheless taken into account in the present study. In addition, pollen from both the local vegetation and the regional vegetation will be incorporated in the assemblage. Whilst a large influx of pollen from local vegetation is useful when attempting to reconstruct *in situ* vegetation communities, it may complicate attempts to relate the local pollen assemblage to the regional pollen assemblage zones.

Preparation of sediment for pollen analysis follows the principles outlined in Moore *et al.* (1991). This involves several stages of physical and chemical extraction, each designed to remove different matrix material in which the pollen may be embedded. Sediment samples of $1cm^3$ volume were placed in centrifuge tubes and subjected to the following chemical treatments: 10% HCl (hydrochloric acid) to remove carbonates; 10% NaOH (sodium hydroxide) to remove soluble humic compounds; 10% $Na_4O_7P_2$ (sodium pyrophosphate) to remove clay; 40% HF (hydrofluoric acid) to remove silicate material; and acetolysis (9:1 mixture of CH_3COOH (acetic anhydride) and H_2SO_4 (sulphuric acid) to remove soluble cellulose. Each stage of the chemical treatment was encouraged by heating the sediment and chemical mixture in a boiling water bath. After each stage of treatment, the extraction supernatant was separated from the remaining sediment by centrifuging at 3000 rpm for 5 minutes and decanted. Physical extraction involved separating the coarse (>100 μm) sediment fraction from the pollen-containing fine fraction. After chemical and physical treatment, safranine was added to the sediment (which stains the pollen grains allowing easier identification) and samples were then mounted in glycerol and stored in phials. Pollen grains were counted and identified with reference to Moore *et al.* (1991) and nomenclature follows Stace (1997). Where possible, a total of 300 pollen grains were counted, excluding aquatics and Pteriodophytes. The percentage pollen diagrams are based on a pollen sum of total land pollen (TLP), excluding aquatics, Pteriodophytes and *Sphagnum*. The excluded categories are expressed as TLP + aquatics, TLP + Pteriodophytes and TLP + *Sphagnum*. The pollen assemblages are presented graphically using the TILIA 2.0 and TILIA GRAPH 2.0 programs.

4.4.3.2 Diatom analysis

Preparation of sediment for diatom analysis follows the principles outlined in Battarbee (1986). Sediment samples of 1cm^3 in volume were oxidized in 30% H_2O_2 (hydrogen peroxide) to remove organic matter. Approximately 2ml of the remaining solution was extracted using a pipette and smeared over a cover slip. Excess liquid was evaporated from the sediment by gentle heating of the cover slip, leaving a sediment residue, which was inverted and mounted in Naphrax on a cover slide. The cover slide was heated on a hot plate at high temperatures to expel excess air and permanently seal the cover slip and slide. For the purpose of statistical analysis 300 diatom valves were counted (Battarbee, 1986; Cooper, 1999), although diatom preservation was variable and the attainment of this sum was not possible for all levels investigated. Diatom valves were identified with reference to Krammer and Lange-Bertalot (1986-1991) and Hartley *et al.* (1996). Nomenclature follows Hartley (1986) with ecological classification based on Denys (1991-92) and Vos & De Wolf (1993a). The diatom counts are expressed as a percentage of total assigned valves (TAV %) with the most common diatom taxa (≥ 5% TAV) presented graphically using the TILIA 2.0 and TILIA GRAPH 2.0 programs.

4.4.4 $\delta^{13}C$ and C/N analysis

Prior to $\delta^{13}C$ and C/N analysis, the plant specimens were washed with deionised water, dried at 50°C and ground to a fine powder using a pestle and mortar. Sediment samples were treated with 5% HCl overnight to remove inorganic carbon. The sediment was separated from the supernatant by filtering through Whatman 42 filter papers, washed several times with deionised water, dried at 50°C and then ground to a fine powder. $\delta^{13}C$ and C/N were measured simultaneously by combustion in a Carlo Erba 1500 on-line to a VG TripleTrap and Optima dual-inlet mass spectrometer, with $\delta^{13}C$ values calibrated to the VPDB scale (Equation 2.1) using a within-run laboratory standard (cellulose, Sigma Chemical prod. no. C-6413) calibrated against NBS-19 and NBS-22. Replicate analysis of well-mixed samples indicated a precision of $\pm$ 0.15‰ (1 SD). C/N ratios are calibrated through an acedanalid standard and replicate analysis of well-mixed samples indicated a precision of $\pm$ <0.1.

Chapter 5

Modern Ince Banks and Mersey Estuary $\delta^{13}C$ and C/N Survey

Sediment $\delta^{13}C$ and C/N values reflect the $\delta^{13}C$ and C/N composition of the dominant source of organic matter to the sediments. Estuarine saltmarshes receive organic sediment from two principal sources: autochthonous plant material and allochthonous tidal-derived material. Estuarine tidal-derived organic carbon, or particulate organic carbon (POC), represents a mixture of marine and freshwater plankton (phytoplankton in particular), terrigenous plant detritus and soil eroded from the catchment. Typical tidal-derived POC $\delta^{13}C$ values may vary from –30.0‰ in upper estuarine and riverine locations, to –18.0‰ in outer estuarine and nearshore locations, with C/N values of around 8.0 throughout the estuary (e.g. Middelburg and Nieuwenhuize, 1998). In contrast, C_3 vascular plant material has higher C/N ratios of around 12.0 and over (Tyson, 1995) and $\delta^{13}C$ values commonly between –28.0‰ and –26.0‰. The similarity in $\delta^{13}C$ between C_3 vascular vegetation and freshwater phytoplankton may be overcome by C/N analysis, as phytoplankton tends to be nitrogen rich, resulting in much lower C/N ratios of between 5.0 and 7.0 (Tyson, 1995).

The difference in $\delta^{13}C$ and C/N between these two end-members (terrestrial C_3 plant material and tidal-derived POC) may allow an estimation of the relative contribution of each organic matter source in surface saltmarsh sediments. Due to the change in the dominant source of organic material in surface saltmarsh sediments from the sub-tidal through to the inter-tidal and supra-tidal zones, it follows that the $\delta^{13}C$ and C/N composition of the sediments should reflect this change. This chapter outlines the results of a $\delta^{13}C$ and C/N survey of modern Mersey Estuary saltmarsh and estuarine sediments, which was conducted in order to verify the hypothesis of changing $\delta^{13}C$ and C/N ratios along the sub-tidal and inter-tidal zones. If the hypothesised relationship between saltmarsh altitude and $\delta^{13}C$ and C/N holds, $\delta^{13}C$ and C/N analysis may then be used to distinguish coastal palaeoenvironments in the sediment record, and may also prove useful in verifying SLIs. The use of $\delta^{13}C$ and C/N values as geochemical 'signatures' of environmental facies (e.g. Andrews *et al.*, 2000), however, may be

compromised by the alteration, through decomposition, of bulk sediment $\delta^{13}C$ and C/N values over time. This chapter presents saltmarsh plant compound-specific $\delta^{13}C$ values in an attempt to quantify the expected shift in bulk sediment $\delta^{13}C$ values as a result of decomposition, and to determine whether $\delta^{13}C$ values can realistically be used as geochemical 'signatures' of environmental facies.

5.1 Ince Banks Saltmarsh $\delta^{13}C$ and C/N Survey

5.1.1 Results

The $\delta^{13}C$ and C/N values of Ince Banks' inter-tidal vegetation and surface sediments are summarised in Figure 5.1 (see Appendix A for datasets). The altitude of the saltmarsh decreases from 5.43m OD near the landward edge, to 3.84m OD at low saltmarsh localities (Figure 5.1a). A cliff (approximately 60cm in height) separates the low saltmarsh from the tidalflats, which are present below 2.82m OD. The altitude of stations IB1 to IB11 are above MHWS, IB12 occurs between MHWN and MHWS and IB13 and IB14 occur below MHWN. Bulk surface sediment $\delta^{13}C$ values range from –27.8‰ at station IB1 to –23.5‰ at station IB13 (Figure 5.1b) and bulk surface sediment C/N ratios range from 9.3 at IB14 to 11.6 at IB1 (Figure 5.1c). The mean and range in vegetation $\delta^{13}C$ and C/N at each station has been calculated using Equation 5.1 (page 72). The equation, developed by Chmura *et al.* (1987), takes into account the range in $\delta^{13}C$ and C/N for each plant species present (based on $\delta^{13}C$ and C/N measurements of three plant specimens of each species), as well as the abundance of each species at each station, which was estimated using a randomly placed 50cm^2 quadrat. Mean vegetation $\delta^{13}C$ shows little variation across the saltmarsh (–28.1‰ to –27.0‰) (Figure 5.1b). The range in vegetation $\delta^{13}C$ at each station is also relatively small across the saltmarsh, only vegetation at station IB1 shows any significant variation, with $\delta^{13}C$ values of between –28.0‰ and –26.0‰. The C/N ratios of saltmarsh vegetation is much more variable, with minimum and maximum mean values of 17.9 and 48.1 at stations IB12 and IB10 respectively (Figure 5.1c). Similarly, the range in vegetation C/N at each station is much greater than that for $\delta^{13}C$, with station IB1 again showing the largest variation in C/N, from 22.6 to 56.0. Mean whole plant $\delta^{13}C$ and mean plant lignin $\delta^{13}C$ are compared in Table 5.1. At each sample station studied across the Ince Banks

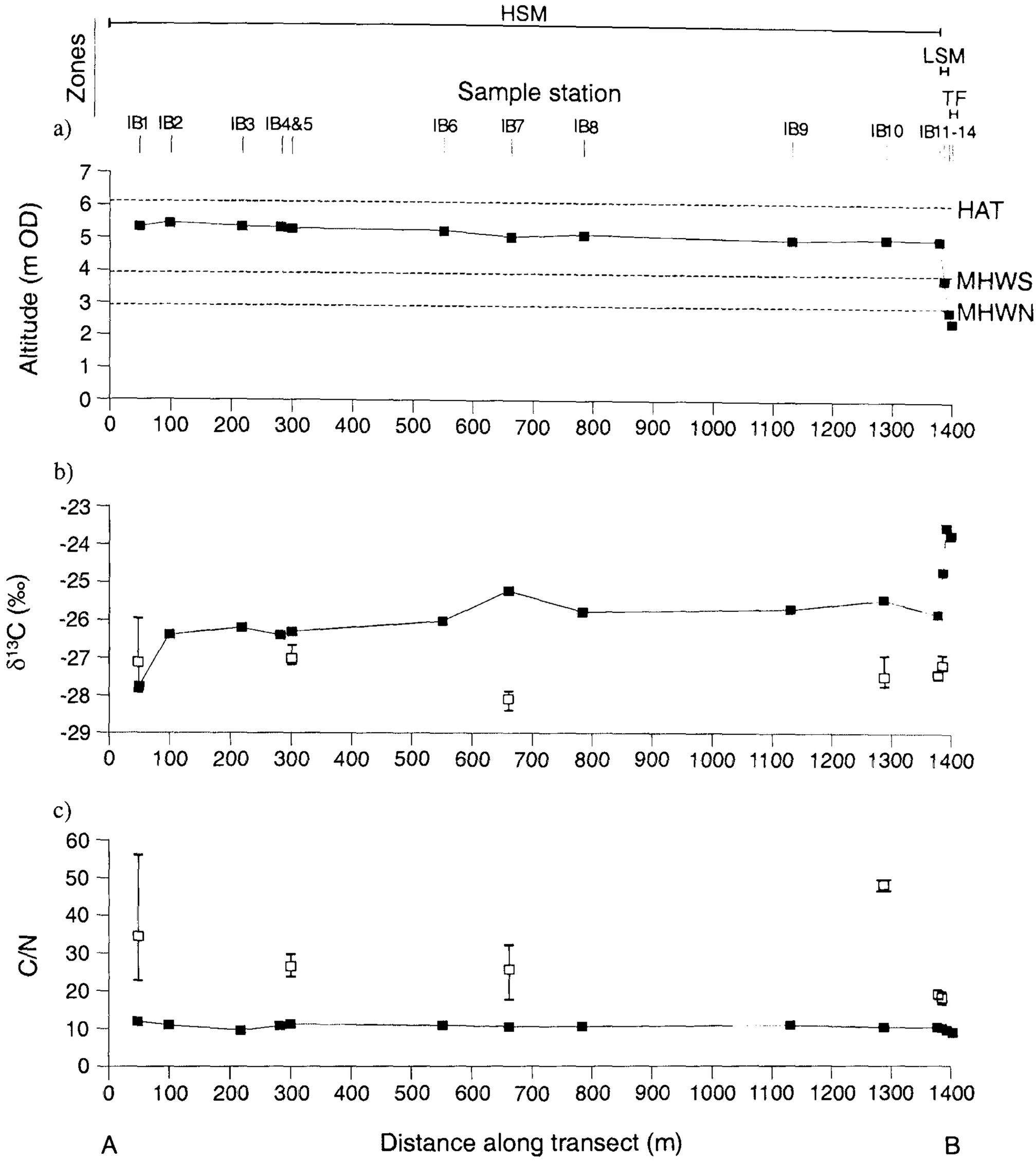

Figure 5.1. a) Ince Banks ground elevation in relation to the tidal frame and location of sampling stations along transect A-B (Figure 4.1), which extends across the high saltmarsh (HSM), through to the low saltmarsh (LSM) and tidalflat (TF) zones; b) Ince Banks surface sediment $\delta^{13}C$ (■) and mean (□) and range (error bars) of vegetation $\delta^{13}C$; c) Ince Banks surface sediment C/N (■) and mean (□) and range (error bars) of vegetation C/N. See Appendix A for datasets.

transect, the mean $\delta^{13}C$ of plant lignin is consistently less than the mean $\delta^{13}C$ of the whole plant by between approximately 2.0‰ and 4.0‰.

Table 5.1. Difference between mean whole plant $\delta^{13}C$ and mean plant lignin $\delta^{13}C$ at sampling stations along Ince Banks transect A-B (Figure 4.1).

Sampling Station	Elevation (m OD)	Mean whole plant $\delta^{13}C$ (‰)	Mean lignin $\delta^{13}C$ (‰)	Difference in $\delta^{13}C$ (‰)
IB 1	5.32	-27.10	-30.96	3.86
IB 5	5.29	-27.03	-30.22	3.19
IB 7	5.05	-28.15	-30.54	2.39
IB10	5.01	-27.41	-31.15	3.74
IB11	5.00	-27.39	-30.11	2.72
IB12	3.84	-27.12	-29.43	2.31
				mean = 3.04

5.1.2 Interpretation

There appears to be no correlation between saltmarsh surface elevation and vegetation $\delta^{13}C$ and C/N (Figure 5.1). In contrast, bulk sediment $\delta^{13}C$ appears to be associated with ground elevation within the tidal frame (Figure 5.1a and 5.1b). In general, surface sediment $\delta^{13}C$ increases with decreasing ground elevation, with abrupt changes in $\delta^{13}C$ occurring between the high saltmarsh, the low saltmarsh and the tidalflats. For example, there is a 1.1‰ increase in $\delta^{13}C$ between the high saltmarsh station IB11 (–25.8‰) and the low saltmarsh station IB12 (–24.7‰), which is located only 10m further seaward, but lies below MHWS. In contrast, the change in $\delta^{13}C$ within saltmarsh zones is more gradual. For example, there is a gradual increase in high saltmarsh surface sediment $\delta^{13}C$ from –27.8‰ at 5.32m OD (IB1) to –25.8‰ at 5.00m OD (IB11) over a horizontal distance of approximately 1380m. Although the change in $\delta^{13}C$ is of a higher magnitude (2.0‰), this is a consequence of the very low $\delta^{13}C$ measurement recorded for the sediments at the most landward station, IB1, (–27.8‰). The vegetation here consisted largely of the more salt intolerant species *Elymus atherica* (70% in a randomly placed 50cm^2 quadrat) and *Agrostis stolonifera* (30% in a randomly

placed 50cm^2 quadrat), which may suggest a significant reduction in the frequency and duration of tidal flooding in this part of the saltmarsh, although more data is needed to support this interpretation.

The tidalflat stations IB13 and IB14 lie below MHWN and are located 5m and 10m away from the low saltmarsh station IB12, and 15m and 20m away from the high saltmarsh station IB11 respectively. Surface sediment $\delta^{13}C$ values of the tidalflat stations IB13 and IB14 are –23.5‰ and –23.7‰ respectively, which are approximately 1.0‰ greater than the low saltmarsh station IB12, and 2.0‰ greater than the high saltmarsh station IB11. Surface sediment C/N ratios also change in relation to ground elevation within the tidal frame, although the relationship is much less pronounced (Figure 5.1a and 5.1c). Surface sediment C/N values fall from 11.6 to 10.2 between the high saltmarsh stations IB1 and IB11. Surface sediment C/N then falls to 10.0 at the low saltmarsh station IB12, and to 9.6 and 9.3 at the tidalflat stations IB13 and IB14.

To determine the provenance of organic carbon in the saltmarsh sediments at each station, the mixing model of Chmura *et al.* (1987) is employed (Equation 5.1). The model attempts to predict surface saltmarsh sediment $\delta^{13}C$ and C/N values (e.g. $\delta^{13}C_{plot}$), based on the weighted averaged $\delta^{13}C$ and C/N values of the overlying vegetation, which is calculated from the relative abundance and associated $\delta^{13}C$ and C/N values of each plant species (% biomass) in a 50cm^2 quadrat (as in Section5.1.1) (See Appendix A for an example). In the present study, such a model is useful in determining the extent to which vegetation is the dominant source of organic carbon.

$$\delta^{13}C_{plot} = \frac{\sum_{n=1}^{i}(\%\text{biomass}_i)(\delta^{13}C)}{\sum^{i}\%\text{biomass}_i} \qquad \text{(Equation 5.1)}$$

The high saltmarsh stations IB1 to IB6, which lie above 5.20m OD and have surface sediment $\delta^{13}C$ values of –26.0‰ or less, probably receive organic carbon mostly from the overlying vegetation. This is particularly evident at the most landward saltmarsh station IB1 (5.32m OD), where the $\delta^{13}C$ composition of the surface sediments (–27.8‰) lies within the range of the $\delta^{13}C$ values of the overlying vegetation (–28.0‰ to

–26.0‰), with mean vegetation $\delta^{13}C$ differing from the underlying surface sediment by only 0.7‰ (Figure 5.1b). At the slightly lower altitude high saltmarsh stations. IB7 (5.05m OD), IB10 (5.01m OD) and IB11 (5.00m OD), the difference between vegetation $\delta^{13}C$ and underlying surface sediment $\delta^{13}C$ is greater (1.6‰ to 2.9‰), with the $\delta^{13}C$ values of surface sediments occurring further outside the range of the $\delta^{13}C$ values of the overlying vegetation. At the low saltmarsh station IB12 (3.84m OD), the difference in $\delta^{13}C$ between the vegetation and the underlying surface sediments is also significant (2.4‰), again with surface sediment $\delta^{13}C$ values occurring outside the range of the $\delta^{13}C$ values of the overlying vegetation. As the $\delta^{13}C$ composition of all of Ince Banks' vegetation is very similar (range in mean vegetation $\delta^{13}C$ across all stations is between –28.1‰ and –27.0‰), the deviation in surface sediment $\delta^{13}C$ from that of vegetation with decreasing saltmarsh height indicates a separate and distinctive tidal-derived source of particulate organic carbon (POC) to the saltmarsh. An Inner Mersey estuarine $\delta^{13}C_{POC}$ of –23.6‰ has been measured as part of this study (Section 5.2). This allochthonous POC appears to be increasingly important with decreasing saltmarsh height, a result of the progressive increase in frequency and duration of tidal inundation of the lower altitude saltmarsh areas.

The extreme variability of saltmarsh vegetation C/N contrasts with the relatively uniform saltmarsh surface sediment C/N ratios. Saltmarsh sediment C/N ratios at all stations are between 10.0 and 11.6, with the exception of station IB3, which has a C/N value of 9.7. Tidalflat C/N ratios are a little lower, with values of 9.3 and 9.6. To a certain extent, this fine distinction arises because saltmarsh vegetation is a more important contributor of organic carbon to saltmarsh sediments, whilst tidalflat sediments will receive most organic carbon from *in situ* algae and, considering the large tidal influence in the Mersey Estuary, from marine phytoplankton, resulting in slightly lower C/N ratios of 6.0 to 8.0 (Tyson, 1995). The faster remineralisation of organic nitrogen in degrading phytoplankton may account for the slightly higher tidalflat C/N ratios of 9.3 and 9.6. Nevertheless, the difference in C/N between the saltmarsh vegetation (range in mean vegetation C/N across all stations is between 17.9 and 48.1) and the underlying surface sediments (9.7 to 11.6) highlights the importance of tidal POC as a source of organic matter in Ince Banks saltmarsh sediments, resulting in the suppression of C/N values that would otherwise be expected if organic matter was derived solely from vegetation.

5.2 Mersey Estuary $\delta^{13}C$ and C/N Survey

5.2.1 Results

The $\delta^{13}C$ and C/N of Mersey Estuary and River Mersey suspended POC ($\delta^{13}C_{POC}$ and C/N_{POC} respectively) at stations between the freshwater end-member at Martinscroft (River Mersey), approximately 38km from the mouth of the Estuary, and the marine end-member at Crosby, is shown in Figure 5.2 (see Appendix B for dataset). $\delta^{13}C_{POC}$ gradually and systematically decreases from between –22.0‰ and –22.8‰ at Crosby to between –27.2‰ and –26.9‰ at Martinscroft (Figure 5.2a). In general, high tide $\delta^{13}C_{POC}$ is slightly greater than low tide $\delta^{13}C_{POC}$ at all stations apart from at Martinscroft. An average (mid tide) $\delta^{13}C_{POC}$ has been calculated for each sampling station and is shown in Figure 5.2b. $\delta^{13}C_{POC}$ averages between –22.4‰ and –22.8‰ for the Outer Estuary, –23.0‰ for the Narrows, –23.9‰ for the Inner Estuary, –24.3‰ for the Upper Estuary and –27.1‰ for the River Mersey. In contrast to $\delta^{13}C_{POC}$, C/N_{POC} shows little variation with distance from the mouth of the Mersey Estuary (Figure 5.2c). C/N_{POC} generally remains between 8.0 and 10.0 from the mouth of the Estuary at Crosby to the Inner Estuary at Pickerings Pasture, just over 25km upstream. C/N_{POC} then increases slightly to 10.5 at Mersey Way, with the highest C/N ratios of between 11.3 and 12.4 encountered in the River Mersey at Martinscroft. There appears to be no relationship between tidal cycle and C/N_{POC}.

The insufficient quantity of organic carbon in Mersey Estuary surficial sediments at most sampling stations prevented longer-term averaged $\delta^{13}C_{POC}$ and C/N_{POC} values from being determined. $\delta^{13}C$ measurement of bulk organic surficial sediments was possible at three stations, however, and the results are presented in Table 5.2. Even based on these limited results, the general decrease in suspended $\delta^{13}C_{POC}$ with distance from the mouth of the estuary is also apparent in the bulk surficial sediments, with Inner Estuary surficial $\delta^{13}C$ values of between –22.8‰ and –23.2‰ contrasting with a River Mersey surficial sediment $\delta^{13}C$ value of –27.6‰.

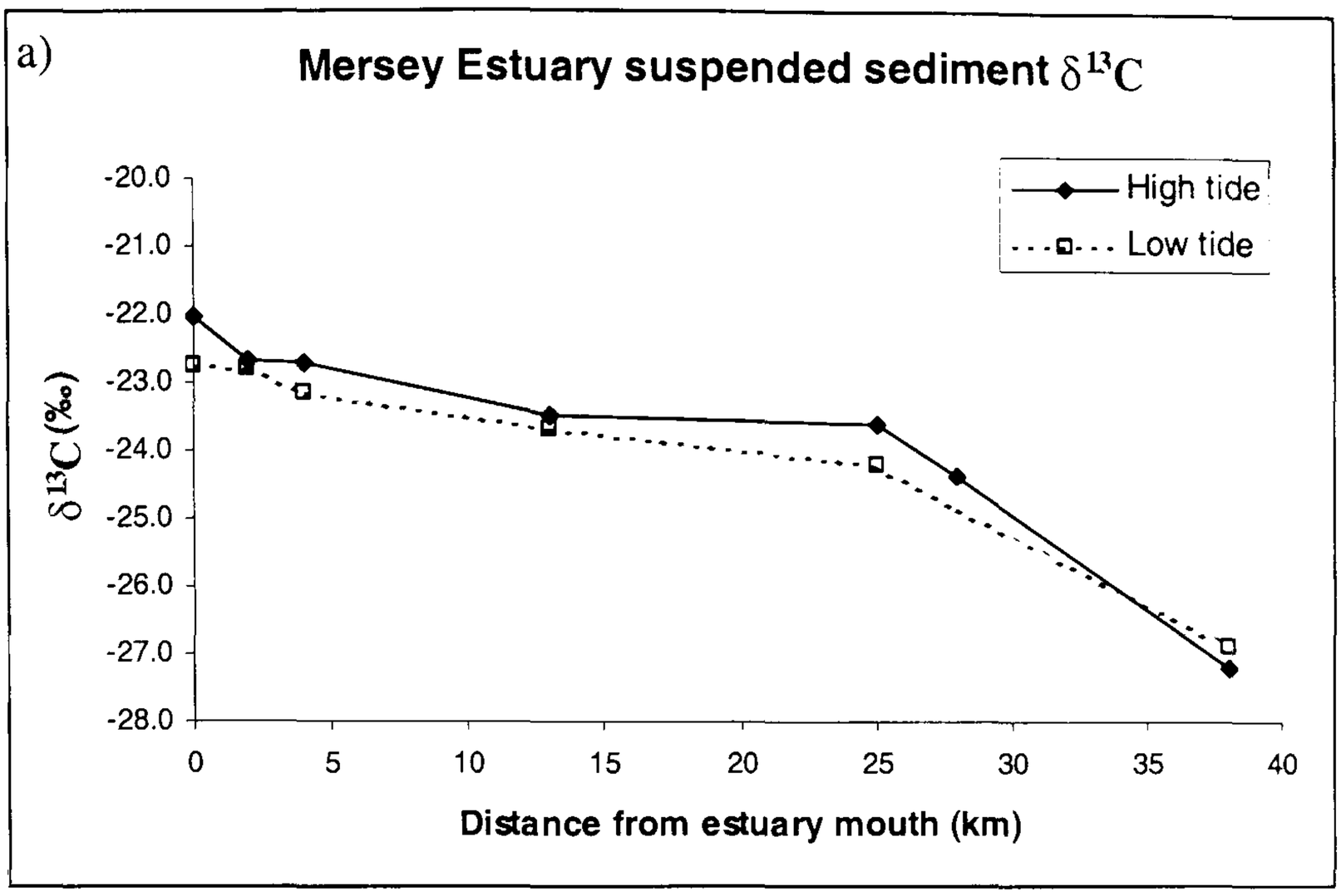

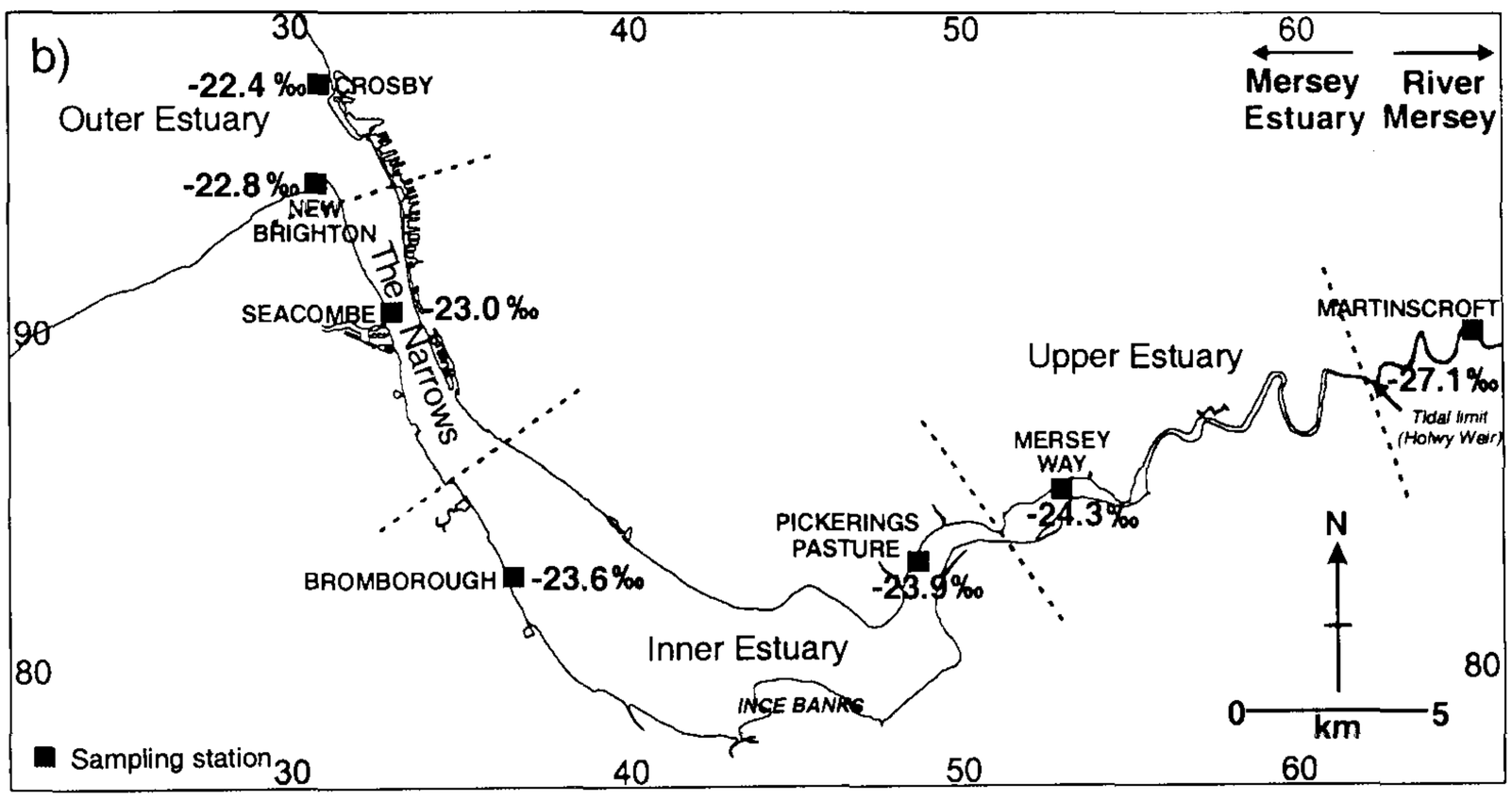

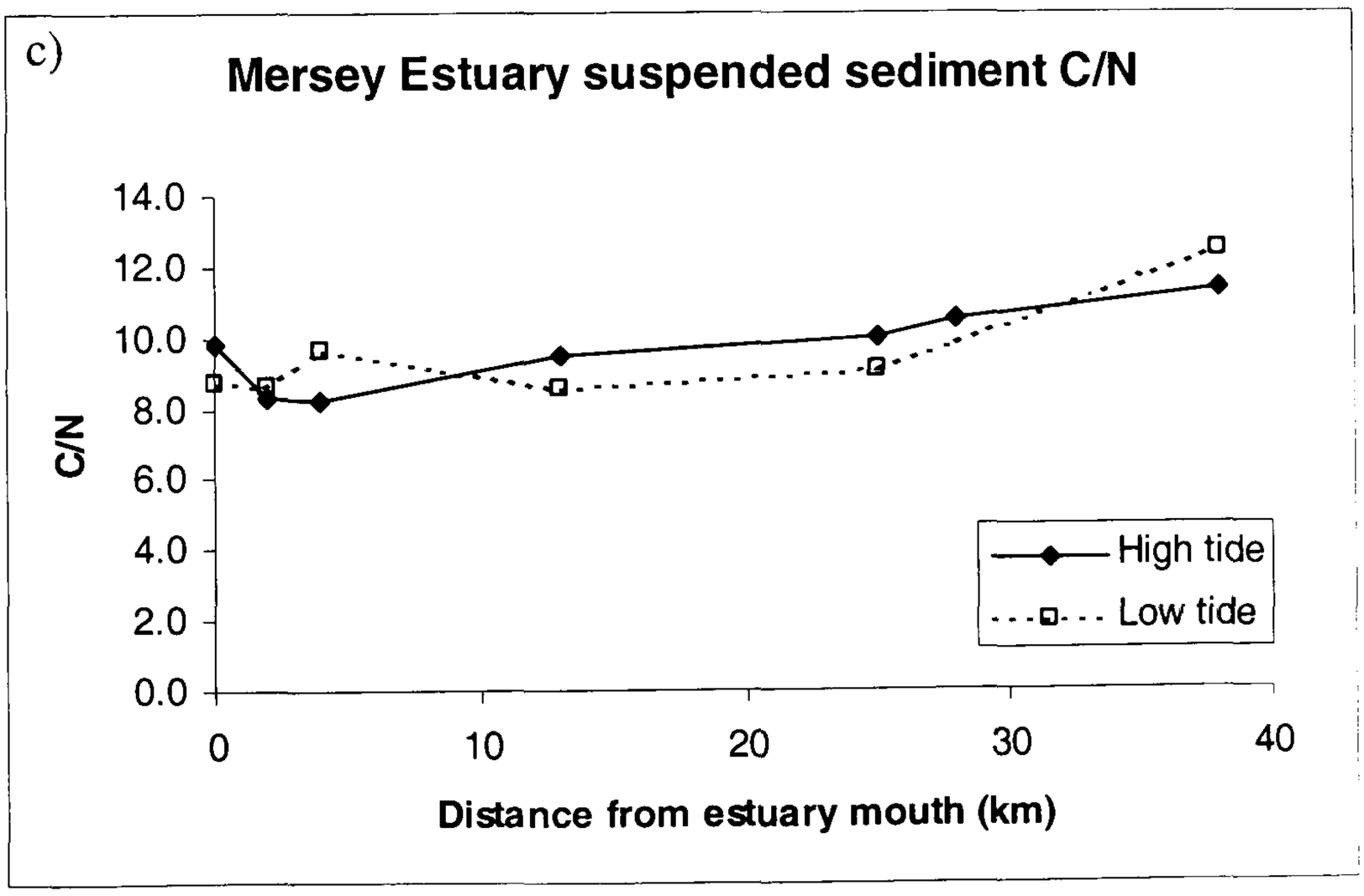

Figure 5.2. a) High and low tide $\delta^{13}C_{POC}$; b) mean tidal $\delta^{13}C_{POC}$; and c) high and low tide C/N_{POC} along the axis of the Mersey Estuary. See Appendix B for datasets.

Table 5.2. Mersey Estuary and River Mersey bulk organic surficial sediment $\delta^{13}C$ (see Figure 5.2b for locations).

Sampling station	Approximate distance from estuary mouth	Bulk organic surficial sediment $\delta^{13}C$
Bromborough (Inner Estuary)	13km	−23.2‰
Pickerings Pasture (Inner Estuary)	25km	−22.8‰
Martinscroft (River)	38km	−27.6‰

5.2.2 Interpretation

It is apparent from the difference in mean $\delta^{13}C_{POC}$ of 4.7‰ and in C/N_{POC} of approximately 2.0 between the marine and freshwater end-members of the Mersey Estuary and River Mersey (Crosby and Martinscroft respectively) that a change occurs in the content and provenance of suspended particulate organic matter (POM). Although microscopic analysis of the components contributing to the POM pool is beyond the scope of this study, it is apparent from the $\delta^{13}C_{POC}$ and C/N_{POC} values in the Outer Estuary, the Narrows and the Inner Estuary, that the POC pool is derived principally from marine plankton. Mean $\delta^{13}C_{POC}$ values of between –22.4‰ and –23.9‰, as observed at Crosby in the Outer Estuary and at Pickerings Pasture in the Inner Estuary respectively, occur within the range of marine POC (e.g. Laane *et al.*, 1990; Middelburg & Nieuwenhuize, 1998), whilst the C/N_{POC} values are relatively similar between the Outer and Inner Estuary and remain between 8.0 and 10.0, values typical of material dominated by phytoplankton (Tyson, 1995). In contrast, the $\delta^{13}C_{POC}$ and C/N_{POC} values of the River Mersey reveal that both terrigenous material and freshwater phytoplankton are important contributors to the POC pool. A $\delta^{13}C_{POC}$ of –27.1‰, as recorded at Martinscroft, is typical of C_3 terrigenous material (e.g. plant detritus, soils, colloidal humic substances and humin) and phytoplankton (Deines, 1980), the presence of both indicated by the slightly higher C/N ratios of between 11.3 and 12.4 recorded here (Tyson, 1995). A $\delta^{13}C_{POC}$ value of –24.3‰ and a C/N_{POC} value of 10.5 (high tide recordings, sediments at low tide were inaccessible) is observed at Mersey Way, indicating that the Upper Estuary zone is transitional between marine and riverine conditions.

The gradual and systematic decrease in $\delta^{13}C_{POC}$ along the axis of the Mersey Estuary with increasing distance from its mouth is also seen in other estuaries, for example the Schelde Estuary on the Netherlands-Belgium border (Middelburg & Nieuwenhuize, 1998) and the Great Ouse Estuary in the UK (Fichez *et al.*, 1993) (Section 2.3.4.1). Such studies have also demonstrated that suspended riverine $\delta^{13}C_{POC}$ is commonly between –29.0‰ and –26.0‰ (e.g. Shultz & Calder, 1976; Middelburg & Nieuwenhuize, 1998), reflecting a combination of C_3 terrigenous material, colloidal humic substances and humin eroded from catchment soils, and freshwater plankton (in particular phytoplankton). Furthermore, suspended marine POC in these estuaries, which consists almost entirely of plankton (phytoplankton in particular, e.g. Megens *et al.*, 2002), have similar $\delta^{13}C$ values as the Outer Mersey Estuary, between –23.0‰ and –20.0‰ (e.g. Laane *et al.*, 1990; Middelburg & Nieuwenhuize, 1998).

$\delta^{13}C$ measurement of bulk surficial sediment samples circumvents any seasonal effects on $\delta^{13}C_{POC}$ (e.g. changes in temperature, phytoplankton populations and numbers, terrigenous input, river discharge and longer-term tidal cycles) and will represent a longer-term average of $\delta^{13}C_{POC}$ for each station. The general decrease in $\delta^{13}C_{POC}$ with distance from the mouth of the Estuary is apparent in the limited bulk surficial sediment data, therefore indicating that this is a typical characteristic of the Mersey Estuary. It is fortunate that the limited surficial sediment $\delta^{13}C$ measurements are from Inner Estuary and River Mersey stations, where changes in $\delta^{13}C_{POC}$ were most pronounced. A significant change in surficial sediment $\delta^{13}C$, of nearly 5.0‰, is also apparent between these two zones of the Estuary. The sharp fall in suspended and surficial sediment $\delta^{13}C$ occurs because the sampling station at Martinscroft is located above the tidal limit at Howley Weir (Figure 5.2b), whilst all the other sampling stations are located within the tidal reaches. Seasonal salinity measurements, recorded over a three year period (see Appendix B for dataset), confirms that the sampling station at Martinscroft is unaffected by the tides, with salinity remaining at 0.5 ± 0.1‰

Aside from establishing the provenance of organic carbon, $\delta^{13}C$ analysis also provides an insight into the hydrological regime of an estuary. The large marine influence in the Mersey Estuary (Section 1.4) is reflected by the relatively high $\delta^{13}C_{POC}$ values recorded at stations up to approximately 30km upstream. Moreover, the comparatively small

freshwater discharge of the River Mersey is revealed by the notably small differences in $\delta^{13}C_{POC}$ between low and high tide, the largest difference being only 0.7‰. In addition, the decreasing $\delta^{13}C$ values with distance from the mouth of the Estuary, evident in both the suspended and surficial sediments, indicates that the Mersey Estuary is generally poorly mixed (although some mixing maybe evident between Bromborough and Pickerings Pasture; Table 5.2). Well-mixed estuaries, the Forth Estuary in Scotland for example, are characterised by relatively uniform suspended and surficial sediment $\delta^{13}C$ values (Graham *et al.*, 2001).

5.3 Mechanism for $\delta^{13}C$ and C/N as Holocene coastal and RSL indicators

$\delta^{13}C$ and C/N values of modern inter-tidal saltmarsh and tidalflat sediments, as well as sub-tidal estuarine sediments, reveals that $\delta^{13}C$ values increase and C/N ratios decrease, to a lesser extent, with decreasing ground elevation within the tidal frame. A difference in $\delta^{13}C$ of 5.0‰ separates the two end-members of the most landward high saltmarsh, organic rich, sediments (–27.8‰) and the sub-tidal, organic poor, estuarine sediments (–22.8‰). A difference in C/N of 2.3 between the most landward high saltmarsh sediments and the tidalflat sediments at station IB14 is also evident. The large difference in $\delta^{13}C$ between these two environments reflects the contrasting $\delta^{13}C$ composition of their source organic carbon. High saltmarsh vegetation has a mean $\delta^{13}C$ value of –27.1‰. The range in $\delta^{13}C$ values of the underlying high saltmarsh surface sediments (–27.8‰ to –25.2‰) indicates that vascular vegetation is an important source of organic carbon in these sediments, especially at stations located on the highest parts of the high saltmarsh. There is also an important organic carbon contribution from tidal-derived POC in the surface saltmarsh sediments, which is particularly well highlighted by the relatively low C/N ratios (9.7 to 11.6). In contrast to the saltmarsh sediment $\delta^{13}C$ and C/N values, $\delta^{13}C$ values of –23.6‰ have been obtained for POC suspended in the Inner Mersey Estuary, which reveals that the organic carbon in Inner Estuarine sub-tidal surficial sediments (–23.2‰ to –22.8‰) and Ince Banks tidalflat sediments (–23.7‰ to –23.5‰) is derived entirely from suspended POC. The range in surface sediment $\delta^{13}C$ and C/N values from low saltmarsh and lower elevated high saltmarsh areas (–25.8‰ to –24.7‰ and 9.3 to 10.8 respectively) reflect the mixing of the two contrasting source of organic carbon.

Surface saltmarsh sediment $\delta^{13}C$ values in the coastal zone appears to vary as a function of the frequency and duration of tidal flooding, which causes changes in the relative contribution of organic carbon in the sediments, from autochthonous, vascular vegetation, on the one hand and allochthonous, tidal-derived POC on the other. Indeed, abrupt and significant changes in surface sediment $\delta^{13}C$ values over short distances were recorded between stations when the ground elevation in these areas fell below an upper tidal limit. Based on modern inter-tidal and sub-tidal sediment analysis, it appears that ground elevation within the tidal frame is the principal controlling factor on both $\delta^{13}C$ and C/N. Indeed, ground elevation was also found to be the most influential variable governing diatom, foraminifera and testate amoebae assemblages (Charman *et al.*, 1998; Zong and Horton, 1998; Horton, 1999). The morphology of Ince Banks saltmarsh, the very wide high saltmarsh zone and the narrow low saltmarsh and tidalflat zones, has resulted in the bias distribution of modern $\delta^{13}C$ and C/N measurements in the high saltmarsh zone. Further $\delta^{13}C$ and C/N measurements on other saltmarshes, ideally with intact reedswamp areas, and with a more even distribution of saltmarsh zones, would perhaps reveal an even greater range in surface sediment $\delta^{13}C$ and C/N values.

It is apparent from the range in average $\delta^{13}C_{POC}$ along the axis of the Mersey Estuary, (from −22.4‰ at the marine-end member at Crosby, to −27.1‰ at the freshwater end-member at Martinscroft), that considerable variation in tidalflat and lower saltmarsh surface sediment $\delta^{13}C$ may result as a consequence of temporal variability in freshwater discharge rather than due to any change in saltmarsh elevation in relation to the tidal frame. This may be a complicating factor in attempting to apply $\delta^{13}C$ analysis to reconstruct Holocene RSL and coastal evolution, in particular at sites with a significant riverine input. Fortunately, variations in $\delta^{13}C$ driven by a change in freshwater discharge will be readily apparent in the sediment record from the C/N ratios. For example, a hypothetical period of high freshwater discharge may result in a change in tidalflat sediment $\delta^{13}C$ from –23.0‰ to –26.0‰. An unchanging C/N ratio would indicate continued plankton deposition, which, taken together with the lower $\delta^{13}C$ value, would indicate an increase in riverine POC. This hypothetical example underlines the importance of using $\delta^{13}C$ and C/N in combination in the field of coastal reconstruction.

It is evident from the results of the modern survey that $\delta^{13}C$ in particular satisfies a basic requirement of a sea-level and coastal environmental indicator, in that it is sensitive to changes in inter-tidal ground elevation in relation to the tidal frame. In addition, by using a combination of $\delta^{13}C$ and C/N analysis of sediment deposits, the complicating factor of variable riverine discharge, which would go undetected using $\delta^{13}C$ analysis alone, may be overcome. The results of the modern survey justify an investigation into the potential of $\delta^{13}C$ and C/N analysis as Holocene coastal palaeoenvironmental and sea-level indicators in the Mersey Estuary sediments.

Chapter 6

Helsby and Ince Marshes Holocene sediment deposits: Results of a multi-proxy investigation

6.1 Lithology

The stratigraphy of Helsby and Ince Marshes and Ince Banks (Figure 4.3) is shown in Figures 6.1 to 6.3 (see Appendix C for lithological descriptions). The pre-Holocene surface of Helsby Marsh was encountered between –1.00m OD and –2.00m OD, whilst the pre-Holocene surface of Ince Marshes and Ince Banks was not reached, and lies below –5.37m OD and –3.90m OD respectively.

6.1.1 Helsby Marsh

Basal peats, containing occasional wood fragments, are recorded between –1.62m OD and –0.76m OD in core Ince 5 and between –1.06m OD and –0.61m OD in core Ince 4 (Figure 6.1). The basal peat units sit on fine to medium sand deposits, which are underlain by glacial till in core Ince 5. Upper peat deposition occurs between +1.79m OD and +3.68m OD in core Ince 5 and between +2.18m OD and +3.63m OD in core Ince 4. Unlike core Ince 5, the upper peat deposition is not continuous in core Ince 4, but is interrupted by clay between +2.91m OD and +3.59m OD. The upper peat of core Ince 5 contains *Phragmites* remains between +1.79m OD and +2.26m OD and wood fragments between +2.26m OD and +3.29m OD. Wood fragments are also present in the upper peat of core Ince 4, occasionally between +2.18m OD and +2.34m OD, and commonly between +2.34m OD and +2.82m OD. Interspersed between the lower and upper peat units of cores Ince 5 and Ince 4 is a thick (c. 2.70m) minerogenic deposit, chiefly consisting of clay and silt. Overlying the upper peat of core Ince 5 is a second minerogenic deposit of clay and silt, from +3.68m OD to the core surface at +4.33m OD, which is mottled towards the base. The corresponding upper minerogenic deposit of core Ince 4, from +3.63 OD to the core surface at +5.42m OD, contains a more complex sequence, consisting of units of clay and silt (some of which contain *Phragmites* remains) and units of silt and sand.

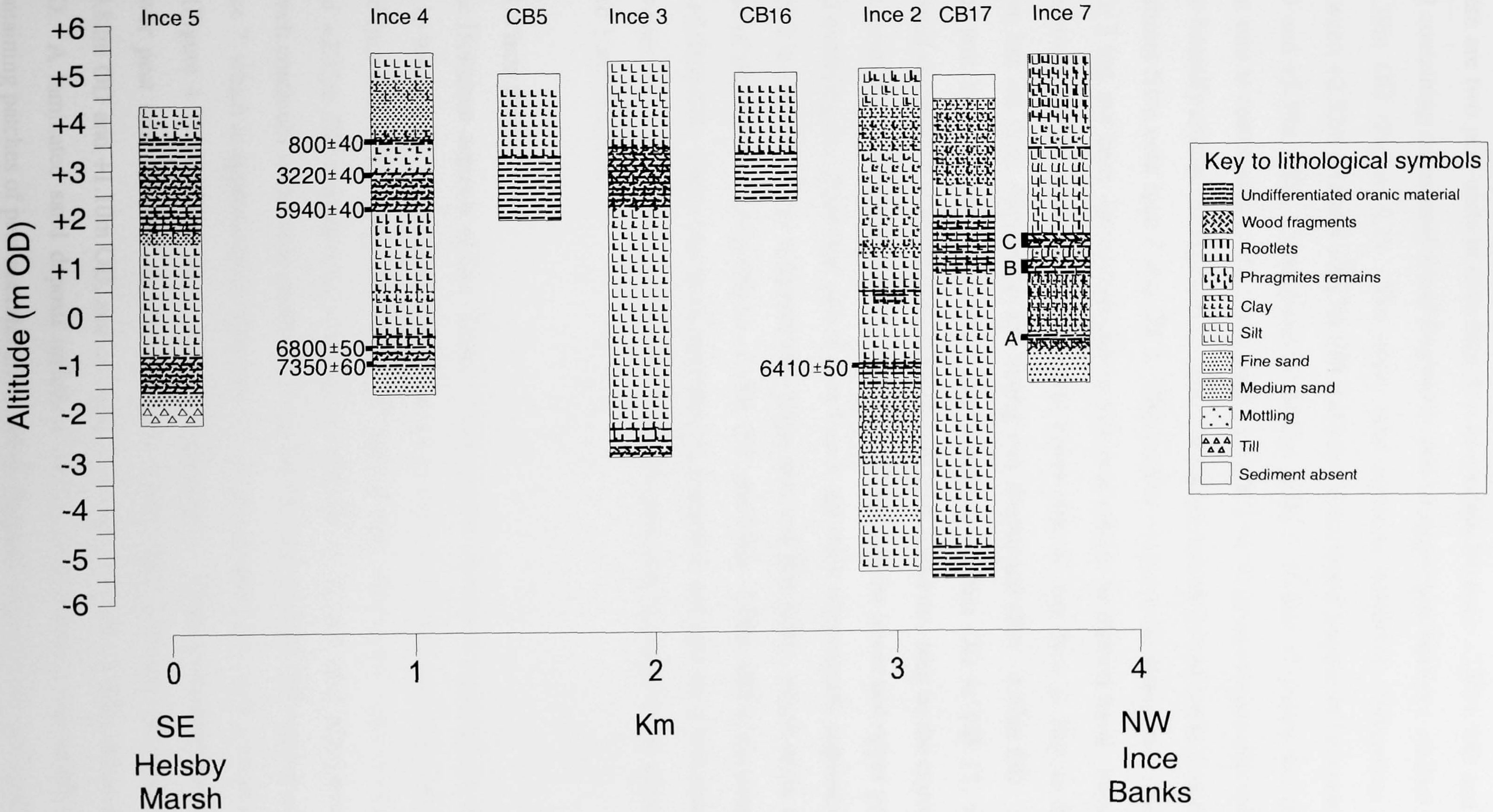

Figure 6.1. Helsby and Ince Marshes stratigraphy. Cores Ince 2 to Ince 7 were taken by the BGS, whilst cores CB5, CB16 and CB17 are commercial boreholes. Dates are in radiocarbon years BP and dates A, B and C from core Ince 7 are shown in Figure 6.3.

6.1.2 Ince Marshes

There are two peat units in core Ince 3: a lower peat between –2.97m OD and –2.63m OD containing occasional wood fragments, and an upper peat between +2.25m OD and +3.39m OD (Figure 6.1). The upper peat contains numerous *Phragmites* remains between +2.32m OD and +3.17m OD and occasional wood fragments between +2.32m OD and +3.39m OD. Commercial boreholes (CB) 5, 16 and 17 shows that the upper peat unit is continuous to the north west, and CB 1 to 13 demonstrates that this unit is also laterally extensive (Figure 6.2). This unit is not recorded in all cores, however, and is absent from core Ince 2 and CB 8. The vertical extent of the lower peat unit in core Ince 3 has not been determined and so this peat cannot be termed basal *sensu stricto*. Moreover, the presence of an equivalent lower peat in core Ince 2, 1km to the north west, has not been determined and coring was abandoned after –5.37m OD. A lower peat unit has been recorded below approximately –4.86m OD in CB 17, which is located around 0.4km to the north west of core Ince 2, and this may be the equivalent of the lower peat unit of core Ince 3. Interspersed between the lower and upper peat units, and overlying the upper peat unit of core Ince 3, are thick minerogenic sequences. Core Ince 2 is almost entirely dominated by clays, silts and fine sands, which occur from the base of the core at –5.37m OD to –1.15m OD, and from –1.08m OD to the core surface at +5.08m OD. These two thick minerogenic sequences are split by a thin muddy peat between –1.15m OD and –1.08m OD. This thin peat unit is absent in the adjacent core Ince 3 and in CB14.

6.1.3 Ince Banks

The Holocene deposits of Ince Banks consist almost entirely of minerogenic sequences up to 9m in thickness (Figure 6.3). Medium to fine sands are persistent in cores Ince 8 and Ince 6 from their base at –3.90m OD and –3.01m OD respectively, to +1.81m OD and +2.33m OD respectively, whereupon a change to silt and clay deposition occurs, which continues to the core surfaces at +5.11m OD and +5.29m OD respectively. Core Ince 7, which is approximately 1km east of core Ince 6 and 1km north west of core Ince 2 (Figure 4.3), records a more complex stratigraphy. Three peat units are present: a lower peat unit between –0.58m OD and –0.44m OD, a middle peat unit between +0.82m OD and +1.10m OD, and an upper peat unit between +3.40m OD and +3.44m OD. A laminated sand deposit underlies the lower peat and a fine sandy silt unit, containing patches of peat material and rootlets, intercalates the lower and middle peat.

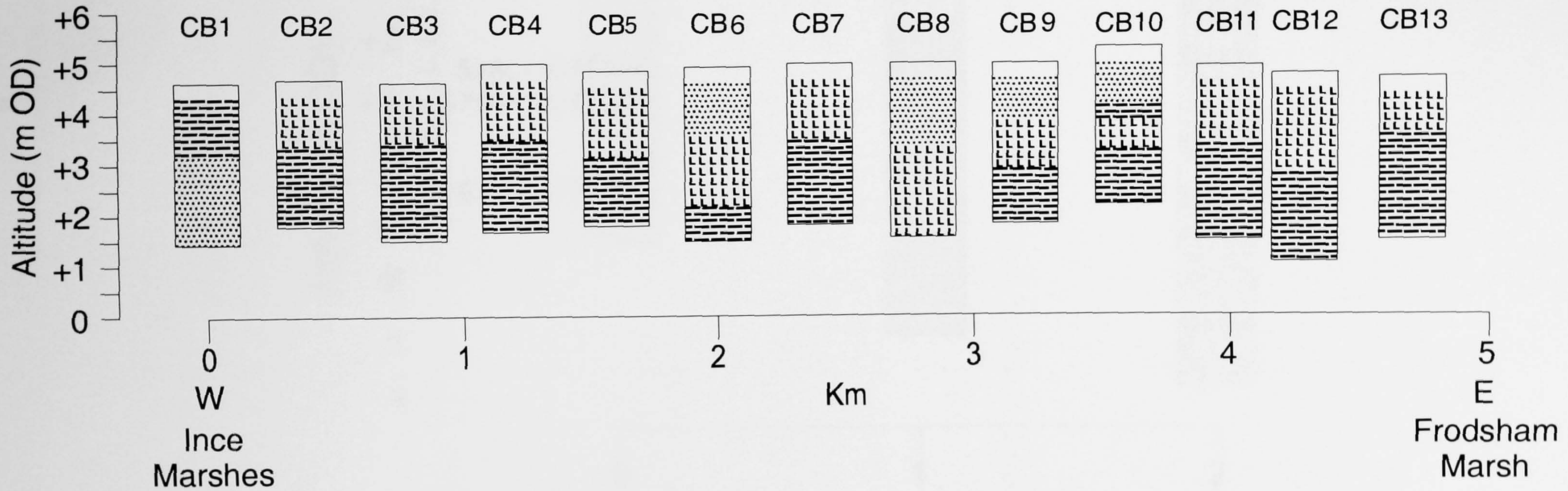

Figure 6.2. Commercial boreholes along an east-west transect between Helsby and Ince Marshes. The key to the lithological symbols is presented in Figure 6.1.

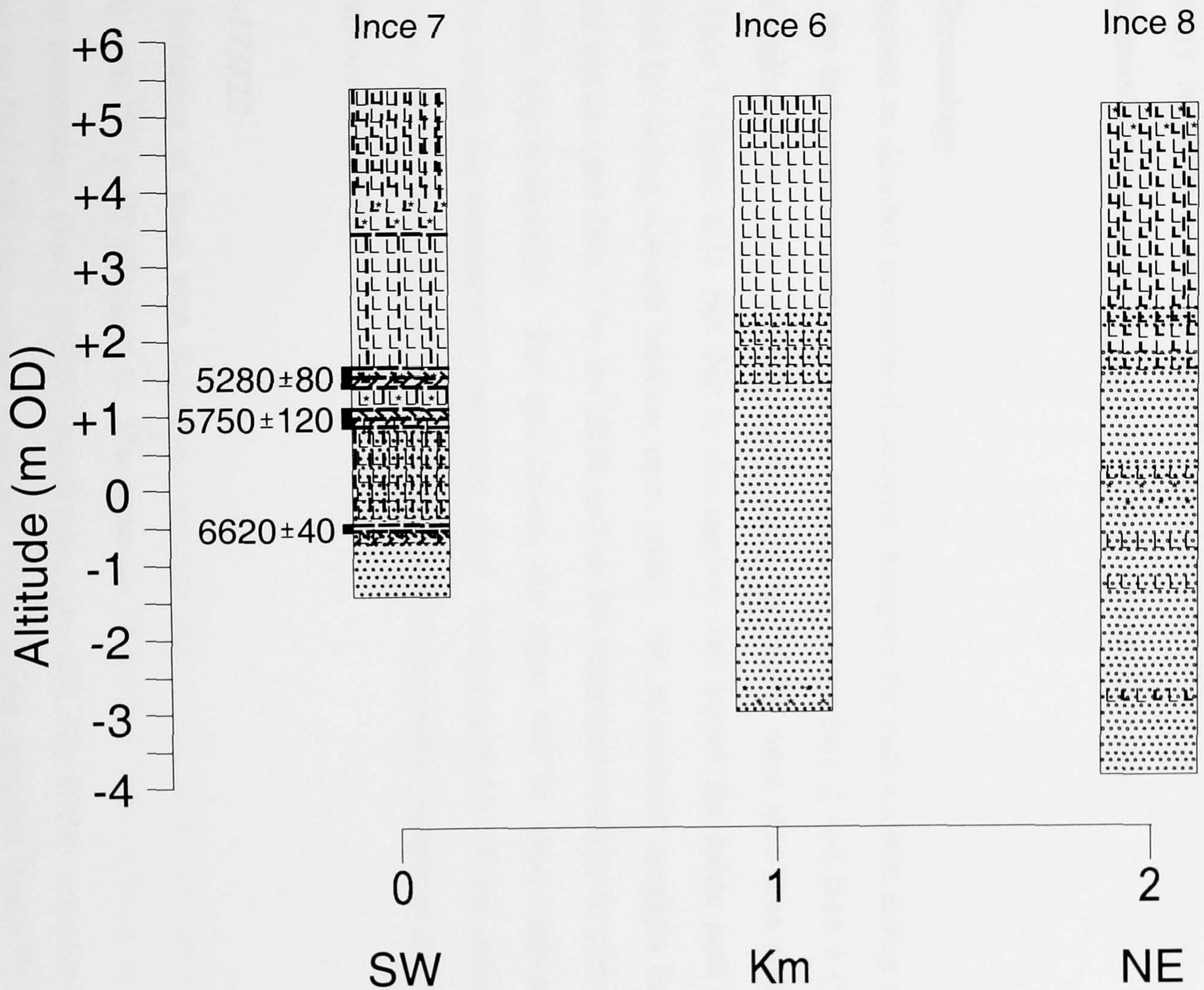

Figure 6.3. Ince Banks stratigraphy. All cores were taken by the BGS. Dates are in radiocarbon years BP. The key to the lithological symbols is presented in Figure 6.1.

The middle and upper peat is intercalated by a mottled silt unit, again containing patches of peat material and rootlets, whilst a thick (1.92m) silty clay unit, containing root fragments, caps the upper peat.

Cores Ince 4 (Helsby Marsh) and Ince 2 (Ince Marshes) have been chosen for detailed multi-proxy analysis in order to capture the range of coastal palaeosedimentary environments that have fringed the Mersey Estuary throughout the Holocene. This is necessary in order to investigate the potential of $\delta^{13}C$ and C/N analysis as coastal palaeoenvironmental indicators across a range of sediment types.

6.2 Chronology

Subsequent to detailed microfossil analysis, samples for radiocarbon dating were taken from the transgressive and regressive overlaps of cores Ince 2 and Ince 4 (Table 6.1). Three radiocarbon dates, relating to the three peat units, have also been obtained from core Ince 7 (Table 6.1), but due to the narrow core barrel the entire peat units were required for dating (Gareth Jenkins, pers. com.). No microfossil analysis has yet been carried out on core Ince 7 by the BGS and so the radiocarbon dates in core Ince 7 are currently uncorroborated. For this reason the dates will be used cautiously in the present study for comparative purposes only. Pollen analysis of the dated sediment horizons of cores Ince 4 and Ince 2 is used as an independent means to accept or reject the radiocarbon dates.

Beta-173722

The initiation of basal peat deposition in core Ince 4 has been radiocarbon dated at 7,350 ± 60 ^{14}C yr BP (Table 6.1). The presence of *Alnus* and the absence of *Tilia* in the pollen assemblage (local pollen assemblage zone (LPAZ) HMa) indicates deposition during the FId / FII chronozone boundary, in particular between 7,460 ^{14}C yr BP and 6,880 ^{14}C yr BP (Figure 6.4) (Hibbert *et al.*, 1971). Based on independent verification, together with its correct chronostratigraphic position in the sediment core, this radiocarbon date appears valid.

Beta-173723

Cessation of the basal peat unit in core Ince 4 has been radiocarbon dated at 6,800 ± 50 ^{14}C yr BP (Table 6.1). The presence of *Alnus*, *Tilia* and *Ulmus* in the pollen assemblage

Table 6.1. Radiocarbon dates from transgressive and regressive overlaps at Helsby and Ince Marshes and Ince Banks. Calibrated ages are based on Stuiver *et al.* (1998).

Site	Core	National Grid Reference	Laboratory Code	Core depth (cm)	Altitude (m OD)	Material	Date (1σ) (^{14}C years BP)	Calibrated age range BP (2σ)	Technique
Helsby Marsh	Ince 4	SJ 4792 7641	Beta-173100	179 to 183	+3.63 to +3.59	Peat	800 ± 40	780-670	AMS
Helsby Marsh	Ince 4	SJ 4792 7641	Beta-173724	251 to 256	+2.91 to +2.86	Peat	3,220 ± 40	3,490-3,360	AMS
Helsby Marsh	Ince 4	SJ 4792 7641	Beta-173099	319 to 324	+2.23 to +2.18	Peat	5,940 ±40	6,860-6,670	AMS
Helsby Marsh	Ince 4	SJ 4792 7641	Beta-173723	603 to 608	–0.61 to –0.66	Peat	6,800 ± 50	7,700-7,580	AMS
Helsby Marsh	Ince 4	SJ 4792 7641	Beta-173722	643 to 648	–1.06 to –1.01	Peat	7,350 ± 60	8,330-8,010	AMS
Ince Marshes	Ince 2	SJ 4668 7730	Beta-173725	616 to 623	–1.08 to –1.15	Organic mud	6,410 ± 50	7,430-7,250	AMS
Ince Banks	Ince 7	SJ 4590 7758	Beta-176449	370 to 400	+1.66 to +1.36	Peat	5,280 ± 80	6,280-5,900	Radiometric
Ince Banks	Ince 7	SJ 4590 7758	Beta-176447	425 to 450	+1.11 to –0.78	Peat	5,750 ± 120	6,790-6,300	Radiometric
Ince Banks	Ince 7	SJ 4590 7758	Beta-176448	580 to 590	–0.44 to –0.54	Peat	6,620 ± 40	7,850-7,440	AMS

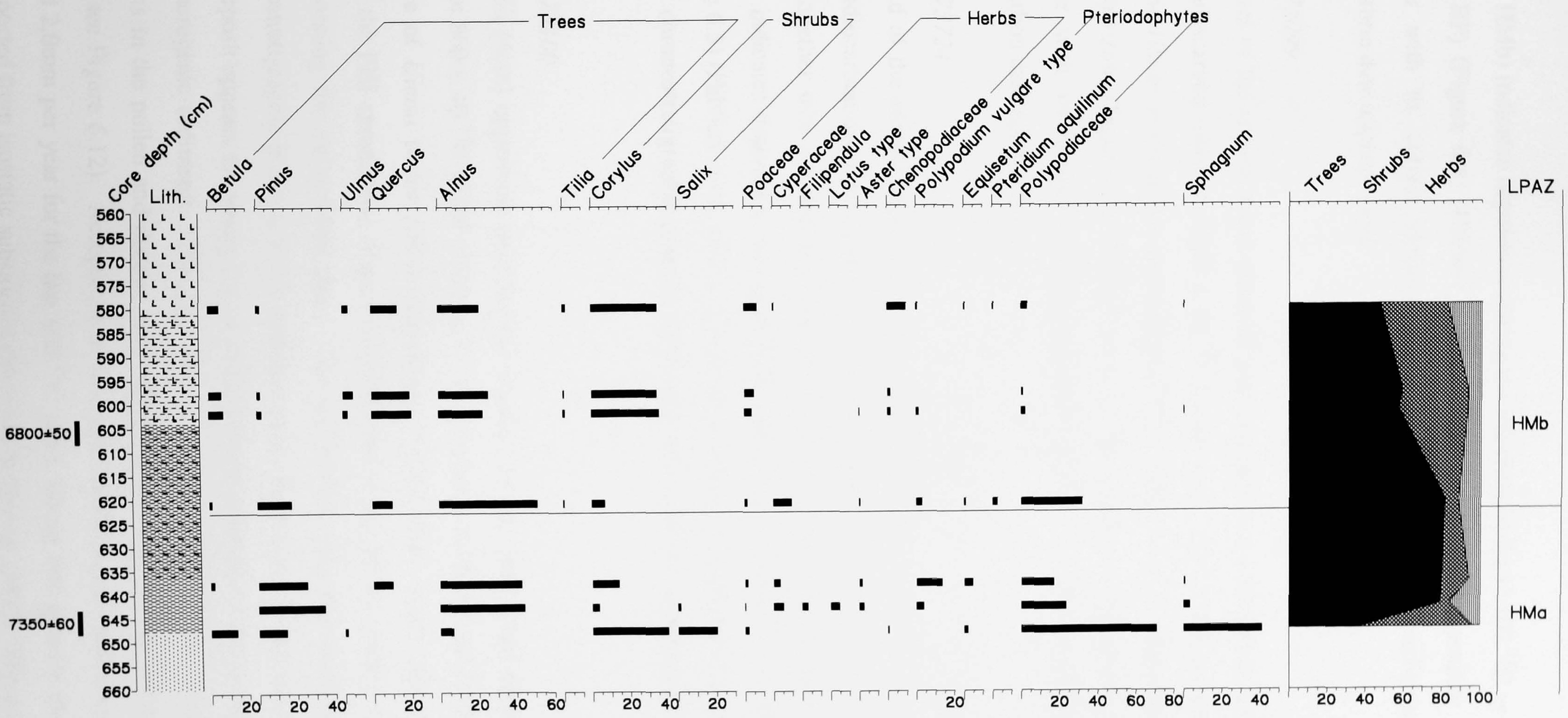

Figure 6.4. Core Ince 4 lower peat pollen assemblages (660cm to 560cm; -1.18m OD to -1.02m OD). Dates are in radiocarbon years BP.

(LPAZ HMb) indicates deposition during the FII chronozone (7,107 ^{14}C yr BP to 5,010 ^{14}C yr BP) (Figure 6.4) (Hibbert *et al.*, 1971). Based on independent verification, together with its correct chronostratigraphic position in the sediment core, this radiocarbon date appears valid.

Beta-173099

The onset of the second major phase of peat accumulation recorded in core Ince 4 has been radiocarbon dated at 5,940 ± 40 ^{14}C (Table 6.1). Again, the presence of *Alnus*, *Tilia* and *Ulmus* in the pollen assemblage (LPAZ HMb) indicates deposition during the FII chronozone (Figure 6.5) (Hibbert *et al.*, 1971). Based on independent verification, together with its correct chronostratigraphic position in the sediment core, this radiocarbon date appears valid.

Beta-173724

The end of the second major phase of peat accumulation recorded in core Ince 4 has been radiocarbon dated at 3,220 ± 40 ^{14}C yr BP (Table 6.1). The presence of *Alnus* and *Tilia*, together with the near total absence of *Ulmus* in the pollen assemblage (LPAZ HMc), indicates deposition during the FIII chronozone (5,010 ^{14}C yr BP to present) (Figure 6.5) (Hibbert *et al.*, 1971). Based on independent verification, together with its correct chronostratigraphic position in the sediment core, this radiocarbon date appears valid.

Beta-173100

The thin (4cm) uppermost peat deposit recorded in core Ince 4 has been radiocarbon dated at 800 ± 40 ^{14}C yr BP (Table 6.1). The presence of *Alnus* and *Tilia* and the near absence of *Ulmus* in the pollen assemblage (LPAZ HMc) again indicate deposition during the FIII chronozone (Figure 6.6) (Hibbert *et al.*, 1971), thereby independently corroborating the radiocarbon date. The radiocarbon date also occupies its correct chronostratigraphic position in the sediment core. However, the age of this uppermost peat deposit appears too young for its stratigraphical position, as it is overlain by 1.79m of minerogenic sediments. This peat unit is unquestionably *in situ*, evident from the changes in the pollen and diatom assemblages of the peat and the adjacent sediment units (see Figure 6.12). Acceptance of this date would require sedimentation rates of around 2.0mm per year for the last 800 ^{14}C years, taking into account the rate of RSL fall expected from isostatic subsidence (Shennan & Horton, 2002). There is evidence of

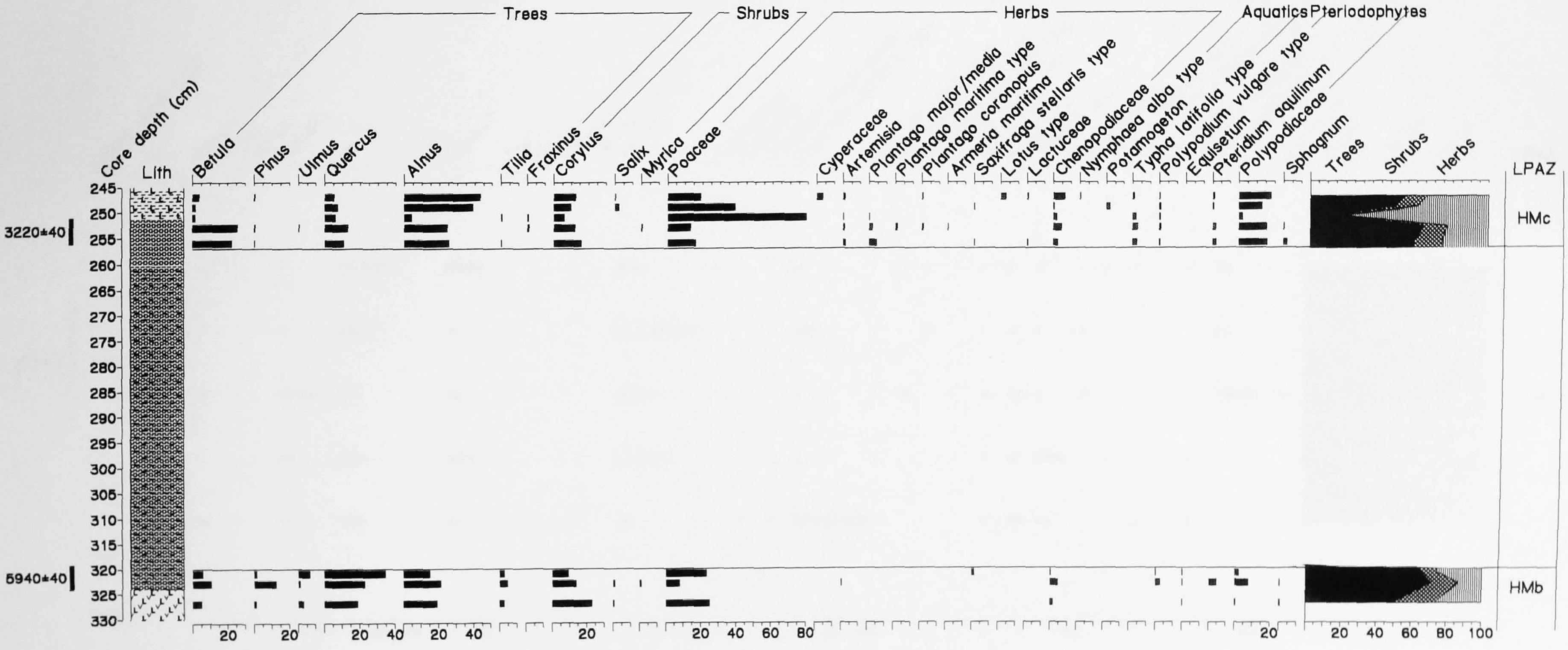

Figure 6.5. Core Ince 4 middle peat pollen assemblages (330cm to 245cm; +2.12m OD to +2.97m OD). Dates are in radiocarbon years BP.

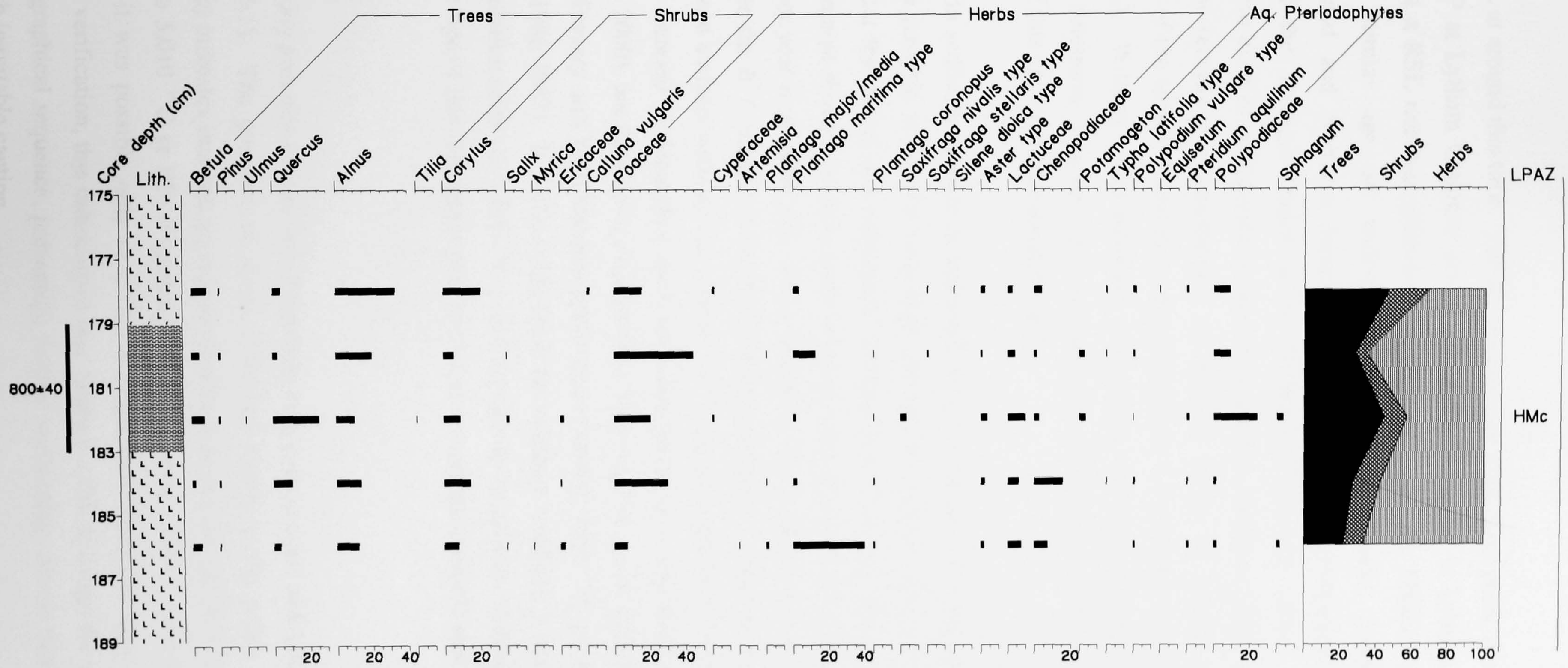

Figure 6.6. Core Ince 4 upper peat pollen assemblages (189cm to 175cm; +3.53m OD to +3.67m OD). Dates are in radiocarbon years BP.

a rise in RSL at around this time. The accumulation of dune slack peats, dated at 805 ± 70 ^{14}C yr BP at Lytham Common and at 830 ± 50 ^{14}C yr BP at Lytham Hall Park. indicates that a RSL rise was underway (Tooley, 1974, 1978a, 1982b). Dune slack peats of a similar age are widespread (e.g. on the Wirral, North Norfolk, Northumberland and Northern Ireland coastlines) and are comparable with the formation of the Younger Dunes in the Netherlands (Tooley, 1990). Historical recordings also exist of an increase in marine conditions. Morton (1887) cites earlier literature that records the abandonment of Stanlow Abbey by monks in 1294 'in consequence of the terrible inundations that flooded the surrounding country' (Morton. 1887, p. 351). Without actual estimates of the rates of RSL rise, however, it is not possible to determine whether an acceleration in RSL rise resulted in the rapid deposition of this uppermost minerogenic unit.

An increase in sediment deposition, unrelated to any movement in RSL, could also be invoked as a possible reason for such high sedimentation rates. Long *et al.* (1999a) speculated that the arrival and subsequent dominance of *Spartina anglica* in a Poole Harbour saltmarsh resulted in an increase in sedimentation rates from 1.14mm per year to 7.17mm per year from 1890 AD. This explanation can be discounted for the present study because the δ^{13}C values of the characteristic saltmarsh sediments, from +4.83m OD to the core surface, indicate the absence of C_4 plants, such as *S. anglica* (Figure 6.16a). An increase in deposition rates may also result from catchment disturbance (Long *et al.*, 2000), but vegetation clearance has been ongoing in the catchment area of the Mersey Estuary and its tributaries since approximately 4,000 ^{14}C yr BP (Innes & Tomlinson, 1986-1987). It is clear that, from the evidence available, a mechanism for high sedimentation rates since 800 ^{14}C yr BP remains to be proven. Consequently, the reality of the age of this thin upper peat unit must remain questionable and is therefore not used.

Beta-173725

The thin muddy peat unit of core Ince 2 has been radiocarbon dated at 6,410 ± 50 ^{14}C yr BP (Table 6.1). The presence of *Alnus*, *Tilia* and *Ulmus* in the pollen assemblage (LPAZ HMb) indicates that this deposit accumulated during the FII chronozone (7,107 ^{14}C yr BP to 5,010 ^{14}C yr BP) (Figure 6.7) (Hibbert *et al.*, 1971). Due to analytical difficulties, it was possible only to obtain a single date from this core. Based on independent verification, this radiocarbon date appears valid, although the absence of a chronostratigraphical sequence, preventing further verification, means that this date is accepted with inevitable caution.

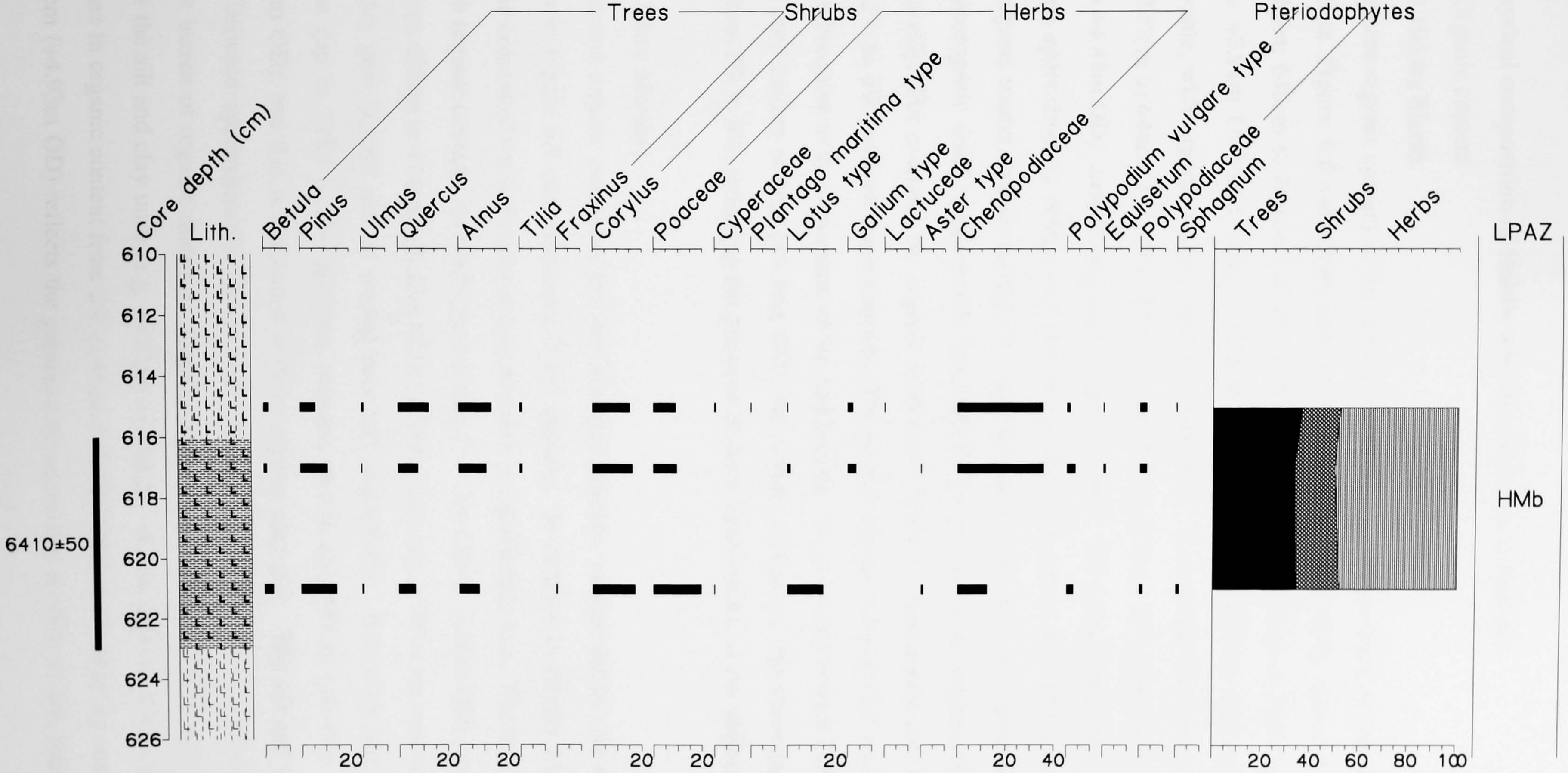

Figure 6.7. Core Ince 2 pollen assemblages (626cm to 610cm; -1.18m OD to -1.02m OD). Dates are in radiocarbon years BP.

6.3 Physical composition of Helsby and Ince Marshes sediments

6.3.1 Organic content

6.3.1.1 Helsby Marsh

The percent organic content of the Helsby Marsh deposits, as recorded in core Ince 4, is shown in Figure 6.8 (see Appendix D for dataset). The three episodes of peat deposition: 648cm to 603cm (–1.06m OD to –0.61m OD), 324cm to 251cm (+2.18m OD to +2.91m OD) and 183cm to178cm (+3.59m OD to +3.64m OD) are clearly observable, with organic content reaching over 80%. In contrast, the fine sand units, from 707cm to 648cm (–1.65m OD to –1.06m OD) and from 153cm to 94cm (+3.89m OD to +4.48m OD), contain negligible organic matter. The intercalated clays and silts between approximately 500cm and 400cm (+0.42m OD and +1.42m OD) also contain little organic matter, approximately 3%. An increase and decrease in organic content of the minerogenic units is discernible immediately before and after organic deposition respectively. For example, the organic content of the lower minerogenic unit increases from 2% to 8% between approximately 401cm and 326cm (+1.41m OD and +2.16m OD), subsequent to the deposition of the middle peat. From 61cm (+4.81m OD) to near to the core surface at 6cm (+5.36m OD), the organic content of this minerogenic unit rises from 2% to 8%, reflecting the presence of occasional rootlets in the sediments.

6.3.1.2 Ince Marshes

The percent organic content of the Ince Marshes deposits, as recorded in core Ince 2, is shown in Figure 6.9 (see Appendix D for dataset). In contrast to Helsby Marsh, the organic content of the sediments at Ince Marshes is significantly less. The two episodes of high organic content, from 623cm to 616cm (–1.15m OD to –1.08m OD) (up to 30%) and from 485cm to 474cm (+0.23m OD to +0.34m OD) (up to 70%) are associated with a muddy peat deposit and an eroded peat ball respectively. Relatively high organic content (up to 22%) is also apparent between 461cm and 457cm (+0.47m and OD +0.51m OD), and this is associated with an organic clay unit. The silt and fine sand units between approximately 930cm and 630cm (–4.22m OD and –1.22m OD) are almost barren of organic material. Slightly more organic matter (2% to 4%) is found within the silt and clay units (e.g. 1042cm to 950cm; –5.34m OD to –4.42m OD). An increase in organic content from 2% at 45cm (+4.63m OD) to 8% near the core surface at 15cm (+4.93m OD) reflects the presence of occasional rootlets in this minerogenic unit.

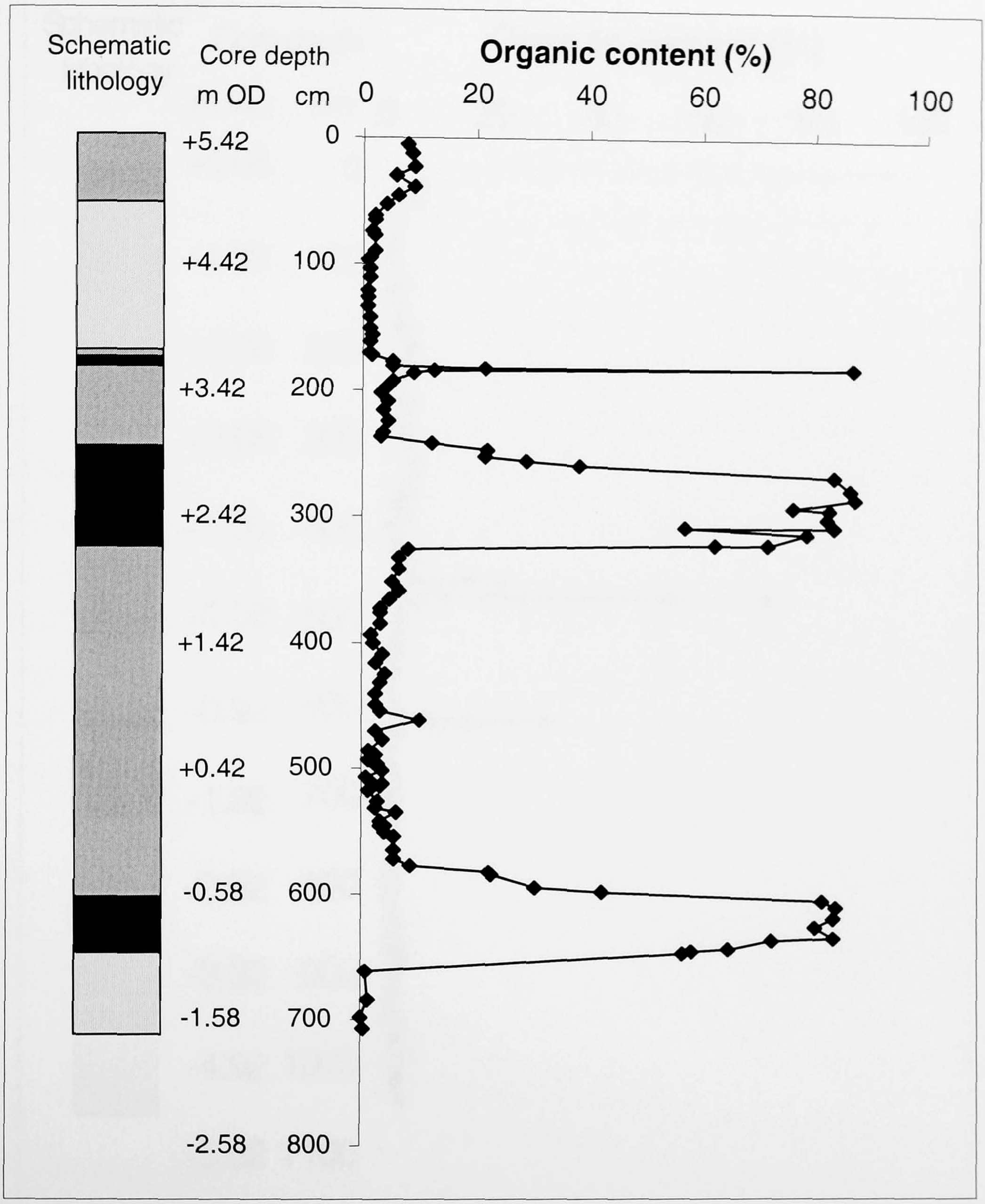

Figure 6.8. Organic content of Helsby Marsh (core Ince 4) sediments by loss on ignition. For the schematic lithology, black represents organic rich horizons, dark grey represents silts and clays, whilst light grey represents sand.

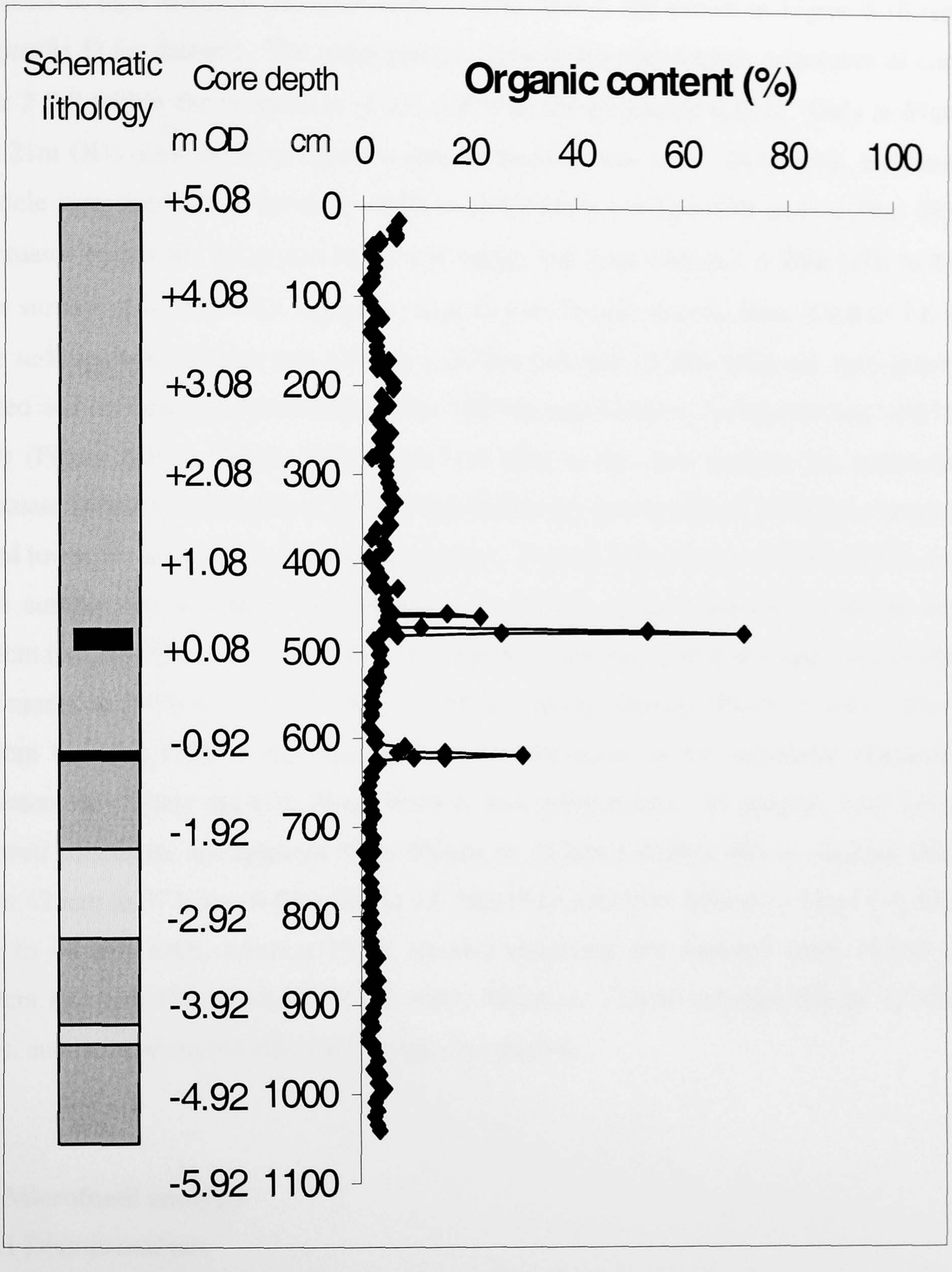

Figure 6.9. Organic content of Ince Marshes (core Ince 2) sediments by loss on ignition. For the schematic lithology, black represents organic rich horizons, dark grey represents silts and clays, whilst light grey represents sand.

6.3.2 Particle size analysis

The mean, sorting and skewness of the particle size distributions of the sediment deposits at Ince Marshes, as represented in core Ince 2, are shown in Figure 6.10 (see Appendix D for dataset). The mean particle sizes of the minerogenic sequences of core Ince 2 fall within the boundaries of silt (4.0 ϕ to 8.0 ϕ) (Figure 6.10a). Only at 87cm (+4.21m OD) does the mean particle size increase to fine sand. In general, the mean particle size distribution between 1043cm and 644cm (–5.35m OD and –1.36m OD) fluctuates within the 4.1 ϕ and 6.5 ϕ size range, but from 644cm (–1.36m OD) to the core surface at +5.08m OD, a greater range in particle size occurs, from 3.8 ϕ to 7.6 ϕ. The sediments at 1043cm and 1035cm (–5.35m OD and –5.27m OD) are very poorly sorted and become poorly sorted between 1027cm and 515cm (–5.19m OD and –0.07m OD) (Figure 6.10b). From 487cm (+0.21m OD) to the core surface, the sediments fluctuate between the classes of poorly sorted and very poorly sorted, although a general trend towards very poorly sorted is discernable. Indeed, from 69cm (+4.39m OD) to the core surface, the sediments are entirely very poorly sorted. Between 1042cm and 644cm (–5.34m OD and –1.36m OD) the sediments are very finely skewed, save for the sediments at 1035cm (–5.27m OD), which are finely skewed (Figure 6.10c). From 644cm (–1.36m OD) to the core surface, the skewness of the sediments fluctuates between very finely skewed, finely skewed and symmetrical. In general, very finely skewed sediments are apparent from 606cm to 487cm (–0.98m OD to +0.21m OD), from 426cm to 373cm (+0.82m OD to +1.35m OD), and from 165cm to 52cm (+3.43m OD to +4.56m OD), whereas finely skewed sediments are apparent from 467cm to 430cm (+0.41m OD to +0.78m OD), from 365cm to 173cm (+1.43m OD to +3.35m OD), and from 46cm (+4.62m OD) to the core surface.

6.4 Microfossil analysis

6.4.1 Diatom analysis

6.4.1.1 Helsby Marsh

Core depth 707cm to 300cm (–1.65m OD to +2.42m OD)

Diatom preservation in the sediments from this part of the core was generally very good, allowing at least 300 diatom valves to be counted for the majority of levels analysed. Between 648cm and 644cm (–1.06m OD and –1.02m OD), the diatom assemblages are dominated by freshwater epiphytes, such as *Gomphonema angustatum*,

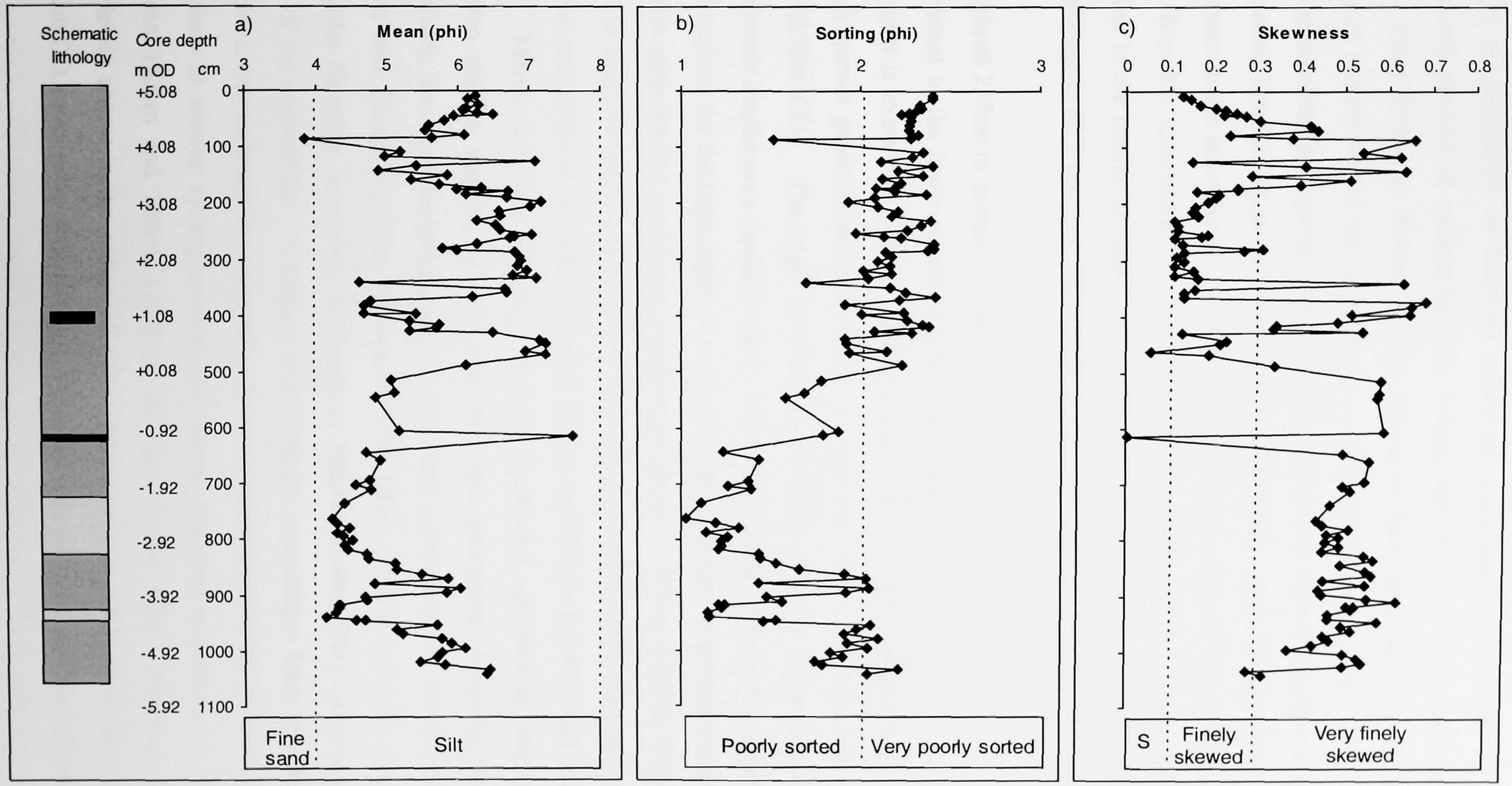

Figure 6.10. Core Ince 2 particle size data: a) mean particle size; b) sorting and c) skewness (S = symmetrical). For the schematic lithology, black represents organic rich horizons, dark grey represents silts and clays, whilst light grey represents sand.

which attains frequencies of over 40% (Figure 6.11, see Appendix E for datasets). A change in dominance to brackish freshwater tychoplankton species, in particular *Fragilaria pinnata*, is evident between 606cm and 581cm (–0.64m OD and –0.39m OD). From 557cm to 384cm (–0.15m OD to +1.58m OD) marine plankton species comprise around 40% of the assemblages, in particular *Paralia sulcata*, which is present in large numbers throughout, and marine tychoplankton, marine brackish epipsammon and marine brackish epipelon species are also common. *Navicula peregrina* becomes prominent in the assemblages at 365cm (+1.77m OD) and at 354cm (+1.88m OD) and then *Nitzschia navicularis* at 333cm (+2.09m OD), significantly contributing to the increase in the marine brackish epipelon ecological group from approximately 10% to approximately 80% between 365cm and 333cm (+1.77m OD and +2.09m OD).

Core depth 255cm to surface (+2.87m OD to +5.42m OD)

In contrast to the lower levels of core Ince 4, diatom preservation in the upper core sediments is extremely variable, but in general relatively poor (Figure 6.12). Marine diatom species generally dominate in the peat between 255cm and 250cm (+2.87m OD and +2.92m OD). The high frequencies of *Paralia sulcata* (approximately 10%), *Rhaphoneis amphiceros* (approximately 25%) and *Delphineis surirella* (approximately 30%) account for the importance of marine plankton, marine tychoplankton and marine brackish epipsammon ecological groups respectively at 255cm (+2.87m OD). Marine brackish epipelon species, in particular *Navicula digito-radiata* and *Navicula peregrina*, become prominent in the assemblages at 252cm and 250cm (+2.90m OD and +2.92m OD). Marine brackish epipelon, brackish freshwater aerophilous and freshwater epipelon diatom species, in particular *Navicula peregrina*, *Navicula pusilla* and *Pinnularia lata var. latestriata,* are all important components of the assemblages at 236cm and 232cm (+3.06m OD and +3.10m OD). Marine brackish epipelons, in particular *Navicula peregrina*, dominates at 196cm (+3.46m OD), comprising around 80% of the assemblage. A change in the diatom assemblages from marine brackish epipelons, marine brackish aerophilous, brackish freshwater aerophilous and freshwater epipelons to marine tychoplanktons and marine brackish epipsammons is apparent between 182cm and 169cm (+3.60m OD and +3.73m OD). Diatoms are almost completely absent in the sediments from 160cm (+3.82m OD) to the core surface at +5.42m OD, save for an assemblage at 93cm (+4.49m OD) consisting of marine

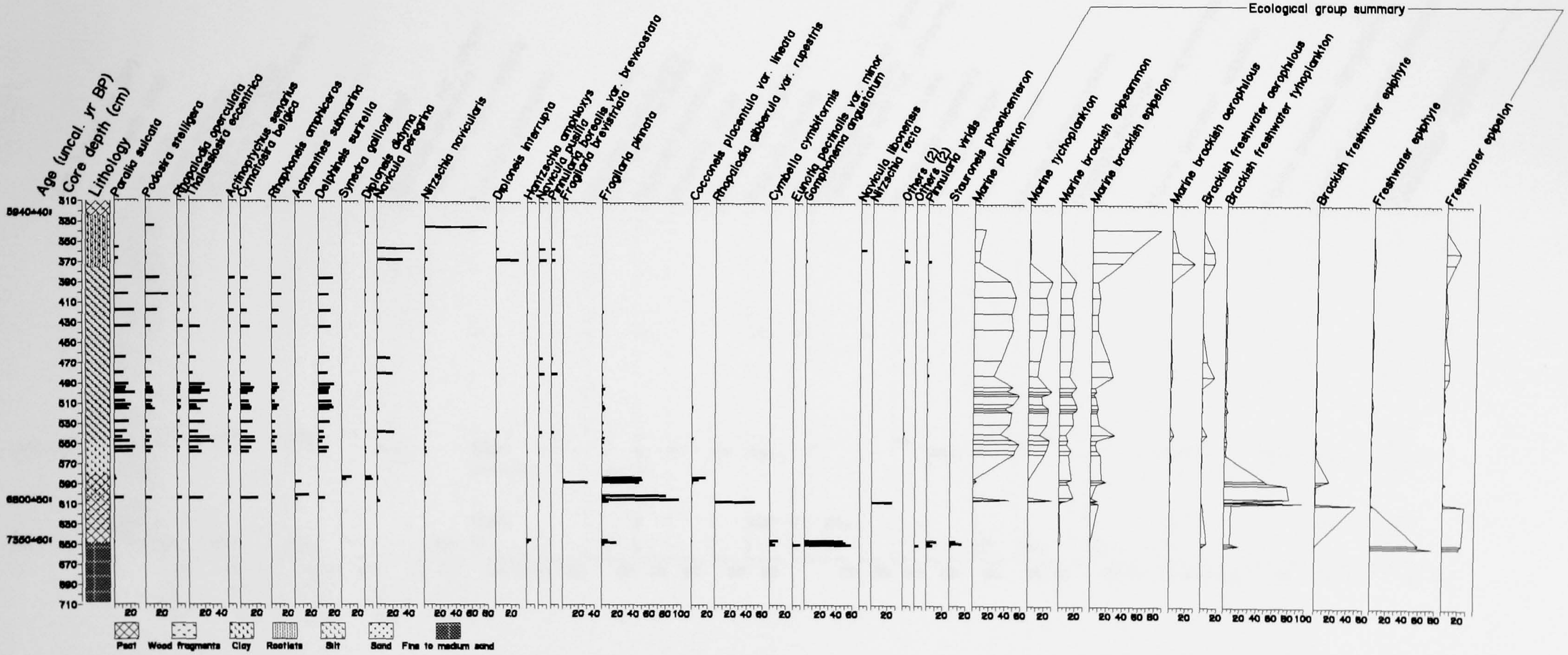

Pinnularia lata var. *latestriata* and *P. microstauron* amalgamated into Others (2)'

Figure 6.11. Core Ince 4 diatom assemblages (707cm to 300cm; -1.65m OD to +2.42m OD). Dates are in radiocarbon years BP.

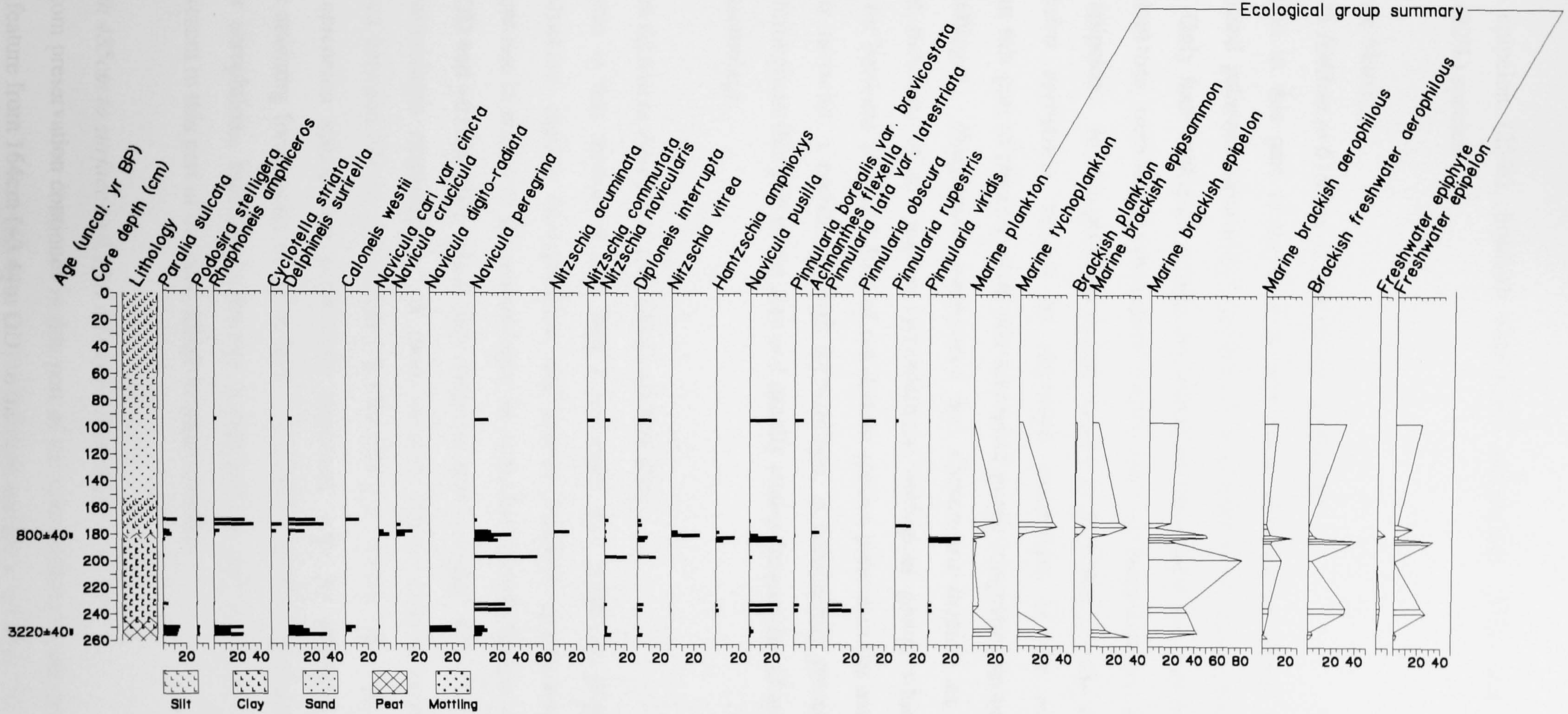

Figure 6.12. Core Ince 4 diatom assemblages (255cm to surface; +2.87m OD to 5.42m OD). Dates are in radiocarbon years BP.

brackish epipelon (25%), brackish freshwater aerophilous (31%) and freshwater epipelon (22%) species.

6.4.1.2 Ince Marshes

Core depth 1043cm to 616cm (–5.35m OD to –1.08m OD)

Preservation in this part of the core is very good, allowing an almost continuous diatom–based palaeoenvironmental reconstruction (Figure 6.13, see Appendix E for dataset). Only four ecological groups are important throughout this part of the core: marine planktons, marine tychoplanktons, marine brackish epipsammons, and marine brackish epipelons. Marine plankton diatom species, in particular *Paralia sulcata* and *Thalassiosira eccentrica*, remain an important component of the assemblages throughout this part of the core, with this ecological group comprising around 40% of the assemblages. *Rhaphoneis amphiceros* and *Cymatosira belgica* are the most prominent members of the marine tychoplankton ecological group, which usually accounts for between 20% and 30% of the diatom species present in the assemblages. *Delphineis surirella*, a marine brackish epipsammon, is consistently present in high numbers throughout this part of the core and usually attains frequencies of at least 20% in each assemblage.

Core depth 623cm to 490cm (–1.15m OD to +0.18m OD)

The diatoms in this section of core Ince 2 are again well preserved (Figure 6.14). Marine plankton, marine tychoplankton and marine brackish epipsammon diatom species continue to dominate the assemblages, in particular between 606cm and 499cm (–0.98m OD and +0.09m OD), where they comprise approximately 40%, 30% and 25% of the assemblages respectively. A more diverse diatom species assemblage is encountered between 621cm and 609cm (–1.13m OD and –1.01m OD). Here, marine brackish epiepelon species are particularly important with, for example, *Navicula peregrina* attaining frequencies of up to 80%. Marine brackish aerophilous, brackish freshwater aerophilous, brackish freshwater tychoplanktons and freshwater epipelons are also present in this part of the core, albeit in small numbers.

Core depth 485cm to surface (+0.23m OD to +5.08m OD)

Good diatom preservation continues in this part of the core, although poor preservation is again a feature from 164cm (+3.44m OD) to the core surface at +5.08m OD

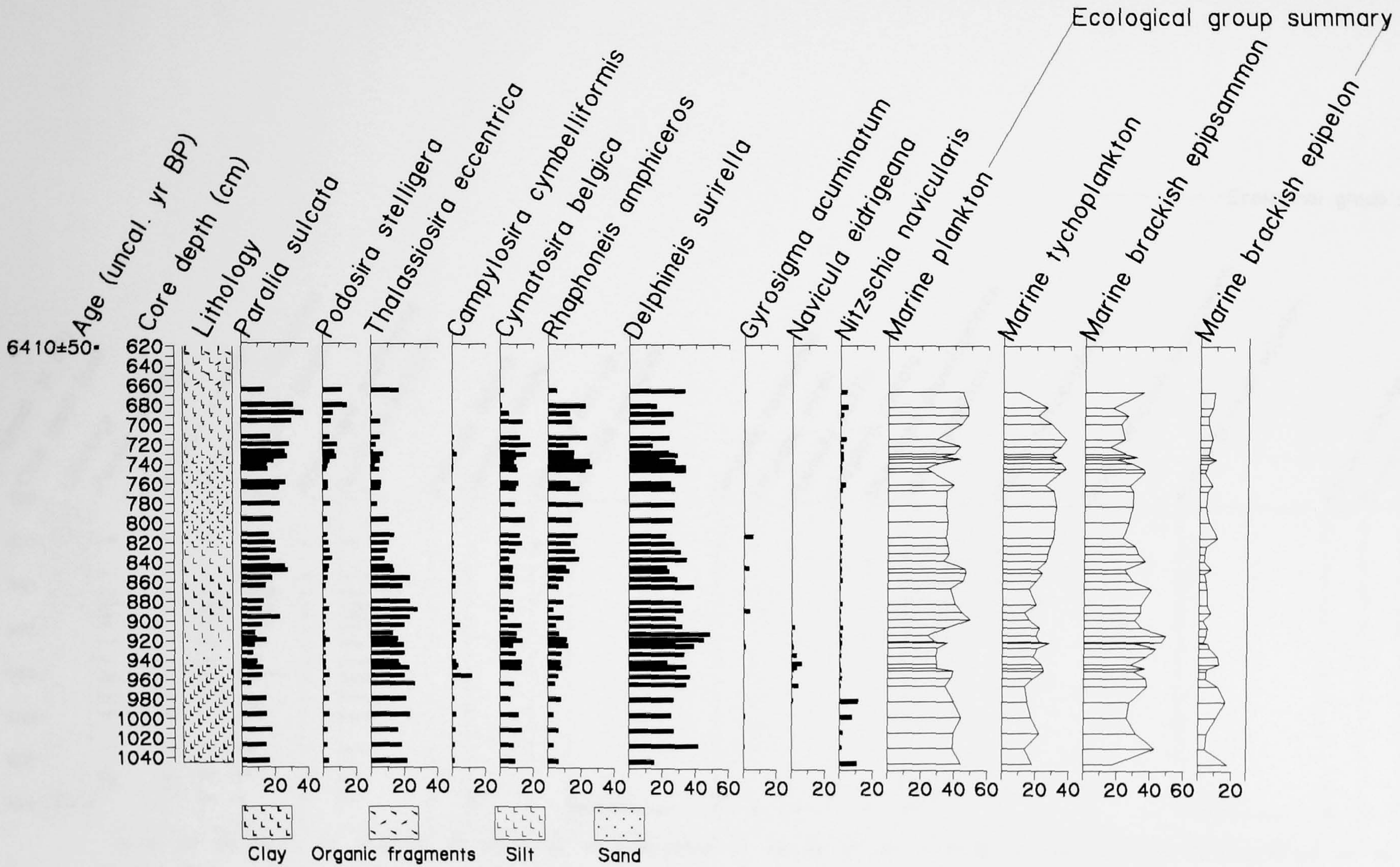

Figure 6.13. Core Ince 2 diatom assemblages (1043cm to 616cm; -5.35m OD to -1.08m OD). Dates are in radiocarbon years BP.

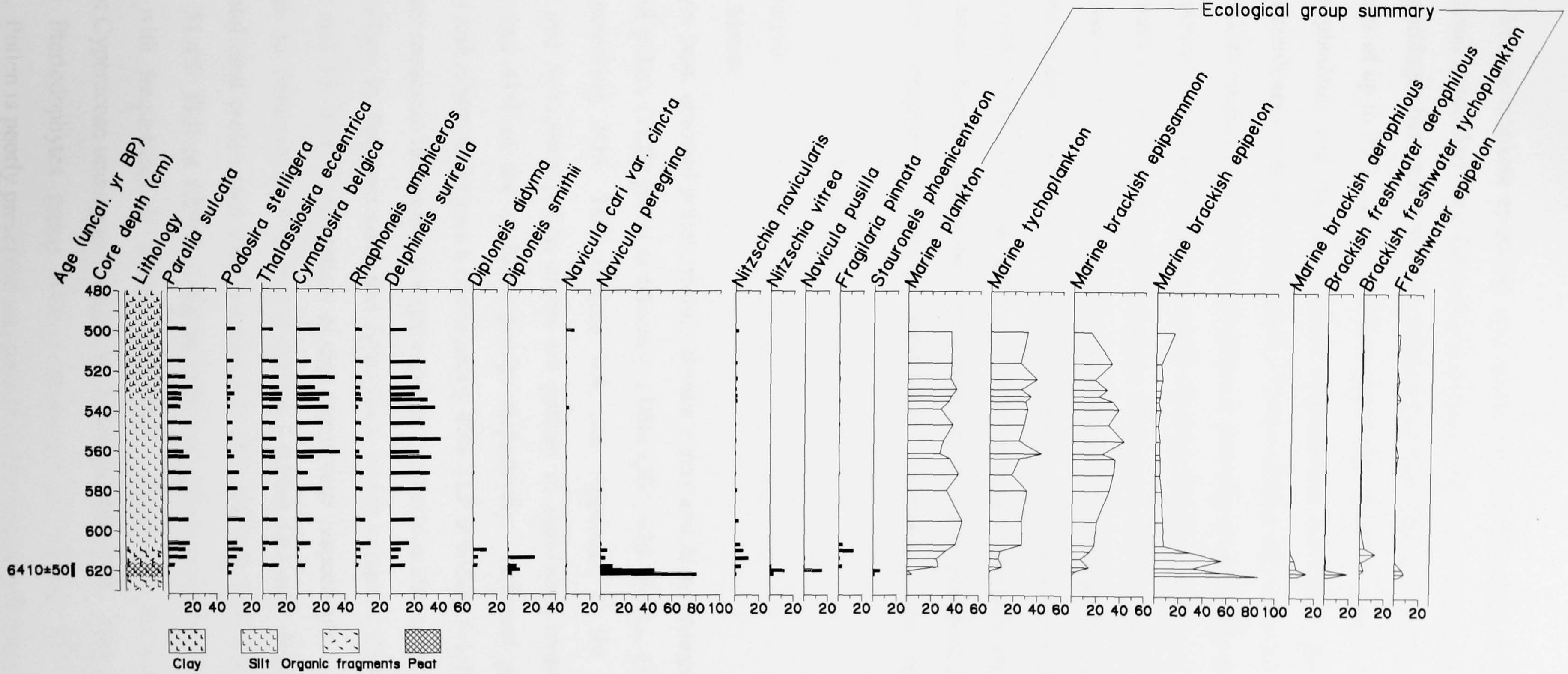

Figure 6.14. Core Ince 2 diatom assemblages (623cm to 490cm; -1.15m OD to +0.18m OD). Dates are in radiocarbon years BP.

(Figure 6.15). Marine brackish epipelons and marine brackish aerophilous species, in particular *Nitzschia navicularis* and *Diploneis interrupta*, are significant components of the diatom assemblages between 474cm and 429cm (+0.34m OD and +0.79m OD) and attain frequencies of up to 80% and up to 40% respectively. Diatoms species belonging to the marine plankton and marine brackish epipsammon ecological groups then dominate the assemblages between 420cm and 177cm (+0.88m OD and +3.31m OD). The marine brackish epipsammon species, *Delphineis surirella,* in particular remains an important component of the assemblages, usually attaining frequencies of over 30%. A return to prominence of marine brackish epipelons is apparent at 171cm (+3.37m OD), with high frequencies of *Caloneis westii* (approximately 50%) significantly contributing to the rise in this ecological group to around 80%. Diatoms are absent in the sediments from 164cm (+3.44m OD) to the core surface, save for an assemblage at 30cm (+4.78m OD), which contains diatoms species belonging mostly to the three ecological groups of marine brackish aerophilous, brackish freshwater aerophilous, and freshwater aerophilous.

6.4.2 Pollen analysis

6.4.2.1 Helsby Marsh

Within the lower peat, arboreal pollen, mainly *Betula*, *Pinus* and *Alnus*, comprise 36% of the total land pollen (TLP) group at 648cm (–1.06m OD), with shrubs, *Corylus* in particular, representing 60% TLP (Figure 6.4, see Appendix E for dataset). Polypodiaceae and *Sphagnum* pollen grains are present in significant numbers and comprise 71% and 41% of the excluded groups respectively. Arboreal pollen, in particular *Pinus* and *Alnus*, undergoes a rise to nearly 80% TLP at 643cm (–1.01m OD), with a significant reduction in shrubs. A slight expansion in herbs is also apparent and a significant reduction in Polypodiaceae and *Sphagnum*, which comprise 23% TLP + Pteriodophytes and 3% TLP + *Sphagnum* of the assemblage respectively. Arboreal pollen continues to dominate at 638cm and 623cm (–0.96m OD and –0.81m OD), although the total land pollen sum only reached 150 TLP and 148 TLP respectively. *Alnus* rises to 51.4% TLP at 623cm (–0.81m OD) and *Quercus* appears at 638cm (–0.96m OD) with frequencies of around 10% TLP. *Corylus* is present in low frequencies, but Cyperaceae undergoes a slight rise to around 10% TLP. Polypodiaceae dominates the Pteriodophytes group with a frequency of around 35% TLP + Pteriodophytes. Pollen is poorly preserved and present in low numbers between 622cm

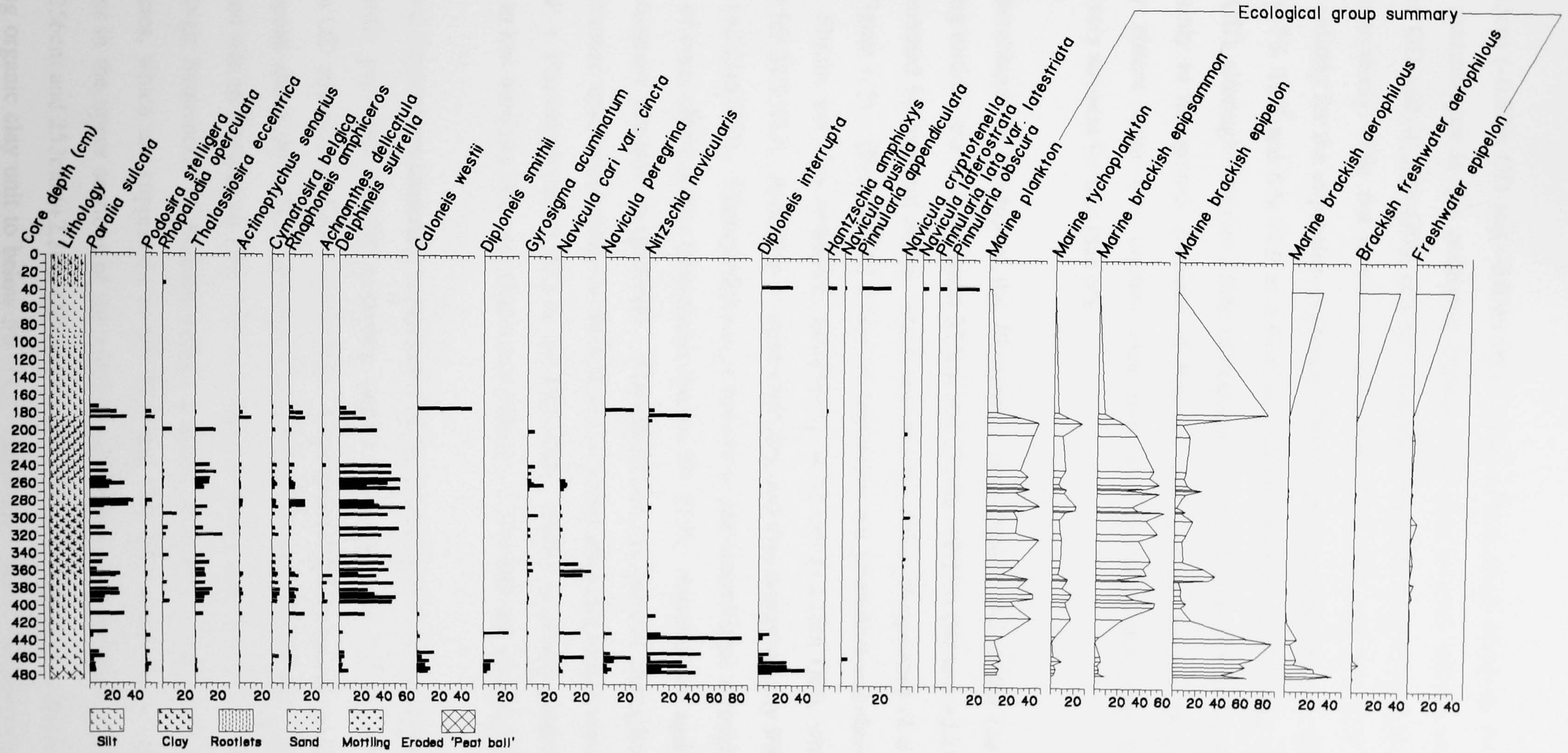

Figure 6.15. Core Ince 2 diatom assemblages (485cm to surface; +0.23m OD to +5.08m OD).

and 603cm (–0.80m OD and –0.62m OD). *Quercus* and *Alnus* dominate the arboreal pollen assemblages in the overlying organic clay unit between 602cm and 580cm (–0.60m OD and –0.38m OD), attaining frequencies approaching 20% TLP and 30% TLP respectively. The rise in *Corylus* to between 34% TLP and 36% TLP accounts almost entirely for the expansion of shrubs. Herbs continue to remain low, accounting for only 7% TLP and 6% TLP at 598cm and 602cm respectively (–0.56m OD and –0.60m OD), although they rise a little in frequency to 18% TLP at 580cm (–0.38m OD), due mainly to the greater presence of Poaceae and Chenopodiaceae. Aquatics are entirely absent from this organic clay unit and Pteriodophytes and *Sphagnum* collectively account for less than 6%.

The assemblages in the top of the *Phragmites* clay deposit and in the base of the overlying middle peat unit, between 327cm and 321cm (+2.15m OD and +2.21m OD), are dominated by arboreal pollen, which consistently attains frequencies of over 50% TLP (Figure 6.5). *Quercus* and *Alnus*, in particular, are prominent members of this group. Shrubs are also important, particularly at 327cm (+2.15m OD), where they account for 24% TLP. A decline in shrubs follows, and they comprise only 9% TLP at 321cm (+2.21m OD). Chenopodiaceae is present in the assemblages throughout this section of core, albeit in low frequencies (below 5% TLP). Aquatics are again absent and *Sphagnum* remains insignificant. Pteriodophytes are present throughout, with Polypodiaceae again accounting for the bulk of this group, attaining frequencies of up to 8% TLP + Pteriodophytes at 323cm (+2.19m OD). Pollen is poorly preserved and present in low numbers between 320cm and 255cm (+2.22m OD and +2.87m OD).

Alnus and Poaceae are important components of the assemblages from the upper part of this middle peat unit and the overlying organic clay, between 256cm and 247cm (+2.86m OD and +2.95m OD) (Figure 6.5). *Alnus* generally remains above 25% TLP and Poaceae above 20% TLP, although a significant fall of *Alnus* to 4% TLP and an associated rise in Poaceae to 79% TLP is evident at 251cm (+2.91m OD). The sharp rise to high frequencies of Poaceae causes a severe reduction in the shrub and tree frequencies, which are suppressed to 6% TLP and 12% TLP respectively. *Betula* is important in the upper sections of the middle peat, attaining frequencies of over 20% TLP at 256cm and 253cm (+2.86m OD and +2.89m OD), but undergoes a decline in the overlying organic clay unit to below 5% TLP. Similarly, *Quercus* undergoes a slight

decrease in frequency, from over 10% TLP to under 8% TLP, between the peat and the overlying organic clay unit. *Corylus* remains important throughout this section of the core and comprises approximately 10% TLP. Herbs in general are well represented and, save for the spike in the herb group owing to the rise in Poaceae, account for between 22% TLP and 27% TLP prior to the Poaceae spike, and between 25% TLP and 40% TLP subsequent to the Poaceae spike. Chenopodiaceae, in particular, is consistently present, although in relatively low frequencies. Aquatics are also present in low frequencies throughout, in particular *Typha latifolia* type. Polypodiaceae is again the most prominent member of the Pteriodophytes group and generally attains frequencies approaching 20% TLP + Pteriodophytes.

The pollen assemblages in the clay deposits below the upper peat, at 186cm and 184cm (+3.56m OD and +3.58m OD), are dominated by herb pollen, which comprises 57% TLP and 67% TLP respectively (Figure 6.6). *Plantago maritima* type is particularly important at 186cm (+3.56m OD), where it accounts for 40% TLP. Chenopodiaceae is also present in appreciable numbers, attaining 16% TLP at 184cm. A rise in Poaceae is apparent from 7% TLP at 186cm (+3.56m OD) to 30% TLP at 184cm (+3.58m OD) and Poaceae attains frequencies of between 16% TLP and 44% TLP throughout this section of the core. Arboreal pollen becomes more important in the assemblages within the peat and the overlying clay unit, accounting for between 29% TLP and 47% TLP. *Quercus* and *Alnus* in particular are prominent members of the arboreal pollen group, with *Alnus* attaining peak frequencies (33% TLP) in the overlying clay unit at 178cm (+3.64m OD) and *Quercus* attaining peak frequencies (25% TLP) in the peat unit at 182cm (+3.60m OD). Polypodiaceae is the most prominent Pteriodophyte within the peat, and reaches frequencies of 24% TLP + Pteriodophytes at 182cm (+3.60m OD). A general rise in trees and shrubs, in particular in *Alnus* and *Corylus*, is apparent between the upper level of the peat at 180cm (+3.62m OD) and the overlying clay unit at 178cm (+3.64m OD). In contrast, there is a decline in the frequencies of herb pollen, from 65% TLP to 31% TLP respectively. Aquatic pollen is present in both the clay units and in the peat, but in very low numbers.

6.4.2.2 Ince Marshes

Pollen is poorly preserved and present in low numbers in the silt unit below the organic clay at 624cm (–1.16m OD). The herb group dominates the thin peat and the base of

the overlying organic clay, between 621cm and 615cm (–1.13m OD and –1.07m OD), accounting for half of the TLP (Figure 6.7, see Appendix E for dataset). In particular, Chenopodiaceae is important throughout, but more so at 617cm and 615cm (–1.09m OD and –1.07m OD), where frequencies of over 35% TLP are encountered. Poaceae is also an important member of this group, approaching 20% TLP at 621cm (–1.13m OD), but subsequently declining to approximately 10% TLP at 617cm and 615cm (–1.09m OD and –1.07m OD), concurrent with the rise in Chenopodiaceae. The arboreal pollen, largely consisting of *Pinus*, *Quercus* and *Alnus*, generally accounts for around 35% TLP in the assemblages throughout, although a slight rise is discernible from 617cm to 615cm (–1.09m OD to –1.07m OD). *Corylus*, the only shrub encountered, remains an important component of the assemblages throughout and accounts for between 16% TLP and 18% TLP. Aquatics are absent and Pteriodophytes comprise less than 8% of each assemblage.

6.5 Geochemical analysis

6.5.1 Helsby Marsh

$\delta^{13}C$ is extremely variable throughout core Ince 4 (Figure 6.16a, see Appendix F for dataset). The lowest $\delta^{13}C$ values are measured in the peat units. The lower peat (648cm to 603cm; –1.06m OD to –0.61m OD) $\delta^{13}C$ values are mostly between –29.0‰ and –28.0‰. Both the middle peat (324cm to 251cm; +2.18m OD to +2.91m OD) and the upper peat (183cm to 179cm; +3.59m OD to +3.63m OD) deposits have similar $\delta^{13}C$ values of between –29.5‰ and –28.5‰. $\delta^{13}C$ values in the thick minerogenic unit between 565cm and 322cm (–0.23m OD and +2.20m OD) remain almost consistently above –26.5‰, and commonly fluctuate around –25.5‰. Similar $\delta^{13}C$ values are also encountered in the minerogenic units between 236cm and 202cm (+3.06m OD and +3.40m OD), and from 177cm (+3.62m OD) to the top of the core at +5.42m OD.

C/N is also extremely variable throughout core Ince 4 (Figure 6.16b, see Appendix F for dataset). The highest C/N is measured in the peat units. C/N values of around 20.0 or above are measured in the lower and middle peat deposits, but C/N values for the thin upper peat reach only around 10.0 and 11.0. C/N values in the thick minerogenic unit between 565cm and 322cm (–0.23m OD and +2.20m OD) are generally below 15.0, and commonly fluctuate around 10.0. Similar C/N values are also encountered in the

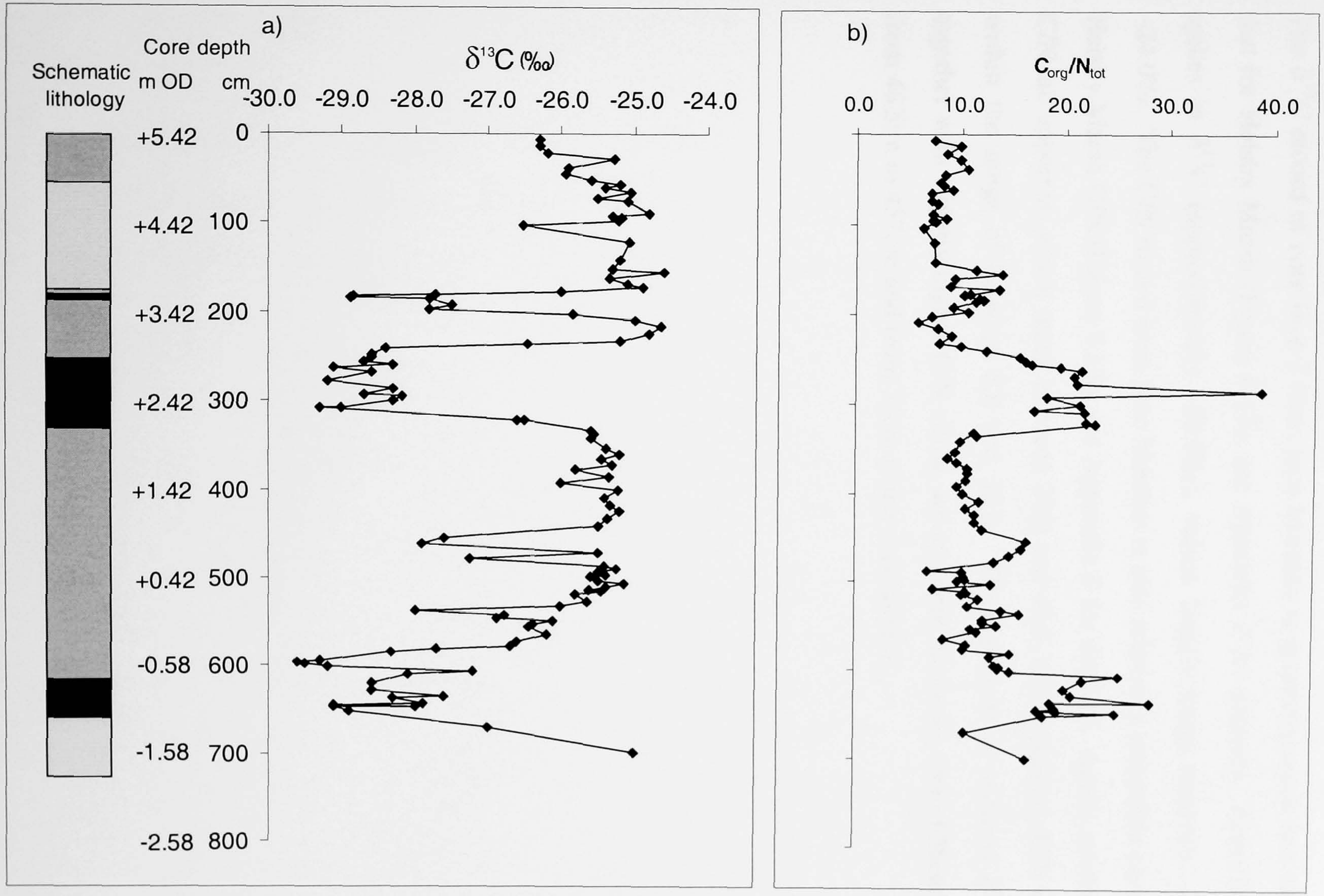

Figure 6.16. a) Core Ince 4 $\delta^{13}C$; b) core Ince 4 C/N. For the schematic lithology, black represents organic rich horizons, dark grey represents silts and clays, whilst light grey represents sand.

minerogenic units between 236cm and 202cm (+3.06m OD and +3.40m OD), and from 177cm (+3.65m OD) to the top of the core.

6.5.2 Ince Marshes

The $\delta^{13}C$ record of core Ince 2 from Ince Marshes is generally much less variable than that for Helsby Marsh (Figure 6.17a, see Appendix F for dataset). Apart from several spikes in $\delta^{13}C$ (approximately –20.0‰), values largely range between –26.0‰ and –24.0‰. The C/N record from Ince Marshes is also relatively invariable compared with Helsby Marsh C/N (Figure 6.17b, see Appendix F for dataset). Again, several spikes in C/N are apparent, which reach between 30.0 and 40.0, but in general, C/N values vary within the range of between 8.0 and 12.0. Three periods of reduced $\delta^{13}C$ values, together with slightly higher C/N ratios, are apparent, however, from 628cm to 609cm, from 482cm to 457cm and from 33cm to the core surface.

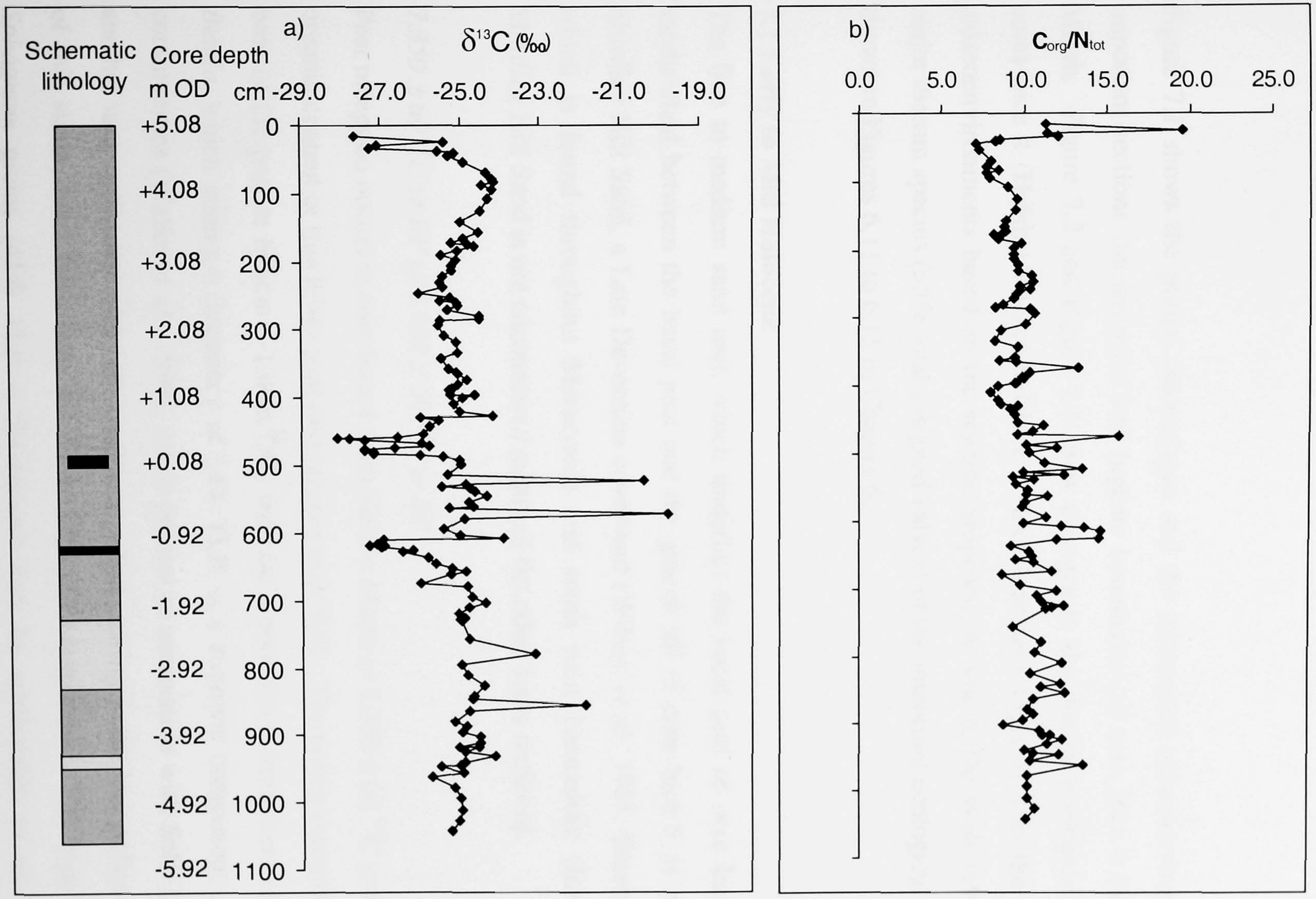

Figure 6.17. a) Core Ince 2 $\delta^{13}C$; b) core Ince 2 C/N. For the schematic lithology, black represents organic rich horizons, dark grey represents silts and clays, whilst light grey represents sand.

Chapter 7

Holocene palaeoenvironments and evolution of the Inner Mersey Estuary

Figure 7.1 shows the pollen assemblages and the interpreted palaeoenvironments for important sections (minerogenic and organic boundaries) of core Ince 4 from Helsby Marsh. Figure 7.2 and Figure 7.3 show changes in the diatom ecological groups of cores Ince 4 (Helsby Marsh) and Ince 2 (Ince Marshes), together with the interpreted palaeoenvironments based on the scheme proposed by Vos & De Wolf (1993a). The major diatom species (>5% total assigned valves) of the important ecological groups are shown in Figures 6.11 to 6.15 in Chapter 6.

7.1 Early to Mid Holocene

The fine to medium sand unit, which underlies the basal peat of core Ince 4 and is sandwiched between the basal peat and the glacial till of core Ince 5, is likely to be Shirdley Hill Sand, a Late Devensian coversand (Wilson *et al.*, 1981; Bateman, 1995), which is found throughout Merseyside and south west Lancashire (Innes, 1986). Shirdley Hill Sand is not encountered in any of the other cores retrieved.

7,350 ±60 ^{14}C yr BP to 6,800 ±50 ^{14}C yr BP

Peat inception occurs in core Ince 4 from Helsby Marsh at 7,350 ± 60 ^{14}C yr BP, and the organic content of this lower peat unit reaches over 80%. The pollen assemblages at the base of the peat at 648cm (–1.06m OD) indicate a poor fen environment (Figure 7.1). *Betula*, which attains a frequency of 14% TLP, is a common component of poor fen communities (Waller *et al.*, 1999), and is present in association with *Salix* (20% TLP), another taxa associated with fen conditions, which, owing to the low pollen production of this shrub, must have been an important local component. The high number of *Sphagnum* grains (41% TLP + *Sphagnum*) may be attributable to its high spore production but may also indicate that acidic bog environments were close by. The presence of *Armeria maritima* and Chenopodiaceae may also indicate some marine influence. The diatom assemblages suggest peat development under freshwater conditions (Figure 7.2), with high frequencies of *Gomphonema angustatum* (freshwater

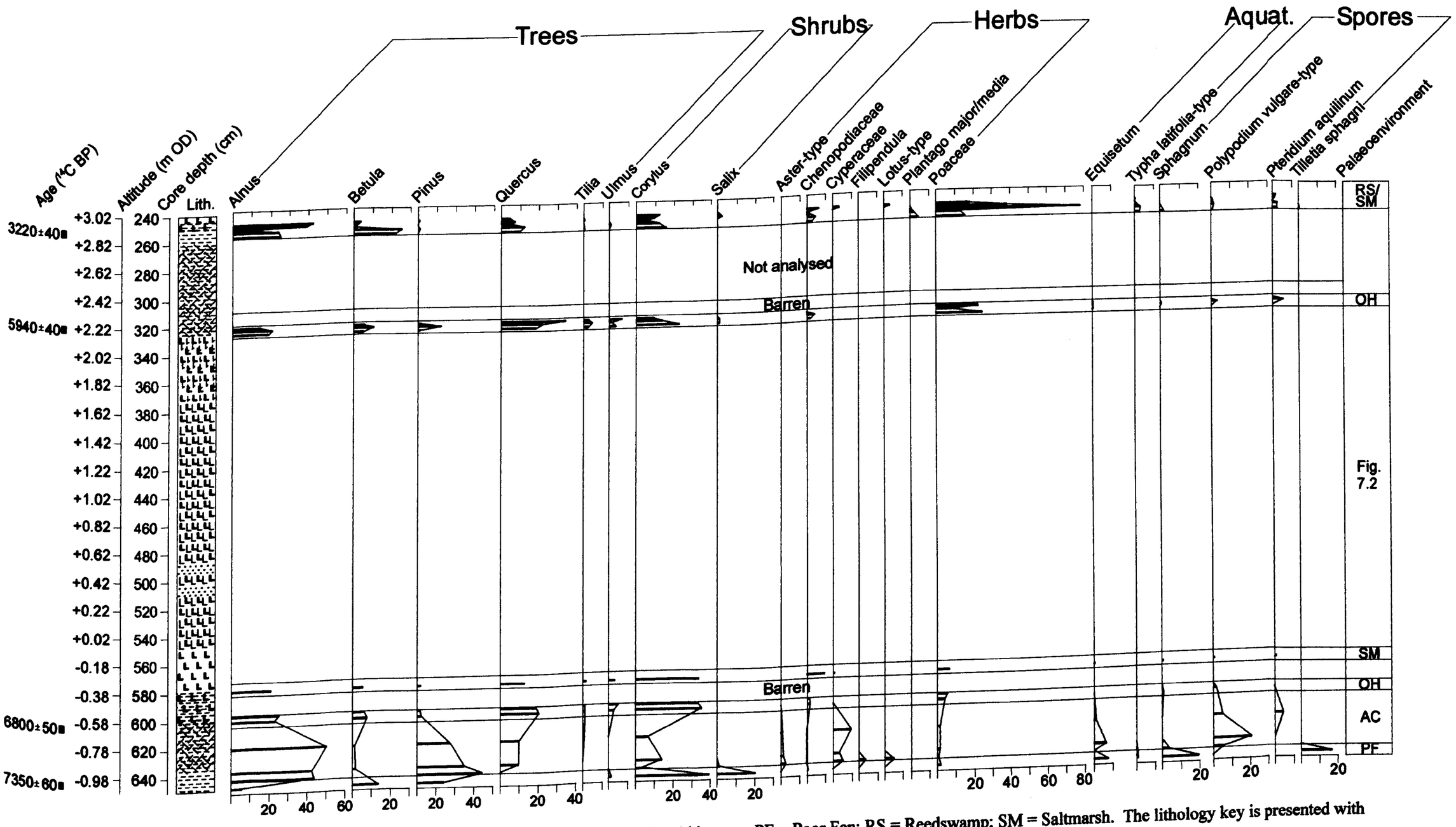

Figure 7.1. Core Ince 4 pollen-inferred palaeoenvironments (OH = Oak-hazel woodland; AC = Alder carr; PF = Poor Fen; RS = Reedswamp; SM = Saltmarsh. The lithology key is presented with Figure 6.1. The diatom assemblages preserved in the thick minerogenic units of core Ince 4 are presented in Figure 7.2.

epiphyte), *Pinnularia viridis* and *Stauroneis phoenicenteron* (freshwater epipelons). The occurrence of *Fragilaria pinnata*, a brackish freshwater tychoplankton, in addition to brackish freshwater allochthonous valves, supports the inference of nearby marine conditions. A rise in *Alnus* to 44% TLP (Figure 7.1) indicates a change to alder carr conditions at 643cm (–1.01m OD), which remain until 623cm (–0.81m OD), although this interpretation must remain tentative because it is based on a pollen sum of 230 TLP and 148 TLP respectively. A mixed oak-hazel woodland environment is apparent towards the top of this lower peat unit between 602cm and 598cm (–0.61m OD and –0.56m OD) from the high frequencies of *Quercus* (approximately 20% TLP) and *Corylus* (approximately 40% TLP). The increase of *Quercus* relative to *Alnus* pollen may indicate a drying of the local environment, although this may also be explained as a result of local competition or pollen production, or as a consequence of changes in the receipt of local *vs.* regional pollen. In addition, wood fragments found in the lower peat of core Ince 3 may indicate the presence of trees and shrubs at, or near to, Ince Marshes. Furthermore, wood fragments in the lower peat in core Ince 7 from Ince Banks, which has been dated at 6,620 ± 40 ^{14}C yr BP, suggest that woodland communities may have been extensive in the Inner Estuary.

6,800 ±50 ^{14}C yr BP to 5,940 ±40 ^{14}C yr BP

An expansion of inter-tidal and sub-tidal conditions is recorded in the Inner Mersey Estuary from around 6,800 ± 50 ^{14}C yr BP. A change in the lithology from peat with wood fragments between 636cm to 603cm (–0.94m OD to –0.61m OD) to organic clay between 603cm to 579cm (–0.61m OD to –0.37m OD) occurs in core Ince 4 from Helsby Marsh (Figure 6.1). This is associated with a fall in the organic content of the sediments from over 80% in the woody peat, to 43% at the base of the overlying organic clay, with the organic content of this unit progressively decreasing to 22% (Figure 6.8), testifying to the reduction in organic sediment deposition.

The diatom assemblages show an increase in marine conditions prior to organic clay deposition (Figure 7.2). High frequencies of *Rhopalodia gibberula* var. *rupestris* (50%) and *Nitzschia recta* (25%), brackish freshwater epiphyte and freshwater epipelon species respectively, are recorded at 606cm (–0.64m OD). These benthic diatoms are almost completely replaced by *Fragilaria pinnata*, a brackish freshwater tychoplankton, at 604cm (–0.62m OD), immediately prior to organic clay deposition. Brackish freshwater tychoplanktons, especially *Fragilaria pinnata*, remain important in the organic clay between 600cm and 582cm (–0.58m OD and –0.40m OD), although a marine episode is recorded by the assemblage at 603cm (–0.61m OD), which is

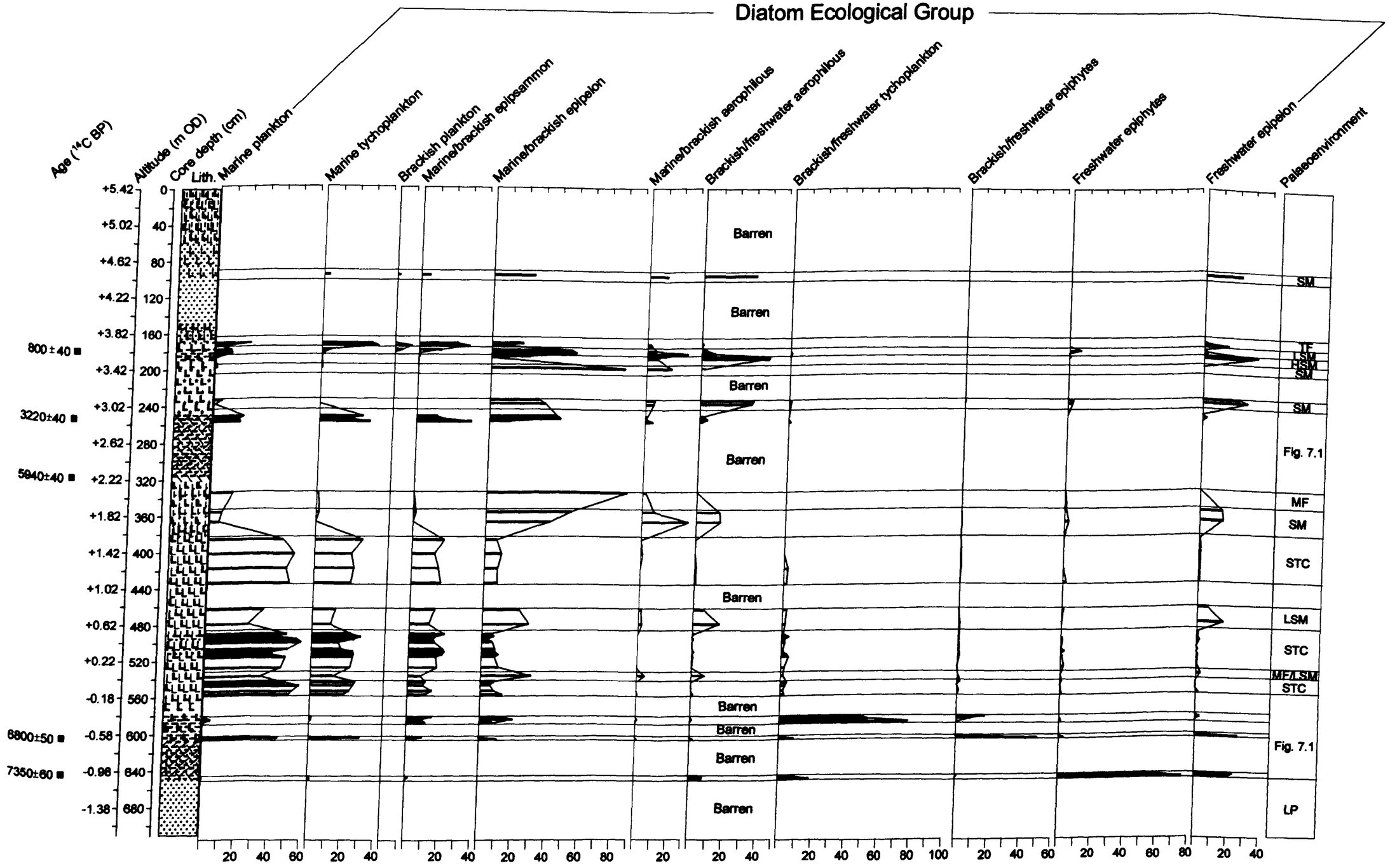

Figure 7.2. Core Ince 4 diatom-inferred palaeoenvironments (LP = Late Pleistocene; STC = Sub-tidal channel; TF = Tidalflat; MF = Mudflat; SM = Saltmarsh, which is further subdivided into Low saltmarsh (LSM) and High saltmarsh (HSM) where possible). The lithology key is presented with Figure 6.1.

dominated by marine plankton and marine tychoplankton species (over 70%), in particular *Thalassiosira eccentrica* and *Cymatosira belgica*. This marine episode appears to be short-lived, as freshwater tychoplankton diatoms, especially *Fragilaria pinnata*, dominate once more from 600cm (–0.58m OD). The presence of marine plankton and tychoplankton diatoms in such high numbers in terrestrial / semi-terrestrial coastal deposits may indicate a storm surge event, several of which were recorded in Morecambe Bay between 6,030 ± 70 ^{14}C yr BP and 5,740 ± 60 ^{14}C yr BP (Zong & Tooley, 1999), although further diatom and organic content analysis is needed at this level to support this inference. Saltmarshes are present at 580cm (–0.38m OD), indicated by the presence of Chenopodiaceae, together with the increase in Poaceae and the presence of aquatic pollen (Figure 7.1).

The replacement of organic clay with clay at 579cm (–0.37m OD) marks the beginning of around 2.5m of minerogenic deposition in core Ince 4 at Helsby Marsh (Figure 6.1). The organic content of these sediments generally remains below 3% throughout (Figure 6.8). Diatoms are absent from the base of the clay unit but towards the top, where silt deposition becomes more important, the diatom assemblages from 557cm to 543cm (–0.15m OD to +0.01m OD) are indicative of sub-tidal channel conditions (Figure 7.2). High frequencies of marine plankton (49% to 57%) and marine tychoplankton (20% to 27%) species are present, in particular *Paralia sulcata* and *Cymatosira belgica*, and the marine brackish epipelon and epipsammon species *Nitzschia navicularis* and *Delphineis surirella* are also important components of the assemblages. Vos & De Wolf (1993a) assign *Delphineis surirella* to the marine tychoplankton ecological group, but this species is associated with an epipsammic habitat in Belgian Holocene coastal deposits (Denys, 1991-92) and is an important component of sandy tidalflats in Britain (Zong & Horton, 1998). Therefore, it is more likely that *Delphineis surirella* belongs to the marine brackish epipsammon ecological group.

A significant rise in marine brackish epipelons at 537cm (+0.05m OD) may indicate a brief change to mudflat conditions (Figure 7.2), although the dominant marine brackish epipelon, *Navicula peregrina*, is often found on low saltmarshes (e.g. Zong & Horton, 1998). With aerophilous species comprising only 11% of the assemblage, the palaeoenvironment represented by the diatom assemblage remains equivocal. A change to interlaminated silt and silty clay deposition from 536cm to 375cm (+0.06m OD to

+1.67m OD) reflects, for the most part, a change to sub-tidal channel conditions, as the sediments from 527cm to 385cm (+0.15m OD to +1.57m OD) are dominated by the marine plankton *Paralia sulcata* and the marine tychoplankton *Cymatosira belgica*. A brief change to low saltmarsh conditions between 479cm and 463cm (+0.63m OD and +0.79m OD) interrupts the otherwise continuous sub-tidal channel deposits. This is indicated by the presence of brackish freshwater aerophilous species (between 6% and 15%), mainly *Navicula pusilla* and *Pinnularia borealis* var. *brevicostata*, and the high frequencies of the low saltmarsh species, *Navicula peregrina*, in association with high frequencies of marine brackish epipelic species (between 22% and 28%).

A return to saltmarsh conditions is apparent from the diatom assemblages in the overlying clay deposit at 366cm and 355cm (+1.76m OD and +1.87m OD) (Figure 7.2). This inference is further supported by the presence of *Phragmites* remains. The diatom assemblages are consistent with those expected on a saltmarsh, with the presence of freshwater epipelons and high frequencies of species associated with marine brackish epipelic and aerophilous habitats. *Navicula peregrina* and *Diploneis interrupta* dominate the assemblage at 366cm (+1.76m OD), comprising 32% and 28% of the species present respectively, whilst at 355cm (+1.87m OD) frequencies of *Navicula peregrina* increase to 46% with *Navicula pusilla* present at 8%. These species are often found in significant numbers on contemporary saltmarsh surfaces (e.g. Shennan *et al.*, 1995; Zong & Horton, 1998; Gehrels *et al.*, 2001). A change to mudflat deposition at the top of this unit at 333cm (+2.09m OD) is evident as the marine brackish epipelon *Nitzschia navicularis*, commonly found on modern mudflats (e.g. Zong & Horton, 1998), accounts for 77% of the diatoms present in the assemblage. Peat development at 5,940 ± 40 ^{14}C yr BP (324cm; +2.18m OD) testifies to significant coastal environmental change. Possible changes in palaeosedimentary environments leading up to peat development, however, remain unresolved due to the absence of diatoms.

Diatom analyses of the c. 2.5m minerogenic sequence in core Ince 4 from Helsby Marsh show that inter-tidal and sub-tidal conditions persisted for 860 ^{14}C years (Figure 7.2). Around 2.5m of minerogenic deposits are recorded at a similar altitude (–0.76m OD to +1.79m OD) in the more landward core of Ince 5 (Figure 6.1), indicating that marine conditions may have penetrated more than 2km inland of the present Mersey Estuary shoreline between 6,800 ± 50 ^{14}C yr BP and 5,940 ± 40 ^{14}C yr BP. In core Ince 7 from

Ince Banks, a change from peat to sandy silt deposition after 6,620 ± 40 ^{14}C yr BP points to a significant change in both the nature and energy of the depositional environment (Figure 6.3) and is probably associated with the marine incursion recorded at Helsby Marsh.

At Ince Marshes, over 4m of minerogenic sediments had accumulated before 6,410 ± 50 ^{14}C yr BP (Figure 6.1). The organic content of these sediments is negligible throughout and generally remains below 3% (Figure 6.9). The diatom assemblages in these deposits are dominated by a handful of species that belong to only four important ecological groups: marine plankton; marine tychoplankton; marine brackish epipsammon and marine brackish epipelon (Figure 6.13). The consistently high frequencies of marine plankton (between 23% and 50%), marine tychoplankton (between 10% and 38%) and marine brackish epipsammon (between 15% and 50%) indicate that sub-tidal channel conditions characterised this area of the Inner Mersey Estuary prior to 6,410 ± 50 ^{14}C yr BP (Figure 7.3). Slight fluctuations in the energy of this environment are highlighted in the mean particle size, sorting and skewness data (Figure 6.10). The mean particle size of the sediments remains between 5.2 ϕ and 6.1 ϕ from 1027cm to 955cm (–5.19m OD to –4.47m OD) and are poorly sorted and very finely skewed. An increase in depositional energy is recorded between 955cm and 940cm (–4.47m OD and –4.32m OD), when mean particle size increases to 4.1 ϕ, and between 871cm and 763cm (–3.63m OD and –2.55m OD), when mean particle size increases from 5.8 ϕ to 4.2 ϕ, together with a change in sorting, from very poorly sorted / poorly sorted to almost moderately sorted sediments. These higher energy conditions nevertheless remain within a tidal setting, with the very finely skewed nature of the sediments indicating the absence of a wave-dominated environment (Friedman, 1961). The two episodes of higher energy conditions are separated by a period of lower energy conditions, indicated by a fall in mean particle size from 4.1 ϕ at 940cm (–4.32m OD) to 6.0 ϕ at 887cm (–3.77m OD), and a change to more poorly sorted sediments.

An overlying silt deposit from 661cm to 623cm (–1.53m OD to –1.15m OD), containing occasional organic fragments, indicates the removal of marine conditions to some extent and this culminates in muddy peat (30% organic content) deposition at 6,410 ± 50 ^{14}C yr BP (Figure 6.1 and Figure 6.9). Unfortunately, absence of diatoms in the silt deposit prevents any further insight into the environmental changes leading up to

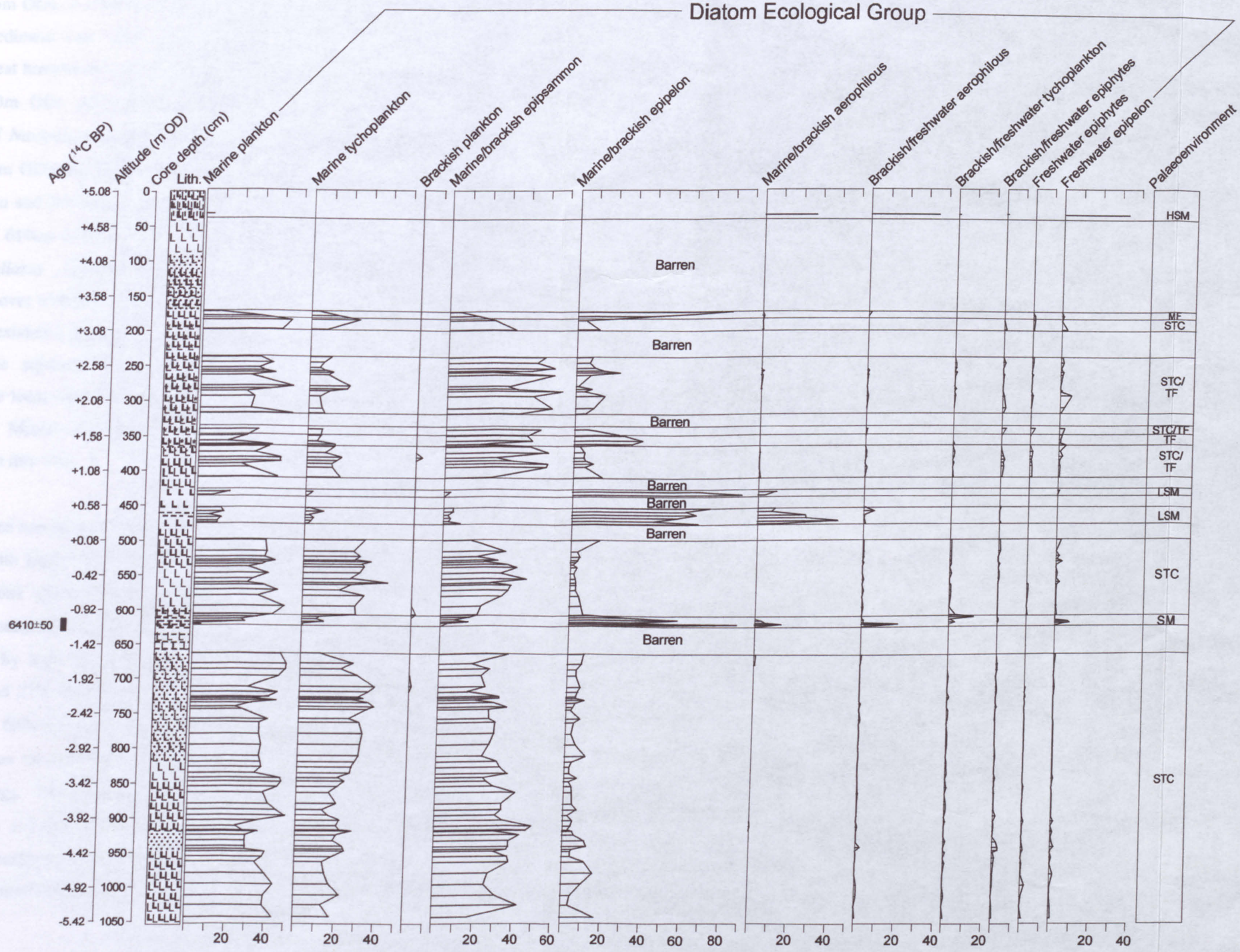

Figure 7.3. Core Ince 2 diatom-inferred palaeoenvironments (abbreviations are as in Figure 7.2). The lithology key is presented with Figure 6.1.

muddy peat development, although a reduction in mean particle size from 4.9 ϕ to 7.6 ϕ between 657cm and 613cm (−1.49m OD and −1.05m OD) testifies to a reduction in depositional energy. The skewness of the sediment population becomes symmetrical at 613cm (−1.05m OD), in contrast to the generally very fine skewed sediments from the base of the sediment core, perhaps indicating a shift to a quieter water environment. The muddy peat horizon may have been deposited under saltmarsh conditions between 621cm (−1.13m OD) and 609cm (−1.01m OD). This is indicated by the high frequencies of *Navicula peregrina*, which reaches 80% of the diatom assemblage at 621cm (−1.13m OD), the significant frequencies of aerophilous species, in particular *Nitzschia vitrea* and *Navicula pusilla*, which attain frequencies of up to 13% and 15% respectively at 619cm (−1.11m OD), and the presence of brackish freshwater species, such as *Fragilaria pinnata*. The presence of Chenopodiaceae, which reaches frequencies of over 35% TLP at 617cm and 615cm (−1.09m OD and −1.07m OD) adds support to the existence of saltmarshes. The absence of organic rich horizons at similar altitudes in the adjacent cores, Ince 3 and CB17, indicates that semi-terrestrial conditions were local, and site-specific factors must have played an important role in their initiation. Moreover, marine conditions are evident at the more landward site of Helsby Marsh at this time.

Increasing marine conditions are apparent between 613cm and 609cm (−1.05m OD and −1.01m OD), with higher frequencies of marine planktons (32%) and a fall in marine brackish epipelons (30%) evident at 609cm (−1.01m OD). Approaching marine conditions are confirmed by a change to sub-tidal channel conditions at 608cm (−1.00m OD), indicated by high frequencies of marine plankton and marine tychoplankton species (40% and 27% respectively). In addition, the sediments are once again very finely skewed at 606cm (−0.98m OD), supporting the interpretation of a return of tidal conditions, and an increase in mean particle size to 5.2 ϕ suggesting an increase in depositional energy. The dominance of *Paralia sulcata* and *Cymatosira belgica* from 608cm to 499cm (−1.00m OD to +0.09m OD) indicates continuous sub-tidal channel conditions. The temporal extent of this environment is unknown as diatoms are absent in the remaining interlaminated silt and silty clay deposit.

7.2 Mid to Late Holocene

5,940 ±40 ^{14}C yr BP to 3,220 ±40 ^{14}C yr BP

A widespread contraction of the sub-tidal and inter-tidal areas is evident in the Inner Estuary during the Mid Holocene. In core Ince 2 from Ince Marshes, the sediments between 515cm and 463cm (–0.07m OD and +0.45m OD) (approximately 1.00m above the dated muddy peat horizon, which was dated at 6,410 ± 50 ^{14}C yr BP) record a fall in mean particle size, from 5.1 ϕ to 6.9 ϕ (Figure 6.10). This is associated with a change in sorting, from poorly sorted to very poorly sorted, and in skewness, from very finely skewed to symmetrical, together suggesting a decrease in depositional energy. This switch to lower energy conditions, which may become non-tidal at 463cm (+0.45m OD) as indicated by the symmetrical distribution of the sediment population, is confirmed by a change in lithology. Interlaminated silt and silty clay deposition gives way to clay deposition at 485cm (+0.23m OD). An eroded 'peat ball' is present in this clay unit between 485cm and 474cm (+0.23m OD and +0.34m OD). Unfortunately, diatoms are absent in the sediments leading up to the peat ball. Consequently, it is not possible to determine the nature of the environmental changes that resulted in an increase in the organic content of the sediments, nor is it possible to determine if the peat ball is an eroded *in situ* peat unit or an inwash deposit.

In core Ince 2, the diatom assemblages between 473cm (+0.35m OD) and 429cm (+0.79m OD) indicate low saltmarsh environments. Marine brackish epipelons remain significant throughout (between 42% and 87%), and the occurrence of marine brackish aerophilous species, in particular the low saltmarsh species *Diploneis interrupta*, which reaches frequencies of over 40% at 471cm (+0.37m OD), indicates aerial exposure. The organic content is also relatively high (16% to 22%) between 461cm and 458cm (+0.47m OD and +0.50m OD), supporting the presence of semi-terrestrial conditions.

Further inland, oak-hazel woodland is present in core Ince 4 from Helsby Marsh at 5,940 ± 40 ^{14}C yr BP, indicated by the high frequencies of *Quercus* (20% to 40% TLP) and *Corylus* (10% to 30% TLP) (Figure 7.1). At Ince Banks, peat deposits, which contain wood fragments, are recorded at 5,750 ± 120 ^{14}C yr BP and at 5,280 ± 80 ^{14}C yr BP, and so woodland communities may have been extensive in the Inner Mersey Estuary at this time. Peat development at a similar altitude is recorded throughout the area between Helsby and Ince Marshes (Figure 6.2). Peat accumulated at Helsby Marsh

for around 2,700 ^{14}C years before approaching marine conditions are recorded in the pollen assemblages, with high frequencies of Poaceae, together with *Typha latifolia* type, *Pteridium aquilinum*, Chenopodiaceae and *Plantago major/media*. This suggests the existence of transitional reedswamp / saltmarsh environments at 3,220 ± 40 ^{14}C yr BP.

3,220 ±40 ^{14}C yr BP to present

An expansion of the inter-tidal areas is recorded in the Inner Mersey Estuary in the Mid to Late Holocene. A reduction in the organic content of the sediments in core Ince 4 (Helsby Marsh), from 83% to 3% between 269cm and 236cm (+2.73m OD and +3.06m OD) (Figure 6.8), emphasises the increasing importance of minerogenic deposition. A return of marine conditions is recorded here around 3,220 ± 40 ^{14}C yr BP, when saltmarshes replace transitional reedswamp / saltmarsh environments (Figure 7.2). Marine plankton and marine tychoplankton species are almost absent, but significant frequencies of marine brackish epipelons (over 30%) testify to saline conditions. High frequencies of *Navicula pussila*, a brackish freshwater aerophilous species often found on mid saltmarshes (e.g. Zong, 1997), and *Pinnularia lata* var. *latestriata*, a freshwater epiphyte, indicate periodic exposure and periods of low salinity.

Diatoms are absent in core Ince 4 between 230cm and 200cm (+3.12m OD and +3.42m OD), but with the organic content of the sediments remaining around 4%, lower inter-tidal conditions seem probable. Saltmarsh conditions are again apparent from 196cm to 169cm (+3.46m OD to +3.73m OD). At 196cm (+3.46m OD), high frequencies of *Navicula peregrina* and *Diploneis interrupta* are present, marine brackish epipelon and marine brackish aerophilous species common to low saltmarshes (e.g. Zong & Horton, 1998). The almost complete absence of marine plankton and tychoplankton species, however, would suggest deposition higher in the inter-tidal zone. High saltmarsh conditions may occur at 184cm (+3.58m OD), as high frequencies of brackish freshwater aerophilous (37%) and freshwater epipelon species (30%) are present. This is accompanied by an increase in the organic content of the sediments, from 5% at 196cm (+3.46m OD) to 13% at 184cm (+3.58m OD). The existence of saltmarshes is also supported by the high numbers of *Plantago maritima* type (40% TLP) at 186cm, and the increase in Chenopodiaceae from 7% TLP at 186cm (+3.56m OD) to 16% TLP at 184cm (+3.58m OD) (Figure 7.1). Peat development between 183cm and 179cm

(+3.59m OD and +3.63m OD) indicates deposition high in the inter-tidal zone. The diatom assemblage at 182cm (+3.60m OD) reveals high saltmarsh conditions as brackish freshwater aerophilous and freshwater epipelon species undergo slight increases to 41% and 33% respectively (Figure 7.2). This interpretation is supported by the high organic content of the sediments at this level, which reaches 87%. The pollen assemblages indicate transitional reedswamp / saltmarsh conditions between 182cm and 178cm (+3.60m OD and +3.64m OD), with high frequencies of Poaceae (up to 44% TLP), *Plantago maritima* type (up to 13% TLP) and Chenopodiaceae (up to 5% TLP) (Figure 7.1). However, the diatom assemblage at 180cm (+3.62m OD) contains high frequencies of marine brackish aerophilous species (25%) and epipelon species (51%) (Figure 7.2). In addition, the organic content of the sediments falls to just 5%. Taken together, a low saltmarsh environment is favoured, with reedswamp conditions nearby.

The peat unit has been dated at 800 ± 40 ^{14}C yr BP, but this date is almost certainly an error, as it appears to be too young for deposits of this depth (Section 6.2). An equivalent peat unit is absent from the adjacent, more seaward, cores of CB5 and Ince 3. In addition, the upper peat unit in the more landward core of Ince 5 continues uninterrupted until +3.68m OD. Therefore, the marine conditions recorded in core Ince 4 from 3,220 ± 40 ^{14}C yr BP may not have penetrated much further inland, as an equivalent minerogenic unit is absent in core Ince 5, less than 1km inland from core Ince 4. A radiocarbon date from the top of the upper peat unit in core Ince 5, and re-dating of the thin upper peat unit in core Ince 4, would be required before this inference can be accepted.

The replacement of low saltmarshes by tidalflats from 172cm (+3.70m OD) to 169cm (+3.73m OD) marks the return of stronger marine conditions (Figure 7.2). This is indicated by a change in lithology from clay to interlaminated sandy silt and silty clay at 174cm (+3.68m OD), and the prominence of marine tychoplankton (between 30% and 34%) and marine brackish epipsammon species (between 24% and 30%) in the assemblages. The presence of the freshwater epipelon *Pinnularia viridis* (14%), and the brackish plankton *Cyclotella striata* (10%), may signify some freshwater input. It is equally likely, however, that these two species may be allochthonous.

Diatoms are absent in the remaining sediments of this deposit. The overlying fine sand deposit, from 104cm to 94cm (+4.38m OD to +4.48m OD), is also barren of diatom valves. A saltmarsh environment is indicated by the diatom assemblage in the fine sandy silt sediments at 93cm (+4.84m OD). Although high frequencies of aerophilous species (43%), especially brackish freshwater aerophilous species such as *Navicula pusilla*, and freshwater epipelic species (22%) may suggest a high saltmarsh environment, this is not supported by the low organic content of this horizon, which is only 2%, and which contrasts with the higher organic content of modern day high saltmarsh sediments on Ince Banks (≥9%, Appendix A). Diatoms are absent, or present in extremely low numbers, in the remainder of the sandy silt deposits and also in the clay and silt deposits from 59cm (+4.83m OD) to the surface of the core at +5.42m OD. The increase in the organic content of the sediments, from 2% at 89cm (+4.53m OD) to 8% just below the core surface at 6cm (+5.36m OD), suggests deposition progressively higher in the inter-tidal zone. This is supported by the appearance of rootlets in the clayey silt unit between 59cm and 4cm (+4.83m OD and +5.38m OD).

The onset of stronger marine conditions, resulting in the accumulation of inter-tidal and sub-tidal sediments in core Ince 4 from Helsby Marsh after 3,220 ± 40 ^{14}C yr BP, is likely to have been experienced earlier at Ince Banks and, in particular, at Ince Marshes, although this remains to be determined through dating. In core Ince 7 from Ince Banks, minerogenic deposits begin to accumulate after 5,280 ± 80^{14}C yr BP, and continue to the core surface, although the depositional context of these sediments remains to be determined through microfossil analysis. In core Ince 2 from Ince Marshes, a change in the sediments from clay to interlaminated silty clay and silt at 428cm (+0.80m OD) may suggest an increase in marine conditions, but absence of diatoms near the base of this unit prevents confirmation. A reduction in the organic content of the sediments to around 3% and an increase in the mean particle size, from 6.5 ϕ to 5.0 ϕ, and in skewness, from finely skewed to very finely skewed, indicates an increase in the energy of the depositional environment. Transitional sub-tidal channel / tidalflat conditions are apparent between 408cm (+1.00m OD) and 364cm (+1.44m OD), indicated by the high frequencies of the marine brackish epipsammon *Delphineis surirella* (23%) and the marine plankton *Paralia sulcata* (31%), together with the presence of marine brackish epipelons.

Tidalflat conditions succeed at 363cm (+1.45m OD) and continue until 349cm (+1.59m OD). This is accompanied by a change to silty clay deposition. Transitional sub-tidal channel / tidalflat conditions return once more at 341cm (+1.67m OD), as revealed by the falling marine brackish epipelons and rising marine brackish epipsammon and marine plankton species. The mean particle size of the sediments increases to 4.6 ϕ and the sediments become very finely skewed, suggestive of a higher energy depositional environment. Transitional sub-tidal channel / tidalflat conditions appear to persist from 317cm (+1.91m OD) to 237cm (+2.71m OD).

Sub-tidal channel conditions prevail at 197cm (+3.11m OD), evident by the high frequencies of marine planktons (41%) in conjunction with marine brackish epipelon and marine brackish epipsammon species, and these conditions continue to 183cm (+3.25m OD). Mudflat conditions follow from 177cm (+3.31m OD) to 171cm (+3.37m OD), with assemblages at this level containing high frequencies of marine brackish epipelons (80%), especially *Caloneis westii,* which is commonly found on modern day mudflats (e.g. Zong & Horton, 1998). Visual inspection of the sediments reveals the coarsening of this deposit up the core, but the absence of diatoms prevents elucidation of the palaeoenvironments. Diatoms are also absent in the overlying sandy silt deposits at 104cm and at 84cm (+4.04m OD and +4.24m OD), as well as in the silt deposit at 84cm and at 36cm (+4.24m OD and +4.72m OD). An increase in the depositional energy is indicated by the particle size data, however. Mean particle size increases from 6.3 ϕ at 171cm (+3.37m OD) to 3.8 ϕ at 87cm (+4.21m OD) and this is associated with a change in skewness from very finely skewed to finely skewed sediments.

A reduction in mean particle size from 3.8 ϕ to 6.2 ϕ, together with the reduction in skewness, initially from very finely skewed to finely skewed, and then to symmetrical, occurs between 87cm (+4.21m OD) and near to the core surface at 7cm (+5.01m OD) (Figure 6.10). The reduction in the energy of the depositional environment is confirmed by changes in the lithology. Sandy silts, which occur between 104cm and 84cm (+4.04m OD and +4.24m OD), are replaced by silts from 84cm to 36cm (+4.24m OD to +4.72m OD) and then by rootlet-containing clays and silts, which continue to the core surface at +5.08m OD (Figure 6.1). An increase in the organic content of the sediments, from less than 1% to 7%, occurs between 94cm (+4.14m OD) and near to the core surface at 7cm (+5.01m OD) (Figure 6.9). Taken together, a move from tidal conditions

to increasingly quiet water conditions is indicated. A single diatom assemblage preserved at 30cm (+4.78m OD) indicates high saltmarsh conditions (Figure 7.3). Brackish freshwater and marine brackish aerophilous species dominate the assemblage, with frequencies of 35% and 27% respectively. Both *Diploneis interrupta* and *Pinnularia appendiculata*, low and high saltmarsh species respectively (e.g. Zong & Horton, 1998), occur in high frequencies in the assemblage. *Pinnularia obscura*, a freshwater epipelon, is also significant and further supports the presence of a high saltmarsh.

7.3 Overview of Inner Mersey Estuary Holocene Evolution

The basal peat in core Ince 4 from Helsby Marsh, dated at between 7,350 ± 60 ^{14}C yr BP and 6,800 ± 50 ^{14}C yr BP, initially accumulated under poor fen conditions, although the presence of saltmarsh pollen grains and brackish diatoms indicate nearby marine conditions. Poor fen conditions were succeeded by alder carr, with oak-hazel woodland becoming established later. The presence of trees and shrubs is supported by the appearance of wood fragments in core Ince 4 and in the equivalent peat units at Ince Marshes and Ince Banks. Terrestrial / semi-terrestrial conditions appear to be extensive in the Inner Mersey Estuary in the Early Holocene, with the change from poor fen to alder carr and then to oak-hazel woodland, recorded at Helsby Marsh in core Ince 4, possibly indicating a seaward movement of the shoreline after 7,350 ± 60 ^{14}C yr BP.

The presence of brackish freshwater benthic diatoms in the top of the basal peat unit in core Ince 4 from Helsby Marsh, and the subsequent replacement by brackish freshwater tychoplanktons at 6,800 ± 50 ^{14}C yr BP, indicates a rise in the water table and an increase in salinity, which suggests approaching marine conditions. The proximity of marine conditions around 6,800 ± 50 ^{14}C yr BP is further supported by a possible storm surge event, several of which have been recorded in Morecambe Bay at around this time (Zong & Tooley, 1999). A change to saltmarsh conditions sometime after 6,800 ± 50 ^{14}C yr BP heralds the return of marine conditions at Helsby Marsh, and marine conditions remain at Helsby Marsh for 860 ^{14}C years. Complete marine inundation of Helsby Marsh occurs on several occasions (when the diatoms record the existence of sub-tidal channel environments in core Ince 4), whilst inter-tidal conditions otherwise occupied this area during the period of marine influence. The presence of minerogenic

deposits in core Ince 5, the more inland Helsby Marsh core, suggests that inter-tidal, and maybe even sub-tidal, environments may have extended over 2km inland from the present Mersey Estuary shoreline.

The deposition of around 3.80m of marine sediments in core Ince 2 from Ince Marshes before 6,410 ± 50 ^{14}C yr BP indicates its closer proximity to the route of marine inundation, and it is therefore likely that the sea inundated Ince Marshes earlier than Helsby Marsh. Sub-tidal channels appear to have existed at Ince Marshes for most of the Early Holocene, although saltmarshes develop locally at around 6,410 ± 50 ^{14}C yr BP. This is in contrast to Helsby Marsh, the more landward site, where saltmarsh and tidalflat environments existed on several occasions between 6,800 ± 50 ^{14}C yr BP and 5,940 ± 40 ^{14}C yr BP, supporting the inference that Ince Marshes is located closer to the route of marine inundation.

A significant reduction in the area of sub-tidal and inter-tidal zones is evident in the Inner Mersey Estuary from the occurrence of a substantial, and widespread, middle peat unit, occurring in most cores from Helsby and Ince Marshes and Ince Banks. The peat unit recorded in core Ince 4 from Helsby Marsh was deposited between 5,940 ± 40 ^{14}C yr BP and 3,220 ± 40 ^{14}C yr BP, and culminated in oak-hazel woodland conditions. At Ince Banks, two peat units, containing wood fragments, are present and have been dated at 5,750 ± 120 ^{14}C yr BP and at 5,280 ± 80 ^{14}C yr BP. At Ince Marshes, a change from sub-tidal channel to low saltmarshes occurs sometime after 6,410 ± 50 ^{14}C yr BP (from 473cm to 429cm (+0.35m OD to +0.79m OD). This may be associated with the contraction of the sub-tidal and inter-tidal areas of the Inner Estuary around 5,940 ± 40 ^{14}C yr, as recorded by the widespread development of peat at Helsby Marsh and in the more landward areas of Ince Marshes. Dating of the change from sub-tidal to saltmarsh conditions at Ince Marshes would be necessary before the two events can be unequivocally linked.

Sub-tidal / tidalflat environments characterise Ince Marshes for much of the Late Holocene, resulting in around 3m of minerogenic deposition. Absence of diatoms in the top 150cm of core Ince 2 means that the nature of sedimentary environments remains undetermined, although high saltmarsh environments are apparent towards the top of the core. Perhaps associated with the change from low saltmarsh to sub-tidal channel /

tidalflat conditions at Ince Marshes from 408cm (+1.00m OD) is a change to transitional reedswamp / saltmarsh environments at Helsby Marsh, concurrent with the deposition of increasingly organic poor, minerogenic sediments at 3,220 ± 40 ^{14}C yr BP. A similar change from organic to minerogenic deposition occurs in the more seaward cores of CB5, Ince 3, CB16 and CB17. In core Ince 7 from Ince Banks, silts and fine sands begin to accumulate after 5,280 ± 80 ^{14}C yr BP. This core is located in a more seaward area than Helsby Marsh, accounting for the earlier onset of marine conditions. It is possible that terrestrial / semi-terrestrial conditions persisted at Helsby Marsh landward of core Ince 4, with continued peat accumulation evident in core Ince 5, although dating of the cessation of peat accumulation in core Ince 5 would be necessary to confirm this.

Saltmarsh conditions continue in core Ince 4 from Helsby Marsh after 3,220 ± 40 ^{14}C yr BP. Although poor diatom preservation has resulted in a patchy environmental reconstruction, occasional preserved diatom assemblages generally indicate saltmarsh conditions. In addition, the organic content of the sediment units remains between 3% and 5%, and the iron oxide mottling of the sediments indicates periodic aerial exposure. The microfossil assemblages in the thin upper organic rich horizon, of uncertain age, also testify to the existence of saltmarsh conditions. An increase in the marine influence results in the cessation of this organic rich horizon and the replacement of saltmarshes with tidalflats. This switch from high inter-tidal conditions to low inter-tidal conditions, as recorded in core Ince 4, may have caused the cessation of peat deposition in core Ince 5, the more landward core from Helsby Marsh. If this is the case, then the Late Holocene expansion in the inter-tidal and sub-tidal areas of the Inner Mersey Estuary may have in fact occurred in two phases. The first phase resulted in minerogenic deposition over former peat surfaces in most cores seaward of core Ince 5 at Helsby Marsh, with sub-tidal and tidalflat conditions not extending further inland than Ince Marshes, and saltmarshes persisting in the more seaward areas of Helsby Marsh. The second phase of sub-tidal and inter-tidal expansion was more extensive, with tidalflats replacing saltmarshes in the seaward areas of Helsby Marsh at one point. This more extensive second phase most probably resulted in the deposition of minerogenic sediments over former peat surfaces in the most landward areas of Helsby Marsh.

This interpretation, however, is based on sparse diatom evidence, and diatom analysis of other cores needs to be completed before this interpretation can be proven. In addition, radiocarbon dating of the cessation of the upper peat in core Ince 5, re-dating of the thin upper peat unit in core Ince 4, and microfossil analysis of the upper minerogenic unit in core Ince 5, is also needed for confirmation. Nevertheless, the Late Holocene expansion in sub-tidal and inter-tidal areas remains less extensive than that experienced in the Early Holocene, when sub-tidal deposits were thicker and more common in core Ince 4 from Helsby Marsh. The less energetic Late Holocene marine conditions in the Inner Mersey Estuary are most obvious in the particle size data. Prior to the change to inter-tidal conditions, which occurred between 473cm and 429cm (+0.35m OD and +0.79m OD), the mean particle size of core Ince 2 sediments was on average 5.0 ϕ, whereas the mean particle size of the sediments above 429cm (+0.79m OD) is 6.0 ϕ. In addition, the sediments above 429cm (+0.79m OD) are generally very poorly sorted and less finely skewed than the sediments below 473cm (+0.35m OD), which are generally poorly sorted and very finely skewed.

Saltmarshes are present at Helsby and Ince Marshes in the recent past, as indicated by the diatom assemblages towards the surface of the sediment cores. The increasing organic content of the sediments, and the presence of rootlets in the uppermost sediments of both cores, indicates that higher inter-tidal conditions probably persisted at Helsby and Ince Marshes. Reclamation and the construction of the Manchester Ship Canal resulted in the isolation of Helsby and Ince Marshes from the Mersey Estuary.

7.4 Comparison of $\delta^{13}C$ and C/N with microfossil-inferred palaeoenvironments

The pollen- and diatom-inferred palaeoenvironments of Helsby and Ince Marshes (Figures 7.1 to 7.3) are shown together with organic $\delta^{13}C$ and C/N (Figure 7.4 and Figure 7.5 respectively) in order to critically assess the accuracy of $\delta^{13}C$ and C/N as coastal palaeoenvironmental indicators.

7.4.1 Helsby Marsh

Significant changes in $\delta^{13}C$ and C/N values occur in association with changes between Holocene sub-tidal, inter-tidal and supra-tidal sediments (Figure 7.4). In general, low $\delta^{13}C$ values of less than –28.0‰, and high C/N ratios of over 20.0, are associated with

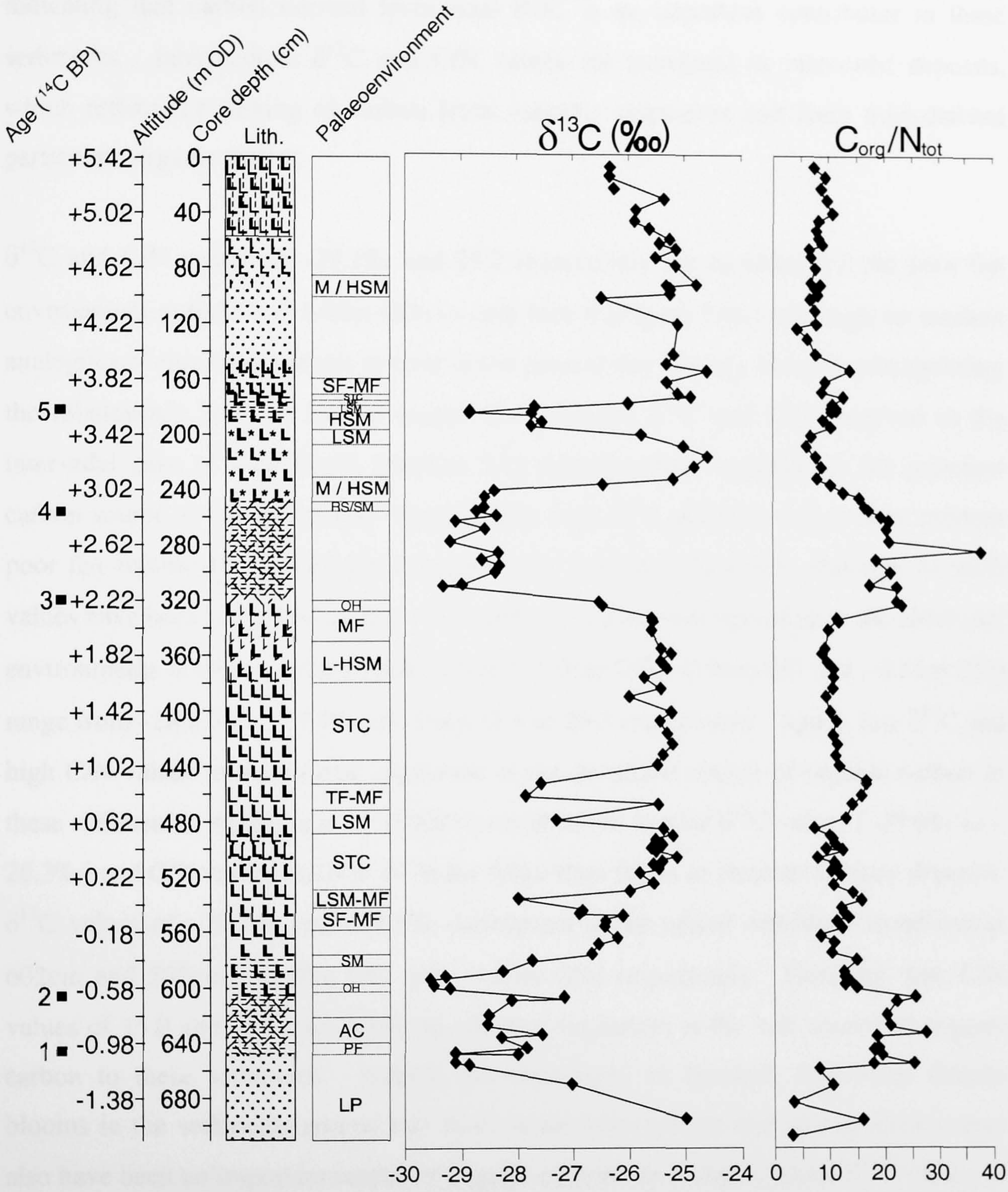

Figure 7.4. Core Ince 4 diatom and pollen-inferred palaeoenvironments and associated $\delta^{13}C$ and C/N. The lithology key is presented with Figure 6.1. Palaeoenvironmental abbreviations are as in Figure 7.2. 1 = 7, 350 ± 60 ^{14}C yr BP; 2 = 6,800 ± 50 ^{14}C yrs BP; 3 = 5,940 ± 50 ^{14}C yrs BP; 4 = 3,220 ± 40 ^{14}C yrs BP; 5 = 800 ± 40 ^{14}C yrs BP.

supra-tidal sediments, which reflect the importance of carbon derived from vascular vegetation in these sediments. In contrast, sub-tidal sediments have much higher $\delta^{13}C$ values of between –26.0‰ and –25.0‰, and much lower C/N ratios of around 10.0, indicating that carbon derived from tidal POC is an important contributor in these sediments. Intermediate $\delta^{13}C$ and C/N values are measured in inter-tidal deposits, which reflect the mixing of carbon from vascular vegetation and from tidal-derived particulate organic matter.

$\delta^{13}C$ and C/N values of –29.1‰ and 25.2 respectively are recorded for the poor fen environment at 648cm (–1.06m OD) in core Ince 4 (Figure 7.4). Although no modern analogues of this environment remain in the present day Mersey Estuary, extrapolating the relationship between carbon source and sediment $\delta^{13}C$ and C/N observed in the inter-tidal zone of Ince Banks (Section 5.1) indicates that vegetation is the principal carbon source to the sediments. Comparisons with $\delta^{13}C$ and C/N values from modern poor fen sediments is necessary to support this inference, however, although no such values have been published to date. $\delta^{13}C$ and C/N values corresponding to the alder carr environments at 643cm, 638cm and 623cm (–1.01m OD, –0.96m OD and –0.81m OD) range from –28.6‰ to –27.9‰ and from 18.9 to 20.2 respectively. Again, low $\delta^{13}C$ and high C/N values indicates that vegetation is the dominant source of organic carbon to these sediments. Andrews *et al.* (2000) have obtained similar $\delta^{13}C$ values (–29.0‰ to –26.3‰) and C/N values (12.9 to 19.3) for Alder Carr facies in Humber Estuary deposits. $\delta^{13}C$ values of –29.2‰ and –29.5‰ correspond to the mixed oak-hazel woodland at 602cm and 598cm (–0.60m OD and –0.56m OD) respectively. However, low C/N values of 15.0 and 13.8 cast doubt on whether vegetation is the sole source of organic carbon to these sediments. Indeed, the occurrence of brackish freshwater diatom blooms in the sediments around this level in the core reveals that phytoplankton may also have been an important source of organic carbon. In contrast, lower $\delta^{13}C$ values of approximately –26.5‰, and higher C/N ratios of between 22.0 and 23.0, are measured for oak-hazel woodland at 323cm and 321cm (+2.19m OD and +2.21m OD) respectively. A wide range in C/N, from 13.3 to 37.2, has also been found for oak-hazel woodland facies in Humber Estuary deposits (Andrews *et al.*, 2000), although associated $\delta^{13}C$ values were a little less variable (–29.1‰ to –27.4‰). A $\delta^{13}C$ and C/N value of –27.7‰ and 15.0 respectively is recorded for the saltmarsh environment at

580cm (–0.38m OD) and indicates that organic carbon is derived predominantly from vascular vegetation. $\delta^{13}C$ is slightly lower, and C/N higher, however, than the corresponding modern Ince Banks saltmarsh sediments, although $\delta^{13}C$ values for the highest parts of the saltmarsh (–27.8‰) are comparable. Similar $\delta^{13}C$ and C/N values have been measured for high saltmarsh sediments in Humber Estuary deposits (–27.8‰ to –23.4‰ and 12.5 to 25.0, respectively), and here too Holocene $\delta^{13}C$ values were on the whole lower than modern equivalent mean high saltmarsh values (–24.3‰).

Diatom assemblages preserved in the thick minerogenic unit between 553cm and 385cm (–0.11m OD and +1.57m OD) indicate deposition under sub-tidal and lower inter-tidal environments (Figure 7.2). The range in $\delta^{13}C$ and C/N of the sub-tidal deposits between 557cm and 543cm (–0.15m OD and –0.01m OD) is relatively narrow, between –26.9‰ and –26.4‰ and between 11.2 and 12.4 respectively (Figure 7.4). $\delta^{13}C$ and C/N indicate a mixture of vascular vegetation and marine plankton derived carbon in the sediments at this level. Comparison with modern Inner Estuary sub-tidal $\delta^{13}C$ (–22.8‰, Table 5.2) reveals that $\delta^{13}C$ is 3.6‰ higher in the modern environment. Unfortunately, C/N values are not available for comparison in the sub-tidal channel sediments of the Mersey Estuary, although contemporary sub-tidal sediment C/N values from the Tay Estuary in Scotland range between 9.0 and 15.7 (e.g. Thornton & McManus, 1994), depending on the distance from the estuary mouth.

A change to low saltmarsh or mudflat conditions is apparent at 537cm (+0.05m OD). $\delta^{13}C$ falls to –28.0‰, whilst C/N is 15.8. The direction of change in $\delta^{13}C$ is consistent with that expected for a reduction in marine conditions. The rise in $\delta^{13}C$ indicates a greater proportion of vascular vegetation derived carbon in the sediments relative to phytoplankton. This inference is further supported by the C/N value. $\delta^{13}C$ is significantly higher, and C/N lower, in modern Ince Banks low saltmarsh and tidalflat surface sediments (Figure 5.1). Low saltmarsh conditions are evident also at 479cm (+0.63m OD) and at 463cm (+0.79m OD), and here also $\delta^{13}C$ (–27.3‰ and –27.9‰ respectively) and C/N (13.5 and 16.0 respectively) is significantly different from the $\delta^{13}C$ and C/N of the modern equivalent environment (–24.7‰ and 10.0 respectively). Only at 366cm and at 355cm (+1.76m OD and +1.87m OD) are the $\delta^{13}C$ (–25.4‰) and C/N (9.7 and 9.6 respectively) of these diatom-inferred saltmarsh sediments comparable

to modern values. However, the occurrence of aerophilous diatom species in greater numbers suggests a decrease in tidal exposure at this level, suggesting an increase in saltmarsh aerial exposure. Therefore, contrary to observed values, this should lead to a decrease in $\delta^{13}C$ and an increase in C/N. A large range in low saltmarsh $\delta^{13}C$ (–28.3‰ to –24.0‰) and C/N (13.7 to 22.0) was also encountered in Humber Estuarine deposits, and modern equivalent mean low saltmarsh $\delta^{13}C$ values were higher here also (–23.6‰) (Andrews *et al.*, 2000).

Sub-tidal channel conditions between 527cm and 490cm (+0.15m OD and +0.52m OD) are apparent from the high frequencies of marine plankton and marine tychoplankton diatom species in the assemblages. $\delta^{13}C$ and C/N values remain in the narrow range of between –25.6‰ and –25.1‰ and between 7.6 and 10.9 respectively, throughout this deposit. Similar $\delta^{13}C$ and C/N values are encountered for the sub-tidal channel deposits from 433cm to 385cm (+1.09m OD and +1.57m OD), although for the sub-tidal channel deposits from 557cm and 543cm (–0.15m OD and –0.01m OD) the range in $\delta^{13}C$ is lower (between –26.9‰ and –26.4‰) and the range in C/N is higher (between 11.2 and 12.4). Both the $\delta^{13}C$ and C/N values in the sub-tidal channel deposits between 527cm and 490cm (+0.15m OD and +0.52m OD) and between 433cm and 385cm (+1.09m OD and +1.57m OD) are indicative of carbon derived from marine POM. Comparison with modern Inner Estuary sub-tidal channel sediment $\delta^{13}C$ (–22.8‰, Table 5.2) shows an apparent shift in $\delta^{13}C$ between modern and Mid Holocene values. Mudflat conditions are present at 333cm (+2.09m OD), and have an associated $\delta^{13}C$ value of –25.6‰ and a C/N value of 11.4. Comparison with modern-day Ince Banks tidalflat $\delta^{13}C$ and C/N measurements (–23.7‰ to –23.5‰, and 9.3 to 9.6, respectively) reveals that $\delta^{13}C$ values are higher, and C/N values are lower, in the modern environment (Figure 5.1). Again, a similar picture emerges for the Humber Estuary, where the mean contemporary mudflat $\delta^{13}C$ value, –22.5‰, is significantly greater than the mean mudflat $\delta^{13}C$ value in the Holocene deposits (–25.2‰) (Andrews *et al.*, 2000).

$\delta^{13}C$ and C/N values of –28.7‰ to –28.6‰ and 15.6 to 16.9 correspond to the transitional wet reedswamp and saltmarsh environment between 256cm and 247cm (+2.86m OD and +2.95m OD). These values suggest that vascular vegetation is the predominant source of organic carbon to these sediments, although again this

assumption would need to be verified by obtaining $\delta^{13}C$ and C/N measurements of contemporary transitional wet reedswamp / saltmarsh sediments (which are not available in the literature to date). There is no indication of marine influence, as the presence of marine plankton would lower the C/N values and cause an increase in the $\delta^{13}C$ values. The $\delta^{13}C$ and C/N values of the saltmarsh environments between 236cm and 232cm (+3.06m OD and +3.10m OD) (–26.5‰ to –25.2‰ and 8.1 to 10.1 respectively) and at 196cm (+3.46m OD) (–27.8‰ and 10.7) reflect a greater presence of marine plankton in the sediments. Similar $\delta^{13}C$ and C/N values are also recorded for the saltmarsh environment at 93cm (+4.49m OD), and these are comparable to Ince Banks high saltmarsh sediment $\delta^{13}C$ and C/N values (between –27.8‰ and –25.2‰, and between 9.7 and 11.6 respectively; Figure 5.1). However, the high saltmarsh environments at 184cm and 182cm (+3.58m OD and +3.60m OD) have lower $\delta^{13}C$ values of –28.9‰, and higher C/N values of 12.2 and 11.7 respectively. This may indicate a greater contribution of carbon from vascular vegetation in these sediments. Similar values are not recorded in Ince Banks high saltmarsh sediments, although the destruction of parts of the high saltmarsh for the construction of the Manchester Ship Canal prevents the measurement of the full range of high saltmarsh sediment $\delta^{13}C$ and C/N. Low saltmarsh conditions are apparent at 180cm and at 177cm (+3.62m OD and +3.65m OD), and $\delta^{13}C$ values of –27.7‰ and –26.0‰, and C/N ratios of 10.3 and 10.9 respectively, are recorded here, indicating a mixture of carbon derived from vascular vegetation and from tidal-derived POM in the sediments. Tidalflat conditions replace the low saltmarsh conditions from 172cm to 169cm (+3.70m OD and +3.73m OD) respectively. $\delta^{13}C$ increases significantly to between –25.1‰ and –24.6‰. Although this may suggest a progressively greater contribution of organic carbon from marine phytoplankton in the sediment, the C/N values do not support this inference, as an increase in C/N from 10.9 to 14.0 between the low saltmarsh and the tidalflat deposits is recorded, although C/N values do fall to 9.1 in the tidalflat deposits at 169cm (+3.73m OD).

7.4.2 Ince Marshes

The conservative range in both $\delta^{13}C$ and C/N values throughout most of core Ince 2 (Figure 7.5) reflects the less diverse coastal palaeoenvironments recorded in this area during the Holocene. Sub-tidal environments have dominated its history, and this is

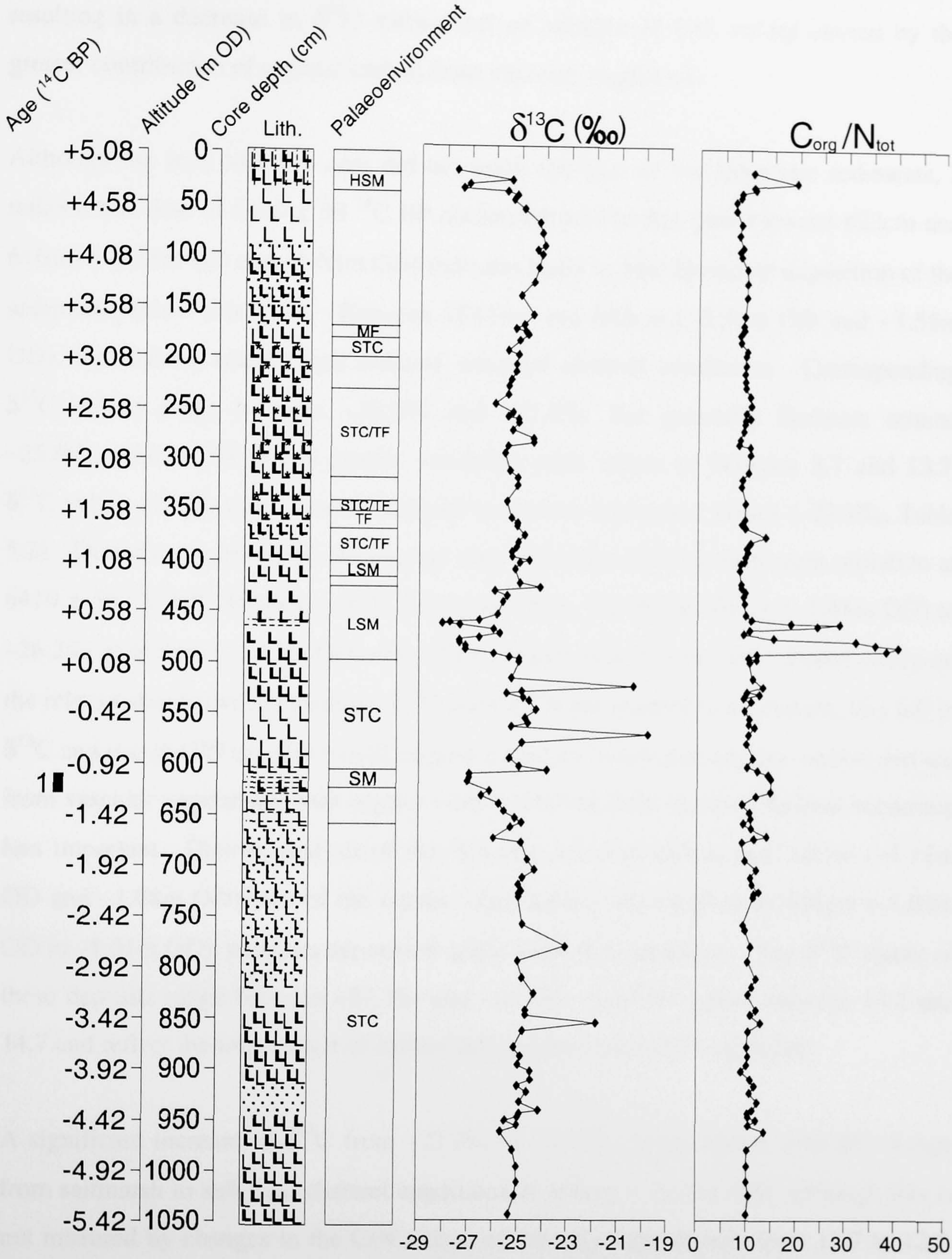

Figure 7.5. Core Ince 2 diatom-inferred palaeoenvironments and associated δ^{13}C and C/N. The lithology key is presented with Figure 6.1. Palaeoenvironmental abbreviations are as in Figure 7.2. 1 = 6,410 ± 50 ^{14}C yrs BP.

reflected by the high $\delta^{13}C$ values (around –25.0) and low C/N ratios (around 10.0‰). Periods of sediment deposition under inter-tidal conditions are apparent, however, resulting in a decrease in $\delta^{13}C$ values and an increase in C/N values caused by the greater contribution of organic carbon from vascular vegetation.

Although the Ince Marshes core did not reach the base of the Holocene sediments, a radiocarbon date of 6410 ± 50 ^{14}C BP obtained from the thin peat between 623cm and 616cm (–1.15m OD and –1.08m OD) indicates Early to Mid Holocene deposition of the sediments below this level. Between 1042cm and 663cm (–5.34m OD and –1.55m OD), the diatom assemblages indicate sub-tidal channel conditions. Corresponding $\delta^{13}C$ values range between –25.7‰ and –21.9‰, but generally fluctuate around –25.0‰, whilst C/N shows greater variability with values of between 8.7 and 13.7. $\delta^{13}C$ values are generally lower compared to modern equivalent values (–22.8‰, Table 5.2). Diatoms are absent in the organic clay sediments leading up to peat initiation at 6410 ± 50 ^{14}C BP. However, $\delta^{13}C$ values fall from –24.9‰ at 656cm (–1.48m OD) to –26.2‰ at 625cm (–1.17m OD) and C/N increases from 9.6 to 14.4. Based solely on the relationship between elevation, $\delta^{13}C$ and C/N in the modern environment; this fall in $\delta^{13}C$ and rise in C/N up-core would suggest a gradual increase in organic carbon derived from vascular vegetation, with organic carbon derived from marine plankton becoming less important. Diatom analysis of the thin peat between 623cm and 616cm (–1.15m OD and –1.08m OD), and of the organic clay deposit from 617cm to 609cm (–1.09m OD to –1.01m OD), suggests deposition under saltmarsh conditions. The $\delta^{13}C$ values of these deposits range between –27.3‰ and –26.9‰, and C/N values between 13.2 and 14.7 and reflect the importance of carbon derived from vascular vegetation.

A significant increase in $\delta^{13}C$ from –27.0‰ to –23.9‰ is associated with the change from saltmarsh to sub-tidal channel conditions at 606cm (–0.98m OD), although this is not mirrored by changes in the C/N ratios, which only falls slightly from 13.7 to 12.7. Nevertheless, the large increase in $\delta^{13}C$ indicates that marine derived POC is an important source of organic matter in the sediments. Sub-tidal channel conditions continue to 499cm (+0.09m OD), and associated $\delta^{13}C$ values generally fluctuate between –25.5‰ and –25.0‰, significantly higher than modern equivalent sub-tidal channel sediment $\delta^{13}C$ values (–22.8‰, Table 5.2), whilst C/N values fluctuate around

10.0. Two prominent spikes in $\delta^{13}C$ are apparent at 571cm and 522cm (–0.63m OD and –0.14m OD), with $\delta^{13}C$ values increasing to –19.8‰ and –20.4‰. No significant change in C/N, lithology or diatoms is associated with these spikes in $\delta^{13}C$. Although contamination could explain the two spikes, the $\delta^{13}C$ values do occur within the range of $\delta^{13}C$ values measured in nearshore sediment deposits (e.g. Middelburg and Nieuwenhuize, 1998).

Sediment deposits from 500cm (+0.08m OD) to the surface are assumed to represent the Mid to Late Holocene, as indicated by a radiocarbon date of 6410 ± 50 ^{14}C BP obtained from the thin peat between 623cm and 616cm (–1.15m OD and –1.08m OD). The diatom assemblages indicate low saltmarsh conditions between 473cm and 429cm (+0.35m OD and +0.79m OD), with corresponding $\delta^{13}C$ values of between –25.5‰ and –27.4‰, and C/N values of between 9.2 and 24.1. Further, $\delta^{13}C$ reaches values of –28.1‰ within this deposit at 461cm (+0.47m OD), although diatom data is not available from this level. From 408cm to 171cm (+1.00m OD to +3.37m OD) the diatom assemblages indicate alternating sub-tidal channel / tidalflat and tidalflat conditions, with mudflats present between 177cm and 171cm (+3.31m OD and +3.37m OD). $\delta^{13}C$ and C/N remains consistent throughout, with the majority of $\delta^{13}C$ values remaining between –25.5‰ and –25.0‰, and the majority of C/N values remaining around 10.0, reflecting the importance of tidal-derived POC. Diatoms are absent in the sediments from 170cm (+3.38m OD) to the top of the core, although a single preserved assemblage at 30cm (+4.78m OD) indicates high saltmarsh conditions and this is associated with a $\delta^{13}C$ value of –27.1‰ and a C/N ratio of 11.4, indicating that vascular vegetation is an important source of organic carbon in these sediments.

Chapter 8

Discussion and Conclusions

8.1 The validity of $\delta^{13}C$ and C/N as coastal palaeoenvironmental indicators

8.1.1 Comparison with microfossil record

Early to Mid Holocene, Mid to Late Holocene and modern $\delta^{13}C$ and C/N data and associated microfossil-inferred palaeoenvironments are presented in a summary diagram (Figure 8.1). The microfossil-inferred palaeoenvironments are split into supra-tidal, inter-tidal and sub-tidal categories and the coastal environments organised within these categories by decreasing elevation in relation to the tidal frame. The mean and standard deviation of $\delta^{13}C$ and C/N values associated with each microfossil-inferred palaeoenvironment is shown. The data is split into Early to Mid Holocene, Mid to Late Holocene and modern time frames in order to investigate if organic matter decomposition has any effect on bulk sediment $\delta^{13}C$ or C/N values.

It is obvious from Figure 8.1 that the relationship between coastal zone ground elevation, sediment $\delta^{13}C$ and sediment C/N is preserved throughout the Holocene. In particular, Holocene supra-tidal environments (mean $\delta^{13}C$ of –29.1‰ to –27.9‰, mean C/N of 16.3 to 25.2) may be distinguished from Holocene inter-tidal environments (mean $\delta^{13}C$ of –26.9‰ to –25.0‰, mean C/N of 10.3 to 13.3), and sub-tidal environments (mean $\delta^{13}C$ of –25.1‰ to –24.9‰, mean C/N of 8.9 to 10.9).

In the supra-tidal zone, oak-hazel woodland, alder carr and poor fen, all have mean $\delta^{13}C$ values of less than around –28.0‰, which is as expected in environments in which C_3 organic material (vascular vegetation and freshwater plankton) is the major contributor to the sediment. Mean C/N values of over 15.0 are also as expected, with vascular vegetation being the dominant organic matter source in each of these environments. It is surprising, however, that the C/N value of poor fen deposits (25.2) is higher than the mean C/N of alder carr deposits (19.5), because the greater presence of freshwater phytoplankton in the poor fen environment would be expected to lower the C/N values. Only a single poor fen deposit was encountered in this study (and hence only a single C/N measurement). Therefore, more C/N measurements of poor fen deposits are

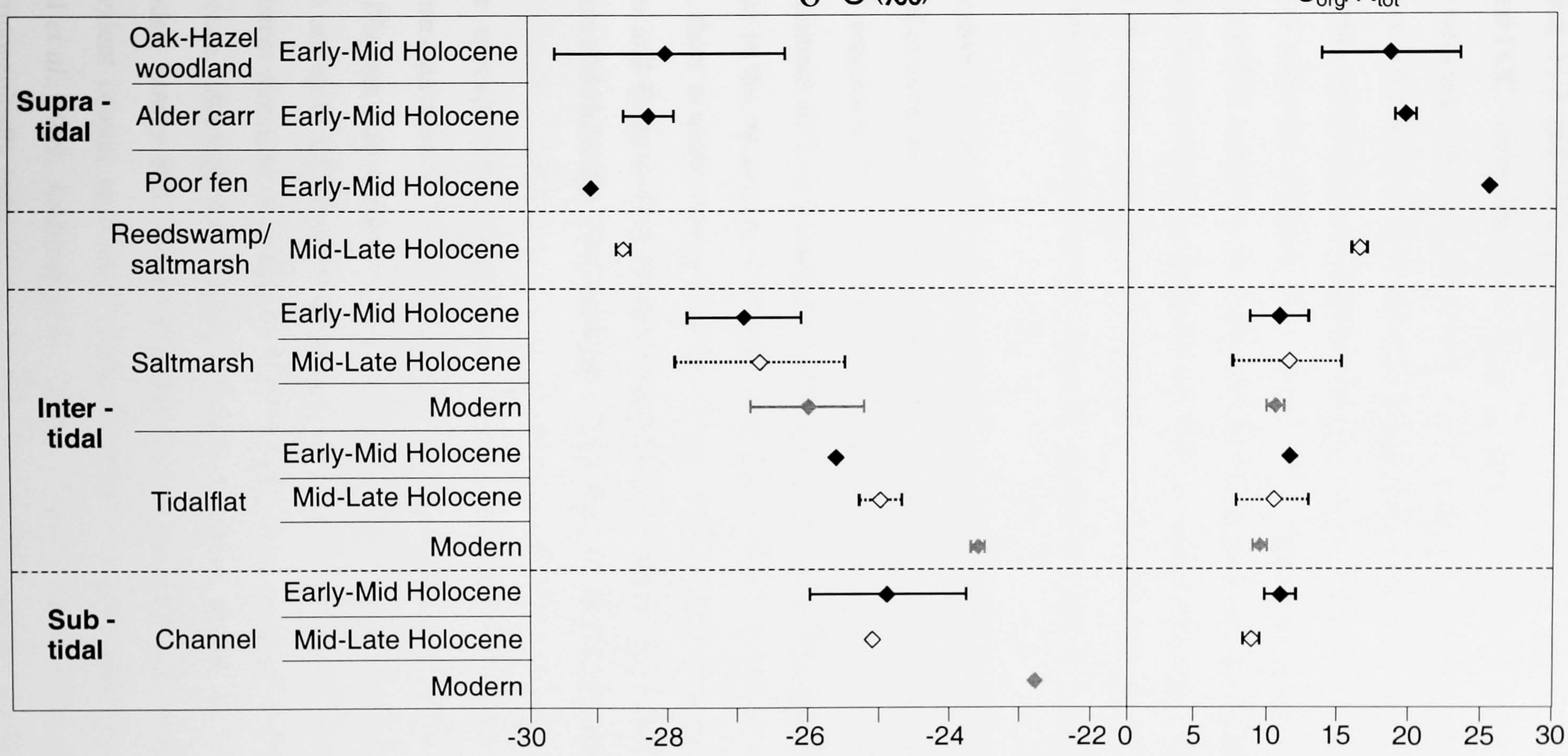

Figure 8.1. Mean Early to Mid Holocene $\delta^{13}C$ and C/N (◆), mean Mid to Late Holocene $\delta^{13}C$ and C/N (◇) and mean modern $\delta^{13}C$ and C/N (◆) values of supra-tidal, inter-tidal and sub-tidal environments in the Inner Mersey Estuary. The standard deviation (error bars) of the group of $\delta^{13}C$ and C/N values measured for each environment in the supra-tidal, inter-tidal and sub-tidal zones are also shown. Data points without error bars indicate an insufficient number of $\delta^{13}C$ and C/N measurements.

needed to attain a mean value. In the inter-tidal zone, mean Holocene and modern saltmarsh $\delta^{13}C$ values range between –26.9‰ and –26.1‰, and mean C/N ratios between 11.3 and 13.3, which reflects the mixing of vascular vegetation with tidal-derived POC. Mean Holocene and modern tidalflat $\delta^{13}C$ values are slightly greater, and range between –25.6‰ and –23.6‰, whilst mean C/N ratios are slightly less, and range between 9.6 and 11.4. This indicates a greater proportion of tidal derived POC in these sediments compared to saltmarsh sediments. In the sub-tidal zone, mean Holocene and modern sub-tidal channel $\delta^{13}C$ values range from –25.1‰ to –22.8‰, and mean Holocene C/N values are 10.9 (Late to Mid Holocene) and 8.9 (Early to Mid Holocene). Again, the importance of tidal derived POC in these sediments is reflected in the $\delta^{13}C$ and C/N ratios, although their similarity to Holocene tidalflat $\delta^{13}C$ and C/N values prevents their distinction in the sediment record using only $\delta^{13}C$ and C/N analysis.

There does appear to be some overlap in both $\delta^{13}C$ and C/N between spatially adjacent coastal environments within tidal zones. In the supra-tidal zone, the large range in oak-hazel woodland $\delta^{13}C$ and C/N (–29.5‰ to –26.5‰ and 13.8 to 23.0) makes this environment difficult to distinguish using $\delta^{13}C$ and C/N. This large range in values may be due to the occurrence of diatom blooms in some of the deposits. In the inter-tidal zone, there is some overlap between Late to Mid Holocene and modern saltmarsh $\delta^{13}C$ values and Early to Mid Holocene tidalflat $\delta^{13}C$ values, whilst the mean and range in modern and Holocene C/N ratios are very similar for both environments.

There appears to be a significant shift in Holocene $\delta^{13}C$ values from their original modern equivalent $\delta^{13}C$ values, with, for example, Late to Mid Holocene $\delta^{13}C$ values up to 4.1‰ less than modern equivalent $\delta^{13}C$ values. Further, Late to Mid Holocene C/N ratios are up to 1.8 greater than modern equivalent C/N ratios. There appears to be no consistent direction of change in $\delta^{13}C$ between Early to Mid Holocene and Late to Mid Holocene, although C/N ratios appear to increase further between these two time periods. Lower $\delta^{13}C$ values in Holocene coastal sediments compared with modern-equivalent coastal sediments is also apparent in other studies (e.g. DeLaune, 1986; Fogel *et al.*, 1989; Andrews *et al.*, 2000). This difference is not caused by the recent, anthropogenically induced, rise in atmospheric CO_2 concentrations (which has resulted in a decrease in the $\delta^{13}C$ composition of atmospheric CO_2 by around 1.5‰ from pre-

industrial levels, Section 2.3.3.1), as this would result in comparatively higher, not lower, Holocene sediment $\delta^{13}C$ values. The change in $\delta^{13}C$ and C/N over time probably reflects the early loss of labile organic matter during decomposition, leading to the relative increase in refractory material, such as lignin in vascular vegetation, or lipids in phytoplankton. Comparison of lignin, for example, with whole plant $\delta^{13}C$ and C/N in saltmarsh vegetation taken from Ince Banks as part of this study reveals that, on average, lignin $\delta^{13}C$ is 3.04‰ less than the whole plant $\delta^{13}C$ (Table 5.1), and average lignin C/N is greater than the whole plant C/N by 3.0. This difference in $\delta^{13}C$ values between the lignin fraction and the whole plant is in agreement with values reported elsewhere (Benner *et al.*, 1987).

The obvious influence of the degree of organic decomposition on bulk sediment $\delta^{13}C$ and C/N values has important implications for $\delta^{13}C$ and C/N-based coastal palaeoenvironmental reconstructions. However, in terms of the application of $\delta^{13}C$ and C/N to RSL reconstruction, changes in the bulk sediment $\delta^{13}C$ values caused by fluctuating RSLs may be enhanced by the associated change in the rates of decomposition, which may result in a more obvious $\delta^{13}C$ signature. Hypothetically, a transgressive overlap (replacement of organic sediments with minerogenic sediments, Section 2.1.3.1) caused by a positive tendency in RSL would result in an increase in $\delta^{13}C$ values due to the deposition of isotopically heavier tidal-derived material. In these anaerobic sediments, decomposition would slow, and any associated decrease in sediment $\delta^{13}C$ values due to decomposition would be minimal. In contrast, in a regressive sequence resulting from a negative tendency of RSL, the lowering water table would enhance the rates of decomposition. The trend of decreasing $\delta^{13}C$ values associated with the regressive overlap may be reinforced by a further decrease in $\delta^{13}C$ values as a result of decomposition.

8.1.2 Evaluation of $\delta^{13}C$ and C/N as coastal palaeoenvironmental indicators

There are two significant limitations associated with comparing $\delta^{13}C$ and C/N values with microfossil-inferred palaeoenvironments in this study. Firstly, although diatoms appear to be the most accurate microfossil indicators in the context of coastal environmental reconstruction (Gehrels *et al.*, 2001), taphanomic processes (Section 2.2.6) may result in a distorted fossil diatom assemblage, and consequently may not

accurately reflect the environment of deposition. This limitation is inherent in microfossil-based, palaeoenvironmental reconstructions and, to some extent, is unquantifiable. The second significant limitation is the uneven number of $\delta^{13}C$ and C/N measurements of each coastal palaeoenvironment (Table 8.1), both spatially and temporally. This is largely due the location of cores investigated and the preservation of coastal palaeoenvironmental indicators. The thick accumulations of minerogenic deposits in both cores Ince 2 and Ince 4 mean that sub-tidal channel and inter-tidal palaeoenvironments are generally well represented in this study, whilst supra-tidal environments are under-represented. $\delta^{13}C$ and C/N measurement of modern supra-tidal areas in the Mersey Estuary is not possible due to their reclamation. Supra-tidal deposits are absent from core Ince 2 and, whilst present in core Ince 4, a combination of poor pollen preservation coupled with the restricted use of pollen analysis in this investigation (to verify radiocarbon dates and to provide palaeoenvironmental information at lithological boundaries) prevented a full exploration of these palaeoenvironments. The collection of more cores in the landward areas of Helsby Marsh and high-resolution pollen, $\delta^{13}C$ and C/N analysis of the organic rich units is necessary to rectify this limitation. Nevertheless, $\delta^{13}C$ and C/N values have been obtained for a broad range of coastal palaeoenvironments over different timescales (Early to Mid Holocene, Mid to Late Holocene, modern), allowing an evaluation of the potential of $\delta^{13}C$ and C/N analysis in the field of Holocene coastal environmental reconstruction.

The relationship between coastal zone ground elevation and sediment $\delta^{13}C$ and C/N in the modern coastal environment is preserved in the sediment record, although this relationship is distorted slightly by the decomposition of organic matter. Due to the presence of organic matter in all coastal deposits, a continuous $\delta^{13}C$ and C/N record of coastal environmental change may be obtained. Although the effects of decomposition may prevent the application of 'signature' $\delta^{13}C$ and C/N values to be applied to each coastal environment, because $\delta^{13}C$ and C/N are governed by ground elevation within the tidal frame, any change in RSL may be detected. $\delta^{13}C$ and C/N analysis is therefore particularly valuable in verifying SLIs. The integrity of SLIs partly relies on the evidence of a gradual increase, or removal, of marine conditions prior to transgressive or regressive overlaps, respectively. An eroded regressive or transgressive overlap contact, or a depositional hiatus, is indicated if this gradual palaeoenvironmental change

is not apparent. The nature of environmental changes prior to an overlap may remain unresolved if microfossils are absent, or poorly preserved, in the sediments. $\delta^{13}C$ and C/N analysis of such sediments would demonstrate whether an increase or removal of marine conditions occurs prior to an overlap. For example, a gradual decrease in $\delta^{13}C$ and an increase in C/N in the sediments leading up to a regressive overlap could indicate a gradual reduction in tidal-derived organic matter and a greater contribution of organic carbon from vascular vegetation. Therefore, $\delta^{13}C$ and C/N may be used reliably to help verify SLIs if microfossils are absent. This is demonstrated in the following section, where $\delta^{13}C$ and C/N are used for the first time to validate SLIs.

Table 8.1. Number of observations of each coastal environment and the associated number of $\delta^{13}C$ and C/N measurements.

Coastal Environment	Early to Mid Holocene		Mid to Late Holocene		Modern	
	$\delta^{13}C$	C_{org}/N_{tot}	$\delta^{13}C$	C_{org}/N_{tot}	$\delta^{13}C$	C_{org}/N_{tot}
Oak-hazel woodland	n=4	n=4	n=0	n=0	n=0	n=0
Alder carr	n=3	n=3	n=0	n=0	n=0	n=0
Poor fen	n=1	n=1	n=0	n=0	n=0	n=0
Reedswamp/saltmarsh	n=0	n=0	n=2	n=2	n=0	n=0
Saltmarsh	n=10	n=10	n=17	n=17	n=12	n=12
Tidalflat	n=1	n=1	n=4	n=4	n=2	n=2
Sub-tidal channel	n=67	n=67	n=2	n=2	n=3	n=3

8.1.3 Verification of Mersey Estuary SLIs using $\delta^{13}C$ and C/N

The relationship between $\delta^{13}C$, C/N and ground altitude within the tidal frame has been demonstrated for the contemporary inter-tidal zone of the Inner Mersey Estuary, and this relationship is retained in Holocene coastal sediment deposits (Figure 8.1). $\delta^{13}C$ and C/N analysis, used in conjunction, can therefore be used effectively to help verify SLIs. The focus of the present study is not one of an exhaustive Holocene RSL reconstruction of the Mersey Estuary, which would require multi-proxy investigations of cores spanning the axis of the estuary and significantly more radiocarbon dates.

Rather, it is concerned with reconstructing the palaeoenvironments of the Inner Mersey Estuary as a basis to evaluate the application of $\delta^{13}C$ and C/N in the field of coastal palaeoenvironmental reconstruction. Nevertheless, the several dated regressive and transgressive overlaps may be evaluated as suitable SLIs using a combination of microfossil and geochemical ($\delta^{13}C$ and C/N) techniques. This will not only demonstrate the potential of $\delta^{13}C$ and C/N analysis in helping to verify SLIs, but the SLIs generated may be correlated with other SLIs from north west England in an effort to identify region-wide RSL changes. Although altitudinal errors are acknowledged in association with the coring exercise as a consequence of compaction and in relation to the interpolation of tidal parameters (Shennan, 1982), they have little bearing on the present study and are therefore not quantified. In addition, the estimates in the literature (Shennan, 1986) of the indicative ranges for each type of SLI encountered in the present study is likely to be a conservative estimate, with greater ranges expected for macrotidal systems such as the Mersey Estuary (Heyworth & Kidson, 1982). SLIs are presented in Table 8.2 and each is evaluated below.

Helsby Marsh: 7,350 ±60 ^{14}C yr BP

The base of the lower peat at Helsby Marsh, which sits on the proposed Shirdley Hill Sand at –1.06m OD, has been dated at 7,350 ± 60 ^{14}C yr BP (Figure 8.2a). Freshwater diatoms dominate in the lower levels of the peat, although brackish freshwater species are present in very small numbers. The pollen assemblage at –1.06m OD indicates a poor fen environment and the presence of saltmarsh taxa (*Armeria maritima* and Chenopodicaceae) also suggests nearby marine conditions. Taken together, the microfossil data indicate little or no direct contact with tidal water. Brackish freshwater diatoms increase further in the upper levels of the peat at –1.02m OD. The pollen assemblage at –1.02m OD indicates a change to alder carr, and the absence of saltmarsh taxa suggests a reduction in environmental salinity, and therefore contradicts the diatom evidence. Little change is evident in $\delta^{13}C$ or in C/N, which indicate peat formation from C_3 vascular vegetation. A slight rise in the organic content of the peat, from around 60% to 70% between –1.06m OD and –1.02m OD, may indicate increasing terrestrial conditions.

Table 8.2. New SLIs from the Mersey Estuary.

Site	Stratigraphic context	Tendency	Altitude (m OD)	Indicative meaning & range (m)	Approx. altitude of MHWS (m OD ± 0.10)	Age (^{14}C yr BP)	2σ age range (Cal. yr BP)
Helsby Marsh	Basis	+	–1.06 to –1.01	MHWS ± 0.4	–1.06 to –1.01 (± 0.40)	7,350 ± 60	8,010–8,330
Helsby Marsh	Transgressive overlap	+	–0.61 to –0.66	MHWS ± 0.10	–0.61 to –0.66	6,800 ± 50	7,580–7,700
Helsby Marsh	Regressive overlap	–	+2.18 to +2.23	MHWS+HAT2 ± 0.10	+1.58 to +1.63	5,940 ± 40	6,670–6,860
Helsby Marsh	Transgressive Overlap	+	+2.86 to +2.91	MHWS ± 0.10	+2.86 to +2.91	3,220 ± 40	3,360–3,490
Ince Marshes	Regressive/ Transgressive overlap	+/-	–1.15 to –1.08	MHWS + 0.60 ± 0.10	–0.55 to –0.48	6,410 ± 50	7,250–7,430

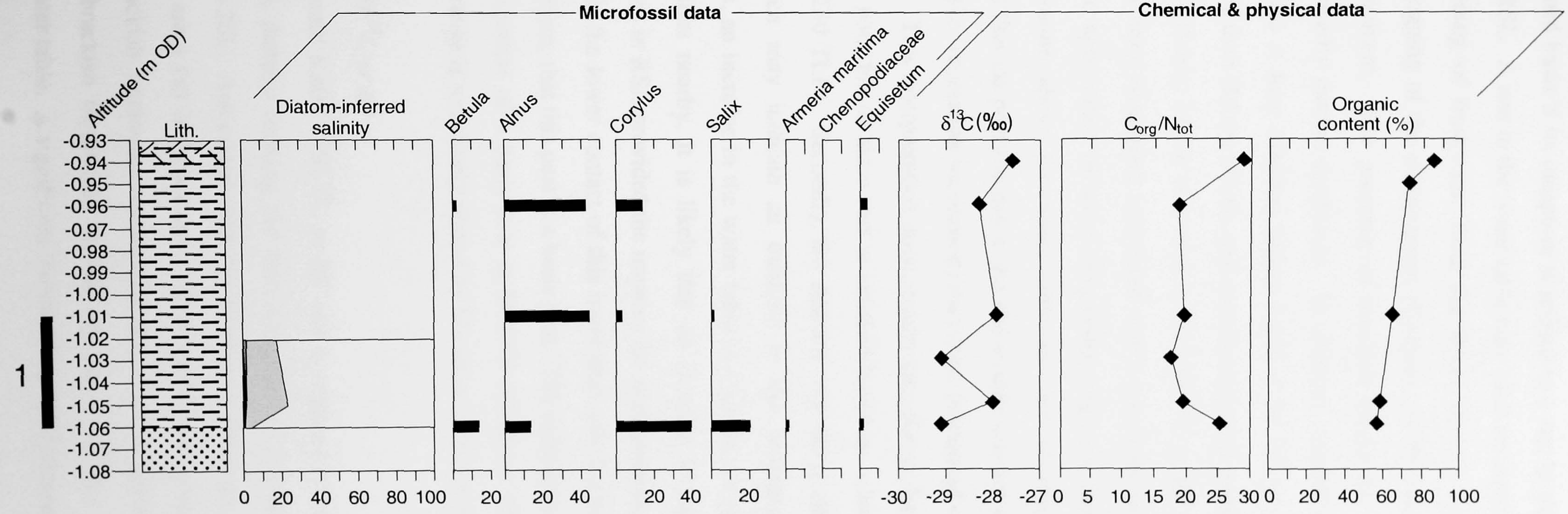

Figure 8.2a. SLI of Helsby Marsh basal peat (1 = 7,350 ± 60 ^{14}C yr BP). Details of the diagrams are given with Figure 8.2e.

A basal peat may be termed basis if its inception is related to a rise in the water table, associated with a rise in RSL. A rise in the water table may have occurred in relation to a rise in RSL, and ponding of freshwater from the River Mersey may also have contributed to the waterlogging of the environment (Godwin, 1978), which may have initiated poor fen development. The presence of brackish freshwater diatoms and saltmarsh taxa supports nearby marine conditions. In addition, around 4m of marine sediments had accumulated at Ince Marshes before 6,410 ± 50 ^{14}C yr BP, which is located 2km more seaward than Helsby Marsh, and so it is likely that marine conditions were in close proximity to Helsby Marsh at around 7,350 ± 60 ^{14}C yr BP. A change to alder carr and then to oak-hazel woodland, associated with a rise in the organic content of the sediments and the appearance of wood fragments, suggests deposition at an increasingly greater elevation above the water table and out of reach of marine conditions. This suggests that the possible rise in the water table was not sustained, and that autogenic processes (i.e. vegetation succession) may have dominated over allogenic processes (i.e. RSL rise). This interpretation must remain speculative for two reasons. Firstly, the change from poor fen to alder carr is inferred based on a low pollen sum (between 148 TLP and 230 TLP). Secondly, the diatoms undergo a rise in brackish freshwater species, which may indicate an increase in the proximity of marine conditions. Nevertheless, an increase in the water table is required for peat formation and with marine conditions nearby, it is likely that an increase in the water table associated with an increase in RSL provided the impetus for peat formation, although it remains uncertain whether the lower contact of this basal peat unit has been subject to erosion. It is likely, therefore, that this peat is a basis peat. The indicative meaning of a poor fen deposit in the context of a basis peat is MHWS (Godwin, 1940; Shennan, 1986) and the indicative range is tentatively placed by Shennan (1986) at 80cm.

Helsby Marsh: 6,800 ±50 ^{14}C yr BP

Peat deposition persists until 6,800 ± 50 ^{14}C yr BP and is replaced by a firm organic clay unit at –0.61m OD, thereby forming the first transgressive overlap recorded at Helsby Marsh (Figure 8.2b). Associated with the change in lithology from peat to organic clay deposition, are a fall in freshwater diatom species and a rise in brackish freshwater species. Brackish freshwater tychoplanktonic species almost completely replace freshwater and brackish freshwater benthic species at –0.62m OD, perhaps indicating a rise in the water table. A significant increase in coastal exposure, albeit of

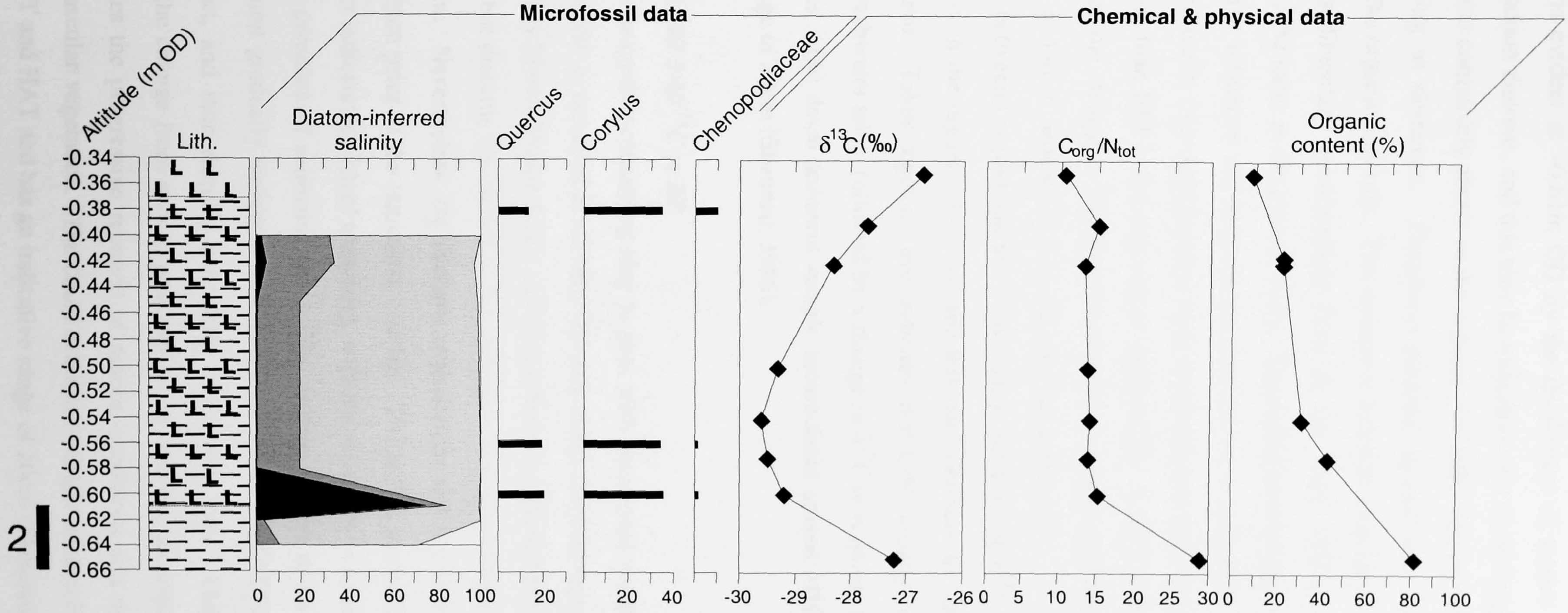

Figure 8.2b. SLI of the first transgressive overlap at Helsby Marsh (2 = 6,800 ± 50 ^{14}C yr BP). Details of the diagrams are given with Figure 8.2e.

short duration, is evident at –0.61m OD by the dominance of marine plankton and marine tychoplankton diatoms, and this may be indicative of a storm surge. Freshwater diatoms are almost completely absent in the organic clay unit, with brackish freshwater species continuing to dominate. *Fragilaria pinnata*, in particular, dominates the assemblages in the organic clay unit. This species is found in association with lagoonal and saltmarsh sedimentary environments (Vos & De Wolf, 1993a), although the lithology favours the latter in the present study. The pollen assemblages also record an increase in marine influence and indicate the presence of a saltmarsh. The organic content of the sediments falls significantly, from approximately 80% in the peat unit at –0.65m OD to less than 10% in the clay unit at –0.35m OD. A fall in C/N from 25.4 to 15.0 accompanies the change in lithology from peat to organic clay deposition. C/N values continue to fall to around 13.0 in the overlying clay unit. Little change is apparent in $\delta^{13}C$ between the peat and the organic clay, but a rise in $\delta^{13}C$ from –29.6‰ to –27.7‰ occurs in the organic clay unit, and this rise continues to –26.7‰ into the overlying clay unit. Taken together, this indicates that C/N initially responds to an increase in the freshwater table, followed by a change in $\delta^{13}C$ in response to more direct marine influences. The dated sediment sample accumulated around MHWST and has an indicative range of 20cm (Shennan, 1986).

Helsby Marsh: 5,940 ±40 ^{14}C yr BP

A change from *Phragmites*-containing clay to peat with occasional wood fragments at 5,940 ± 40 ^{14}C yr BP is recorded at +2.18m OD and marks the first regressive overlap registered at Helsby Marsh (Figure 8.2c). A fall in salinity is apparent from +1.57m OD to +2.09m OD, but diatoms are absent in the sediments deposited immediately before peat development. Nevertheless, the diatoms assemblages and the lithology indicate saltmarsh deposition prior to the regressive overlap. The pollen assemblages from the regressive contact indicate oak-hazel woodland, with the proximity of marine conditions indicated by the presence of saltmarsh taxa. The organic content of the *Phragmites*-containing clay unit gradually increases from less than 5% to nearly 10% towards the regressive contact, and then rises to over 60% in the peat unit. The fall in $\delta^{13}C$ associated with the change from clay to peat deposition, and the accompanying rise in C/N, demonstrates the progressive removal of marine conditions and the increase in importance of vascular vegetation. The dated sediment sample accumulated mid-way between MHWST and HAT and has an indicative range of 20cm (Shennan, 1986).

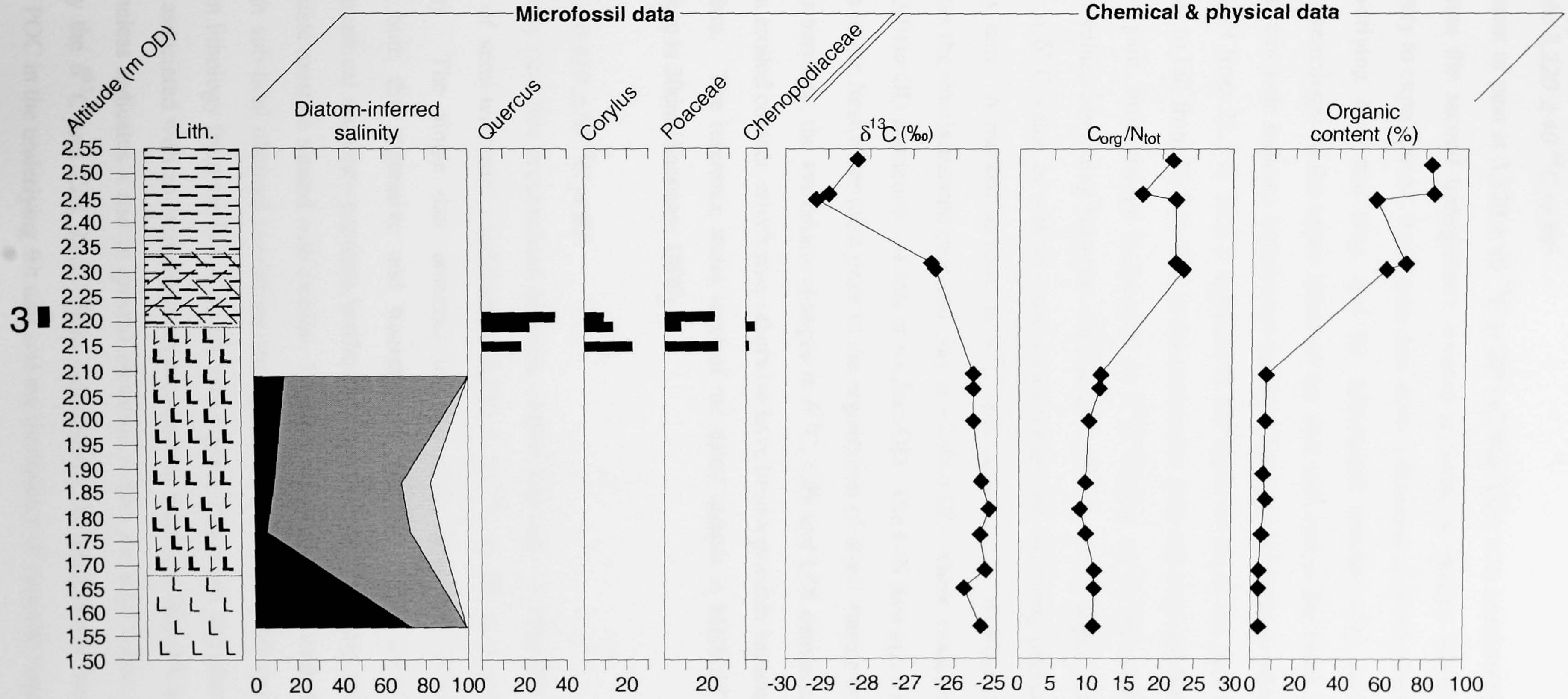

Figure 8.2c. SLI of the first regressive overlap at Helsby Marsh (3 = 5,940 ± 40 ^{14}C yr BP). Details of the diagrams are given with Figure 8.2e.

Helsby Marsh: 3,220 ±40 ^{14}C yr BP

The replacement of peat at 3,220 ± 40 ^{14}C yr BP (+2.91m OD) with interlaminated peat and clay forms the second transgressive overlap recorded at Helsby Marsh (Figure 8.2d). Contrary to expectations, the diatom data show a decrease in salinity between the peat, the overlying peat and clay, and the subsequent mottled clay units. The microfossil assemblages in the upper levels of the peat unit and in the lower levels of the peat and clay unit indicate transitional reedswamp and saltmarsh conditions. A decrease in C/N from 21.7 to 16.2 is apparent in the upper levels of the peat unit, and C/N continues to fall from 15.6 to 10.1 in the successive peat and clay and the mottled clay units. Again, little change is apparent in $\delta^{13}C$ leading up to the transgressive overlap, with values remaining between –28.3‰ and –28.7‰ in the upper peat levels. Furthermore, a $\delta^{13}C$ value of –28.6‰ also characterises the overlying interlaminated peat and clay unit. A marked increase in $\delta^{13}C$ only occurs in the mottled clay unit, which replaces the interlaminated peat and clay at +2.99m OD, where values rise from –28.4‰ at +3.01m OD and reach –24.6‰ at +3.26m OD. The C/N data again indicates an initial rise in the freshwater table prior to the registration of direct marine conditions by $\delta^{13}C$. Furthermore, the systematic changes in $\delta^{13}C$, C/N and LOI demonstrates the absence of an eroded contact, which may otherwise have been a possible explanation for the diatom data. The reference water level of the dated sample is MHWST and the indicative range is 20cm (Shennan, 1986).

Ince Marshes: 6,410 ±50 ^{14}C yr BP

The thin muddy peat that accumulated between –1.08m OD and –1.15m OD marks a brief period of semi-terrestrial conditions at 6,410 ± 50 ^{14}C yr BP at Ince Marshes (Figure 8.2e). The single date obtained for the whole peat unit consequently incorporates both the regressive and transgressive overlap. The absence of a chronostratigraphical sequence prevents verification beyond relative dating and so this radiocarbon date must be treated with caution. Diatoms are absent in the underlying silt unit, although sub-tidal channel conditions are apparent in the sandy silt unit below. The change in lithology from sandy silt, to silt with organic fragments and ultimately to muddy peat, associated with an increase in organic content from less than 2% to around 30%, nevertheless indicates a rise in ground elevation within the tidal frame. This is confirmed by the $\delta^{13}C$ and C/N data, which demonstrate the progressive removal of tidal-derived POC in the underlying silt unit and the dominance of vascular vegetation

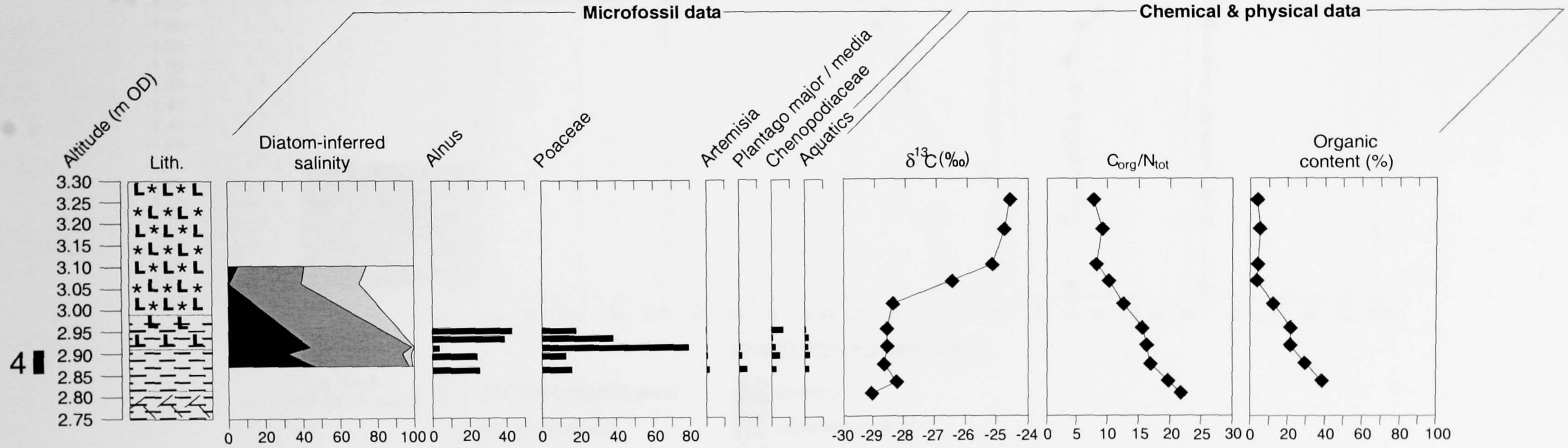

Figure 8.2d. SLI of the second transgressive overlap at Helsby Marsh (4 = 3,220 ± 40 ^{14}C yr BP). Details of the diagrams are given with Figure 8.2e.

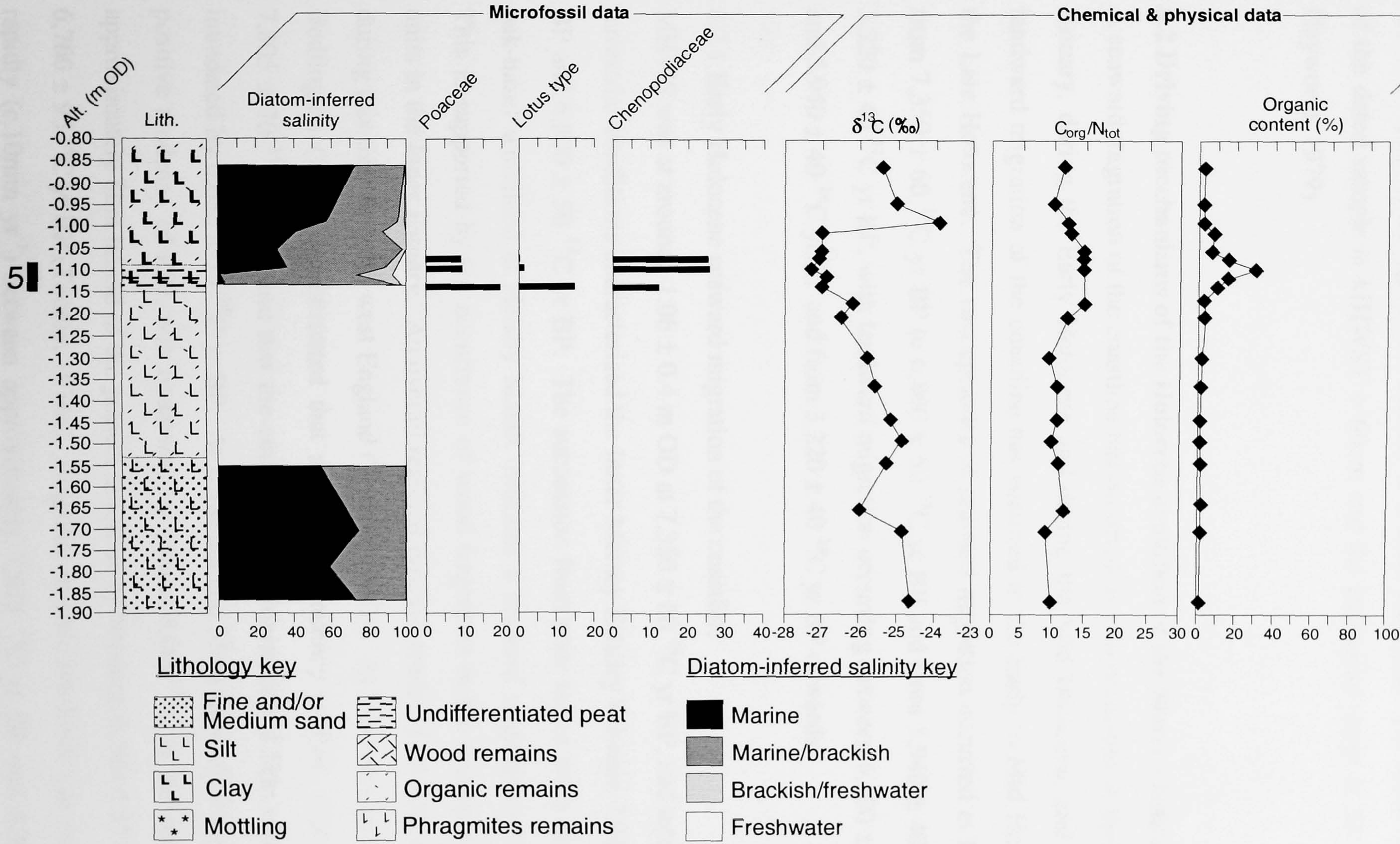

Figure 8.2e. SLI from Ince Marshes (5 = 6,410 ± 50 ^{14}C yr BP). Diatoms are summarised into the categories outlined in Vos & De Wolf (1993a) and are presented as a percentage. Pollen is expressed as a percentage of total land pollen, excluding aquatics, Pteriodophytes and *Sphagnum*. Only key pollen taxa are shown.

and freshwater plankton in the muddy peat unit. The microfossils in the muddy peat unit indicate saltmarsh conditions, which are subsequently replaced by sub-tidal channel deposits. This is supported by the $\delta^{13}C$ and C/N data, which show an increase in tidal derived POC, consisting almost entirely of marine plankton. The reference water level of the dated sample is MHWST + 60cm and the indicative range is 20cm (Kidson & Heyworth, 1979).

8.2 Driving mechanisms of the Holocene evolution of the Mersey Estuary

A seaward migration of the coastline has occurred on two occasions in the Inner Mersey Estuary, during the Early Holocene and during the Mid Holocene, and a subsequent landward migration of the coastline has occurred in the Early to Mid Holocene and in the Late Holocene. The two episodes of seaward migration occurred at Helsby Marsh from 7,350 ± 60 ^{14}C yr BP to 6,800 ± 50 ^{14}C yr BP and from 5,940 ± 40 ^{14}C yr BP to 3,220 ± 40 ^{14}C yr BP, with landward migration occurring between 6,800 ± 50 ^{14}C yr BP and 5,940 ± 40 ^{14}C yr BP and from 3,220 ± 40 ^{14}C yr BP onwards.

8.2.1 Early Holocene seaward migration of the coastline

MHWS was at around –1.06 ± 0.4 m OD at 7,350 ± 60 ^{14}C yr BP, and terrestrial / semi-terrestrial conditions characterised the Inner Mersey Estuary between 7,350 ± 60 ^{14}C yr BP and 6,800 ± 50 ^{14}C yr BP. The succession from poor fen to alder carr and then to oak-hazel woodland at Helsby Marsh indicates a seaward migration of the coastline. This is supported by the occurrence of wood fragments in the widespread lower peat units in the Inner Estuary. An overall regional positive tendency of RSL was underway during this time in north west England (Tooley, 1982b). At Newton Carr on the Wirral, Bedlington (1994) demonstrated that a positive tendency of RSL was underway by 7,805 ± 70 ^{14}C yr BP, and that the entire site (approximately 2.5km inland) had been inundated by 6,680 ± 75 ^{14}C yr BP. At Downholland Moss in south west Lancashire, a positive tendency of RSL was underway by around 8,000 ^{14}C yr BP and had reached approximately 8km inland of the present coastline by between 6,980 ± 55 ^{14}C yr BP and 6,760 ± 95 ^{14}C yr BP (Tooley, 1978a). Regional eustatic sea-level was rising extremely rapidly (c.10mm yr^{-1}) between approximately 7,925 ^{14}C yr BP and 6,300 ^{14}C yr BP (Mörner, 1984), and this is associated with glacial meltwater flux into the ocean basins (e.g. Fairbanks, 1989). Within this time period a catastrophic sea-level rise event

occurred, when glacio-eustatic sea-level rose by approximately 6m at around 7,500 ^{14}C yr BP (Blanchon *et al.*, 2002), possibly as a result of Antarctic ice-sheet instability (Blanchon & Shaw, 1995). Zong & Tooley (1996) invoke this event as an explanation for the rapid RSL rise rates (up to 36.7mm yr^{-1}) observed at around this time in Morecambe Bay, north west England.

The continued accumulation of peat at Helsby Marsh between 7,350 ± 60 ^{14}C yr BP and 6,800 ± 50 ^{14}C yr BP appears to contradict the regional trend of rapidly rising RSL. This apparent inconsistency may be explained as a result of the location of Helsby Marsh in relation to the present-day coastline and also as a result of fluctuations in regional eustatic sea-level at around this time. Helsby Marsh is located just over 2km inland of the present-day banks of the Inner Mersey Estuary, which itself is located approximately 20km from the mouth of the Mersey Estuary. Consequently, the regional rise in eustatic sea-level during the Early Holocene had not reached Helsby Marsh by 7,350 ± 60 ^{14}C yr BP, unlike the more sea-proximal sites of Newton Carr in the Wirral and Downholland Moss in south west Lancashire. Nevertheless, marine conditions were not far away, as indicated by the presence of brackish freshwater diatoms, and even some marine plankton and marine tychoplankton diatoms in the sediments. In addition, around 4m of marine sediments had accumulated at Ince Marshes before 6,410 ± 50 ^{14}C yr BP, which is located 2km more seaward of Helsby Marsh, and so it is likely that marine conditions were in close proximity to Helsby Marsh at 7,350 ± 60 ^{14}C yr BP. Furthermore, the encroachment of marine conditions may have resulted in ponding of riverine water, which may have acted as the initial catalyst for peat formation at Helsby Marsh, although this remains speculative. A fall in eustatic sea-level occurred between approximately 7,600 ^{14}C yr BP and 7,200 ^{14}C yr BP (Mörner, 1984). In addition, south Lancashire was undergoing isostatic uplift at this time (Shennan, 1989) and Tooley (1974) identified a period of slow RSL rise and subsequent fall between 7,600 ^{14}C yr BP and 7,200 ^{14}C yr BP. Furthermore, a withdrawal of marine conditions was recorded at a number of sites along the North Wales and Wirral coasts around 7,000 ^{14}C yr BP (Bedlington, 1994). A slowdown in sea-level rise or a fall in sea-level may explain why forested environments were able to eventually succeed poor fens in the Inner Mersey Estuary at some time after 7,350 ± 60 ^{14}C yr BP.

8.2.2 Early to Mid Holocene landward migration of the coastline

An expansion of the inter-tidal and sub-tidal areas in the Inner Mersey Estuary is recorded at Helsby Marsh between 6,800 ± 50 ^{14}C yr BP and 5,940 ± 40 ^{14}C yr BP. Approaching marine conditions are apparent from the occurrence of marine and brackish diatoms and the appearance of saltmarsh pollen in the upper layers of the basal peat. The presence of marine plankton and tychoplankton diatoms in the largely organic sediments at –0.61m OD may indicate a storm surge. Either way, the presence of these diatoms testifies to a significant increase in exposure to marine conditions. Subsequently, MHWS intersects the coastline at around –0.61 ± 0.1m OD at 6,800 ± 50 ^{14}C yr BP when saltmarshes replace oak-hazel woodland, which, in turn, is replaced by lower inter-tidal and then sub-tidal channel environments. Newton Carr was experiencing marine conditions at around this time (Bedlington, 1994). Indeed, much of the north west coastline was experiencing extensive marine inundation from 6,885 ^{14}C yr BP (Tooley, 1974), indicating that a regional positive sea-level tendency was underway. Regional eustatic sea-level continued to rise rapidly (c. 6mm yr^{-1}) between these time periods (Mörner, 1984) in response to deglaciation. Bedlington (1994) calculates slightly lower rates of RSL rise of approximately 3mm to 4mm per ^{14}C year at Newton Carr, and this is partly due to the ongoing isostatic uplift of the area (Shennan, 1989).

The positive tendency of sea-level, recorded at Helsby Marsh at 6,800 ± 50 ^{14}C yr BP, may have influenced Ince Marshes much earlier. Sub-tidal channel conditions characterised Ince Marshes for some time before 6,410 ± 50 ^{14}C yr BP. The continuous deposition of sub-tidal sediments from –5.37m OD to –1.54m OD indicates a RSL rise of around 3.83m over an undefined time period. The almost complete lack of organic matter in the sediments, evident by loss on ignition values of less than 4%, indicate relatively high rates of RSL rise, probably greater than 3mm per year (Shennan, 1995). Saltmarshes formed locally at this site at around 6,410 ± 50 ^{14}C yr BP, and MHWS was between –0.55 ± 0.1m OD and –0.48 ± 0.1m OD.

Organic sediments began to accumulate at Helsby Marsh from 5,940 ± 40 ^{14}C yr BP, indicating a reduction in the rate of RSL rise, and MHWS intersects the coast at around +1.58 ± 0.1m OD (assuming a constant tidal range). Marine conditions persisted at Helsby Marsh for around 860 ^{14}C years. Assuming that no erosion has occurred, and a

constant sedimentation rate prevailed, RSL rose at a rate of approximately 2.5mm per ^{14}C year, a similar rate experienced at Newton Carr (Bedlington, 1994). At approximately 1km inland of core Ince 4 at Helsby Marsh, the transgressive and regressive contact of this positive tendency was dated at 5,470 ± 155 ^{14}C yr BP (+0.73m OD) and 5,250 ± 385 ^{14}C yr BP (+1.29m OD) respectively by Tooley (1978a).

8.2.3 Mid Holocene seaward migration of the coastline

Peat deposits envelop most areas of the Inner Mersey Estuary, indicating a second seaward movement of the coastline, and this again results in oak-hazel woodland development. Peat deposition occurred at Helsby Marsh between 5,940 ± 40 ^{14}C yr BP and 3,220 ± 40 ^{14}C yr BP. A change from marine to terrestrial / semi-terrestrial conditions was also widespread at Newton Carr between 5,465 ± 90 ^{14}C yr BP and 2,825 ± 40 ^{14}C yr BP (Bedlington, 1994), which may indicate a more widespread operational process, and dunes began to form along the Formby foreshore. A slowdown in the rate of rise of regional eustatic sea-level occurs during this time period (Mörner, 1984). In addition, uplift continued in south Lancashire until approximately 5,000 ^{14}C yr BP. A combination of continued uplift and a slowdown of regional eustatic sea-level rise must have resulted in a reduced rate of RSL and this allowed the expansion of the supra-tidal zone over former inter-tidal and sub-tidal areas. Peat accumulated at Helsby Marsh for around 2,700 ^{14}C yrs, before a change to transitional reedswamp / saltmarsh conditions heralds the return of marine conditions at 3,220 ± 40 ^{14}C yr BP, when MHWS intersected the coastline at +2.86 ± 0.1m OD.

8.2.4 Late Holocene landward migration of the coastline

A second expansion of the sub-tidal and inter-tidal zones is apparent in the Inner Mersey Estuary from 3,220 ± 40 ^{14}C yr BP. Saltmarsh sediments occur at Helsby Marsh after 3,220 ± 40 ^{14}C yr BP, and these high inter-tidal zone deposits culminate in a period of peat deposition (erroneously dated at 800 ± 40 ^{14}C yr BP). A return of stronger marine conditions ends peat deposition, and tidalflat conditions characterise the Inner Mersey Estuary as far inland as Helsby Marsh. At Newton Carr, marine deposits replace terrestrial / semi-terrestrial deposits at 2,825 ± 40 ^{14}C yr BP (Bedlington, 1994), and again a larger scale process may be in operation. Although oscillations in regional eustatic sea-level with amplitudes of over 1m are apparent, the overall trend is one of slow rates of sea-level rise (<1mm yr^{-1}) (Mörner, 1984). The isostatic adjustment of the

Merseyside region was almost complete by the Mid Holocene, with only very small rates (–0.28mm yr^{-1}) of subsidence evident since 3,700 ^{14}C yr BP (Shennan & Horton, 2002). Consequently, local processes will be more important and will exert a major influence over landform development.

The change from organic to minerogenic deposition after the Mid Holocene is characteristic of several UK estuaries (e.g. Thames Estuary (Devoy, 1979), Severn Estuary (Allen & Haslett, 2002), Southampton Water (Long *et al.*, 2000) and the Humber Estuary (Metcalfe *et al.*, 2000)). There is no evidence of an increase in the rate of regional eustatic sea-level (Mörner, 1984) or in north west England RSL (Tooley, 1982b; Figure 3.3) to account for this. A more likely explanation is the increase in minerogenic sediment supply (Long *et al.*, 2000). An increase in terrigenous sediment flux has been demonstrated in both the Tees Estuary (Plater *et al.*, 2000a) and the Humber Estuary (Long *et al.*, 1998; Metcalfe *et al.*, 2000) in the Late Holocene, and this has been linked to vegetation clearance and associated soil erosion in the catchments. Long *et al.* (2000) argue that the rate of RSL rise in the Late Holocene would have been insufficient to support a high water table, which is required to maintain the anaerobic conditions necessary for peat accumulation. Consequently, the greater minerogenic sediment supply would promote tidalflat development, and the succession to high marsh and freshwater peat development would have been arrested.

There is evidence of anthropogenically-induced widespread forest clearance within the catchment of the Mersey Estuary and its tributaries in the Late Holocene. A major clearance phase, probably in relation to cultivation, has been recorded at Chat Moss, approximately 10km west of Manchester, at 3,070 ± 150 ^{14}C yr BP and at 2,645 ± 100 ^{14}C yr BP, (Birks, 1964). Furthermore, a period of intensive land use in the region is recorded at Knowsley Park Moss, approximately 2km west of St Helens, between approximately 4,000 ^{14}C yr BP and 2,500 ^{14}C yr BP, with a further widespread period of clearance occurring from approximately 1,700 ^{14}C yr BP onwards (Innes & Tomlinson, 1986/1987). Although widespread catchment disturbance would generate an increase in terrigenous sediment flux to the Mersey Estuary, geochemical sediment tracing techniques (e.g. Plater *et al.*, 2000a; Rees *et al.*, 2000) would have to be applied to the Late Holocene Mersey Estuary sediment deposits before this hypothesis can be accepted.

8.2.5 Summary

Multi-proxy analysis of the Inner Mersey Estuary sediment deposits, using conventional techniques (diatom, pollen, particle size and loss on ignition analysis), as well as new techniques ($\delta^{13}C$ and C/N analysis), applied for the first time to RSL reconstruction in an estuary within a C_3 vegetated catchment, provide evidence of Holocene RSL changes and associated Inner Mersey Estuarine evolution. At 7,350 ± 60 ^{14}C yr BP, MHWS was approximately 6m below present levels. The Early Holocene rise in RSL may have affected the Inner Mersey Estuary indirectly by initiating freshwater peat development through raising the water table and promoting a waterlogged environment, although this remains speculative. The pivotal position occupied by the Inner Mersey Estuary in the Early Holocene, coupled with a momentary reduction in the rate of regional eustatic sea-level rise, and subsequent fall, may have allowed the seaward expansion of terrestrial / semi-terrestrial conditions up to 6,800 ± 50 ^{14}C yr BP. RSL rose by 1.13m at a rate of approximately 2.5mm per ^{14}C year in the Inner Mersey Estuary between 6,800 ± 50 ^{14}C yr BP and 5,940 ± 40 ^{14}C yr BP, and this resulted in the expansion of sub-tidal and lower inter-tidal environments over former supra-tidal areas. A slowdown in regional eustatic sea-level encouraged the advancement of upper inter-tidal and then supra-tidal environments after 5,940 ± 40 ^{14}C yr BP, and freshwater peat deposition persisted in the Inner Mersey Estuary for approximately 2,700 ^{14}C years. Intensive catchment disturbance from around 4,000 ^{14}C yr BP may have caused an increase in the terrigenous sediment flux into the estuary, which may in turn have encouraged the development of lower inter-tidal and sub-tidal environments in the Inner Estuary after 3,220 ± 40 ^{14}C yr BP. Succession to supra-tidal environments may have been prevented by the slow rates of RSL rise, which were perhaps insufficient to support a rising water table, a fundamental requirement for the accumulation of peat.

The Holocene evolution of the Inner Mersey Estuary conforms to the tripartite model of deposition (minerogenic / organic / minerogenic) noted in other UK estuaries (Long *et al.*, 2000). This suggests similar driving mechanisms and estuarine responses. The tripartite estuarine evolution model is a result of an Early Holocene rapid RSL rise causing a landward expansion in the inter-tidal and sub-tidal zones, a Mid Holocene slowdown in RSL causing the seaward expansion of the supra-tidal zone, and a Late Holocene expansion in inter-tidal areas predominantly as a result of an increase in terrigenous sediment flux associated with human disturbance. The evolution of the

Inner Mersey Estuary departs slightly from the tripartite model in the Early Holocene, as a widespread seaward movement of the coastline is recorded. This is due in part to the location of the Inner Mersey Estuary in relation to the height of RSL, and in part as a result of a slowdown and subsequent fall in regional eustatic sea-level.

8.3 Overall Conclusions

1) Contemporary Inner Mersey Estuary high inter-tidal, low inter-tidal and sub-tidal surface sediments have distinctly different $\delta^{13}C$ values, with variation in C/N ratios also evident. This reflects the change in the dominant source of organic matter, with high saltmarsh sediments receiving organic carbon chiefly from the overlying vegetation, and sub-tidal sediments receiving organic carbon entirely from suspended particulate organic matter. The gradual increase in the surface sediment $\delta^{13}C$ and the lowering of C/N with decreasing ground elevation is a reflection of the greater frequency of tidal inundation and duration of lower inter-tidal environments, depositing greater quantities of tidal-derived particulate organic matter onto the saltmarsh surface.

2) Comparison of $\delta^{13}C$ and C/N with the more established coastal palaeoenvironmental proxies of diatoms and pollen in the Holocene sediment deposits of the Inner Mersey Estuary reveal that $\delta^{13}C$ and C/N are good indicators of palaeoenvironmental change. Despite decomposition effects, the relationship between ground elevation, $\delta^{13}C$ and C/N is preserved in the sediment record, with an obvious gradual increase in $\delta^{13}C$ and decrease in C/N from supra-tidal, through to inter-tidal and to sub-tidal environments.

3) Organic matter decomposition results in a change in bulk sediment $\delta^{13}C$ and C/N over time. Bulk sediment $\delta^{13}C$ values generally decrease by approximately 3.0‰ as a result of the preferential degradation of isotopically heavier labile material such as cellulose and hemi-cellulose, and the preferential preservation of isotopically lighter refractory organic compounds such as lignin and lipids. Consequently, 'signature' $\delta^{13}C$ and C/N values cannot be assigned to coastal

palaeoenvironmental zones and, therefore, $\delta^{13}C$ and C/N analysis cannot be used in isolation as a coastal palaeoenvironmental indicator.

4) The relationship between $\delta^{13}C$, C/N and ground elevation within the tidal frame is preserved in the sediment record. For example, an increase in marine conditions resulting in the replacement of sub-tidal channel deposits with inter-tidal and then supra-tidal deposits would be manifest in the $\delta^{13}C$ record by a gradual fall in values and in the C/N record by a gradual rise in values, as a result of the change in deposition from marine-derived particulate organic matter, to a mixture of marine derived particulate organic matter and vascular vegetation, to predominantly vascular vegetation. The effects of decomposition on $\delta^{13}C$ and C/N may accentuate the trend. Based on this relationship, $\delta^{13}C$ and C/N has been successfully used both independently, and in combination with more established proxies, to verify SLIs. This study demonstrates that $\delta^{13}C$ and C/N can be used in conjunction to confidently verify SLI points if microfossils are absent or poorly preserved in the sediments.

5) $\delta^{13}C$ and C/N measurement is rapid and relatively inexpensive, and these parameters are measurable in all coastal sediments.

6) The Early to Mid Holocene evolution of the Inner Mersey Estuary was principally controlled by RSL change, whilst the Late Holocene evolution may have been principally controlled by sediment supply. Indirect marine conditions were first recorded at Helsby Marsh at 7,350 ± 60 ^{14}C yr BP, when a rise in the water table and ponding of riverine water may have occurred in response to the rising RSL, which may have triggered freshwater peat development. Direct marine conditions may have been present at around this time in the more seaward location of Ince Marshes. As a result of a reduced rate of rise and a subsequent fall in regional eustatic sea-level, and due to the more protected and distant location of the Inner Mersey Estuary, a seaward expansion of the supra-tidal zone occurred. A rise in regional RSL resulted in the subsequent expansion of sub-tidal and inter-tidal zones, which reached as far inland as Helsby Marsh from 6,800 ± 50 ^{14}C yr BP (which is located approximately 20km upstream from the mouth of the Mersey Estuary, and approximately 2km inland of the estuary

itself). Marine conditions persisted at Helsby Marsh for 860 ^{14}C years, during which time RSL rose by 1.13m at a rate of approximately 2.5mm per ^{14}C year. A slowdown in the rate of regional RSL rise in the Mid Holocene resulted in the expansion of freshwater peat deposits over former sub-tidal and inter-tidal surfaces at 5,940 ± 40 ^{14}C yr BP. Terrestrial / semi-terrestrial conditions persisted at Helsby Marsh for approximately 2,700 ^{14}C years. Catchment disturbance from approximately 4,000 ^{14}C yr BP may have triggered an increase in the terrigenous sediment flux to the estuary. The greater availability of sediment, coupled with the low rates of RSL rise, may have encouraged the development and maintenance of tidalflats from 3,220 ± 40 ^{14}C yr BP.

7) The Holocene evolution of the Inner Mersey Estuary generally follows the tripartite model of estuarine evolution common to other UK estuaries (Long *et al.*, 2000). Early Holocene expansion and Mid Holocene contraction of the coastal zone was driven by changes in the rate of regional RSL rise, and a possible increase in terrigenous sediment flux in the Late Holocene may have allowed the re-establishment of lower inter-tidal conditions. These processes led to the minerogenic-organic-minerogenic sediment structures observed in the Inner Mersey Estuary Holocene deposits, which is the characteristic sediment stacking pattern of estuarine deposits associated with the tripartite model of evolution.

8.4 Future work

1. The morphology of Ince Banks saltmarsh, a very wide high saltmarsh zone, with narrow low saltmarsh and tidalflat zones, has resulted in a high saltmarsh sampling bias. A more comprehensive dataset of bulk surface sediment δ^{13}C and C/N measurements needs to be collected for a range of saltmarshes morphologies. This will further improve our knowledge of the relationship between δ^{13}C and C/N values and flooding frequency.

2. Due to the construction of the Manchester Ship Canal, large parts of the upper saltmarsh have been destroyed, and supra-tidal zones no longer exist in the

Mersey Estuary. As a result, assumptions have to be made on the likely $\delta^{13}C$ and C/N values of these environments. It is important to measure and publish the $\delta^{13}C$ and C/N values of existing supra-tidal environments, as this data is not available in the literature.

3. In this study, supra-tidal environments in the sediment record are under-represented, resulting in an insufficient number of $\delta^{13}C$ and C/N measurements for these environments. Cores with more extensive peat units need to be collected, and high-resolution pollen analysis carried out, in order to fully investigate the relationship between $\delta^{13}C$ and C/N and environments in the supra-tidal zone.

4. The sediments preserved in the Inner Mersey Estuary contain a detailed record of its Holocene evolution. The collection and analysis of cores from a more extensive area around the Mersey Estuary will allow an insight into the Holocene evolution of the estuary as a whole in response to various forcing factors (e.g. climate and RSL change, changes in terrigenous sediment delivery).

5. The new sea-level index points presented in this study may be combined with existing sea-level index points from the north Wirral coastline (Bedlington, 1994; Cowell & Innes, 1994) to generate a Holocene relative sea-level curve for Liverpool Bay.

References

Admiraal, W., 1977. Salinity tolerance of benthic estuarine diatoms as tested with a rapid polarographic measurement of photosynthesis. *Marine Biology*, **39**, 11-18.

Admiralty Tide Tables, 2003. Volume 1, UK and Ireland. UK Hydrographic Office.

Allen, J.R.L., 1990. Salt-marsh growth and stratification: A numerical model, with special reference to the Severn Estuary, southwest Britain. *Marine Geology*, **95**, 77-96.

Allen, J.R.L., 1999. Geological impacts on coastal wetland landscapes: some general effects of sediment autocompaction in the Holocene of northwest Europe. *The Holocene*, **9**, 1-12.

Allen, J.R.L. & Haslett, S.K., 2002. Buried salt-marsh edges and tide-level cycles in the mid-Holocene of the Caldicot Level (Gwent), South Wales, UK. *The Holocene*, **12**, 303-324.

Allen, J.R.L. & Pye, K., 1992. Coastal saltmarshes: their nature and importance. *In:* J.R.L. Allen & K. Pye, eds. *Saltmarshes: morphodynamics, conservation and engineering significance*. Cambridge: Cambridge University Press, 1-18.

Amspoker, M.C. & McIntire, D.C., 1978. Distribution of intertidal diatoms associated with sediments in Yaquina Estuary, Oregon. *Journal of Phycology*, **14**, 387-395.

Andrews, J.E., Brimblecombe, P., Jickells, T.D. & Liss, P.S., 1996. *An Introduction to Environmental Chemistry*. Oxford: Blackwell Science.

Andrews, J.E., Greenway, A.M. & Dennis, P.F., 1998. Combined carbon isotope and C/N ratios as indicators of source and fate of organic matter in a poorly flushed, tropical estuary: Hunts Bay, Kingston Harbour, Jamaica. *Estuarine, Coastal and Shelf Science*, **46**, 743-756.

Andrews, J.E., Samways, G., Dennis, P.F. & Maher, B.A., 2000. Origin, abundance and storage of organic carbon and sulphur in the Holocene Humber Estuary: emphasizing human impact on storage changes. *In*: I. Shennan & J.E. Andrews, eds. *Holocene Land-Ocean Interaction and Environmental Change around the North Sea*. Geological Society, London, Special Publications, **166**, 145-170.

Austin, W.E.N. & McCarroll, D., 1992. Foraminifera from the Irish Sea glacigenic deposits at Aberdaron, western Lleyn, North Wales: palaeoenvironmental implications. *Journal of Quaternary Science*, **7**, 311-317.

Bard, E., Hamelin, B., Fairbanks, R.G. & Zindler, A., 1990a. Calibration of the ^{14}C

timescale over the past 30,000 years using mass spectromentric U-Th ages from Barbados corals. *Nature*, **345**, 405-409.

Bard, E., Hamelin, B. & Fairbanks, R.G., 1990b. U/Th ages obtained by mass spectrometry in corals from Barbados: sea level during the last 130,000 years. *Nature*, **382**, 242-244.

Bard, E., Hamelin, B., Arnold, M., Montaggioni, L., Cabioch, G., Faure, G. & Rougerie, F., 1996. Deglacial sea-level record from Tahiti corals and the timing of global meltwater discharge. *Nature*, **382**, 241-244.

Barth, J.A.C., Veizer, J. & Mayer, B., 1998. Origin of particulate organic carbon in the upper St. Lawrence: isotopic constraints. *Earth and Planetary Science Letters*, **162**, 111-121.

Bateman, M.D., 1995. Thermoluminescence dating of the British coversand deposits. *Quaternary Science Reviews*, **14**, 791-798.

Bathurst, R.G.C. & Brenchley, P.J., 1975. The geology of Liverpool Bay. *In*: Liverpool Bay Study Group, ed. *Liverpool Bay: An Assessment of Present Knowledge*. Natural Environmental Research Council, London, Series C, 14, 8-10.

Battarbee, R.W., 1986. Diatom analysis. *In*: B.E. Berglund, ed. *Handbook of Holocene Palaeoecology and Palaeohydrology*. Chichester: John Wiley, 527-570.

Bedlington, D.J., 1994. *Holocene sea-level changes and crustal movements in north Wales and Wirral*. Unpublished Ph.D. Thesis, University of Durham.

Bengstsson, L & Enell, M., 1986. Chemical Analysis. *In*: B.E. Berglund, ed. *Handbook of Holocene Palaeoecology and Palaeohydrology*. Chichester: John Wiley, 423-451.

Benner, R., Fogel, M.L., Sprague, K.E. & Hodson, R.E., 1987. Depletion of ^{13}C in lignin and its implications for stable carbon isotope studies. *Nature*, **329**, 708-710.

Benner, R., Fogel, M.L. & Sprague, E.K., 1991. Diagenesis of belowground biomass of *Spartina alterniflora* in salt-marsh sediments. *Limnology Oceanography*, **36**, 1358 -1374.

Beyens, L. & Denys, L., 1982. Problems in diatom analysis of deposits: allochthonous valves and fragmentation. *Geologie en Mijnbouw,* **61**, 159-162.

Bhiry, N., Garneau, M. & Filion, L., 2000. Macrofossil record of a middle Holocene drop in relative sea level at the St. Lawrence Estuary, Québec. *Quaternary Research*, **54**, 228-237.

Binney, E.W. & Talbot, J.H., 1868. On the petroleum found in the Downholland Moss.

near Ormskirk. *Transactions of the Manchester Geological Society*, **7**, 41-48.

Birks, H.J.B., 1964. Chat Moss, Lancashire. *Memoirs and Proceedings of the Manchester Literary and Philosophical Society*, **106**, 22-45.

Birks, H.J.B., Line, J.M., Juggins, S., Stevenson, A.C. & ter Braak, C.J.F., 1990. Diatoms and pH Reconstruction. *Philosophical Transactions of the Royal Society of London B*, **327**, 263-278.

Blanchon, P. & Shaw, J., 1995. Reef drowning during the last deglaciation: Evidence for catastrophic sea-level rise and ice-sheet collapse. *Geology*, **23**, 4-8.

Blanchon, P., Jones, B. & Ford, D.C., 2002. Discovery of a submerged relic reef and shoreline off Grand Cayman: further support for an early Holocene jump in sea level. *Sedimentary Geology*, **147**, 253-270.

Bloom, A.L., 1967. Pleistocene shorelines: a new test of isostasy. *Geological Society of America Bulletin*, **78**, 1477-1494.

Bloom, A.L., 1977. *Atlas of sea-level curves*. IGCP Project 61. New York: Cornell University.

Boutton, T.W., Archer, S.R., Midwood, A.J., Zitzer, S.F. & Bol, R., 1998. $\delta^{13}C$ values of soil organic carbon and their use in documenting vegetation change in a subtropical savanna ecosystem. *Geoderma*, **82**, 5-41.

Bowen, D.Q., Phillips, F.M., McCabe, A.M., Knutz, P.C. & Sykes, G.A., 2002. New data for the Last Glacial Maximum in Great Britain and Ireland. *Quaternary Science Reviews*, **21**, 89-101.

Brinson, M.M. & Matson, E.A., 1983. Carbon isotope distribution in the Pamlico River Estuary, North Carolina and tributaries. *Estuaries*, **6**, 306.

Bull, I.D., van Bergen, P.F., Bol, R., Brown, S., Gledhill, A.R., Gray, A.J., Harkness, D.D., Woodbury, S.E. & Evershed, R.P., 1999. Estimating the contribution of *Spartina anglica* biomass to salt-marsh sediments using compound specific carbon isotope measurements. *Organic Geochemistry*, **30**, 477-483.

Byrne, R., Ingram, L.B., Starratt, S. & Malamud-Roam, F., 2001. Carbon-isotope, diatom, and pollen evidence for late Holocene salinity change in a brackish marsh in the San Francisco Estuary. *Quaternary Research*, **55**, 66-76.

Cazenave, A., Dawson, A.G., Frezzotti, M., Long, A.J., Raper, S.C.B., Reeh, N., Tooley, M., De Wolde, J. & Woodworth, P., 2000. Global changes in the volume and mass of the ocean. *In*: D. Smith, S.C.B. Raper, S. Zerbini & A. Sánchez-

Arcilla, eds. *Sea level Change and Coastal Processes: Implications for Europe.* Luxembourg: European Communities, 9-81.

Chapman, V.J., 1977. *Ecosystems of the World I: Wet Coastal Ecosystems.* Amsterdam: Elsevier Scientific Publishing Company.

Chappell, J., Omura, A., Esat, T., McCulloch, M., Pandolfi, J., Ota, Y. & Pillans, B., 1996. Reconciliation of late Quaternary sea levels derived from coral terraces at Huon Peninsula with deep sea oxygen isotope records. *Earth and Planetary Science Letters*, **141**, 227-236.

Charman, D.J., Roe, H.M. & Gehrels, R., 1998. The use of testate amoebae in studies of sea-level change: a case study from the Taf Estuary, south Wales, UK. *The Holocene,* **8**, 209-218.

Charman, D.J., Roe, H.M. & Gehrels, W.G., 2002. Modern distribution of saltmarsh testate amoebae: regional variability of zonation and response to environmental variables. *Journal of Quaternary Science*, **17**, 387-409.

Chmura, G.L. & Aharon, P., 1995. Stable carbon isotope signatures of sedimentary carbon in coastal wetlands as indicators of salinity regime. *Journal of Coastal Research*, **11**, 124-135.

Chmura, G.L., Aharon, P., Socki, R.A. & Abernethy, R., 1987. An inventory of ^{13}C abundances in coastal wetlands of Louisiana, USA: vegetation and sediments. *Oecologia*, **74**, 264-271.

Cifuentes, L.A., 1991. Spatial and temporal variations in terrestrially-derived organic matter from sediments of the Delaware Estuary. *Estuaries*, **14**, 414-429.

Clark, J.A., 1976. Greenland's rapid postglacial emergence: A result of ice-water gravitational attraction. *Geology*, **4**, 310-312.

Clark, J.A., Farrell, W.E. & Peltier, R.W., 1978. Global changes in postglacial sea level: A numerical calculation. *Quaternary Research*, **9**, 265-287.

Cloern, J.E., Canuel, E.A. & Harris, D., 2002. Stable carbon and nitrogen isotope composition of aquatic and terrestrial plants of the San Francisco Bay estuarine system. *Limnology and Oceanography*, **47**, 713-729.

Cooper, S., 1999. Estuarine paleoenvironmental reconstructions using diatoms. In: E.F. Stoermer & P. Smol, eds. *The Diatoms: Application for the Environmental and Earth Sciences.* Cambridge: Cambridge University Press, 352-373.

Cowell, R.W. & Innes, J.B., 1994. *The Wetlands of Merseyside, Northwest Wetlands Survey 1.* Lancaster Imprints 2, English Heritage and Lancaster University.

Craft, C.B., Brooe, S.W., Seneca, E.D. & Showers, W.J., 1988. Estimating sources of soil organic matter in natural and transplanted estuarine marshes using stable isotopes of carbon and nitrogen. *Estuarine, Coastal and Shelf Science*, **26**, 633 -641.

Craig, H., 1957. Isotopic standards for carbon and oxygen and correction factors for mass spectrometric analysis of carbon dioxide. *Geochimica et Cosmochimica Acta*, **12**,133-149.

Crawford, R.M.M., 1989. *Studies in Plant Survival*. Oxford: Blackwell.

Davidson, N.C., Laffoley, D.d'A., Doody, P., Way, L.S., Gordon, J., Key, R., Pienkowski, M.W., Mitchell, R. & Duff, K.L., 1991. *Nature Conservation and Estuaries in Great Britain*. Peterborough: Nature Conservancy Council.

Davies, H.J.L., 1964. A morphogenic approach to world shorelines. *Zeitschrift für Geomorphologie*, **8**, 127-142.

Davies, M.B., 1963. On the theory of pollen analysis. *American Journal of Science*, **261**, 897-912.

Deines, P., 1980. The isotopic composition of reduced organic carbon. *In*: P. Fritz & J.C. Fontes, eds. *Handbook of Environmental Isotope Geochemistry*. Amsterdam: Gisewir, 329-406.

DeLaune, R.D., 1986. The use of $\delta^{13}C$ signature of C_3 and C_4 plants in determining past depositional environments in rapidly accreting marshes of the Mississippi River deltaic plain, Louisiana, U.S.A. *Chemical Geology*, **59**, 315-320.

Denys, L., 1984. Diatom analysis of coastal deposits: methodological aspects. *Bulletin van de Belgische Vereniging voor Geologie*, **93**, 291-295.

Denys, L., 1991-2. *A check-list of the diatoms in the Holocene deposits of the western Belgian coastal plain with a survey of their apparent ecological requirements. I. Introduction, ecological code and complete list*. Professional Paper 246, Belgium: Belgian Geological Survey.

Denys, L. & De Wolf, H., 1999. Diatoms as indicators of coastal paleoenvironments and relative sea-level change. *In*: E.F. Stoermer & J.P. Smol, eds. *The Diatoms: Applications for the Environmental and Earth Sciences*. Cambridge: Cambridge University Press, 1999, 277-297.

Devoy, R.J.N., 1979. Flandrian sea-level changes and vegetation history of the lower Thames Estuary. *Philosophical Transactions of the Royal Society of London*, **B285**, 355-410.

De Wolf, H., 1982. Method of coding of ecological data from diatoms for computer utilization. *Mededelingen Rijks Geologische Dienst*, **36-2**, 95-113.

Dixit, S.S., Smol, J.P., Kingston, J.C. & Charles, D.F., 1992. Diatoms: powerful indicators of environmental change. *Environmental Science and Technology*, **26**, 23-33.

Eady, J., 1976. The monitoring of tide gauges by the Ordnance Survey. *In*: *Proceedings of the Symposium on Tide Recording*, (Southampton 14-15 April 1976). Hydrographical Society Special Publication 4, 37-45.

Eisma, D., 1998. *Intertidal Deposits: River Mouths, Tidal Flats, and Coastal Lagoons.* Bergen aan Zee, Netherlands: CRC Press.

Ember, L.M., Williams, D.F. & Morris, J.T., 1987. Processes that influence carbon isotope variations in salt marsh sediments. *Marine Ecology Progress Series*, **36**, 33-42.

Eyles, N. & McCabe, M.A., 1989. The late Devensian (<22,000 BP) Irish Sea Basin: the sedimentary record of a collapsed ice sheet margin. *Quaternary Science Reviews*, **8**, 307-351.

Fairbanks, R.G., 1989. A 17,000 year glacio-eustatic sea level record: influence of glacial melting rates on the Younger Dryas event and deep-ocean circulation. *Nature*, **342**, 637-642.

Fairbridge, R.W., 1961. Eustatic changes in sea-level. *In*: L.H. Ahrens, F. Press, K. Rankama & S.K. Runcorn, eds. *Physics and Chemistry of the Earth*. London: Pergamon, 99-185.

Farquhar, G.D., O'Leary, M.H. & Berry, J.A., 1982a. On the relationship between carbon isotope discrimination and the intercellular carbon dioxide concentration in leaves. *Australian Journal of Plant Physiology*, **9**, 121-137.

Farquhar, G.D., Ehleringer, J.R. & Hubick, K.T., 1989a. Carbon isotope discrimination and photosynthesis. *Annual Review of Plant Physiology and Plant Molecular Biology*, **40**, 503-537.

Farquhar, G.D., Hubick, K.T., Condon, A.G. & Richards, R.A., 1989b. Carbon isotope fractionation and plant water-use efficiency. *In*: P.W. Rundel, J.R. Ehleringer, & K.A. Nagy, eds. *Stable Isotopes in Ecological Research*. New York: Springer -Verlag, 21-40

Fichez, R., Dennis, P., Fontaine, M.F. & Jickells, T.D., 1993. Isotopic and biochemical composition of particulate organic matter in a shallow water estuary (Great Ouse,

North Sea, England). *Marine Chemistry*, **43**, 263-276.

Fleming, K., Johnston, P., Zwartz, D., Yokoyama, Y., Lambeck, K. & Chappell, J., 1998. Refining the eustatic sea-level curve since the Last Glacial Maximum using far-and intermediate-field sites. *Earth and Planetary Science Letters*, **163**, 327-342.

Flower, R.J., 1993. Diatom preservation: experiments and observations on dissolution and breakage in modern and fossil material. *Hydrobiologia*, **269/270**, 473-484.

Fogel, M.L., Sprague, K.E., Gize, A.P. & Frey, R.W., 1989. Diagenesis of organic matter in Georgia salt marshes. *Estuarine, Coastal and Shelf Science*, **28**, 211-230.

Folk, R.T. & Ward, W.C., 1957. Brazos River Bar: A study in the significance of grain size parameters. *Journal of Sedimentary Petrology*, **27**, 3-26.

Freitas, M.C., Andrade, C., Rocha, F., Tassinari, C., Munhá, J.M., Cruces, A., Vidinha, J. & Silva, M., 2003. Lateglacial and Holocene environmental changes in Portuguese coastal lagoons 1: the sedimentological and geochemical records of the Santo André coastal area. *The Holocene*, **13**, 433-446.

Friedli, H., Lötscher, H., Oeschger, H., Siegenthaler, U. & Stauffer, B., 1986. Ice core record of the $^{13}C/^{12}C$ ratio of atmospheric CO_2 in the past two centuries. *Nature*, **324**, 237-238.

Friedman, G.M., 1961. Distinction between dune, beach and river sands from their textural characteristics. *Journal of Sedimentary Petrology* **31**, 514-529.

Friedman, G.M. & Sanders, J.E., 1978. *Principles of Sedimentology*, New York: Wiley.

Fry, B. & Sherr, E.B., 1989. $\delta^{13}C$ measurements as indicators of carbon flow in marine and freshwater ecosystems. *In*: P.W. Rundel, J.R. Ehleringer & K.A. Nagy, eds. *Stable Isotopes in Ecological Research*. New York: Springer-Verlag, 196-229.

Gearing, J.N., Gearing, P.J., Rudnick, D.T., Requejo, A.G. & Hutchins, M.J., 1984. Isotopic variability of organic carbon in a phytoplankton-based, temperate estuary. *Geochimica et Cosmochimica Acta*, **48**, 1089-1098.

Gehrels, R.W., 1999. Middle and late Holocene sea-level changes in eastern Maine reconstructed from foraminiferal saltmarsh stratigraphy and AMS ^{14}C dates on basal peat. *Quaternary Research*, **52**, 350-359.

Gehrels, R.W., Belknap, D.F., Pearce, B.R. & Gong, B., 1995. Modeling the contribution of M_2 tidal amplification to the Holocene rise of mean high water in the Gulf of Maine and the Bay of Fundy. *Marine Geology*, **124**, 71-85.

Gehrels, R.W., Roe, H.M. & Charman, D.J., 2001. Foraminifera, testate amoebae and

diatoms as sea-level indicators in UK saltmarshes: a quantitative multiproxy approach. *Journal of Quaternary Science*, **16**, 201-220.

Godwin, H., 1940. Studies of the post-glacial history of British vegetation III. Fenland pollen diagrams. IV. Post-glacial changes of relative land- and sea-level in the English Fenland. *Philosophical Transactions of the Royal Society B*, **230**, 239-303.

Godwin, H., 1978. *Fenland: its ancient past and uncertain future*. Cambridge: Cambridge University Press.

Goñi, M.A., Teixeira, M.J. & Perkey, D.W., 2003. Sources and distribution of organic matter in a river-dominated estuary (Winyah Bay, SC, USA). *Estuarine, Coastal and Shelf Science*, **57**, 1023-1048.

Gonzalez, S., Huddart, D. & Roberts, G., 1996. Holocene development of the Sefton coast: a multidisciplinary approach to understanding the archaeology. *In*: A. Sinclair, E. Slater & J. Gowlett, eds. *Proceedings of a Conference on the Application of Scientific Techniques to the Study of Archaeology*. Oxford Monograph **64**, 271-281.

Graham, M.C., Eaves, M.A., Farmer, J.G., Dobson, J. & Fallick, A.E. 2001. A study of carbon and nitrogen stable isotope and elemental ratios as potential indicators of source and fate of organic matter in sediments of the Forth Estuary, Scotland. *Estuarine, Coastal and Shelf Science*, **51**, 375-380.

Gray, A.J., 1992. Saltmarsh plant ecology: zonation and succession revisited. *In:* J.R.L. Allen & K. Pye, eds. *Saltmarshes: morphodynamics, conservation and engineering significance*. Cambridge: Cambridge University Press, 63-79.

Greensmith, J.T. & Tucker, E.V., 1986. Compaction and consolidation. *In*: Plassche, O. van de, ed. *Sea-level Research: a manual for the collection and evaluation of data*. Norwich: Geo Books, 591-603.

Griffiths, J.C. 1967. *Scientific Method in Analysis of Sedimentary Environments*. New York: McGraw-Hill.

Guy, R.D., Reid, D.M. & Krouse, R.H., 1980. Shifts in carbon isotope ratios of two C_3 halophytes under natural and artificial conditions. *Oecologia*, **44**, 241-247.

Hageman, B.P., 1969. Development of the western part of the Netherlands during the Holocene. *Geologie en Mijnbouw*, **48**, 373-388.

Haines, E.B., 1976. Stable carbon isotope ratios in biota, soils and tidal water of a Georgia salt marsh. *Estuarine and Coastal Marine Science*, **4**, 609-616.

Hanebuth, T., Stattegger, K. & Grootes, P.M., 2000. Rapid flooding of the Sunda Shelf:

A late-glacial sea-level record. *Science*, **288**, 1033-1035.

Hartley, B., 1986. A check-list of the freshwater, brackish and marine diatoms of the British Isles and adjoining coastal waters. *Journal of Marine Biological Association UK*, **66**, 531-610.

Hartley, B., Barber, H.G., Carter, J.R & Sims, P.A., 1996. An Atlas of British Diatoms. Bristol: Biopress.

Harvey, G.R. & Boran, D.A., 1985. Geochemistry of humic substances in seawater. *In*: G.R. Aiken, D.M. McKnight, R.L. Wershaw & P. McCarthy, eds. *Humic Substances in Soil, Sediment, and Water: Geochemistry, Isolation and Characterisations*. New York: Wiley, 233-247.

Hatcher, P.G. & Spiker, E.C., 1988. Selective degradation of plant biomolecules. *In*: F.H. Frimmel & R.F. Christman, eds. *Humic Substances and Their Role in the Environment*. Chichester: John Wiley & Sons Limited, 59-74.

Hayes, M.O., 1975. Morphology of sand accumulation in estuaries: an introduction to the symposium. *In*: L.E. Cronin, ed. *Estuarine Research, Vol. II: Geology and Engineering*. London, Academic Press, Inc., 3-22.

Hedges, J.I., 1988. Polymerization of humic substances in natural environments. *In*: F.H. Frimmel & R.F. Christman, eds. *Humic Substances and Their Role in the Environment*. Chichester: John Wiley & Sons Limited, 45-58.

Hedges, J.I., Keil, R.G. & Benner, R., 1997. What happens to terrestrial organic matter in the ocean? *Organic Geochemistry*, **27**, 195-212.

Hemphill-Haley, E., 1995. Intertidal diatoms from Willapa Bay, Washington: applications to studies of small-scale sea-level changes. *Northwest Science* **69**, 29 -45.

Hendey, N.I., 1964. *An introductory account of the smaller algae of British coastal waters*, Part V, *Bacillariophyceae* (*diatoms*). London: HMSO.

Heyworth, A. & Kidson, C., 1982. Sea-level changes in southwest England and Wales. *Proceedings of the Geologists' Association*, **93**, 91-111.

Hibbert, F.A., Switsur, V.R. & West, R.G., 1971. Radiocarbon dating of Flandrian pollen zones at Red Moss, Lancashire. *Proceedings of the Royal Society of London B*, **177**, 161-176.

Hinga, K.R., Arthur, M.A., Pilson, M.E.Q. & Whitaker, D., 1994. Carbon-isotope fractionation by marine-phytoplankton in culture – the effects of CO_2 concentration, pH, temperature and species. *Global Biogeochemical Cycles*, **8**, 91

-102.

Hoefs, J., 1997. *Stable Isotope Geochemistry*. Berlin: Springer-Verlag.

Horton, B.P., 1999. The distribution of contemporary intertidal foraminifera at Cowpen Marsh, Tees Estuary, UK: implications for studies of Holocene sea-level changes. *Palaeogeography, Palaeoclimatology, Palaeoecology*, **149**, 127-149.

Horton, B.P., Edwards, R.J. & Lloyd, J.M., 1999. UK intertidal foraminiferal distributions: implications for sea-level studies. *Marine Micropaleontology*, **36**, 205-223.

Howell, F.T., 1973. The sub-drift surface of the Mersey and Weaver catchment and adjacent areas. *Geological Journal*, **8**, 285-296.

Huddart, D., 1992. Coastal environmental changes and morphostratigraphy in southwest Lancashire, England. *Proceedings of the Geologists' Association*, **103**, 217-236.

Huddart, D., 1993. Controversial Irish Sea basin glacial models: some answers from the Cumbrian lowlands. *Proceedings of the Cumberland Geological Society*, **5**, 476-480.

Huddart, D., 1994. The Late Quaternary glacigenic sequence: Landforms and environments in coastal Cumbria. *In*: J. Boardman & J. Walden, eds. *Cumbria: field guide*. Oxford: Quaternary Research Association, 59-77.

Huddart, D., 2002a. Lytham. *In*: D. Huddart & N.F. Glasser, eds. *Quaternary of Northern England*. Geological Conservation Review Series, No. **25**, Joint Nature Conservation Committee, Peterborough, 539-554.

Huddart, D., 2002b. Downholland Moss. *In*: D. Huddart & N.F. Glasser, eds. *Quaternary of Northern England*. Geological Conservation Review Series, No. **25**, Joint Nature Conservation Committee, Peterborough, 554-569.

Huddart, D. & Clark, R., 1993. Conflicting interpretations of glacial sediments and landforms in Cumbria. *Proceedings of the Cumberland Geological Society*, **5**, 419-436.

Huddart, D., Roberts, G. & Gonzalez, S., 1999a. Holocene human and animal footprints and their relationships with coastal environmental change, Formby Point, NE England. *Quaternary International*, **55**, 29-41.

Huddart, D., Gonzalez, S. & Roberts, G., 1999b. The archaeological record and mid-Holocene marginal coastal palaeoenvironments around Liverpool Bay. *Quaternary Proceedings*, **7**, 563-574.

Hunt, J.M., 1970. The significance of carbon isotope variations in marine sediments. *In*: G.D. Hobson & G.C. Speers, eds. *Advances in Organic Geochemistry. Proceedings of the Third International Congress, London, 1966.* International Series of Monographs in Earth Science, **32**, Oxford: Pergamon Press, 27-35.

Hustedt, F., 1953. Die Systematik der Diatomeen in Ihren Beziehungen zur Geologie und Ökologie nebst einer Revision des Halobien-systems. *Svensk Botanisk Tedskrift*, **47**, 509-519.

Hustedt, F., 1957. Die Diatomeen Flora des Fluss-systems der Weser im Gebiet der Hansestadt Bremen. *Abhandlungen Naturwissenschaftlichen Verein, Bremen*, **34**, 181-440.

Indermühle, A., Stocker, T.F., Fischer, H., Smith, H.J., Joos, F., Wahlen, M., Deck, B., Mastroianni, D., Tschumi, J., Blunier, T., Meyer, R. & Stauffer, B., 1998. High resolution Holocene CO_2 – Record from the Taylor Dome ice core (Antarctica). *Nature*, **398**, 121-126.

Innes, J.B., 1986. The history of the Shirdley Hill Sand revealed by examination of associated organic deposits. *North of England Soils Discussion Group Proceedings*, **21**, 31-43.

Innes, J.B. & Tomlinson, P.R., 1986-1987. Environmental archaeology in Merseyside. *Journal of the Merseyside Archaeological Society*, **7**, 1-20.

Innes, J.B., Bedlington, D.J., Kenna, R.J.B. & Cowell, R.W., 1990. A preliminary investigation of coastal deposits at Newton Carr, Wirral, Merseyside. *Quaternary Newsletter*, **62**, 5-12.

Innes, J.B., Shennan, I., Twiddy, E.J. & Zong, Y., 1996. The contemporary diatom and pollen flora and foraminiferal fauna of Kentra Bay and Moss SSSI, Lochaber. *Scottish Natural Heritage Research, Survey and Monitoring Report No. 31.*

Jelgersma, S., 1961. Holocene sea-level changes in the Netherlands. *Mededelingen van de Geologische Stichting, Serie C. VI*, **7**, 1-100.

Jennings, A.E., Nelson, A.R., Scott, D.B. & Aravena, J.C., 1995. Marsh foraminiferal assemblages in the Valdivia estuary, south-central Chile, relative to vascular plants and sea level. *Journal of Coastal Research*, **11**, 107-123.

Juggins, S., 1992. Diatoms in the Thames Estuary, England: ecology, palaeoecology, and salinity transfer function. *Bibliotheca Diatomologica*, Band **25**, 1-216.

Kato, M., Tanimura, Y., Matsuoka, K. & Fukusawa, H., 2003. Plankton diatoms from

sediment traps in Omura Bay, western Japan with implications for ecological and taphonomic studies of coastal marine environments. *Quaternary International*. **105**, 25-31.

Keeley, J.E. & Sandquist, D.R., 1992. Carbon: freshwater plants. *Plant, Cell and Environment*, **15**, 1021-1035.

Keeling, C.D., Whorf, T.P., Wahlen, M. & van der Plicht, J., 1995. Interannual extremes in the rate of rise of atmospheric carbon dioxide since 1980. *Nature*, **375**, 666-670.

Kenna, R.J.B., 1986. The Flandrian sequence of north Wirral (N.W. England). *Geological Journal*, **21**, 1-27.

Kidson, C & Heyworth, A., 1979. Sea level. *In:* Proceedings of the 1978 International Symposium on Coastal Evolution in the Quaternary. São Paulo: Universidade de São Paulo, 1-28.

Kohorn, L.U., Goldstein, G. & Rundel, P.W., 1994. Morphological and isotopic indicators of growth environment: variability in $\delta^{13}C$ in Simmondsia chinensis, a dioecious desert shrub. *Journal of Experimental Botany*, **45**, 1817-1822.

Kolbe, R.W., 1927. Zur Ökologie, Morphologie und Systematik der Brackwasser -Diatomeen. *Pflanzenforschung*, **7**, 1-146.

Kosugi, M., 1987. Limiting factors on the distribution of benthic diatoms in coastal regions: salinity and substratum. *Diatom*, **3**, 21-31.

Krammer, K & Lange-Bertalot, H., 1986-1991. Bacillariophyceae. 1. Teil: Naviculaceae, pp 876, 1986; 2. Teil: Bacillariaceae, Epithemiaceae, Surirellaceae, pp 596, 1988; 3. Teil: Centrales, Fragilariaceae, Eunotiaceae, pp 576, 1991; 4. Teils: Achnanthaceae. Kritische Erganzungen zu *Navicula* (Lineolatae) und *Gomphonema*, 1991. *In* Ettl, H., Gerloff, J., Heynig, H. & Mollenhauer, D. eds. *Susswasserflora von Mitteleuropa 2/1-4*. Stuttgart: Fischer Verlag.

Krishnamurthy, R.V. & Epstein, S., 1990. Glacial-interglacial excursion in the concentration of atmospheric CO_2: effects in the $^{13}C/^{12}C$ ratio in wood cellulose. *Tellus*, **42B**, 423-434.

Laane, R.W.P.M., Turkstra, E & Mook, W.G., 1990. Stable carbon isotope composition of pelagic and benthic organic matter in the North Sea and adjacent estuaries. *In*: V. Ittekkot, S. Kempe, W. Michaelis & A. Spitzy, eds. *Facets of Modern Biogeochemistry*. Berlin: Springer-Verlag, 214-224.

Lamb, A.L., Leng, M.J., Mohammed, M.U. & Lamb, H.F., 2004. Holocene climate and

vegetation change in the Main Ethiopian Rift Valley, inferred from the composition (C/N and $\delta^{13}C$) of lacustrine organic matter. *Quaternary Science Reviews*, **23**, 881-891.

Lambeck, K. & Chappell, J., 2001. Sea level changes through the last glacial cycle. *Science*, **292**, 679-686.

Lambeck, K. & Purcell, A.P., 2001. Sea-level change in the Irish Sea since the Last Glacial Maximum: constraints from isostatic modelling. *Journal of Quaternary Science*, **16**, 497-506.

Lambeck, K., Yokoyama, Y. & Purcell, T., 2002. Into and out of the Last Glacial Maximum: sea-level change during Oxygen Isotope Stages 3 and 2. *Quaternary Science Reviews*, **21**, 343-360.

Lee, C. & Wakeman, S.G., 1992. Organic matter in the water column: future research challenges. *Marine Chemistry*, **39**, 95-118.

Leeder, M.R., 1982. *Sedimentology, Process and Product.* London: George Allen & Unwin.

Leeder, M., 1999. *Sedimentology and Sedimentary Basins: From Turbulence to Tectonics*. Oxford: Blackwell Science.

Lerch, F.J., Herem, R.S., Putney, B.H., Felsentreger, T.L., Sanchez, B.V. & Marshall, J.A., 1994. A geopotential model from satellite tracking, altimeter and surface gravity data: GEM:T3. *Journal of Geophysical Research*, **99**, 2815-2839.

Lloyd, J.M., Shennan, I., Kirby, J.R. & Rutherford, M.M., 1999. Holocene relative sea-level changes in the inner Solway Firth. *Quaternary International*, **60**, 83-105.

Long, A.J., 1992. Coastal responses to changes in sea-level in the East Kent Fens and southeast England, UK over the last 7500 years. *Proceedings of the Geologists' Association*, **103**, 187-199.

Long, A.J., Plater, A.J. Waller, M.P. & Innes, J.B., 1996. Holocene coastal sedimentation in the Eastern English Channel: New data from the Romney Marsh region, United Kingdom. *Marine Geology*, **136**, 97-120.

Long, A.J., Innes, J.B., Kirby, J.R., Lloyd, J.M., Rutherford, M.M., Shennan, I. & Tooley, M.J., 1998. Holocene sea-level change and coastal evolution in the Humber estuary, eastern England: an assessment of rapid coastal change. *The Holocene*, **8**, 229-247.

Long, A.J., Scaife, R.G. & Edwards, R.J., 1999a. Pine pollen in intertidal sediments

from Poole Harbour, UK: implications for late-Holocene sediment accretion rates and sea-level rise. *Quaternary International*, **55**, 3-16.

Long, A.J., Innes, J.B., Shennan, I. & Tooley, M.J., 1999b. Coastal stratigraphy: a case study from Johns River, Washington, U.S.A. *In*: A.P. Jones, M.E. Tucker & J.K. Hart, eds. *The description and analysis of Quaternary stratigraphic field sections.* Quaternary Research Association Technical Guide No. 7. London: Quaternary Research Association, 267-286.

Long, A.J., Scaife, R.G. & Edwards, R.J., 2000. Stratigraphic architecture, relative sea -level, and models of estuary development in southern England: new data from Southampton Water. *In*: K. Pye & J.R.L. Allen , eds. *Coastal and Estuarine Environments: sedimentology, geomorphology and geoarchaeology.* Geological Society, London, Special Publications, **175**, 253-279.

Long, A.J., Roberts, D.H. & Rasch, M., 2003. New observations on the relative sea level and deglacial history of Greenland from Innaarsuit, Disko Bugt. *Quaternary Research*, **60**, 162-171.

Luternauer, J.L., Atkins, R.J., Moody, A.I., Williams, H.F.L. & Gibson, J.W., 1995. Salt marshes. *In*: G.M.E. Perillo, ed. *Geomorphology and Sedimentology of Estuaries. Developments in Sedimentology 53.* Amsterdam: Elsevier Science, 307-332.

Maccubbin, A.E. & Hodson, R.E., 1980. Mineralization of detrital lignocelluloses by salt marsh sediment microflora. *Applied and Environmental Microbiology*, **40**, 735-740.

MacLaren, C., 1842. The glacial theory of Professor Aggasiz. *American Journal of Science*, **42**, 346-365.

Malamud-Roam, F. & Ingram, B.L., 2001. Carbon isotopic compositions of plants and sediments of tide marshes in the San Francisco Estuary. *Journal of Coastal Research*, **17**, 17-29.

Marsh, J.G. & Martin,J.V., 1982. The SEASAT altimeter mean sea surface model. *Journal of Geophysical Research*, **87**, 3269-3280.

Mayer, L.M., 1985. Geochemistry of humic substances in estuarine environments. *In*: G.R. Aiken, D.M. McKnight, R.L. Wershaw & P. McCarthy, eds. *Humic Substances in Soil, Sediment, and Water: Geochemistry, Isolation and Characterisations.* New York: Wiley, 211-232.

Mayer, L.M., Jorgensen, J. & Schnitker, D., 1991. Enhancement of diatom frustule

dissolution by iron oxides. *Marine Geology*, **99**, 263-266.

McCarroll, D., 2001. Deglaciation of the Irish Sea Basin: a critique of the glaciomarine hypothesis. *Journal of Quaternary Science*, **16**, 393-404.

McCarroll, D. & Harris, 1992. The glacigenic deposits of western Lleyn, north Wales: terrestrial or marine? *Journal of Quaternary Science*, **7**, 19-29.

McManus, J., 1988. Grain size determination and interpretation. *In*: M. Tucker, ed. *Techniques in Sedimentology*. UK: Blackwell Scientific Publications, 63-85.

McPherson, G.R., Boutton, T.W. & Midwood, A.J., 1993. Stable carbon isotope analysis of soil organic matter illustrates vegetation change at the grassland/woodland boundary in southeastern Arizona, USA. *Oecologia*, **93**, 95 -101.

Megens, L., van der Plicht, J., de Leeuw, J.W. & Smedes, F., 2002. Stable carbon and radiocarbon isotope compositions of particle size fractions to determine origins of sedimentary organic matter in an estuary. *Organic Geochemistry*, **33**, 945-952.

Melillo, J.M., Aber, J.D., Linkins, A.E., Ricca, A., Fry, B. & Nadelhoffer, K.J., 1989. Carbon and nitrogen dynamics along the decay continuum: plant litter to soil organic matter. *Plant and Soil*, **115**, 189-198.

Metcalfe, S.E., Ellis, S., Horton, B.P., Innes, J.B., McArthur, J., Mitlehner, A., Parkes, A., Pethick, J. S, Rees, J., Ridgway, J., Rutherford, M.M., Shennan, I. & Tooley, M.J., 2000. The Holocene evolution of the Humber Estuary: reconstructing change in a dynamic environment. *In*: I. Shennan & J. Andrews, eds. *Holocene Land-Ocean Interaction and Environmental Change around the North Sea*. Geological Society, London, Special Publications, **166**, 97-118.

Meyers, P.A., 1994. Preservation of elemental and isotopic source identification of sedimentary organic matter. *Chemical Geology*, **114**, 289-302.

Meyers, P.A., 1997. Organic geochemical proxies of paleoceanographic, paleolimnologic, and paleoclimatic processes. *Organic Geochemistry*, **27**, 213-250.

Meyers, P.A. & Eadie, B.J., 1993. Sources, degradation and recycling of organic matter associated with sinking particles in Lake Michigan. *Organic Geochemistry*, **20**, 47-56.

Meyers, P.A. & Teranes, J.L., 2001. Sediment organic matter. *In*: W.M. Last & J.P. Smol, eds. *Tracking Environmental Change Using Lake Sediments. Volume 2: Physical and Geochemical Methods*. The Netherlands, Kluwer Academic Publishers, 239-269.

Middelburg, J.J. & Nieuwenhuize, J., 1998. Carbon and nitrogen stable isotopes in suspended matter and sediments from the Schelde Estuary. *Marine Chemistry*, **60**, 217-225.

Middelburg, J.J., Nieuwenhuize, J., Lubberts, R.K. & van de Plassche, O., 1997. Organic carbon isotope systematics of coastal marshes. *Estuarine, Coastal and Shelf Science*, **45**, 681-687.

Milne, G.A., Mitrovica, J.X. & Schrag, D.P., 2002. Estimating past continental ice volume from sea-level data. *Quaternary Science Reviews*, **21**, 361-376.

Mix, A.C., Bard, E. & Schneider, R., 2001. Environmental processes of the ice age: land, oceans, glaciers (EPILOG). *Quaternary Science Reviews*, **20**, 627-657.

Moore, P.D., Webb, J.A & Collinson, M.E., 1991. *An Illustrated Guide to Pollen Analysis*, 2nd ed. Oxford: Blackwell Scientific.

Mörner, N-A., 1969. Eustatic and climatic changes during the last 15,000 years. *Geologie en Mijnbouw*, **48**, 389-399.

Mörner, N-A., 1971. The Holocene eustatic sea-level problem. *Geologie en Mijnbouw*, **50**, 699-702.

Mörner, N-A., 1976. Eustasy and geoid changes. *The Journal of Geology*, **84**, 123-151.

Mörner, N-A., 1980. The northwest European 'sea-level laboratory' and regional Holocene eustasy. *Palaeogeography, Palaeoclimatology, Palaeoecology*, **29**, 281-300.

Mörner, N-A., 1984. Planetary, solar, atmospheric and endogene processes as origin of climate changes on the Earth. *In*: N-A Mörner & W. Karlen, eds. *Climate changes on a Yearly to Millennial basis*. Reidel: Dordrecht, 483-507.

Morton, G.H., 1887. Stanlow, Ince, and Frodsham Marshes. *Proceedings of the Liverpool Geological Society*, **5**, 349-351.

Müller, A. & Mathesius, U., 1999. The palaeoenvironments of coastal lagoons in the southern Baltic Sea, I. The application of sedimentary C_{org}/N ratios as source indicators of organic matter. *Palaeogeography, Palaeoclimatology, Palaeoecology*, **145**, 1-16.

Müller, A. & Voss, M., 1999. The palaeoenvironments of coastal lagoons in the southern Baltic Sea, II. $\delta^{13}C$ and $\delta^{15}N$ ratios of organic matter – sources and sediments. *Palaeogeography, Palaeoclimatology, Palaeoecology*, **145**, 17-32.

Neal, A., 1993. *Sedimentology and morphodynamics of a Holocene coastal dune*

barrier complex, northwest England. Unpublished Ph.D Thesis. University of Reading.

Neales, T.F., Fraser, M.S. & Roksandic, Z., 1983. Carbon isotope composition of the halophyte Disphyma clavellatum (Haw.) Chinnock (Aizoaceae), as affected by salinity. *Australian Journal of Plant Physiology*, **10**, 437-444.

Nelson, A.R. & Kashima, K., 1993. Diatom zonation in southern Oregon tidal marshes relative to vascular plants, foraminifera, and sea level. *Journal of Coastal Research*, **9**, 673-697.

Neumann, A.C., 1969. Quaternary sea-level data from Bermuda. VIII Congress INQUA, Paris, Resumes des Communications, 228-229.

Nier, A.O., 1950. A redetermination of the relative abundances of the isotopes of carbon, nitrogen, oxygen, argon and potassium. *Physical Review*, 77, 789-793.

Nunn, P.D. & Peltier, R.W., 2001. Far-field test of the ICE-4G model of global isostatic response to deglaciation using empirical and theoretical Holocene sea-level reconstructions for the Fiji Islands, Southwestern Pacific. *Quaternary Research*, **55**, 203-214.

O'Leary, M.H. & Osmond, C.B., 1980. Diffusional contribution to carbon isotope fractionation during dark CO_2 fixation in CAM plants. *Plant Physiology*, **66**, 931 -934.

O'Leary, M.H., Madhavan, S. & Paneth, P., 1992. Physical and chemical basis of carbon isotope fractionation in plants. *Plant, Cell and Environment*, **15**, 1099 -1104.

Oppenheim, D.R., 1988. The distribution of epipelic diatoms along an intertidal shore in relation to principal physical gradients. *Botanica Marina*, **31**, 65-72.

Osmond, C.B., Allaway, W.G., Sutton, B.G., Troughton, J.H., Queroz, O., Luttge, N. & Winter, K., 1973. Carbon isotope discrimination in photosynthesis of CAM plants. *Nature*, **246**, 41-42.

Otero, E., Culp, R., Noakes, J.E. & Hodson, R.E., 2003. The distribution and $\delta^{13}C$ of dissolved organic carbon and its humic fraction in estuaries of southeastern USA. *Estuarine, Coastal and Shelf Science*, **56**, 1187-1194.

Palmer, A.J.M. & Abbott, W.H., 1986. Diatoms as indicators of sea-level change. *In*: O. van de Plassche, ed. *Sea-Level Research: A Manual for the Collection and Evaluation of Data*. Norwich: Geo Books, 457-473.

Park, R. & Epstein, S., 1960. Carbon isotope fractionation during photosynthesis.

Geochimica et Cosmochimica Acta, **21**, 110-126.

Park, R. & Epstein, S., 1961. Metabolic fractionation of C^{13} & C^{12} in plants. *Plant Physiology*, **36**, 133-138.

Patterson, R.T., Hutchinson, I., Guilbault, J.-P. & Clague, J.J., 2000. A comparison of the vertical zonation of diatom, foraminifera, and macrophyte assemblages in a coastal marsh: implications for greater paleo-sea level resolution. *Micropaleontology*, **46**, 229-244.

Paul, M.A. & Barra, B.F., 1998. A geotechnical correction for post-depositional sediment compression: examples from the Forth valley, Scotland. *Journal of Quaternary Science*, **13**, 171-176.

Peltier, W.R., 1998. Postglacial variations in the level of the sea: Implications for climate dynamics and solid earth geophysics. *Reviews of Geophysics*, **36**, 603-689.

Peltier, W.R., 2002. On eustatic sea level history: Last Glacial Maximum to Holocene. *Quaternary Science Reviews*, **21**, 377-396.

Peltier, W.R., Shennan, I., Drummond, R. & Horton, B., 2002. On the postglacial isostatic adjustment of the British Isles and the shallow viscoelastic structure of the Earth. *Geophysical Journal International*, **148**, 443-475.

Petersen, B.J., 1943. Some halobian spectra (Diatoms). *Det Kgl. Danske Videnskabernes Selskab Biologiske Meddelelser*, **17**, 1-95.

Peterson, B.J., Howarth, R.W., Lipschultz, F. & Ashendorf, D., 1980. Salt marsh detritus: an alternative interpretation of stable carbon isotope ratios and the fate of *Spartina alterniflora*. *Oikos*, **34**, 173-177.

Peterson, B.J., Fry, B., Hullar, M., Saupe, S. & Wright, R., 1994. The distribution and stable carbon isotope composition of dissolved organic carbon in estuaries. *Estuaries*, **17**, 111-121.

Peypouquet, J.-P., 1979-80. Les ostracodes et la recherche des paléorivages, indicateurs des niveaux marins. *Oceanis*, **5**, 273-281.

Picton, J.A., 1849. The changes of sea levels on the west coast of England during the historic period (Abstract). *Proceedings of the Literary and Philosophical Society of Liverpool*, **5**, 113-115.

Plassche, O. van de, 1986. *Sea-level Research: a manual for the collection and evaluation of data*. Norwich: Geo Books.

Plater, A.J. & Poolton, N.R.J., 1992. Interpretation of Holocene sea level tendency and

intertidal sedimentation in the Tees estuary using sediment luminescence techniques: a viability study. *Sedimentology*, **39**, 1-15.

Plater, A.J. & Shennan, I., 1992. Evidence of Holocene sea-level change from the Northumberland coast, eastern England. *Proceedings of the Geologists' Association*, **103**, 201-216.

Plater, A.J., Long, A.J., Huddart, D., Gonzalez, S. & Tooley, M.J., 1999. The land of the Mersey Basin: sea-level changes. *In*: E.F. Greenwood, ed. *Ecology and Landscape Development: A History of the Mersey Basin.* Liverpool: Liverpool University Press, National Museums and Galleries on Merseyside, 13- 20.

Plater, A.J., Ridgway, J., Rayner, B., Shennan, I., Horton, B.P., Hayworth, E.Y., Wright, M.R., Rutherford, M.M. & Wintle, A.G., 2000a. Sediment provenance and flux in the Tees Estuary: the record from the Late Devensian to the present. *In*: I. Shennan & J.E. Andrews, eds. *Holocene Land-Ocean Interaction and Environmental Change around the North Sea.* Geological Society, London, Special Publications, **166**, 171-195.

Plater, A.J., Horton, B.P., Haworth, E.Y., Appleby, P.G., Zong, Y., Wright, M.R. & Rutherford, M.M., 2000b. Holocene tidal levels and sedimentation rates using a diatom-based palaeoenvironmental reconstruction: the Tees estuary, northeastern England. *The Holocene*, **10**, 441-452.

Postma, H., 1967. Sediment transport and sedimentation in the estuarine environment. *In*: G.H Lauff ed. *Estuaries.* Washington, DC: American Association for the Advancement of Science, Publication 83, (158-179).

Preston, C.D., Pearman, D.A. & Dines, T.D., 2002. *New Atlas of the British and Irish Flora.* Oxford: Oxford University Press.

Pye, K. & Neal, A., 1993a. Stratigraphy and age structure of the Sefton dune complex: Preliminary results of field drilling investigations. *In*: D. Atkinson & J. Houston, eds. *The Sand Dunes of the Sefton Coast.* National Museums & Galleries on Merseyside in association with Sefton Metropolitan Borough Council, 41-44.

Pye, K. & Neal, A., 1993b. Late Holocene dune formation on the Sefton coast, northwest England. In: K. Pye, ed. *The Dynamics and Environmental Context of Aeolian Sedimentary Systems.* Geological Society Special Publication No. **72**. Bath: Geological Society Publishing House, 201-217.

Rackham, O., 1986. *The History of the Countryside.* London: Dent.

Ranwell, D.S., 1974. The salt marsh to tidal woodland transition. *Hydrobiological*

Bulletin, **8**, 139-151.

Rashid, M.A., 1985. *Geochemistry of Marine Humic Compounds*. New York: Springer-Verlag.

Rashid, M.A. & Reinson, G.E., 1979. Organic matter in surficial sediments of the Miramichi Estuary, New Brunswick, Canada. *Estuarine and Coastal Marine Science*, **8**, 23-36.

Raymond, P.A. & Bauer, J.E., 2001. Use of ^{14}C and ^{13}C natural abundances for evaluating riverine, estuarine, and coastal DOC and POC sources and cycling: a review and synthesis. *Organic Geochemistry*, **32**, 469-485.

Reade, T.M., 1871. The geology and physics of the post glacial period, as shewn in the deposits and organic remains in Lancashire and Cheshire. *Proceedings of the Liverpool Geological Society*, **2**, 36-88.

Reade, T.M., 1872. The post-glacial geology and physiography of west Lancashire and the Mersey Estuary. *Geological Magazine*, **9**, 111-119.

Rees, J.G., Ridgway, J., Ellis, S., Knox, O'B. R.W., Newsham, R & Parkes, A., 2000. Holocene sediment storage in the Humber Estuary. *In*: I. Shennan & J.E. Andrews, eds. *Holocene Land-Ocean Interaction and Environmental Change around the North Sea*. Geological Society, London, Special Publications, **166**, 119-143.

Roberts, G., Gonzalez, S. & Huddart, D., 1996. Intertidal Holocene footprints and their archaeological significance. *Antiquity*, **70**, 647-651.

Roep, Th. B. & Beets, D.J., 1988. Sea level rise and paleotidal levels from sedimentary structures in the coastal barriers in the western Netherlands since 5600 BP. *Geologie en Mijnbouw*, **67**, 53-60.

Roeske, C.A. & O'Leary, M.H., 1984. Carbon isotope effects on the enzyme catalysed carboxylation of ribulose bisphosphate. *Biochemistry*, **23**, 6275-6284.

Romankevich, E.A., 1984. *Geochemistry of Organic Matter in the Ocean*. Berlin: Springer-Verlag.

Round, F.E., 1971. Benthic marine diatoms. *Oceanography and Marine Biology: An Annual Review*, **9**, 83-139.

Round, F.E., Crawford, R.M. & Mann, D.G., 1990. *The Diatoms: Biology & Morphology of the Genera*. Cambridge: Cambridge University Press.

Ryves, D.B., Juggins, S., Fritz, S.C. & Battarbee, R.W., 2001. Experimental diatom dissolution and the quantification of microfossil preservation in sediments. *Palaeogeography, Palaeoclimatology, Palaeoecology*, **172**, 99-113.

Sackett, W.M., 1964. The depositional history and isotopic organic carbon composition of marine sediments. *Marine Geology*, **2**, 179-185

Sackett, W.M. & Thompson, R.R., 1963. Isotopic organic carbon composition of recent continental derived clastic sediments of Eastern Gulf Coast, Gulf of Mexico. *Bulletin of the American Association of Petroleum Geologists*, **47**, 525-531.

Sackett, W.M., Eckelmann, W.R., Bender, M.L. & Be, A.W.H., 1965. Temperature dependence of carbon isotope composition in marine plankton and sediments. *Science*, **148**, 235-237.

Salomons, W. & Mook, W.G., 1981. Field observations of the isotopic composition of particulate organic carbon in the southern North Sea and adjacent estuaries. *Marine Geology*, **41**, M11-M20.

Sancetta, C., 1999. Diatoms and marine paleoceanography. *In*: E.F. Stoermer & J.P. Smol, eds. *The Diatoms: Applications for the Environmental and Earth Sciences.* Cambridge: Cambridge University Press, 374-386.

Sawai, Y., 2001. Distribution of living and dead diatoms in tidal wetlands of northern Japan: relations to taphonomy. *Palaeogeography, Palaeoclimatology, Palaeoecology*, **173**, 125-141.

Schidlowski, M., 1987. Application of stable carbon isotopes to early biochemical evolution of the Earth. *Annual Review of Earth and Planetary Sciences*, **15**, 47-72.

Schleser, G.H., 1995. Parameters determining carbon isotope ratios in plants. *In*: B. Frenzel, B. Stauffer & M. Weib, eds. *Problems of Stable Isotopes in Tree-Rings, Lake Sediments and Peat Bogs as Climate Evidence for the Holocene*. Stuttgart: Gustave, Fischer Verlag, 71-96.

Scholl, D.W., Frank, C., Craighead Sr. & Stuiver, M., 1969. Florida submergence curve revised: its relation to coastal sedimentation rates. *Science*, **163**, 562-564.

Scott, D.B. & Medioli, F.S., 1978. Vertical zonations of marsh foraminifera as accurate indicators of former sea-levels. *Nature*, **272**, 528-531.

Scott, D.B. & Medioli, F.S., 1980. Quantitative studies of marsh foraminiferal distributions in Nova Scotia: implications for sea level studies. *Journal of Foraminiferal Research*, Special Publication No. **17**, 1-58.

Seemann, J.R. & Critchley, C., 1985. Effects of salt stress on the growth, ion content, stomatal behaviour and photosynthetic capacity of a salt-sensitive species, *Phaseolus vulgaris* L. *Planta*, **164**, 151-162.

Shackleton, N.J., 2000. The 100,000-year ice-age cycle identified and found to lag

temperature, carbon dioxide, and orbital eccentricity. *Science*, **289**, 1897-1902.

Shaw, D.F., 1975. Water inputs to Liverpool Bay. *In*: Liverpool Bay Study Group, ed. *Liverpool Bay: An Assessment of Present Knowledge*. Natural Environmental Research Council, London, Series C, 14, 11-12.

Shennan, I., 1980. *Flandrian sea-level changes in the Fenland*. Unpublished Ph.D Thesis, University of Durham.

Shennan, I., 1982. Interpretation of Flandrian sea-level data from the Fenland, England. *Proceedings of the Geologists' Association*, **93**, 53-63.

Shennan, I., 1983. A problem of definition in sea-level research methods. *Quaternary Newsletter*, **39**, 17-19.

Shennan, I., 1986. Flandrian sea-level changes in the Fenland. II: tendencies of sea -level movement, altitudinal changes, and local and regional factors. *Journal of Quaternary Sciecne*, **1**, 155-179.

Shennan, I., 1989. Holocene crustal movements and sea-level changes in Great Britain. *Journal of Quaternary Science*, **4**, 77-89.

Shennan, I., 1995. Sea-level and coastal evolution: Holocene analogues for future changes. *Coastal Zone Topics: Process, Ecology & Management*, **1**, 1-9.

Shennan, I. & Horton, B., 2002. Holocene land- and sea-level changes in Great Britain. *Journal of Quaternary Science*, **17**, 511-526.

Shennan, I., Tooley, M.J., Davis, M.J. & Haggart, B.A., 1983. Analysis and interpretation of Holocene sea-level data. *Nature*, **302**, 404-406.

Shennan, I., Innes, J.B., Long, A.J. & Zong, Y., 1995. Holocene relative sea-level changes and coastal vegetation history at Kentra Moss, Argyll, northwest Scotland. *Marine Geology*, **124**, 43-59.

Shennan, I., Long, A.J., Rutherford, M.M., Green, F.M., Innes, J.B., Lloyd, J.M., Zong, Y. & Walker, K.J., 1996. Tidal marsh stratigraphy, sea-level change and large earthquakes, I: a 5000 year record in Washington ,U.S.A. *Quaternary Science Reviews*, **15**, 1023-1059.

Shennan, I., Tooley, M.J., Green, F., Innes, J., Kennington, K., Lloyd, J. & Rutherford, M., 1999. Sea level, climate change and coastal evolution in Morar, northwest Scotland. *Geologie en Mijnbouw*, **77**, 247-262.

Shennan, I., Lambeck, K., Horton, B., Innes, J., Lloyd, J., McArthur, J. & Purcell, T.,

Rutherford, M., 2000a. Late Devensian and Holocene records of relative sea-level changes in northwest Scotland and their implications for glacio-hydro-isostatic modelling. *Quaternary Science Reviews*, **19**, 1103-1135.

Shennan, I., Lambeck, K, Flather, R., Horton, B., McArthur, J., Innes, J., Lloyd, J., Rutherford, M. & Wingfield, R., 2000b. Modelling western North Sea palaeogeographies and tidal changes during the Holocene. *In*: I. Shennan & J.E. Andrews, eds. *Holocene Land-Ocean Interaction and Environmental Change around the North Sea.* Geological Society, London, Special Publications, **166**, 299-319.

Shennan, I., Peltier, W.R., Drummond, R. & Horton, B., 2002. Global to local scale parameters determining relative sea-level changes and the post-glacial isostatic adjustment of Great Britain. *Quaternary Science Reviews*, **21**, 397-408.

Sherr, E.B., 1982. Carbon isotope composition of organic seston and sediments in a Georgia salt marsh estuary. *Geochimica et Cosmochimica Acta*, **46**, 1227-1232.

Shultz, D.J. & Calder, J.A., 1976. Organic carbon $^{13}C/^{12}C$ variations in estuarine sediments. *Geochimica et Cosmochimica Acta*, **40**, 381-385.

Simonsen, R., 1969. Diatoms as indicators in estuarine environments. *Veröffenth Institut Meeresforschung Bremerhaven*, **11**, 287-291.

Spencer, C.D., Plater, A.J. & Long, A.J., 1998. Rapid coastal change during the mid- to late Holocene: the record of barrier estuary sedimentation in the Romney Marsh region, southeast England. *The Holocene*, **8**, 143-163.

Spiker, E.C. & Hatcher, P.G., 1987. The effects of early diagenesis on the chemical and stable carbon isotopic composition of wood. *Geochimica et Cosmochimica Acta*, **51**, 1385-1391.

Stace, C., 1997. *New Flora of the British Isles,* 2nd ed. Cambridge: Cambridge University Press.

Stevenson, F.J., 1985. Geochemistry of soil humic substances. *In*: G.R. Aiken, D.M. McKnight, R.L. Wershaw & P. McCarthy, eds. *Humic Substances in Soil, Sediment, and Water: Geochemistry, Isolation and Characterisations.* New York: Wiley, 19-52.

Stout, J.D., Rafter, T.A. & Troughton, J.H., 1975. The possible significance of isotope ratios in palaeoecology. *Bulletin, - Royal Society of New Zealand*, **13**, 279-286.

Street-Perrott, A.F., Ficken, K.F., Huang, Y. & Eglington, G., 2004. Late Quaternary

changes in carbon cycling on Mt. Kenya, East Africa: an overview of the $\delta^{13}C$ record in lacustrine organic matter. *Quaternary Science Reviews*, **23**, 861-879.

Stuiver, M., Reimer, P., Bard, D., Beck, W.J., Burr, G.S., Hughen, K.A., Kromer, B., McCormac, G., Van Der Plicht, J. & Spurk, M., 1998. INTCAL 98 Radiocarbon age calibration, 24,000-0 cal BP. *Radiocarbon*, **40**, 1041-1083.

Stupples, P., 2002. Tidal cycles preserved in late Holocene tidal rhythmites, the Wainway Channel, Romney Marsh, southeast England. *Marine Geology*, **182**, 231-246.

Suess, E., 1906. *The Face of the Earth*, volume 2. Oxford: Clarendon Press.

Tan, F.C., 1989. Stable carbon isotopes in dissolved inorganic carbon in marine and estuarine environments. *In*: P. Fritz & J. Fontes, eds. *Handbook of Environmental Isotope Geochemistry. Volume 3. The Marine Environment, A*. The Netherlands: Elsevier, 171-190.

Tanner, W.F., 1991. Applications of suite statistics to stratigraphy and sea-level changes. *In*: J.P.M. Syvitski, ed. *Principles, Methods and Applications of Particle Size Analysis*. Cambridge: Cambridge University Press, 283-292.

TAPPI, 1988. Acid-insoluble lignin in wood and pulp. *Technical Association of the Pulp and Paper Industry, T 222 om-88.*

TAPPI, 1997. Solvent extractives of wood and pulp. *Technical Association of the Pulp and Paper Industry, T 204 cm-97.*

Thomas, G.S.P., Chester, D.K. & Crimes, P., 1998. The Late Devensian glaciation of the eastern Lleyn Peninsula, North Wales: evidence for terrestrial depositional environments. *Journal of Quaternary Science*, **13**, 255-270.

Thornton, S.F. & McManus, J., 1994. Applications of organic carbon and nitrogen stable isotope and C/N ratios as source indicators of organic matter provenance in estuarine systems: Evidence from the Tay Estuary, Scotland. *Estuarine, Coastal and Shelf Science*, **38**, 219-233.

Tooley, M.J., 1969. *Sea-level changes and the development of coastal plant communities during the Flandrian in Lancashire and adjacent areas*. Unpublished Ph.D Thesis, University of Lancashire.

Tooley, M.J., 1974. Sea-level changes during the last 9000 years in north-west England. *The Geographical Journal*, **140**, 18-42.

Tooley, M.J., 1978a. *Sea-level changes: North-England during the Flandrian Stage*. Oxford: Clarendon Press.

Tooley, M.J., 1978b. Interpretation of Holocene sea-level changes. *Geologiska Föreningens i Stockholm Förhandlingar*, **100**, 203-212

Tooley, M.J., 1982a. Introduction. *Proceedings of the Geologists' Association*, **83**, 3-6.

Tooley, M.J., 1982b. Sea-level changes in northern England. *Proceedings of the Geologists' Association*, **93**, 43-51.

Tooley, M.J., 1985. Climate, sea-level and coastal changes. *In*: M.J. Tooley & G.M. Sheail, eds. *The Climatic Scene*. London: Allen & Unwin, 206-234.

Tooley, M.J., 1990. The chronology of coastal dune development in the United Kingdom. *Catena Supplement*, **18**, 81-88.

Törnqvist, T.E., Van Ree, M.H.M., Van't Veer, R. & Van Geel, B., 1998. Improving methodology for high-resolution reconstruction of sea-level rise and neotectonics by paleoecological analysis ad AMS ^{14}C dating on basal peats. *Quaternary Research*, **49**, 72-85.

Turney, C.S.M., Barringer, J., Hunt, J.E. & McGlone, M.S., 1999. Estimating past leaf-to-air vapour pressure deficit from terrestrial plant $\delta^{13}C$. *Journal of Quaternary Science*, **14**, 437-442.

Twiddy, E.J., 1996. *Applications of stable carbon and oxygen isotope analysis to some aspects of coastal environmental change*. Unpublished Ph.D Thesis, University of Durham.

Tyson, R.V., 1995. *Sedimentary Organic Matter: Organic Facies and Palynofacies*. London: Chapman & Hall.

Van Dam, H., Mertens, A. & Sinkeldam, J., 1994. A coded checklist and ecological indicator values of freshwater diatoms from The Netherlands. *Netherlands Journal of Aquatic Ecology*, **28**, 117-133.

Van Heemst, J.D.H., Megens, L., Hatcher, P.G. & de Leeuw, J.W., 2000. Nature, origin and average age of estuarine ultrafiltered dissolved organic matter as determined by molecular and carbon isotope characterization. *Organic Geochemistry*, **31**, 847 -857.

Vos, P.C. & De Wolf, H., 1988. Methodological aspects of paleo-ecological diatom research in coastal areas of the Netherlands. *Geologie en Mijnbouw*, **67**, 31-40.

Vos, P.C. & De Wolf, H., 1993a. Diatoms as a tool for reconstructing sedimentary environments in coastal wetlands; methodological aspects. *Hydrobiologia* **269/270**, 285 -296.

Vos, P.C. & De Wolf, H., 1993b. Reconstruction of sedimentary environments in Holocene coastal deposits of the southwest Netherlands; the Poortvliet boring, a case study of palaeoenvironmental diatom research. *Hydrobiologia*, **269/270**, 297-306.

Vos, P.C. & van Kesteren, W.P., 2000. The long-term evolution of intertidal mudflats in the northern Netherlands during the Holocene; natural and anthropogenic processes. *Continental Shelf Research*, **20**, 1687-1710.

Waller, M.P., Long, A.J., Long, D. & Innes, J.B., 1999. Patterns and processes in the development of coastal mire vegetation: Multi-site investigations from Walland Marsh, Southeast England. *Quaternary Science Reviews*, **18**, 1419-1444.

Watts, W.A., 1977. The Late Devensian vegetation of Ireland. *Philosophical Transactions of the Royal Society, London*, **B280**, 273-293.

Werff, van der, A. & Huls, H., 1957-1974. *Diatomeënflora van Nederland*. Reprint 1976. Koenigstein: Otto Koeltz Science Publishers.

Westman, P. & Hedenström, A., 2002. Environmental changes during isolation processes from the Litorina Sea as reflected by diatoms and geochemical parameters – a case study. *The Holocene*, **12**, 531-540.

Wilson, P., Bateman, R.M. & Catt, J.A., 1981. Petrography, origin and environment of deposition of the Shirdley Hill Sand of southwest Lancashire, England. *Proceedings of the Geologists' Association*, **92**, 211-229.

Wong, W.W. & Sackett, W.M., 1978. Fractionation of stable carbon isotopes by marine phytoplankton. *Geochimica et Cosmochimica Acta*, **42**, 1809-1815.

WPRL, 1974. Effect of Polluting Discharges on the Mersey Estuary. Report of Investigations on behalf of the Steering Committee on Pollution of the Mersey Estuary. WPRL Report 447R.

Yamaguchi, H., Montani, S., Tsutsumi, H., Hamada, K. & Ueda, N., 2003. Estimation of particulate organic carbon flux in relation to photosynthetic production in a shallow coastal area in the Seto Inland Sea. *Marine Pollution Bulletin*, **47**, 18-24.

Yokoyama, Y., Lambeck, K., De Deckker, P., Johnston, P. & Fifield, K.L., 2000. Timing of the Last Glacial Maximum from observed sea-level minima. *Nature*, **406**, 713-716.

Zong, Y., 1997. Mid- and late-Holocene sea-level changes in Roundsea Marsh, northwest England: a diatom biostratigraphical investigation. *The Holocene*, **7**, 311-323.

Zong, Y. & Horton, B.P., 1998. Diatom zones across intertidal flats and coastal saltmarshes in Britain. *Diatom Research*, **13**, 375-394.

Zong, Y. & Horton, B.P., 1999. Diatom-based tidal-level transfer functions as an aid in reconstructing Quaternary history of sea-level movements in the UK. *Journal of Quaternary Science*, **14**, 153-167.

Zong, Y. & Tooley, M.J., 1996. Holocene sea-level changes and crustal movements in Morecambe Bay, northwest England. *Journal of Quaternary Science*, **11**, 43-58.

Zong, Y. & Tooley, M.J., 1999. Evidence of mid-Holocene storm-surge deposits from Morecambe Bay, northwest England: A biostratigraphical approach. *Quaternary International*, **55**, 43-50.

Appendix A
Modern saltmarsh survey

A.1. Location of Ince Banks saltmarsh sampling stations along transect A-B (Figure 4.1).

Station name	Zone	National Grid Reference (SJ)	Distance along transect A-B (m)	Altitude (m OD)
IB1	High saltmarsh	4749 7790	50	5.317
IB2	High saltmarsh	4688 7764	100	5.429
IB3	High saltmarsh	4693 7777	210	5.313
IB4	High saltmarsh	4679 7776	290	5.291
IB5	High saltmarsh	4717 7799	300	5.231
IB6	High saltmarsh	4673 7804	550	5.212
IB7	High saltmarsh	4685 7823	670	5.048
IB8	High saltmarsh	4664 7826	790	5.157
IB9	High saltmarsh	4658 7851	1120	4.969
IB10	High saltmarsh	4642 7869	1290	5.068
IB11	High saltmarsh	4637 7879	1380	4.998
IB12	Low saltmarsh	4639 7883	1390	3.838
IB13	Tidalflat	4643 7883	1395	2.818
IB14	Tidalflat	4642 7886	1400	2.448

Table A.2. Saltmarsh sediment organic content, $\delta^{13}C$ and C/N along Ince Banks transect A-B.

Station name	Organic content (%)	$\delta^{13}C$ (‰)	C_{org}/N_{tot}
IB1	17	–27.8	11.6
IB2	16	–26.4	10.9
IB3	15	–26.2	9.7
IB4	16	–26.4	10.9
IB5	16	–26.3	11.0
IB6	12	–26.0	10.8
IB7	8	–25.2	10.5
IB8	16	–25.8	10.5
IB9	11	–25.7	10.8
IB10	9	–25.4	10.2
IB11	8	–25.8	10.2
IB12	6	–24.7	10.0
IB13	5	–23.5	9.6
IB14	5	–23.7	9.3

A.3a. Dominant saltmarsh species at selected stations and associated whole plant $\delta^{13}C$ and C/N measurements of three plant specimens of each species.

Station	Important species	Percentage cover within 50 cm^2 quadrat	Whole plant $\delta^{13}C$ (‰)			Whole plant C_{org}/N_{tot}		
			Specimen			Specimen		
			1	2	3	1	2	3
IB1	*Elymus atherica*	70%	-28.4	-27.3	-27.7	67.1	22.3	22.7
	Agrostis stolonifera	30%	-22.8	-26.7	-26.9	30.1	28.2	23.2
IB5	*Atriplex hastata*	39%	-26.4	-27.1	-27.0	17.4	21.9	14.5
	Puccinellia maritima	59%	-27.4	-27.3	-26.8	31.2	29.4	34.6
	Festuca rubra	2%	-26.4	-26.8	-26.7	31.3	34.6	27.6
IB7	*Atriplex hastata*	32%	-27.2	-27.9	-28.4	22.5	18.1	21.4
	Puccinellia maritima	68%	-28.4	-28.3	-28.2	16.9	30.1	36.6
IB10	*Atriplex hastata*	95%	-26.8	-26.7	-27.1	15.1	15.6	17.6
	Puccinellia maritima	100%	-28.0	-27.1	-28.7	32.1	33.2	33.0
IB11	*Atriplex hastata*	44%	-26.7	-27.0	-26.3	13.4	16.1	15.4
	Puccinellia maritima	100%	-27.0	-27.3	-27.9	36.4	32.3	33.2
IB12	*Atriplex hastata*	45%	-26.9	-27.2	-27.3	13.8	15.7	16.7
	Puccinellia maritima	5%	-27.6	-27.4	-26.6	38.0	40.0	44.2
	Limonium vulgare							

A.3b. Dominant saltmarsh species at selected stations and associated plant lignin $\delta^{13}C$ and C/N measurements of three plant specimens of each species.

Station	Important species	Percentage cover within 50 cm^2 quadrat	Lignin $\delta^{13}C$ (‰)			Lignin C_{org}/N_{tot}		
			Specimen			Specimen		
			1	2	3	1	2	3
IB1	*Elymus atherica*	68%	-30.9	-32.2	-	8.0	9.1	-
	Agrostis stolonifera	32%	-29.7	-	-	23.0	-	-
IB5	*Atriplex hastata*	21%	-29.8	-29.7	-29.5	16.3	20.2	17.5
	Puccinellia maritima	65%	-30.3	-31.4	-29.6	16.0	25.2	21.2
	Festuca rubra	14%	-30.5	-29.6	-	34.3	29.9	-
IB7	*Atriplex hastata*	52%	-29.8	-29.4	-30.6	10.6	13.0	10.0
	Puccinellia maritima	48%	-31.2	-	-	15.7	-	-
IB10	*Atriplex hastata*	95%	-30.2	-30.6	-30.8	15.3	16.7	16.6
	Puccinellia maritima	100%	-31.3	-32.1	-31.9	21.2	21.8	27.0
IB11	*Atriplex hastata*	28%	-29.1	-30.2	-29.9	14.9	13.4	13.7
	Limonium vulgare	14%	-31.1	-31.2	-31.6	25.4	21.5	25.6
	Armeria maritima	58%	-30.0	-	-	19.7	-	-
IB12	*Atriplex hastata*	64%	-30.1	-28.1	-30.1	16.1	13.9	15.7

A.4. Predicted surface sediment and degraded surface sediment $\delta^{13}C$ and C/N based on the mixing model of Chmura *et al.* (1987).

Station	Predicted surface sediment $\delta^{13}C$ (‰)			Predicted surface sediment C_{org}/N_{tot}			Predicted degraded surface sediment $\delta^{13}C$ (‰)			Predicted degraded surface sediment C_{org}/N_{tot}		
	Min.	Mean	Max.	Min.	Mean	Max.	Min.	Mean	Max.	Min.	Mean	Max.
IB1	-28.0	-27.1	-26.0	22.6	34.3	56.0	-31.4	-31.0	-30.5	12.8	13.2	13.5
IB5	-27.3*	-27.0*	-26.6*	23.6	26.3	29.6	-30.9	-30.2	-29.6	18.0	21.8	25.4
IB7	-28.4	-28.1	-27.9	17.3	25.6	32.1	-30.9	-30.5	-30.3	12.6	13.3	14.3
IB10	-27.8	-27.4	-26.9	46.4	48.1	50.0	-31.5	-31.1	-30.7	18.3	19.8	22.0
IB11	-27.5	-27.4	-27.3	18.2	19.0	20.0	-30.3	-30.1	-29.9	16.1	17.4	18.5
IB12	-27.3	-27.1	-26.9	16.2	17.9	19.4	-30.1	-29.4	-28.1	13.9	15.2	16.1

*Example

Plant species	Percentage cover	Plant specimen $\delta^{13}C$			Summary statistics		
		1	2	3	Min. $\delta^{13}C$	Mean $\delta^{13}C$	Max. $\delta^{13}C$
A	39%	-27.1‰	-27.0‰	-26.4‰	-27.1‰	-26.83‰	-26.4‰
B	59%	-27.4‰	-27.3‰	-26.8‰	-27.4‰	-27.17‰	-26.8‰
C	2%	-26.8‰	-26.7‰	-26.4‰	-26.8‰	-26.63‰	-26.4‰

Using Equation 5.1: $\delta^{13}C_{plot} = \frac{\sum_{n=1}^{i}(\%\text{biomass}_i)(\delta^{13}C)}{\sum_{n=1}^{i}\%\text{biomass}_i}$

Predicted minimum $\delta^{13}C$

$$\delta^{13}C_{plot} = \frac{(39\times-27.1)+(59\times-27.4)+(2\times-26.8)}{100}$$

$$= \mathbf{-27.3‰}$$

Predicted mean $\delta^{13}C$

$$\delta^{13}C_{plot} = \frac{(39\times-26.83)+(59\times-27.17)+(2\times-26.63)}{100}$$

$$= \mathbf{-27.0‰}$$

Predicted maximum $\delta^{13}C$

$$\delta^{13}C_{plot} = \frac{(39\times-26.4)+(59\times-26.8)+(2\times-26.4)}{100}$$

$$= \mathbf{-26.6‰}$$

Appendix B
Modern estuary survey

B.1. Location of sampling stations along the axis of the Mersey Estuary.

Location	National Grid Reference	Distance from Estuary mouth
Crosby	308 974	0km
New Brighton	301 943	2km
Seacombe	323 915	5km
Marina	343 889	7km
Bromborough	363 821	13km
Liverpool Airport	450 819	21km
Pickerings Pasture	489 835	25km
Mersey Way	528 849	29km
Martinscroft	656 888	38km

B.2a. Salinity, conductivity, total dissolved solids and pH of estuarine waters during a high tide in summer 2001 along the axis of the Mersey Estuary.

	16-17 August 2001 – High Tide			
Location	Salinity (gl^{-1})	Conductivity (Ms)	TDS (gl^{-1})	pH
Crosby	22.4	36.8	22.1	7.55
New Brighton	24.9	39.5	23.7	7.88
Seacombe	25.1	39.7	23.8	7.94
Marina	21.8	35.9	21.5	7.55
Bromborough	21.6	35.7	21.4	7.51
Liverpool Airport	10.5	21.1	12.6	7.09
Pickerings Pasture	11.3	22.4	13.3	7.01
Mersey Way	1.8	4.2	2.5	7.08
Martinscroft	0.5	0.5	0.3	6.87

B.2b. Salinity, conductivity, total dissolved solids and pH of estuarine waters during a low tide in summer 2001 along the axis of the Mersey Estuary.

	16-17 August 2001 – Low Tide			
Location	Salinity (gl^{-1})	Conductivity (Ms)	TDS (gl^{-1})	pH
Crosby	23.2	37.6	22.5	7.68
New Brighton	23.2	37.5	22.5	7.78
Seacombe	22.9	37.3	22.4	7.69
Marina		Unavailable		
Bromborough	17.4	30.7	18.4	7.4
Liverpool Airport		Unavailable		
Pickerings Pasture	0.4	0.7	0.4	7.00
Mersey Way	0.4	0.6	0.4	7.03
Martinscroft	0.3	0.5	0.3	6.57

B.3a. Salinity, conductivity, total dissolved solids and pH of estuarine waters during a high tide in spring 2001 along the axis of the Mersey Estuary.

Location	23-25 March 2001 – High Tide Salinity (gl^{-1})	Conductivity (Ms)	TDS (gl^{-1})	pH
Crosby		Unavailable		
New Brighton	32.5	48.0	28.1	7.56
Seacombe	33.4	45.6	29.1	6.74
Marina	29.1	41.3	29.3	6.61
Bromborough	27.0	39.6	25.2	6.34
Liverpool Airport	12.7	28.9	16.1	6.95
Pickerings Pasture	13.5	13.7	15.1	6.57
Mersey Way	8.9	19.8	11.5	6.48
Martinscroft	0.6	0.8	0.5	6.94

B.3.b. Salinity, conductivity, total dissolved solids and pH of estuarine waters during a low tide in spring 2001 along the axis of the Mersey Estuary.

Location	23-25 March 2001 – Low Tide Salinity (gl^{-1})	Conductivity (Ms)	TDS (gl^{-1})	pH
Crosby		Unavailable		
New Brighton	27.4	42.1	25.6	6.22
Seacombe	23.6	38.6	23.8	6.87
Marina		Unavailable		
Bromborough	21.1	35.4	21.3	6.49
Liverpool Airport		Unavailable		
Pickerings Pasture	1.7	3.9	2.4	6.81
Mersey Way	1.0	1.9	13.0	6.69
Martinscroft	0.4	0.7	0.6	6.96

B.4a. Salinity, conductivity, total dissolved solids and pH of estuarine waters during a high tide in winter 2002 along the axis of the Mersey Estuary.

Location	24-25 February 2002 – High Tide Salinity (gl^{-1})	Conductivity (Ms)	TDS (gl^{-1})	pH
Crosby	15.6	28.9	17.2	7.53
New Brighton	24.9	39.2	23.6	7.58
Seacombe	24.0	38.4	23.1	7.62
Marina	11.6	22.4	13.6	7.56
Bromborough	15.2	27.9	16.7	7.60
Liverpool Airport	2.1	3.5	2.1	7.22
Pickerings Pasture	0.8	1.1	0.7	6.91
Mersey Way	0.5	0.5	0.3	7.18
Martinscroft	0.4	0.4	0.2	7.08

B.4b. Salinity, conductivity, total dissolved solids and pH of estuarine waters during a low tide in winter 2002 along the axis of the Mersey Estuary.

Location	24-25 February 2002 – Low Tide Salinity (gl^{-1})	Conductivity (Ms)	TDS (gl^{-1})	pH
Crosby	13.6	25.5	15.6	7.43
New Brighton	13.1	24.4	14.8	7.38
Seacombe	9.5	19.6	11.7	7.14
Marina		Unavailable		
Bromborough	3.3	7.6	4.6	7.23
Liverpool Airport		Unavailable		
Pickerings Pasture	0.5	0.4	0.3	7.27
Mersey Way		Unavailable		
Martinscroft	0.4	0.4	0.2	6.64

B.5a. Salinity, conductivity, total dissolved solids and pH of estuarine waters during a high tide in winter 2002 along the axis of the Mersey Estuary.

Location	28-31 January 2002 – High Tide Salinity (gl^{-1})	Conductivity (Ms)	TDS (gl^{-1})	pH
Crosby	21.3	34.5	21.2	7.07
New Brighton	26.1	40.9	24.5	7.45
Seacombe	25.1	39.7	23.8	7.58
Marina	20.3	32.5	20.4	7.46
Bromborough	19	31.2	19.5	7.43
Liverpool Airport	6.7	14.1	8.5	7.47
Pickerings Pasture	5.7	12.6	7.6	7.27
Mersey Way	1.6	3.5	2.1	7.43
Martinscroft	0.4	0.4	0.2	7.03

B.5b. Salinity, conductivity, total dissolved solids and pH of estuarine waters during a low tide in winter 2002 along the axis of the Mersey Estuary.

Location	28-31 January 2002 – Low Tide Salinity (gl^{-1})	Conductivity (Ms)	TDS (gl^{-1})	pH
Crosby		Unavailable		
New Brighton	18.8	32.4	19.4	7.71
Seacombe	14.3	28.8	17.0	7.60
Marina		Unavailable		
Bromborough	12.6	25.2	14.7	7.69
Liverpool Airport		Unavailable		
Pickerings Pasture	0.7	1.1	0.7	7.37
Mersey Way		Unavailable		
Martinscroft	0.4	0.4	0.2	7.26

B.6a. Salinity, conductivity, total dissolved solids and pH of estuarine waters during a high tide in summer 2003 along the axis of the Mersey Estuary

Location	25-27 August 2003 – High Tide Salinity (gl^{-1})	Conductivity (Ms)	TDS (gl^{-1})	pH
Crosby	28.6	42.8	25.9	7.75
New Brighton	33.4	47.7	28.9	7.07
Seacombe	32.4	47.1	28.3	7.59
Marina		Unavailable		
Bromborough	29.1	43.0	26.1	7.60
Liverpool Airport		Unavailable		
Pickerings Pasture	16.9	29.4	17.9	7.34
Mersey Way	6.6	14.4	8.6	7.12
Martinscroft	0.5	0.6	0.4	6.99

B.6b. Salinity, conductivity, total dissolved solids and pH of estuarine waters during a low tide in summer 2003 along the axis of the Mersey Estuary.

Location	25-27 August 2003 – Low Tide Salinity (gl^{-1})	Conductivity (Ms)	TDS (gl^{-1})	pH
Crosby	26.9	42.6	26.0	-
New Brighton	29.9	43.9	26.7	-
Seacombe	27.7	42.1	25.5	-
Marina		Unavailable		
Bromborough	23.2	37.6	22.6	-
Liverpool Airport		Unavailable		
Pickerings Pasture	1.4	3.2	1.9	7.16
Mersey Way		Unavailable		
Martinscroft	0.5	0.6	0.4	7.03

B.7. Suspended sediment organic $\delta^{13}C$ and C/N of estuarine waters during low and high tides along the axis of the Mersey Estuary. Bedload estuarine sediment bulk organic $\delta^{13}C$ and C/N is also show, together with associated organic content. Many bedload sediment samples contained negligible organic matter preventing the measurement of $\delta^{13}C$ and C/N. C/N was unobtainable in all of the bedload sediment samples.

25-27 August 2003

Location	Suspended sediment				Bedload sediment		
	High Tide		Low tide		Low tide		
	$\delta^{13}C$ (‰)	C_{org}/N_{tot}	$\delta^{13}C$ (‰)	C_{org}/N_{tot}	$\delta^{13}C$ (‰)	C_{org}/N_{tot}	Organic content (%)
Crosby	-22.0	9.8	-22.8	8.7	Unavailable		0
New Brighton	-22.7	8.3	-22.8	8.6	Unavailable		0
Seacombe	-22.7	8.2	-23.2	9.6	Unavailable		0
Bromborough	-23.5	9.5	-23.7	8.5	-23.2	-	1
Pickerings Pasture	-23.6	10.0	-24.2	9.0	-22.8	-	2
Mersey Way	-24.3	10.5	Unavailable		Unavailable		-
Martinscroft	-27.2	11.3	-26.9	12.4	-27.6	-	6

Appendix C
Holocene sediment cores

C.1. Core Ince 5 lithology.

Borehole: SJ47NE81 (INCE 5)
Location: Helsby Marsh
NGR: SJ 4862 7613
Ground level: +4.33m OD
Logged by David Brew (30/06/00)

Core depth (m)	Altitude (m OD)	Lithological description
0 to 0.04	4.33 to 4.29	Core missing
0.04 to 0.27	4.29 to 4.06	Very dark greyish brown firm clayey silt
0.27 to 0.51	4.06 to 3.82	Dark yellowish brown mottled grey firm silty clay
0.51 to 0.65	3.82 to 3.68	Grey mottled dark yellowish brown firm clay
0.65 to 1.04	3.68 to 3.29	Very dark brown to black peat
1.04 to 2.07	3.29 to 2.26	Very dark brown wood peat
2.07 to 2.54	2.29 to 1.79	Very dark brown *Phragmites* peat
2.54 to 2.62	1.79 to 1.71	Very dark brown *Phragmites*-rich silty clay
2.62 to 2.86	1.71 to 1.47	Grey soft very fine sandy silt
2.86 to 3.37	1.47 to 0.96	Greyish brown soft interlaminated silt and silty clay
3.37 to 4.22	0.96 to 0.11	Dark grey soft interlaminated silt and silty clay. Occasional very fine sand partings. Laminae disturbed
4.22 to 5.07	0.11 to -0.74	Dark grey soft interlaminated silt and silty clay
5.07 to 5.09	-0.74 to -0.76	Dark grey soft clayey silt
5.09 to 5.95	-0.76 to -1.62	Very dark brown peat. Occasional wood and *Phragmites* fragments. Layer of wood between 5.42m and 5.52m
5.95 to 6.18	-1.62 to -1.85	Greyish brown gravelly fine to medium sand
6.18 to 6.34	-1.85 to -2.01	Grey firm clayey silt with occasional chalk fragments (till).
6.34 to 6.57	-2.01 to -2.24	Greyish brown medium sand
6.57 to 6.60	-2.24 to -2.27	Grey firm clayey silt (till)

C.2. Core Ince 4 lithology.

Borehole: SJ47NE80 (INCE 4)
Location: Helsby Marsh
NGR: SJ 4792 7641
Ground level: +5.42m OD
Logged by David Brew (30/06/00)

Core depth (m)	Altitude (m OD)	Lithological description
0 to 0.04	5.42 to 5.38	Core missing
0.04 to 0.59	5.38 to 4.83	Dark brown firm clayey silt. Occasional rootlets
0.59 to 0.94	4.83 to 4.48	Yellowish brown soft slightly very fine sandy silt with partings of silty clay
0.94 to 1.04	4.48 to 4.38	Yellowish brown soft very fine sand
1.04 to 1.07	4.38 to 4.35	Core missing
1.07 to 1.53	4.35 to 3.89	Yellowish brown to brown very fine sand
1.53 to 1.74	3.89 to 3.68	Dark grey soft interlaminated very fine sandy silt and silty clay
1.74 to 1.79	3.68 to 3.63	Dark grey soft clay
1.79 to 1.83	3.63 to 3.59	Very dark brown peat
1.83 to 1.89	3.59 to 3.53	Dark grey clay
1.89 to 2.43	3.53 to 2.99	Grey mottled brown soft clay
2.43 to 2.51	2.99 to 2.91	Dark brown and dark grey interlaminated peat and clay
2.51 to 2.60	2.91 to 2.82	Very dark brown peat
2.60 to 3.08	2.82 to 2.34	Very dark brown and black peat. Wood fragments throughout
3.08 to 3.24	2.34 to 2.18	Very dark brown peat. Occasional wood fragments
3.24 to 3.75	2.18 to 1.67	Grey soft clay. Occasional *Phragmites*
3.75 to 4.53	1.67 to 0.89	Dark grey soft interlaminated silt and silty clay
4.53 to 5.36	0.89 to 0.06	Dark grey soft interlaminated silt and silty clay with occasional beds of very fine sand: 4.91m to 4.95m and 5.06m to 5.12m
5.36 to 5.50	0.06 to -0.08	Dark grey soft silty clay with partings of silt
5.50 to 5.79	-0.08 to -0.37	Dark grey soft clay with occasional partings of silt towards the top.
5.79 to 6.03	-0.37 to -0.61	Black firm organic clay
6.03 to 6.36	-0.61 to -0.94	Very dark brown to black peat. Occasional wood fragments
6.36 to 6.48	-0.94 to -1.06	Very dark brown peat
6.48 to 7.07	-1.06 to -1.65	Greyish brown fine to medium sand

C.3. Core Ince 3 lithology.

Borehole: SJ47NE 79 (INCE 3)
Location: Ince Marshes
NGR: SJ 4702 7674
Ground level: +5.24m OD
Logged by David Brew (22/06/00)

Core depth (m)	Altitude (m OD)	Lithological description
0 to 0.04	5.24 to 5.20	Core missing
0.04 to 0.17	5.20 to 5.07	Disturbed ground
0.17 to 0.65	5.07 to 4.59	Dark grey into dark brown at 0.32m, into grey at 0.52m, firm silty clay
0.65 to 0.80	4.59 to 4.44	Greyish brown soft silt
0.80 to 0.92	4.44 to 4.32	Brown soft silty clay, occasional organic fragments
0.92 to 1.04	4.32 to 4.20	Grey soft clay
1.04 to 1.07	4.20 to 4.17	Core missing
1.07 to 1.16	4.17 to 4.08	Very soft clay
1.16 to 1.57	4.08 to 3.67	Yellowish brown very soft clayey silt
1.57 to 1.75	3.67 to 3.49	Grey soft clay
1.75 to 1.85	3.49 to 3.39	Very dark greyish brown organic silty clay
1.85 to 2.07	3.39 to 3.17	Black peat. Occasional wood fragments
2.07 to 2.92	3.17 to 2.32	Black to very dark brown peat. *Phragmites* fragments throughout. Occasional wood fragments.
2.92 to 2.99	2.32 to 2.25	Very dark brown peat
2.99 to 3.10	2.25 to 2.14	Grey soft silty clay. *Phragmites* throughout but more abundant towards top
3.10 to 3.66	2.14 to 1.58	Soft clayey silt
3.66 to 4.58	1.58 to 0.66	Grey soft interlaminated silt and silty clay
4.58 to 4.94	0.66 to 0.30	Grey soft clay
4.94 to 5.58	0.30 to -0.34	Grey soft interlaminated silt and silty clay
5.58 to 6.58	-0.34 to -1.34	Grey soft interlaminated silt and silty clay
6.58 to 7.58	-1.34 to -2.34	Grey soft interlaminated silt and silty clay
7.58 to 7.60	-2.34 to -2.36	Very dark greyish brown organic silty clay
7.60 to 7.83	-2.36 to -2.59	Grey soft clay with occasional *Phragmites*
7.83 to 7.87	-2.59 to -2.63	Dark grey organic clay
7.87 to 8.05	-2.63 to -2.81	Very dark brown peat. Occasional wood fragments
8.05 to 8.21	-2.81 to -2.97	Black and very dark brown peat. Occasional wood fragments

C.4. Core Ince 2 lithology.

Borehole: SJ47NE78 (INCE 2)
Location: Ince Marshes
NGR: SJ 4668 7730
Ground level: +5.08m OD
Logged by David Brew (21/06/00)

Core depth (m)	Altitude (m OD)	Lithological description
0 to 0.04	5.08 to 5.04	Core missing
0.04 to 0.36	5.04 to 4.72	Very dark greyish brown firm clayey silt. Occasional rootlets
0.36 to 0.84	4.72 to 4.24	Dark yellowish brown firm silt. Some parts are clayey
0.84 to 1.04	4.24 to 4.04	Dark yellowish brown soft slightly very fine sandy silt. Poorly laminated
1.04 to 1.07	4.04 to 4.01	Core missing
1.07 to 1.72	4.01 to 3.36	Brown soft, interlaminated silty very fine sandy silt and silty clay. Laminae of silty clay increasing in number down core (i.e. coarsening upwards)
1.72 to 1.84	3.36 to 3.24	Dark grey soft silty clay with partings of silt
1.84 to 2.58	3.24 to 2.50	Very dark grey mottled very dark greyish brown very soft silty clay with occasional partings of silt
2.58 to 2.84	2.50 to 2.24	Very dark greyish brown very soft, interbedded silty clay and silt
2.84 to 3.63	2.24 to 1.45	Very dark grey mottled very dark greyish brown very soft silty clay with occasional partings of silt
3.63 to 3.84	1.45 to 1.24	Very dark grey very soft, interbedded silty clay and very fine sand
3.84 to 3.95	1.24 to 1.13	Very dark grey very soft interlaminated silty clay and silt
3.95 to 4.28	1.13 to 0.80	Greyish brown very soft interlaminated silty clay and silt
4.28 to 4.58	0.80 to 0.50	Grey very soft clay
4.58 to 4.61	0.50 to 0.47	Very dark grey very soft organic clay
4.61 to 4.85	0.47 to 0.23	Grey soft clay. Eroded peat 'ball' between 4.74m to 4.85m
4.85 to 5.32	0.23 to -0.24	Grey very soft interlaminated silt and silty clay
5.32 to 5.61	-0.24 to -0.53	Grey very soft laminated silt
5.61 to 6.08	-0.53 to -1.00	Grey very soft silt with partings of silty clay
6.08 to 6.16	-1.00 to -1.08	Grey soft clay with occasional organic fragments
6.16 to 6.23	-1.08 to -1.15	Very dark grey muddy peat / organic mud
6.23 to 6.61	-1.15 to -1.53	Grey soft silt with occasional organic fragments
6.61 to 7.29	-1.53 to -2.21	Grey soft very fine sandy silt
7.29 to 7.61	-2.21 to -2.53	Grey soft silty very fine sand
7.61 to 8.24	-2.53 to -3.16	Grey soft laminated silty very fine sand
8.24 to 8.45	-3.16 to -3.37	Grey soft laminated silt
8.45 to 8.96	-3.37 to -3.88	Grey soft interlaminated silt and silty clay
8.96 to 9.17	-3.88 to -4.09	Grey soft silt with partings of silty clay
9.17 to 9.45	-4.09 to -4.37	Grey soupy very fine sand
9.45 to 10.45	-4.37 to -5.37	Grey soft interlaminated silt and silty clay

C.5. Core Ince 7 lithology.

Borehole: INCE 7
Location: Ince Banks
NGR: SJ 4590 7758
Ground level: +5.36m OD
Logged by Gareth Jenkins

Core depth (m)	Altitude (m OD)	Lithological description
0 to 1.40	5.36 to 3.96	Dark greyish brown silty clay with common root fragments
1.40 to 1.46	3.96 to 3.90	Clast of red sandstone
1.46 to 1.90	3.90 to 3.46	Dark greyish brown silty clay with light grey mottling. Anoxic towards base
1.90 to 1.92	3.46 to 3.44	Light grey silt
1.92 to 1.96	3.44 to 3.40	Peat with erosive top and base
1.96 to 2.12	3.40 to 3.24	Light grey silt with patches of black peaty material and moderate roots
2.12 to 3.40	3.24 to 1.96	Dark greyish brown massive silt with numerous rootlets and peat patches
3.40 to 3.70	1.96 to 1.66	Light grey silt with moderate roots and moderate black peaty patches. Roots more numerous towards base
3.70 to 4.00	1.66 to 1.36	Fibrous peat with mottled light grey clay interspersed. Occasional small woody fragments
4.00 to 4.26	1.36 to 1.10	Mottled greyish brown and light grey silt with particles of peaty material and moderate roots
4.26 to 4.44	1.10 to 0.92	Well developed fibrous peat with numerous small brown woody fragments
4.44 to 4.54	0.92 to 0.82	Silty peat
4.54 to 5.80	0.82 to -0.44	Light grey fine sandy silt with common roots and peat patches
5.80 to 5.94	-0.44 to -0.58	Well developed fibrous peat with numerous brown woody fragments
5.94 to 6.00	-0.58 to -0.64	Light grey fine sandy silt with common roots
6.00 to 6.80	-0.64 to -1.44	Light grey fine sand, wood fragments at 6.10

C.6. Core Ince 6 lithology.

Borehole: INCE 6
Location: Ince Banks
NGR: SJ 4668 7792
Ground level: +5.29m OD
Logged by Gareth Jenkins

Core depth (m)	Altitude (m OD)	Lithological description
0 to 0.76	5.29 to 4.52	Greyish brown silt with numerous roots
0.76 to 1.96	4.52 to 3.32	Greyish brown muddy silt with rare roots. Moderate black mottling (organic rich).
1.96 to 2.96	3.32 to 2.32	Greyish brown muddy silt. Numerous patches of black organic rich mud throughout bed
2.96 to 3.96	2.32 to 1.32	Greyish brown fine sandy silt with numerous black anoxic patches throughout bed
3.96 to 4.42	1.32 to 0.86	Greyish brown silty clay. Moderate black anoxic mottling
4.42 to 4.96	0.86 to 0.32	Greyish brown fine sandy silt with moderate black anoxic mottling. Rare light brown roots
4.96 to 5.56	0.32 to -0.27	Light brown medium sand. Rare thin muddy laminae towards base. Anoxic black patches towards base of bed.
5.56 to 5.66	-0.27 to -0.37	Light brown medium sand. Rare thin muddy laminae towards base. More anoxic black patches.
5.66 to 6.62	-0.37 to -1.33	Light brown medium sand.
6.62 to 8.26	-1.33 to -2.98	Light brown medium sand. Rare black mottling towards base of bed
8.26 to 8.30	-2.98 to -3.01	Dark grey anoxic fine sand

C.7. Core Ince 8 lithology.

Borehole: INCE 8
Location: Ince Banks
NGR: SJ 4758 7811
Ground level: +5.11m OD
Logged by Gareth Jenkins

Core depth (m)	Altitude (m OD)	Lithological description
0 to 0.50	5.11 to 4.60	Dark brown silty clay with iron oxide mottling. Moderate roots
0.50 to 2.78	4.60 to 2.32	Dark brown silty clay with numerous roots and black peaty patches
2.78 to 3.00	2.32 to 2.10	Dark brown fine sandy clay. Large proportion (70%) of black anoxic material
3.00 to 3.30	2.10 to 1.80	Dark brown silty clay with moderate (40%) black anoxic patches
3.30 to 3.34	1.80 to 1.76	Medium sand
3.34 to 3.60	1.76 to 1.50	Black anoxic fine sandy silt / clay
3.60 to 4.32	1.50 to 0.78	Medium brown medium sand interspersed with rare anoxic horizons (0.3mm) and black anoxic patches
4.32 to 4.36	0.78 to 0.74	Dark brown anoxic silt
4.36 to 4.56	0.74 to 0.54	Medium brown medium sand with black anoxic patches
4.56 to 4.72	0.54 to 0.38	Medium brown medium sand with anoxic horizon at top
4.72 to 4.725	0.38 to 0.375	Medium brown medium sand with anoxic silty clay
4.72 to 4.84	0.375 to 0.26	Medium brown medium sand
4.84 to 5.00	0.26 to 0.10	Medium to dark brown fine silt and sand with faint anoxic horizons
5.00 to 5.52	0.10 to –0.42	Medium brown medium sand with rusty patches and clasts of black peaty material, increasing towards base
5.52 to 5.70	-0.42 to -0.60	Medium brown medium sand with faint anoxic horizons throughout
5.70 to 6.00	-0.60 to -0.90	Medium brown medium sand interbedded with silty anoxic horizons
6.00 to 6.30	-0.90 to -1.20	Medium brown medium sand with common anoxic black staining throughout (>40%)
6.30 to 6.54	-1.20 to -1.44	Medium brown medium sand with black silty material
6.54 to 7.00	-1.44 to -1.90	Medium brown medium sand with occasional anoxic staining
7.00 to 7.30	-1.90 to -2.20	Very dark grey medium anoxic sand with occasional medium brown patches
7.30 to 7.68	-2.20 to -2.58	Yellow brown medium sand
7.68 to 7.86	-2.58 to -2.76	Dark greyish brown and yellowish brown medium sand
7.86 to 8.00	-2.76 to -2.90	Dark greyish brown and yellowish brown medium sand with silty clay layer at top of bed
8.00 to 8.56	-2.90 to -3.46	Yellowish brown medium sand with dark greyish brown silty mottling, decreasing towards base
8.56 to 9.00	-3.46 to -3.90	Dark greyish brown medium sand

Appendix D
Physical composition of cores Ince 4 and Ince 2

D.1a. Core Ince 4 sediment organic content by loss on ignition.

Core Depth (cm)	Altitude (m OD)	Crucible weight (g)	Sample + crucible (g)	Dry sample + crucible (g)	Ash + crucible (g)	Loss on ignition (g)	Loss on ignition (%)
6	5.36	15.393	16.032	16.016	15.967	0.077	7.865
13	5.29	16.005	16.716	16.610	16.559	0.072	8.430
22	5.20	15.812	16.526	16.492	16.432	0.084	8.824
29	5.13	15.484	16.173	16.056	16.024	0.046	5.594
38	5.04	16.125	16.761	16.745	16.689	0.088	9.032
45	4.97	16.182	16.786	16.664	16.635	0.048	6.017
53	4.89	16.130	16.681	16.580	16.561	0.034	4.222
61	4.81	15.373	15.944	15.941	15.929	0.021	2.113
65	4.77	14.850	15.405	15.346	15.335	0.020	2.218
73	4.69	15.677	16.283	16.206	16.198	0.013	1.512
76	4.65	15.120	16.258	16.105	16.084	0.018	2.132
89	4.53	15.076	15.910	15.834	15.817	0.020	2.243
95	4.47	15.389	15.989	15.954	15.947	0.012	1.239
97	4.45	16.055	16.811	16.773	16.767	0.008	0.836
103	4.39	14.945	15.626	15.601	15.594	0.010	1.067
110	4.32	15.416	15.982	15.980	15.973	0.012	1.241
121	4.21	16.242	16.754	16.712	16.709	0.006	0.638
126	4.16	15.862	16.494	16.493	16.488	0.008	0.792
133	4.09	15.568	16.153	16.141	16.136	0.009	0.873
142	4.00	15.431	15.960	15.959	15.952	0.013	1.326
151	3.91	15.186	15.791	15.791	15.784	0.012	1.157
155	3.87	15.931	16.557	16.556	16.546	0.016	1.600
161	3.81	15.592	16.218	16.206	16.199	0.011	1.140
169	3.73	15.189	15.908	15.893	15.884	0.013	1.278
172	3.70	15.078	15.586	15.577	15.568	0.018	1.804
177	3.65	15.358	15.897	15.882	15.854	0.052	5.344
179	3.62	15.449	16.234	15.994	15.965	0.037	5.321
181	3.60	15.373	15.881	15.626	15.571	0.109	21.739
181	3.60	15.447	15.960	15.517	15.456	0.119	87.143
183	3.58	15.212	16.025	15.725	15.660	0.080	12.671
186	3.56	14.944	15.588	15.531	15.478	0.082	9.029
192	3.50	15.233	15.758	15.744	15.717	0.051	5.284
196	3.46	15.381	16.210	15.994	15.966	0.034	4.568
202	3.40	15.314	15.903	15.758	15.743	0.025	3.378
208	3.34	15.633	16.289	16.275	16.245	0.046	4.673
216	3.26	15.102	16.285	16.041	16.008	0.028	3.514
224	3.18	15.224	15.766	15.728	15.706	0.041	4.365
232	3.10	15.501	16.502	16.224	16.196	0.028	3.873
236	3.06	15.786	16.568	16.403	16.383	0.026	3.241
241	3.01	15.797	16.377	16.353	16.285	0.117	12.230
247	2.95	15.687	16.320	16.280	16.150	0.205	21.922
252	2.90	15.044	15.688	15.334	15.271	0.098	21.724
256	2.86	15.055	15.740	15.337	15.255	0.120	29.078

D.1a continued

Core Depth (cm)	Altitude (m OD)	Crucible weight (g)	Sample + crucible (g)	Dry sample + crucible (g)	Ash + crucible (g)	Loss on ignition (g)	Loss on ignition (%)
260	2.82	15.250	15.980	15.542	15.430	0.153	38.356
269	2.73	15.518	16.125	15.633	15.537	0.158	83.478
278	2.64	15.650	16.463	15.812	15.672	0.172	86.420
286	2.56	15.666	16.243	15.777	15.680	0.168	87.387
293	2.49	15.574	16.269	15.722	15.609	0.163	76.351
295	2.47	15.752	16.312	15.868	15.772	0.171	82.759
302	2.40	14.664	15.239	14.785	14.685	0.174	82.645
308	2.34	15.739	16.286	15.850	15.757	0.170	83.784
309	2.33	15.566	16.216	15.730	15.636	0.145	57.317
313	2.29	15.126	15.657	15.234	15.149	0.160	78.704
322	2.20	15.626	16.175	15.732	15.656	0.138	71.698
323	2.19	15.372	15.907	15.495	15.418	0.144	62.602
326	2.16	14.835	15.351	15.331	15.291	0.078	8.065
333	2.09	15.597	16.293	16.058	16.027	0.045	6.725
342	2.00	15.566	16.123	16.104	16.069	0.063	6.506
353	1.89	15.493	16.097	15.935	15.912	0.038	5.204
358	1.84	15.568	16.403	16.365	16.314	0.061	6.399
366	1.76	15.403	16.132	15.924	15.899	0.034	4.798
373	1.69	15.381	15.889	15.883	15.866	0.033	3.386
377	1.65	15.652	16.287	16.192	16.174	0.028	3.333
385	1.57	15.092	15.853	15.786	15.762	0.032	3.458
393	1.49	15.521	16.195	16.190	16.179	0.016	1.644
401	1.41	15.947	17.181	16.995	16.975	0.016	1.908
409	1.33	14.820	15.398	15.394	15.373	0.036	3.659
417	1.25	15.290	16.091	15.973	15.957	0.020	2.343
425	1.17	16.036	16.656	16.648	16.623	0.040	4.085
433	1.09	15.958	16.755	16.675	16.651	0.030	3.347
441	1.01	15.175	15.843	15.838	15.821	0.025	2.564
450	0.92	14.968	15.519	15.513	15.500	0.024	2.385
455	0.87	15.052	15.638	15.555	15.539	0.027	3.181
462	0.80	15.552	16.274	16.063	16.010	0.073	10.372
471	0.71	15.907	16.567	16.566	16.550	0.024	2.428
478	0.64	15.663	16.589	16.431	16.404	0.029	3.516
487	0.55	15.717	16.382	16.378	16.370	0.012	1.210
490	0.52	16.113	16.871	16.761	16.746	0.020	2.315
494	0.48	15.394	16.241	16.172	16.161	0.013	1.414
497	0.45	15.312	16.184	16.017	15.997	0.023	2.837
499	0.43	15.055	15.654	15.544	15.531	0.022	2.658
503	0.39	15.591	16.215	16.212	16.188	0.038	3.865
507	0.35	15.983	16.631	16.595	16.589	0.009	0.980
511	0.31	15.084	16.044	15.977	15.964	0.014	1.456
513	0.29	15.502	16.268	16.107	16.084	0.030	3.802
515	0.27	15.278	16.089	15.983	15.959	0.030	3.404
519	0.23	15.046	15.727	15.722	15.713	0.013	1.331
527	0.15	15.430	16.706	16.473	16.443	0.024	2.876
533	0.09	15.520	16.089	16.085	16.071	0.025	2.478
537	0.05	14.665	15.406	15.162	15.131	0.042	6.237
542	0.000	15.356	16.125	15.931	15.912	0.025	3.304

D.1a continued

Core Depth (cm)	Altitude (m OD)	Crucible weight (g)	Sample + crucible (g)	Dry sample + crucible (g)	Ash + crucible (g)	Loss on ignition (g)	Loss on ignition (%)
546	-0.04	14.820	15.328	15.202	15.190	0.024	3.141
547	-0.05	15.897	16.770	16.531	16.504	0.031	4.259
551	-0.09	15.877	16.793	16.548	16.521	0.029	4.024
555	-0.13	15.190	15.697	15.538	15.518	0.039	5.747
565	-0.23	14.925	15.722	15.703	15.659	0.055	5.656
572	-0.30	15.655	16.575	16.272	16.238	0.037	5.511
577	-0.35	15.344	15.970	15.933	15.882	0.081	8.659
584	-0.42	15.810	16.338	16.029	15.980	0.093	22.374
584	-0.42	15.217	16.040	15.630	15.536	0.114	22.760
596	-0.54	15.393	15.994	15.617	15.548	0.115	30.804
599	-0.57	15.078	15.720	15.285	15.197	0.137	42.512
607	-0.65	15.596	16.283	15.747	15.624	0.179	81.457
611	-0.69	15.832	16.356	15.939	15.849	0.172	84.112
621	-0.79	15.110	15.759	15.258	15.134	0.191	83.784
628	-0.86	15.429	15.902	15.531	15.449	0.173	80.392
636	-0.94	15.118	15.725	15.246	15.139	0.176	83.594
637	-0.95	15.355	15.973	15.517	15.399	0.191	72.840
644	-1.02	15.342	15.901	15.496	15.396	0.179	64.935
647	-1.05	15.499	16.330	15.751	15.604	0.177	58.333
648	-1.06	15.685	16.248	15.859	15.760	0.176	56.897
661	-1.19	16.035	16.907	16.800	16.794	0.007	0.784
684	-1.42	15.947	17.049	16.880	16.867	0.012	1.393
699	-1.57	15.120	15.680	15.679	15.678	0.002	0.179
707	-1.65	14.835	15.531	15.475	15.472	0.004	0.469

D.1b. Core Ince 2 sediment organic content by loss on ignition.

Core Depth (cm)	Altitude (m OD)	Crucible weight (g)	Sample + crucible (g)	Dry sample + Crucible (g)	Ash + crucible (g)	Loss on ignition (g)	Loss on ignition (%)
15	4.93	15.483	16.463	16.273	16.220	0.054	6.709
25	4.83	14.819	15.727	15.533	15.491	0.046	5.882
30	4.78	16.129	16.819	16.655	16.623	0.046	6.084
33	4.75	14.849	15.648	15.504	15.463	0.051	6.260
37	4.71	15.675	16.500	16.379	16.357	0.027	3.125
41	4.67	15.120	15.730	15.629	15.614	0.025	2.947
45	4.63	15.075	16.079	15.949	15.933	0.016	1.831
53	4.55	15.387	16.189	16.099	16.088	0.014	1.545
61	4.47	16.052	17.230	17.045	17.023	0.019	2.216
69	4.39	14.943	15.897	15.747	15.728	0.020	2.363
77	4.31	16.240	17.076	16.928	16.915	0.016	1.890
83	4.25	15.566	16.364	16.274	16.263	0.014	1.554
86	4.22	15.590	16.192	16.150	16.141	0.015	1.607
94	4.14	15.187	15.774	15.729	15.726	0.005	0.554
108	4.00	15.447	16.993	16.709	16.691	0.012	1.426
116	3.92	15.371	16.268	16.079	16.064	0.017	2.119
124	3.84	15.211	16.113	15.944	15.918	0.029	3.547
132	3.76	15.381	16.730	16.520	16.502	0.013	1.580
140	3.68	15.313	16.442	16.244	16.230	0.012	1.504
148	3.6	15.101	16.297	16.075	16.049	0.022	2.669
156	3.52	15.501	16.847	16.584	16.557	0.020	2.493
164	3.44	15.785	16.973	16.714	16.690	0.020	2.583
171	3.37	16.179	17.375	17.088	17.043	0.038	4.950
173	3.35	15.492	16.753	16.512	16.484	0.022	2.745
177	3.31	15.751	16.763	16.491	16.460	0.031	4.189
183	3.25	15.597	16.365	16.194	16.178	0.021	2.680
189	3.19	15.289	16.119	15.828	15.803	0.030	4.638
197	3.11	15.400	17.168	16.482	16.421	0.035	5.638
205	3.03	15.551	16.566	16.206	16.168	0.037	5.802
213	2.95	15.091	15.839	15.586	15.569	0.023	3.434
221	2.87	15.956	16.554	16.349	16.329	0.033	5.089
229	2.79	15.945	17.235	16.849	16.816	0.026	3.650
237	2.71	15.662	16.479	16.257	16.240	0.021	2.857
245	2.63	16.112	17.184	16.857	16.829	0.026	3.758
253	2.55	15.393	16.152	15.891	15.864	0.036	5.422
257	2.51	15.312	16.328	15.988	15.955	0.032	4.882
259	2.49	15.055	15.653	15.478	15.464	0.023	3.310
263	2.45	15.984	16.778	16.549	16.528	0.026	3.717
271	2.37	15.083	16.161	15.868	15.833	0.032	4.459
279	2.29	15.501	16.980	16.666	16.634	0.022	2.747
283	2.25	15.276	15.929	15.790	15.781	0.014	1.751
285	2.23	15.430	16.048	15.866	15.846	0.032	4.587
293	2.15	14.665	15.438	15.201	15.176	0.032	4.664
301	2.07	15.355	16.333	16.081	16.049	0.033	4.408
309	1.99	16.034	16.896	16.628	16.598	0.035	5.051
317	1.91	15.897	16.819	16.527	16.493	0.037	5.397
325	1.83	15.876	16.954	16.621	16.583	0.035	5.101
333	1.75	15.189	16.111	15.825	15.786	0.042	6.132

D.1b continued

Core Depth (cm)	Altitude (m OD)	Crucible weight (g)	Sample + crucible (g)	Dry sample + crucible (g)	Ash + crucible (g)	Loss on ignition (g)	Loss on ignition (%)
341	1.67	15.655	16.451	16.152	16.125	0.034	5.433
349	1.59	15.217	16.459	16.092	16.052	0.032	4.571
357	1.51	14.118	15.124	14.765	14.731	0.034	5.255
362	1.46	15.947	16.859	16.623	16.604	0.021	2.811
364	1.44	14.836	15.623	15.423	15.396	0.034	4.600
372	1.36	14.589	15.207	15.112	15.102	0.016	1.912
380	1.28	13.725	14.370	14.269	14.248	0.033	3.860
385	1.23	14.529	15.690	15.346	15.308	0.033	4.651
389	1.19	14.263	15.277	15.026	14.997	0.029	3.801
394	1.14	13.940	14.845	14.648	14.629	0.021	2.684
396	1.12	15.109	15.803	15.685	15.677	0.012	1.389
400	1.08	14.562	15.537	15.359	15.346	0.013	1.631
408	1.00	14.846	15.615	15.459	15.442	0.022	2.773
416	0.92	14.894	16.027	15.742	15.713	0.026	3.420
420	0.88	15.092	15.845	15.671	15.657	0.019	2.418
427	0.81	14.304	15.134	14.984	14.965	0.023	2.794
429	0.79	13.659	14.219	14.009	13.985	0.043	6.857
433	0.75	15.192	16.368	16.024	15.988	0.031	4.327
441	0.67	13.721	14.503	14.284	14.260	0.031	4.263
449	0.59	14.908	15.870	15.580	15.549	0.032	4.613
453	0.55	13.466	14.274	14.030	14.002	0.035	4.965
457	0.51	14.349	15.124	14.870	14.840	0.039	5.758
459	0.49	15.100	15.975	15.615	15.533	0.094	15.922
461	0.47	15.688	16.234	15.981	15.916	0.119	22.184
462	0.46	15.224	16.176	15.864	15.833	0.033	4.844
466	0.42	12.876	14.351	13.911	13.866	0.031	4.348
470	0.38	14.243	15.292	14.941	14.907	0.032	4.871
472	0.36	14.788	15.826	15.481	15.440	0.039	5.916
474	0.34	16.041	17.075	16.655	16.586	0.067	11.238
476	0.32	15.579	16.484	15.844	15.702	0.157	53.585
478	0.3	15.143	15.816	15.290	15.184	0.158	72.109
480	0.28	15.430	16.211	15.742	15.660	0.105	26.282
482	0.26	15.091	16.094	15.764	15.719	0.045	6.686
484	0.24	15.192	15.970	15.807	15.785	0.028	3.577
488	0.20	13.960	15.911	15.566	15.533	0.017	2.055
498	0.10	15.051	15.723	15.588	15.568	0.030	3.724
506	0.02	14.657	16.426	16.057	16.015	0.024	3.000
514	-0.06	13.230	14.319	14.136	14.104	0.029	3.532
522	-0.14	14.724	16.163	15.863	15.833	0.021	2.634
527	-0.19	14.171	15.197	15.002	14.980	0.021	2.647
531	-0.23	14.115	15.094	14.890	14.865	0.026	3.226
533	-0.25	14.943	15.752	15.608	15.595	0.016	1.955
537	-0.29	15.089	16.284	16.033	16.007	0.022	2.754
545	-0.37	15.210	15.959	15.835	15.821	0.019	2.240
553	-0.45	14.832	15.431	15.330	15.322	0.013	1.606
560	-0.52	15.551	16.318	16.186	16.172	0.018	2.205
563	-0.55	16.111	16.991	16.823	16.810	0.015	1.826
571	-0.63	15.656	16.775	16.558	16.543	0.013	1.663

D.1b continued

Core Depth (cm)	Altitude (m OD)	Crucible weight (g)	Sample + crucible (g)	Dry sample + crucible (g)	Ash + crucible (g)	Loss on ignition (g)	Loss on ignition (%)
575	-0.67	15.946	16.570	16.449	16.441	0.013	1.590
587	-0.79	15.101	15.744	15.621	15.613	0.012	1.538
594	-0.86	16.180	16.726	16.618	16.606	0.022	2.740
602	-0.94	15.354	16.211	16.040	16.025	0.018	2.187
606	-0.98	15.393	16.335	16.134	16.113	0.022	2.834
609	-1.01	15.380	16.145	15.907	15.866	0.054	7.780
613	-1.05	15.749	16.408	16.159	16.131	0.042	6.829
615	-1.07	15.429	16.087	15.768	15.715	0.081	15.634
617	-1.09	16.241	17.025	16.550	16.457	0.119	30.097
619	-1.11	15.054	16.044	15.582	15.500	0.083	15.530
621	-1.13	15.251	15.994	15.705	15.660	0.061	9.912
624	-1.16	15.896	16.612	16.461	16.445	0.022	2.832
628	-1.20	15.218	16.423	16.154	16.125	0.024	3.098
637	-1.29	15.500	16.421	16.218	16.204	0.015	1.950
644	-1.36	15.590	17.011	16.708	16.690	0.013	1.610
652	-1.44	14.666	15.655	15.449	15.439	0.010	1.277
656	-1.48	15.055	15.614	15.507	15.502	0.009	1.106
662	-1.54	15.313	15.925	15.808	15.801	0.011	1.414
671	-1.63	15.662	16.432	16.270	16.258	0.016	1.974
679	-1.71	15.311	16.033	15.891	15.880	0.015	1.897
687	-1.79	15.955	16.993	16.760	16.743	0.016	2.112
695	-1.87	16.054	16.952	16.768	16.757	0.012	1.541
703	-1.95	15.187	15.920	15.773	15.764	0.012	1.536
712	-2.03	15.598	16.511	16.326	16.311	0.016	2.060
718	-2.10	15.120	16.233	16.018	16.002	0.014	1.782
726	-2.18	15.447	16.337	16.174	16.159	0.017	2.063
728	-2.20	15.566	16.196	16.070	16.067	0.005	0.595
731	-2.23	14.847	15.518	15.388	15.379	0.013	1.664
735	-2.27	16.035	16.580	16.477	16.471	0.011	1.357
740	-2.32	15.277	16.016	15.904	15.898	0.008	0.957
744	-2.36	15.372	15.973	15.876	15.868	0.013	1.587
757	-2.49	15.290	16.026	15.902	15.894	0.011	1.307
763	-2.55	15.075	15.684	15.570	15.561	0.015	1.818
771	-2.63	15.501	16.293	16.139	16.128	0.014	1.724
778	-2.70	15.084	15.845	15.700	15.686	0.018	2.273
787	-2.79	15.984	16.736	16.605	16.596	0.012	1.449
795	-2.87	15.403	16.223	16.065	16.054	0.013	1.662
803	-2.95	15.484	16.661	16.433	16.419	0.012	1.475
810	-3.02	14.349	15.299	15.096	15.080	0.017	2.142
818	-3.10	14.561	15.898	15.644	15.630	0.010	1.293
826	-3.18	14.893	16.726	16.340	16.317	0.013	1.589
834	-3.26	14.303	15.126	14.965	14.954	0.013	1.662
842	-3.34	14.780	15.897	15.664	15.644	0.018	2.262
846	-3.38	14.172	15.440	15.168	15.135	0.026	3.313
854	-3.46	13.930	14.986	14.765	14.749	0.015	1.916
863	-3.55	13.230	14.220	14.021	14.002	0.019	2.402
870	-3.62	14.243	14.970	14.805	14.787	0.025	3.203
878	-3.70	14.589	15.970	15.696	15.679	0.012	1.536

D.1b continued

Core Depth (cm)	Altitude (m OD)	Crucible weight (g)	Sample + crucible (g)	Dry sample + crucible (g)	Ash + crucible (g)	Loss on ignition (g)	Loss on ignition (%)
886	-3.78	13.941	15.704	15.252	15.214	0.022	2.899
894	-3.86	14.787	16.321	15.963	15.927	0.023	3.061
902	-3.94	15.191	17.477	17.008	16.967	0.018	2.256
910	-4.02	15.108	16.071	15.881	15.864	0.018	2.199
916	-4.08	14.154	14.825	14.701	14.693	0.012	1.463
918	-4.10	13.661	14.292	14.169	14.160	0.014	1.772
923	-4.15	14.909	15.672	15.541	15.528	0.017	2.057
931	-4.23	13.961	15.037	14.830	14.819	0.010	1.266
940	-4.32	13.466	14.546	14.381	14.367	0.013	1.530
944	-4.36	15.224	16.373	16.140	16.121	0.017	2.074
946	-4.38	15.190	15.963	15.864	15.849	0.019	2.226
954	-4.46	14.528	16.288	15.926	15.889	0.021	2.647
963	-4.55	13.751	14.732	14.507	14.484	0.023	3.042
970	-4.62	14.262	16.358	15.943	15.906	0.018	2.201
978	-4.70	14.577	16.878	16.362	16.299	0.027	3.529
986	-4.78	15.051	17.082	16.636	16.585	0.025	3.218
994	-4.86	15.664	17.396	16.987	16.930	0.033	4.308
1002	-4.94	15.092	16.314	16.050	16.022	0.023	2.923
1010	-5.02	14.117	16.602	16.062	16.006	0.023	2.879
1018	-5.10	14.846	16.793	16.368	16.324	0.023	2.891
1026	-5.18	13.723	15.859	15.404	15.361	0.020	2.558
1034	-5.26	14.115	15.717	15.316	15.278	0.024	3.164
1042	-5.34	14.725	16.455	16.019	15.971	0.028	3.709

D.2. Core Ince 2 particle size analysis.

		Phi										
Core Depth (cm)	Altitude (m OD)	Mean	Median	Mode	Percentile 5	25	50	75	95	Mean	Sorting	Skewness
7	5.01	4.631288	6.100855	3.632897	2.965784	4.426005	6.100855	7.925242	10.50321	6.245891	2.39697	0.127406
15	4.93	4.463708	5.962182	3.632897	2.859352	4.290251	5.962182	7.81425	10.44775	6.14299	2.403624	0.145184
25	4.83	4.999538	6.091971	3.632897	3.224317	4.514243	6.091971	7.92349	10.55653	6.279755	2.334661	0.166441
30	4.78	4.848505	5.884274	3.632897	3.143054	4.334098	5.884274	7.746074	10.51161	6.124665	2.336728	0.201858
33	4.75	4.862706	5.800676	3.632897	3.171368	4.310432	5.800676	7.68127	10.45381	6.079366	2.312518	0.225386
38	4.70	5.066125	5.925769	5.077772	3.306145	4.640974	5.925769	7.782457	10.58063	6.262552	2.267858	0.248234
42	4.66	5.124818	6.186525	5.077772	3.476338	4.856424	6.186525	7.991255	10.65312	6.490074	2.229088	0.222071
46	4.62	4.811979	5.607529	3.632897	3.176577	4.17371	5.607529	7.509767	10.39629	5.943674	2.278975	0.269658
52	4.56	4.717098	5.427867	3.632897	3.11904	4.013917	5.427867	7.418334	10.32054	5.816637	2.27724	0.302311
61	4.47	4.534161	4.994011	3.632897	3.054093	3.817054	4.994011	7.176472	10.24857	5.579121	2.267635	0.416691
69	4.39	4.48746	4.910502	3.632897	3.020926	3.784085	4.910502	7.125422	10.23983	5.536256	2.2738	0.437104
77	4.31	4.920953	5.806317	3.764346	3.23243	4.257873	5.806317	7.738351	10.50321	6.097426	2.321074	0.235517
83	4.25	4.567639	5.110293	3.632897	3.03623	3.846221	5.110293	7.228747	10.25561	5.627564	2.275691	0.376839
87	4.21	3.507173	3.415961	3.239226	2.632182	3.064917	3.415961	4.032212	8.836172	3.847265	1.511854	0.656497
109	3.99	4.140507	4.370042	3.370191	2.797864	3.374973	4.370042	6.953394	10.16338	5.199192	2.34687	0.539158
117	3.91	4.002079	4.021629	3.239226	2.752437	3.283492	4.021629	6.594225	10.0413	4.967025	2.283886	0.62644
125	3.83	5.984845	6.909548	6.654136	4.120043	5.532157	6.909548	8.492777	10.92875	7.077942	2.115917	0.148542
133	3.75	4.25044	4.818885	3.239226	2.798868	3.429731	4.818885	7.207481	10.26623	5.416584	2.400847	0.406053
141	3.67	3.983247	3.972563	3.239226	2.76415	3.284897	3.972563	6.406292	9.900901	4.888419	2.211705	0.63451
149	3.59	4.690405	5.468172	3.501606	3.054093	3.957244	5.468172	7.49668	10.41587	5.842227	2.346143	0.286054
157	3.53	4.46339	4.669694	3.632897	3.124063	3.784682	4.669694	6.669767	10.05505	5.341672	2.123986	0.511662
165	3.45	4.733891	5.198129	3.764346	3.220278	4.046206	5.198129	7.242226	10.32609	5.734723	2.225551	0.396799
171	3.37	5.264235	6.021863	4.815225	3.569008	4.69115	6.021863	7.795218	10.58505	6.33291	2.188458	0.254037
173	3.35	5.017183	5.693015	4.815225	3.37049	4.450084	5.693015	7.35532	10.11458	5.973088	2.085401	0.254371
178	3.32	5.473931	6.49981	5.077772	3.638456	5.0613	6.49981	8.190102	10.68127	6.696868	2.193857	0.159304
183	3.25	4.85517	5.853918	3.632897	3.132894	4.249616	5.853918	7.810683	10.51794	6.120163	2.36596	0.211614

D.2 continued

Core Depth (cm)	Altitude (m OD)	Phi										
					Percentile							
		Mean	Median	Mode	5	25	50	75	95	Mean	Sorting	Skewness
189	3.19	5.660543	6.457356	5.340514	3.85225	5.199189	6.457356	8.014196	10.69555	6.692608	2.074652	0.204328
197	3.11	6.2227	6.975737	6.654136	4.511279	5.811169	6.975737	8.384192	10.87358	7.161436	1.931892	0.184593
205	3.03	5.732356	6.805509	6.522178	3.916154	5.552326	6.805509	8.345667	10.86548	7.012596	2.093711	0.15884
214	2.94	5.32945	6.402626	5.077772	3.487136	4.950983	6.402626	8.059278	10.63465	6.576222	2.209176	0.1499
221	2.87	5.459259	6.416115	5.340514	3.575013	5.041684	6.416115	8.02957	10.66947	6.606675	2.173702	0.164568
230	2.78	4.933243	6.161524	5.340514	2.975964	4.547594	6.161524	7.915457	10.55436	6.260005	2.394439	0.109287
238	2.70	5.222162	6.400187	6.522178	3.277884	4.835265	6.400187	8.131478	10.70998	6.523825	2.341098	0.118048
246	2.62	5.311578	6.470089	6.522178	3.418736	4.965334	6.470089	8.116986	10.65777	6.594728	2.259171	0.118698
254	2.54	6.076311	6.844106	6.522178	4.364682	5.61458	6.844106	8.326089	10.78436	7.039877	1.973593	0.187125
257	2.51	5.585886	6.567981	5.734659	3.736773	5.259806	6.567981	8.184215	10.71968	6.789164	2.130313	0.171903
260	2.48	5.4618	6.59562	6.522178	3.468012	5.141526	6.59562	8.222054	10.69078	6.729515	2.226344	0.111335
272	2.36	4.960384	6.149185	3.501606	3.085589	4.446934	6.149185	7.94715	10.61416	6.268634	2.408243	0.128409
279	2.29	4.584847	5.350486	3.501606	2.96917	3.815022	5.350486	7.514771	10.46396	5.785014	2.406211	0.310512
283	2.25	4.771618	5.618119	3.632897	3.111539	4.06685	5.618119	7.693164	10.4907	5.982673	2.37208	0.269332
286	2.22	5.604718	6.639535	6.522178	3.678349	5.259806	6.639535	8.218182	10.66713	6.801094	2.136344	0.132525
294	2.14	5.619537	6.719528	6.522178	3.656717	5.300164	6.719528	8.293133	10.74174	6.855651	2.170125	0.114254
302	2.06	5.451031	6.711946	6.391683	3.702374	5.440342	6.711946	8.231562	10.69795	6.885901	2.099106	0.132563
310	1.98	5.484873	6.7029	6.522178	3.614757	5.292228	6.7029	8.292228	10.68839	6.841577	2.165249	0.110987
318	1.90	5.707265	6.77596	6.391683	3.949868	5.563199	6.77596	8.251209	10.70275	6.963943	2.021722	0.152094
326	1.82	5.511608	6.655153	6.522178	3.578284	5.253189	6.655153	8.206628	10.68602	6.782009	2.174103	0.110467
333	1.75	6.064676	6.925944	6.522178	4.242772	5.651088	6.925944	8.442222	10.89265	7.108195	2.042792	0.162526
341	1.67	4.122303	4.080454	3.764346	3.114035	3.6254	4.080454	4.978009	9.491738	4.630173	1.694659	0.631502
350	1.58	5.498505	6.475214	5.603314	3.61865	5.111789	6.475214	8.102639	10.63925	6.665394	2.161345	0.158091
358	1.50	5.44662	6.53952	6.522178	3.545908	5.02327	6.53952	8.215607	10.74669	6.687865	2.25344	0.132123
365	1.43	4.877897	6.097888	3.632897	3.097888	4.228368	6.097888	7.931921	10.58727	6.206115	2.415183	0.13113
373	1.35	3.813804	3.76729	3.370191	2.627716	3.240588	3.76729	6.115785	9.869522	4.775185	2.213349	0.681282

D.2 continued

Core Depth (cm)	Altitude (m OD)	Phi										
					Percentile							
		Mean	Median	Mode	5	25	50	75	95	Mean	Sorting	Skewness
381	1.27	4.016483	3.960609	3.632897	2.929061	3.451978	3.960609	5.424765	9.590606	4.694876	1.909044	0.651189
394	1.14	4.419507	4.663831	3.632897	3.051698	3.707265	4.663831	6.992908	10.20195	5.404666	2.239457	0.51484
397	1.11	3.956348	3.908767	3.370191	2.827256	3.341245	3.908767	5.662004	9.693164	4.699078	2.012685	0.647261
409	0.99	4.325106	4.642775	3.501606	2.93126	3.59231	4.642775	6.865984	10.15514	5.321702	2.256823	0.482123
416	0.92	4.588661	5.277604	3.632897	3.046921	3.853918	5.277604	7.416608	10.42179	5.748994	2.345921	0.341419
419	0.89	4.520521	5.227557	3.501606	2.956796	3.735428	5.227557	7.400918	10.4139	5.692242	2.38194	0.334665
426	0.82	4.48455	4.635943	3.764346	3.196277	3.831769	4.635943	6.538178	10.03978	5.329339	2.079542	0.539019
430	0.78	5.257597	6.360527	6.654136	3.423526	4.748554	6.360527	8.042065	10.65312	6.476009	2.284854	0.130161
442	0.68	6.262019	6.910589	6.391683	4.635943	5.781504	6.910589	8.384192	10.85475	7.155558	1.911884	0.228971
448	0.60	6.319622	6.998616	6.522178	4.665661	5.850585	6.998616	8.470089	10.89815	7.229127	1.918239	0.214434
463	0.45	5.432844	6.888541	6.785477	3.606123	5.474573	6.888541	8.335845	10.7319	6.941682	2.149239	0.057991
467	0.41	6.257597	7.023551	6.522178	4.54692	5.863966	7.023551	8.479842	10.90643	7.233106	1.942093	0.19087
487	0.21	5.039785	5.647467	4.158429	3.502587	4.335262	5.647467	7.709981	10.45786	6.113633	2.23305	0.339862
515	-0.07	4.494922	4.507009	4.027028	3.382927	3.923359	4.507009	5.818478	9.739276	5.071222	1.779299	0.582377
538	-0.30	4.602263	4.594225	4.158429	3.51837	4.046683	4.594225	5.799069	9.67536	5.104742	1.688313	0.578684
546	-0.38	4.420743	4.402626	4.027028	3.396232	3.902929	4.402626	5.355793	9.417841	4.834128	1.57904	0.575586
606	-0.98	4.494597	4.525829	4.027028	3.342854	3.924673	4.525829	6.040734	9.866826	5.171118	1.878613	0.590524
613	-1.05	6.411195	7.578146	7.048162	4.566271	6.408742	7.578146	8.828937	10.48036	7.607603	1.789401	0.003094
644	-1.36	4.545908	4.5245	4.289686	3.641694	4.116786	4.5245	5.126833	8.949288	4.711726	1.235808	0.496334
657	-1.49	4.603314	4.576217	4.289686	3.637917	4.128093	4.576217	5.321928	9.429731	4.904724	1.436321	0.55846
695	-1.87	4.514903	4.485196	4.289686	3.58554	4.050981	4.485196	5.170849	9.28411	4.764044	1.375887	0.546174
703	-1.95	4.366466	4.365277	4.158429	3.479714	3.945415	4.365277	4.95814	8.919643	4.549835	1.260956	0.495685
711	-2.03	4.505369	4.507993	4.289686	3.51837	4.037651	4.507993	5.223239	9.241571	4.767123	1.390516	0.512757
735	-2.27	4.250715	4.246601	4.027028	3.410121	3.850376	4.246601	4.789462	8.196859	4.394005	1.112796	0.467888
763	-2.55	4.103333	4.105318	3.89561	3.263958	3.727953	4.105318	4.60964	7.672414	4.224397	1.022066	0.43525
771	-2.63	4.072665	4.126077	3.89561	3.131629	3.707454	4.126077	4.710661	8.264457	4.286968	1.193324	0.451423

D.2 continued

Core Depth (cm)	Altitude (m OD)	Phi										
					Percentile							
		Mean	Median	Mode	5	25	50	75	95	Mean	Sorting	Skewness
779	-2.71	4.23596	4.244412	4.027028	3.297608	3.799671	4.244412	4.905737	8.845432	4.476151	1.323445	0.50931
787	-2.79	4.12356	4.135935	3.89561	3.221623	3.721658	4.135935	4.724325	8.008241	4.300366	1.13647	0.458932
795	-2.87	4.198394	4.206362	4.027028	3.304719	3.787468	4.206362	4.790659	8.82697	4.379086	1.259483	0.48993
803	-2.95	4.30244	4.337594	4.158429	3.369595	3.865648	4.337594	5.009263	8.430229	4.520895	1.23025	0.457025
811	-3.03	4.221354	4.227557	4.027028	3.33468	3.818885	4.227557	4.798667	8.6878	4.401033	1.229601	0.48864
819	-3.11	4.239771	4.279004	4.027028	3.307573	3.814007	4.279004	4.934566	8.297665	4.456809	1.212213	0.451505
827	-3.19	4.395018	4.39684	4.158429	3.431442	3.945638	4.39684	5.112787	9.280517	4.70413	1.435286	0.544822
835	-3.27	4.425075	4.38896	4.158429	3.475535	3.949868	4.38896	5.135935	9.273357	4.728088	1.440094	0.568887
843	-3.35	4.729292	4.781107	4.421052	3.622554	4.222431	4.781107	5.711039	9.576217	5.096772	1.529257	0.494144
855	-3.47	4.649639	4.670796	4.289686	3.546245	4.102094	4.670796	5.798266	9.703953	5.119593	1.659642	0.548982
863	-3.55	4.789462	4.845598	4.289686	3.581044	4.177882	4.845598	6.447249	10.07359	5.48858	1.914155	0.564375
871	-3.63	4.969396	5.284897	4.421052	3.5944	4.380521	5.284897	7.073393	10.27157	5.844731	2.030855	0.452815
879	-3.71	4.517875	4.497527	4.289686	3.550127	4.042873	4.497527	5.240043	9.355084	4.811463	1.432506	0.549693
887	-3.79	5.149697	5.452294	4.552326	3.726233	4.489403	5.452294	7.348251	10.36361	6.015558	2.055458	0.441154
895	-3.87	5.090496	5.32945	4.552326	3.722991	4.487783	5.32945	6.825006	10.21732	5.819921	1.9179	0.449579
903	-3.95	4.3629	4.346958	4.027028	3.367955	3.868384	4.346958	5.185999	9.213892	4.691583	1.474168	0.552162
911	-4.03	4.305004	4.246601	4.027028	3.346812	3.815834	4.246601	5.064193	9.382747	4.713324	1.56559	0.619755
917	-4.09	4.160234	4.144074	4.027028	3.309002	3.768666	4.144074	4.664562	8.644433	4.318575	1.204816	0.508558
918	-4.10	4.168512	4.149441	4.027028	3.311864	3.774577	4.149441	4.680012	8.800355	4.342448	1.24174	0.52386
923	-4.15	4.158429	4.141271	4.027028	3.311864	3.76415	4.141271	4.672635	8.714217	4.326274	1.222929	0.51803
932	-4.24	4.141271	4.150978	4.027028	3.275088	3.776355	4.150978	4.635943	8.435214	4.279665	1.146287	0.462671
940	-4.32	3.975056	3.984388	3.764346	3.035047	3.604191	3.984388	4.517214	8.082163	4.142204	1.154159	0.463866
944	-4.36	4.311864	4.296758	4.027028	3.32974	3.836501	4.296758	5.146116	9.325163	4.697073	1.53029	0.580097
947	-4.39	4.201311	4.196013	4.027028	3.265345	3.769649	4.196013	4.891964	9.150209	4.552823	1.459276	0.577578
955	-4.47	4.825824	5.070967	4.289686	3.497038	4.221085	5.070967	6.954468	10.24857	5.703818	2.058037	0.496156
963	-4.55	3.95411	4.481002	4.027028	2.668409	3.892178	4.481002	5.948753	9.84278	5.128348	1.983221	0.518225

D.2 continued

Core Depth (cm)	Altitude (m OD)	Phi										
					Percentile							
		Mean	Median	Mode	5	25	50	75	95	Mean	Sorting	Skewness
971	-4.63	4.032212	4.70275	4.289686	2.811979	4.033156	4.70275	5.996772	9.817826	5.211806	1.912192	0.454514
979	-4.71	4.811574	5.146116	4.289686	3.454348	4.216518	5.146116	7.108998	10.29676	5.76405	2.107167	0.46923
987	-4.79	5.151234	5.424765	4.683715	3.744681	4.555036	5.424765	6.92139	10.26623	5.895382	1.928377	0.430073
995	-4.87	5.115285	5.623087	4.683715	3.639175	4.58762	5.623087	7.404336	10.30952	6.08499	2.04382	0.370231
1003	-4.95	5.106312	5.24168	4.683715	3.818885	4.53483	5.24168	6.649494	10.15021	5.768799	1.836249	0.500681
1011	-5.03	4.929721	5.071937	4.552326	3.664197	4.402016	5.071937	6.661419	10.13715	5.691702	1.907335	0.533346
1019	-5.11	4.838977	4.932361	4.552326	3.665477	4.353137	4.932361	6.177099	9.916154	5.456498	1.746333	0.543237
1027	-5.19	5.175534	5.300164	4.815225	3.894107	4.625222	5.300164	6.652538	10.09394	5.814926	1.787961	0.500688
1035	-5.27	5.125321	6.02844	4.815225	3.44332	4.784682	6.02844	7.985028	10.62323	6.446698	2.218725	0.278648
1043	-5.35	5.234058	6.009728	4.815225	3.817257	4.883848	6.009728	7.713611	10.51372	6.39933	2.047602	0.314028

Appendix E
Microfossil analysis of cores Ince 4 and Ince 2

E.1a. Core Ince 4 lower peat unit pollen. Data are expressed as total pollen grains recorded at each level.

		Trees						Shrubs			Herbs										Aquatics		Pteriodophytes			
Core depth (cm)	Altitude (m OD)	Betula	Pinus	Ulmus	Quercus	Alnus	Tilia	Corylus	Salix	Ericaceae	Poaceae	Cyperaceae	Filipendula	Plantago maritima type	Armeria maritima	Saxifraga stellaris type	Lotus type	Aster type	Chenopodiaceae	Potamogeton	Typha latifolia type	Polypodium type	Equisetum	Pteridium aquilinum	Polypodiaceae	Sphagnum
580	-0.38	17	6	9	40	63	5	102	0	0	20	2	0	1	0	0	0	0	29	0	0	3	2	2	10	1
598	-0.56	20	5	16	61	80	2	106	0	0	16	0	0	0	0	1	0	0	4	0	0	0	0	0	3	0
602	-0.60	28	9	9	75	84	4	129	0	3	14	0	0	0	1	1	0	1	6	0	0	5	0	0	8	1
604	-0.62	1	1	0	0	2	0	1	0	0	0	0	0	0	0	0	0	0	0	0	0	1	2	0	0	0
608	-0.64	1	13	1	5	6	0	11	0	0	0	1	0	0	0	0	0	0	0	0	0	2	0	0	9	0
621	-0.79	2	26	0	15	75	1	10	0	0	2	14	0	0	0	0	0	1	0	1	0	7	2	6	76	0
638	-0.96	3	38	0	15	64	0	21	0	0	2	5	0	0	0	0	0	2	0	0	0	31	10	0	39	1
643	-1.01	0	80	0	0	102	0	8	3	0	1	12	7	0	0	0	11	6	0	0	1	12	0	0	74	8
648	-1.06	43	46	4	0	21	0	125	64	0	6	0	0	0	4	0	0	0	2	0	3	0	24	0	822	218

E.1b. Core Ince 4 middle peat unit pollen. Data are expressed as total pollen grains recorded at each level.

		Trees							Shrubs			Herbs												Aquatics			Pteriodophytes				
Core depth (cm)	Altitude (m OD)	Betula	Pinus	Ulmus	Quercus	Alnus	Tilia	Fraxinus	Corylus	Salix	Myrica	Poaceae	Cyperaceae	Artemisia	Plantago major/media	Plantago maritima type	Plantago coronopus	Armeria maritima	Saxifraga stellaris type	Lotus type	Lactuceae	Chenopodiaceae	Nymphaea alba type	Potamogeton	Typha latifolia type	Polypodium vulgare type	Equisetum	Pteridium aquilinum	Polypodiaceae	Sphagnum
247	+2.95	12	2	0	16	131	0	0	38	1	0	57	11	4	0	0	2	0	0	9	2	20	1	0	2	1	0	4	68	0
249	+2.93	6	0	0	23	121	0	0	30	7	0	120	0	0	0	0	0	0	1	0	0	2	0	7	0	3	0	3	47	0
251	+2.91	5	0	0	18	12	1	2	18	0	0	242	0	1	1	0	0	0	0	0	0	6	0	0	6	2	0	0	6	0
253	+2.89	84	2	1	42	80	0	3	40	0	2	43	0	3	6	4	3	1	0	0	0	15	0	0	10	4	0	8	63	1
256	+2.86	70	1	0	33	80	1	0	50	0	0	51	0	5	14	0	0	0	1	0	2	8	0	0	8	2	0	8	61	7
259	+2.83	0	0	0	0	1	0	0	3	0	0	1	0	0	0	0	0	0	0	0	0	0	0	0	0	0	0	0	1	0
309	+2.33	0	1	0	4	5	0	0	0	1	0	0	4	0	0	0	0	0	0	0	0	0	0	0	0	0	0	0	2	0
315	+2.27	3	1	0	8	9	0	2	1	2	0	5	0	0	0	0	0	0	0	0	0	0	0	0	0	3	0	0	101	0
321	+2.21	17	4	20	104	45	8	0	28	0	0	70	0	0	0	0	0	0	4	0	0	1	0	0	0	1	1	0	7	0
323	+2.19	21	25	2	46	43	9	0	28	2	2	16	0	1	0	0	0	0	0	0	0	9	0	0	0	6	1	11	18	1
327	+2.15	16	4	10	61	62	8	0	74	2	0	81	0	0	0	0	0	0	0	0	0	5	0	0	0	0	1	0	2	0

E.1c. Core Ince 4 upper peat unit pollen. Data are expressed as total pollen grains recorded at each level.

		Trees						Shrubs					Herbs															Aquatics		Pteriodophytes			
Core depth (cm)	Altitude (m OD)	Betula	Pinus	Ulmus	Quercus	Alnus	Tilia	Corylus	Salix	Myrica	Ericaceae	Calluna vulgaris	Poaceae	Cyperaceae	Artemisia	Plantago major/media	Plantago maritima type	Plantago coronopus	Saxifraga nivalis type	Saxifraga stellaris type	Silene dioica type	Aster type	Lactuceae	Chenopodiaceae	Potamogeton	Typha latifolia type	Polypodium vulgare type	Equisetum	Pteridium aquilinum	Polypodiaceae	Sphagnum
178	+3.64	26	2	0	14	101	0	63	0	0	0	5	48	4	0	0	10	0	0	2	1	7	8	13	0	2	6	1	4	31	0
180	+3.62	13	4	0	8	58	0	17	1	0	0	0	129	0	0	1	37	1	0	3	0	3	12	4	9	1	3	0	0	30	0
182	+3.60	20	3	1	74	30	1	27	4	0	6	0	59	3	0	0	5	1	10	0	0	10	29	7	11	0	1	0	5	93	10
184	+3.58	6	3	0	33	43	0	46	0	0	2	0	93	0	0	1	7	2	0	0	0	7	19	49	0	1	3	0	1	4	0
186	+3.56	16	2	0	12	39	0	25	1	1	8	0	23	0	1	5	126	3	0	0	0	6	24	23	0	0	3	0	3	5	0

E.1d. Core Ince 2 pollen. Data are expressed as total pollen grains recorded at each level.

		Trees							Shrubs	Herbs										Pteriodophytes			
Core depth (cm)	Altitude (m OD)	Betula	Pinus	Ulmus	Quercus	Alnus	Tilia	Fraxinus	Corylus	Poaceae	Cyperaceae	Plantago maritima type	Lotus type	Galium type	Lactuceae	Aster type	Chenopodiaceae	Polypodium vulgare type	Equisetum	Polypodiaceae	Sphagnum
615	-1.07	6	19	3	39	41	3	0	47	28	2	1	1	6	1	0	107	4	1	9	1
617	-1.09	4	33	1	24	33	3	0	48	28	0	0	4	10	0	1	104	11	3	9	0
621	-1.13	11	44	2	21	25	0	1	53	60	1	0	45	0	0	3	37	9	0	4	0

E.2a. Core Ince 4 principal diatom species. Data are expressed as total valves recorded at each level. Only levels with preserved diatom assemblages are shown.

Core depth (cm)	Altitude (m OD)	Total number of assigned valves	Paralia sulcata	Podosira stelligera	Thalassiosira eccentrica	Actinoptychus senarius	Cymatosira belgica	Delphineis surirella	Rhaphoneis amphiceros	Cyclotella striata	Caloneis westii	Synedra gaillonii	Diploneis didyma	Navicula crucicula	Navicula digito-radiata	Navicula peregrina	Nitzschia acuminata	Nitzschia commutata	Nitzschia navicularis	Achnanthes submarina	Rhopalodia operculata	Diploneis interrupta	Nitzschia vitrea	Navicula cari var. cincta	Fragilaria brevistriata	Fragilaria pinnata	Rhopalodia gibberula var. rupestris	Cocconeis placentula var. lineata	Gomphonema angustatum	Cymbella cymbiformis	Eunotia pectinalis var. minor	Navicula libonensis	Nitzschia recta	Pinnularia microstauron	Pinnularia obscura	Pinnularia viridis	Stauroneis phoenicenteron	Hantzschia amphioxys	Navicula pusilla	Pinnularia borealis var. brevicostata	Achnanthes flexella	Pinnularia lata var. latestriata	Pinnularia rupestris
93	4.49	210	0	0	0	2	1	6	4	3	0	0	0	0	0	25	0	13	10	0	0	24	0	0	0	0	0	0	0	0	0	0	0	0	24	1	2	0	49	16	0	0	5
169	3.73	208	25	13	1	7	0	48	55	0	25	0	0	0	0	4	0	0	7	0	0	5	0	0	0	0	0	0	0	0	0	0	0	0	0	0	0	0	2	0	0	0	0
172	3.70	195	0	0	6	0	0	59	66	18	0	0	2	7	0	0	0	0	1	0	0	7	0	0	0	0	0	0	0	0	0	0	0	0	0	0	0	0	0	0	0	0	26
177	3.65	215	11	0	9	0	3	29	9	9	0	0	1	30	0	30	28	0	3	0	0	1	11	8	0	0	0	0	0	0	0	0	0	0	0	0	6	1	0	14	0	0	
180	3.62	354	26	2	5	1	2	4	2	0	1	0	0	25	0	111	0	0	1	0	0	0	87	31	0	1	0	0	0	0	0	0	0	0	2	0	0	26	3	0	0	0	
182	3.60	274	1	0	0	0	0	0	0	0	0	0	0	0	0	44	0	0	2	0	0	22	0	0	0	0	0	0	1	0	0	0	0	10	0	75	0	44	65	1	0	0	0
184	3.58	265	4	0	0	0	0	2	0	0	0	0	0	0	0	53	0	0	5	0	0	16	0	1	0	0	0	0	0	0	0	0	0	3	0	51	0	16	73	0	0	0	0
196	3.46	319	3	1	0	1	0	0	0	0	1	0	15	0	0	173	0	0	61	0	0	49	0	0	0	0	0	0	0	0	0	0	0	0	0	0	0	0	8	0	0	0	0
232	3.10	356	15	2	1	0	0	1	1	0	0	0	2	0	0	95	0	0	8	0	0	18	0	0	0	3	0	3	0	0	0	0	0	7	0	10	0	7	88	16	0	44	0
236	3.06	324	2	0	0	0	0	1	0	0	0	0	0	0	0	103	0	0	0	0	0	14	2	0	0	1	0	0	0	0	0	0	0	0	7	10	0	8	70	12	0	63	0
250	2.92	310	44	8	1	1	1	38	77	0	27	0	0	0	59	26	0	0	7	0	0	4	0	2	0	0	0	0	0	0	0	0	0	0	0	0	0	5	2	0	0	0	
252	2.90	216	28	4	0	3	1	38	30	0	11	0	0	0	49	24	0	0	4	0	0	2	0	0	0	0	0	0	0	0	0	0	0	0	2	0	0	8	1	0	1	0	
255	2.87	201	24	5	0	7	3	66	50	0	1	0	0	0	0	13	0	0	12	0	0	9	0	0	0	1	0	0	0	0	0	0	0	0	1	0	0	3	0	0	0	0	
333	2.09	235	3	22	0	1	0	0	0	0	0	0	9	0	0	1	0	0	154	0	0	3	0	0	0	0	0	0	0	0	0	0	0	0	0	0	0	0	0	0	0	0	
355	1.87	326	18	3	0	0	3	4	2	0	1	0	0	0	2	139	0	0	8	0	0	11	12	0	0	0	0	0	3	0	0	22	0	0	0	0	0	2	23	14	0	13	0
366	1.76	317	14	3	0	0	0	1	1	0	0	0	0	0	1	95	0	0	11	0	0	85	0	1	0	0	0	1	4	0	0	0	0	0	2	12	0	1	27	14	0	20	0
385	1.57	308	67	53	11	23	27	55	34	0	0	0	0	0	0	3	0	0	8	0	0	0	0	0	0	0	0	0	0	0	0	0	0	0	0	2	0	0	0	0	0	0	0

E.2a continued

Core depth (cm)	Altitude (m OD)	Total number of assigned valves	Paralia sulcata	Podosira stelligera	Thalassiosira eccentrica	Actinoptychus senarius	Cymatosira belgica	Delphineis surirella	Rhaphoneis amphiceros	Cyclotella striata	Caloneis westii	Synedra gaillonii	Diploneis didyma	Navicula crucicula	Navicula digito-radiata	Navicula peregrina	Nitzschia acuminata	Nitzschia commutata	Nitzschia navicularis	Achnanthes submarina	Rhopalodia operculata	Diploneis interrupta	Nitzschia vitrea	Navicula cari var. cincta	Fragilaria brevistriata	Fragilaria pinnata	Rhopalodia gibberula var. rupestris	Cocconeis placentula var. lineata	Gomphonema angustatum	Cymbella cymbiformis	Eunotia pectinalis var. minor	Navicula libonensis	Nitzschia recta	Pinnularia microstauron	Pinnularia obscura	Pinnularia viridis	Stauroneis phoenicenteron	Hantzschia amphioxys	Navicula pusilla	Pinnularia borealis var. brevicostata	Achnanthes flexella	Pinnularia lata var. latestriata	Pinnularia rupestris
401	1.41	302	52	85	8	11	15	38	35	0	0	0	4	0	0	5	0	0	12	0	0	1	0	0	0	0	0	2	0	0	0	0	0	0	0	1	0	0	0	0	0	0	0
417	1.25	309	75	44	9	20	23	45	25	0	0	0	3	0	0	3	0	0	8	0	0	0	0	0	0	5	0	1	0	0	0	0	0	0	0	0	1	0	0	0	0	0	0
433	1.09	307	62	20	41	9	36	48	20	0	0	0	3	0	0	3	0	0	10	0	0	0	0	0	0	3	0	0	1	0	0	0	0	0	0	1	0	1	0	0	0	0	0
463	0.79	304	43	21	25	8	19	40	10	0	1	0	0	0	0	48	0	0	6	0	0	4	0	2	0	5	0	0	0	0	0	0	0	0	0	4	0	0	12	6	0	2	0
479	0.63	328	38	24	15	4	17	37	15	0	3	0	2	2	3	62	0	0	12	0	0	6	0	2	0	4	0	1	0	0	0	0	0	0	0	7	0	2	23	25	0	0	0
490	0.52	319	56	17	61	7	38	62	22	0	0	0	1	0	0	2	0	0	5	0	0	0	0	1	0	2	0	1	0	0	0	0	0	0	0	0	0	0	1	0	0	0	0
494	0.48	327	46	26	50	8	55	46	28	0	0	0	4	0	0	4	0	0	3	0	0	1	0	1	0	12	0	1	0	0	0	0	0	0	0	0	0	0	2	0	0	0	0
497	0.45	301	41	29	78	7	47	39	18	0	0	0	1	0	0	0	0	0	5	0	0	0	0	0	0	4	0	0	0	0	0	0	0	0	0	0	0	0	0	0	0	0	0
499	0.43	306	80	32	46	9	27	39	11	0	0	0	1	0	0	1	0	0	6	0	1	0	0	0	0	5	0	1	0	0	0	0	0	0	1	0	0	0	0	0	0	0	0
507	0.35	327	44	26	75	3	34	53	11	0	0	0	0	0	2	4	0	0	10	0	0	1	0	0	0	3	0	1	2	0	0	0	0	0	0	0	0	0	2	0	0	0	0
511	0.31	276	56	17	25	11	31	46	24	0	0	0	1	1	0	3	0	0	5	0	0	0	0	0	0	7	0	3	0	0	0	0	0	0	0	0	0	0	0	0	0	0	0
513	0.29	323	50	26	31	7	44	60	19	0	0	0	3	0	0	2	0	0	10	0	1	0	0	0	0	12	0	2	0	0	0	0	0	0	0	1	0	0	2	0	0	0	0
515	0.27	300	55	34	42	9	39	40	19	0	1	0	2	0	0	7	0	0	3	0	0	0	0	0	0	5	0	2	0	0	0	0	0	0	0	0	0	0	0	0	0	0	0
527	0.15	340	62	9	66	7	50	47	15	0	0	0	1	0	2	2	0	0	15	0	0	0	0	0	0	6	0	0	0	0	0	0	0	0	0	0	0	0	0	0	0	0	0
537	0.05	300	46	13	33	4	25	19	11	0	3	0	5	0	4	63	0	0	5	0	0	13	0	1	0	3	0	1	0	0	0	0	0	0	0	0	0	10	10	0	4	0
543	-0.01	303	30	21	76	3	53	22	18	0	0	0	1	0	1	4	0	0	6	0	1	0	0	0	0	9	0	6	0	0	0	0	0	0	0	0	0	0	0	0	0	0	0
547	-0.05	293	57	15	91	5	54	15	10	0	0	0	1	0	0	0	0	0	6	0	0	0	0	0	0	7	0	0	0	0	0	0	0	0	0	0	0	0	0	0	0	0	0
553	-0.11	306	78	27	36	10	41	39	16	0	0	0	4	0	0	0	0	0	6	0	0	0	0	0	0	2	0	1	0	0	0	0	0	0	0	0	0	0	0	0	0	0	0

E.2a continued

Core depth (cm)	Altitude (m OD)	Total number of assigned valves	Paralia sulcata	Podosira stelligera	Thalassiosira eccentrica	Actinoptychus senarius	Cymatosira belgica	Delphineis surirella	Rhaphoneis amphiceros	Cyclotella striata	Caloneis westii	Synedra gaillonii	Diploneis didyma	Navicula crucicula	Navicula digito-radiata	Navicula peregrina	Nitzschia acuminata	Nitzschia commutata	Nitzschia navicularis	Achnanthes submarina	Rhopalodia operculata	Diploneis interrupta	Nitzschia vitrea	Navicula cari var. cincta	Fragilaria brevistriata	Fragilaria pinnata	Rhopalodia gibberula var. rupestris	Cocconeis placentula var. lineata	Gomphonema angustatum	Cymbella cymbiformis	Eunotia pectinalis var. minor	Navicula libonensis	Nitzschia recta	Pinnularia microstauron	Pinnularia obscura	Pinnularia viridis	Stauroneis phoenicenteron	Hantzschia amphioxys	Navicula pusilla	Pinnularia borealis var. brevicostata	Achnanthes flexella	Pinnularia lata var. latestriata	Pinnularia rupestris
557	-0.15	302	69	20	47	8	31	31	18	0	0	0	5	0	2	6	0	0	8	0	0	3	0	0	0	4	0	0	0	0	0	0	0	1	2	0	0	0	0
582	-0.40	328	4	1	0	1	0	1	1	0	0	40	26	0	5	3	0	0	3	0	8	0	0	0	0	162	0	56	0	0	0	0	0	0	0	0	0	0	0	0	0	0	0
584	-0.42	297	8	2	0	0	0	0	1	0	0	15	28	0	6	3	1	0	6	0	5	0	1	0	8	148	0	25	0	0	0	0	0	0	0	0	0	1	0	0	0	0	0
587	-0.45	492	1	0	1	0	0	0	0	0	0	0	0	0	0	0	0	0	1	38	0	0	0	0	152	227	0	6	0	0	0	0	0	0	0	0	0	0	0	0	0	0	0
600	-0.58	1635	1	0	0	0	0	0	1	0	0	0	0	0	0	2	0	0	0	282	0	0	0	0	0	1313	0	3	0	0	0	0	0	0	0	0	0	0	0	0	0	0	0
603	-0.61	302	36	23	52	8	65	25	10	0	1	0	3	0	0	3	0	0	6	2	1	1	0	0	0	13	0	2	0	0	0	0	0	0	0	0	0	0	0	0	0	0	0
604	-0.62	2633	0	0	0	0	0	0	0	0	0	0	0	0	0	1	0	0	0	73	0	0	0	0	0	2535	0	0	0	0	0	0	0	0	0	0	0	0	0	0	0	0	0
606	-0.64	297	0	0	0	0	0	0	0	0	0	0	0	0	0	11	0	0	1	0	0	0	0	0	0	25	146	0	0	0	0	0	74	0	0	0	0	0	4	0	0	0	0
645	-1.03	128	0	0	0	0	0	0	0	0	0	0	0	0	0	0	0	0	0	0	0	0	0	0	0	9	0	1	58	13	0	0	0	0	0	15	9	7	0	0	0	0	0
647	-1.05	122	1	0	0	0	1	0	0	0	0	0	0	0	0	0	0	0	0	0	0	0	0	0	0	22	0	0	61	4	1	0	0	0	0	5	18	3	0	0	0	0	0
649	-1.07	155	0	0	0	0	1	0	0	0	0	0	0	0	0	0	0	0	0	0	0	0	0	0	0	5	0	0	90	11	15	0	0	8	0	12	3	0	0	0	0	0	0

E.2b. Core Ince 2 principal diatom species. Data are expressed as total valves recorded at each level. Only levels with preserved diatom assemblages are shown.

Core depth (cm)	Altitude (m OD)	Total number of assigned valves	Paralia sulcata	Podosira stelligera	Thalassiosira eccentrica	Actinoptychus senarius	Campylosira cymbelliformis	Cymatosira belgica	Delphineis surirella	Rhaphoneis amphiceros	Diploneis smithii	Caloneis westii	Diploneis didyma	Navicula eidrigeana	Navicula peregrina	Nitzschia navicularis	Achnanthes delicatula	Rhopalodia operculata	Diploneis interrupta	Nitzschia vitrea	Navicula cari var. cincta	Fragilaria pinnata	Gyrosigma acuminatum	Navicula cryptotenella	Pinnularia obscura	Stauroneis phoenicenteron	Hantzschia amphioxys	Navicula pusilla	Pinnularia lata var. latestriata	Pinnularia appendiculata
30	4.78	209	0	0	0	0	0	0	0	0	0	0	0	0	0	0	0	0	55	0	0	1	0	0	40	0	16	3	12	52
171	3.37	200	16	0	0	1	0	1	12	6	0	96	1	0	51	10	0	0	0	0	0	0	0	0	0	0	3	0	0	0
177	3.31	206	48	11	2	5	0	0	29	24	0	0	0	0	1	77	0	0	1	0	0	0	0	0	0	0	0	0	0	0
183	3.25	212	69	18	0	22	0	1	50	30	0	0	0	0	0	7	0	0	0	0	0	0	0	0	0	0	0	0	0	0
197	3.11	335	43	3	54	1	7	8	100	5	0	0	0	0	0	0	5	0	0	1	0	0	18	8	0	0	0	0	0	0
237	2.71	379	56	3	48	7	4	14	171	16	0	0	0	0	1	1	13	0	0	0	0	0	23	1	0	0	0	0	0	0
245	2.63	311	50	1	56	4	4	6	140	7	0	0	0	0	0	2	0	0	0	0	0	1	8	3	0	0	0	0	0	0
253	2.55	403	57	2	51	2	5	7	212	6	0	0	0	0	0	0	1	0	0	0	17	2	13	0	0	0	0	0	0	0
257	2.51	319	61	1	38	3	0	9	133	11	0	0	0	0	0	1	0	0	3	0	20	0	17	0	0	0	0	0	0	0
259	2.49	318	96	0	20	4	2	14	74	17	0	0	0	0	0	2	0	0	0	0	17	2	44	5	0	0	0	1	0	0
263	2.45	330	56	0	25	4	5	7	175	15	0	0	0	0	0	0	2	0	1	0	10	0	4	2	0	0	0	0	0	0
279	2.29	234	83	13	1	7	0	7	66	30	0	0	0	0	0	10	0	0	3	0	0	0	0	0	0	0	0	0	0	0
283	2.25	201	68	3	0	5	0	6	71	28	0	0	0	0	0	6	0	0	0	0	1	1	0	0	0	0	0	0	0	0
285	2.23	354	43	0	36	3	8	18	202	5	0	0	0	0	0	2	2	0	1	0	3	1	1	2	0	0	0	0	0	0
294	2.14	391	31	1	19	1	4	7	148	5	0	0	0	0	0	1	3	0	0	0	6	1	32	20	0	0	0	0	0	0
310	1.98	317	40	4	20	3	5	7	159	5	0	0	0	0	0	1	3	0	0	0	6	0	7	3	0	0	0	0	0	0
317	1.91	346	65	5	79	1	6	17	124	4	0	0	0	0	0	0	0	0	0	0	1	0	8	1	0	0	0	0	0	0
341	1.67	315	48	2	24	1	4	8	138	6	0	0	0	0	0	0	2	0	0	0	3	0	5	7	0	0	0	0	0	0
349	1.59	361	40	4	44	2	5	10	143	6	0	0	0	0	0	4	3	0	0	0	59	0	15	3	0	0	0	0	0	0

E.2b continued

Core depth (cm)	Altitude (m OD)	Total number of assigned valves	Paralia sulcata	Podosira stelligera	Thalassiosira eccentrica	Actinoptychus senarius	Campylosira cymbelliformis	Cymatosira belgica	Delphineis surirella	Rhaphoneis amphiceros	Diploneis smithii	Caloneis westii	Diploneis didyma	Navicula eidrigeana	Navicula peregrina	Nitzschia navicularis	Achnanthes delicatula	Rhopalodia operculata	Diploneis interrupta	*Nitzschia vitrea*	Navicula cari var. cincta	Fragilaria pinnata	Gyrosigma acuminatum	Navicula cryptotenella	Pinnularia obscura	Stauroneis phoenicenteron	Hantzschia amphioxys	Navicula pusilla	Pinnularia lata var. latestriata	Pinnularia appendiculata
357	1.51	349	22		28	0	2	9	150	5	0	0	0	0	0	1	1	0	0	0	96	0	17	0	0	0	0	0	0	0
362	1.46	329	86	7	27	10	4	15	54	15	0	0	0	0	2	4	1	0	0	0	65	1	5	1	0	0	0	0	0	0
364	1.44	298	66	4	26	5	2	10	95	23	0	0	0	0	0	2	26	0	0	0	0	0	0	1	0	3	0	0	0	0
373	1.35	339	52	1	28	3	1	17	156	7	1	0	0	0	0	0	13	0	1	0	3	2	1	2	0	0	0	0	0	0
380	1.28	311	77	3	46	7	1	20	77	25	0	0	0	0	1	1	2	0	0	0	0	1	0	1	0	0	0	0	0	0
385	1.23	333	84	5	40	10	5	20	100	14	0	1	0	0	0	1	7	0	0	0	5	0	1	1	0	0	0	0	0	0
389	1.19	357	45	1	27	3	4	14	172	19	0	0	0	0	3	1	7	0	0	0	3	1	4	0	0	0	0	0	0	0
394	1.14	234	26	2	16	3	5	9	102	9	0	0	0	0	0	0	10	0	0	0	1	0	2	0	0	0	0	0	0	0
408	1.00	201	61	5	14	4	2	1	45	27	0	4	1	0	0	15	3	0	1	1	1	1	0	1	0	0	0	0	0	0
429	0.79	306	48	2	1	1	0	1	10	9	68	2	1	0	23	37	0	0	29	1	57	0	4	2	0	0	0	0	0	0
434	0.74	315	9	14	2	1	0	0	0	1	1	7		0	2	264	0	0	12	0	0	0	0	0	0	0	0	0	0	0
452	0.56	307	25	11	0	1	0	0	14	4	1	47	2	0	19	147	0	0	29	0	0	0	0	0	0	0	0	1	0	0
457	0.51	305	40	3	0	3	0	18	15	6	0	13	0	0	74	8	0	0	13	10	66	0	0	0	0	0	0	17	0	0
462	0.46	307	10	4	4	0	1	1	6	5	29	32	1	0	29	95	0	0	77	0	6	0	0	0	0	0	1	0	0	0
467	0.41	303	15	16	4	0	0	3	10	5	19	23	3	0	10	107	0	0	77	0	1	0	1	0	0	0	0	0	0	0
471	0.37	297	15	9	4	2	0	0	7	4	19	35	2	0	22	38	0	0	122	0	3	0	0	0	0	0	0	0	0	0
474	0.34	306	17	7	7	1	0	1	25	2	10	29	0	0	12	131	0	0	36	3	9	0	0	0	0	0	0	1	0	0
499	0.09	323	49	22	30	10	3	62	44	18	1	0	0	0	1	7	1	0	0	0	21	1	1	7	0	0	1	0	0	0
515	-0.07	313	45	18	42	8	10	38	90	20	0	0	1	0	0	3	4	0	0	0	3	2	1	0	0	0	0	0	0	0
523	-0.15	210	30	8	29	4	0	64	37	11	0	0	0	0	1	2	0	0	0	0	1	1	1	3	0	0	0	0	0	0

E.2b continued

Core depth (cm)	Altitude (m OD)	Total number of assigned valves	Paralia sulcata	Podosira stelligera	Thalassiosira eccentrica	Actinoptychus senarius	Campylosira cymbelliformis	Cymatosira belgica	Delphineis surirella	Rhaphoneis amphiceros	Diploneis smithii	Caloneis westii	Diploneis didyma	Navicula eidrigeana	Navicula peregrina	Nitzschia navicularis	Achnanthes delicatula	Rhopalodia operculata	Diploneis interrupta	Nitzschia vitrea	Navicula cari var. cincta	Fragilaria pinnata	Gyrosigma acuminatum	Navicula cryptotenella	Pinnularia obscura	Stauroneis phoenicenteron	Hantzschia amphioxys	Navicula pusilla	Pinnularia lata var. latestriata	Pinnularia appendiculata
528	-0.20	249	50	8	35	10	6	37	60	10	0	0	0	0	0	1	1	0	0	0	0	1	2	1	0	0	0	0	0	0
531	-0.23	309	34	19	51	7	2	81	61	13	0	0	0	0	0	3	0	0	0	0	3	1	0	10	0	0	0	0	0	0
534	-0.26	315	36	9	49	5	7	57	95	17	0	0	0	0	0	3	3	0	0	0	0	2	0	0	0	0	0	0	0	0
538	-0.30	209	21	5	26	0	5	53	76	4	0	0	0	0	0	0	1	0	0	0	4	0	0	0	0	0	0	0	0	0
546	-0.38	306	60	14	33	5	1	66	87	14	0	0	0	0	0	1	3	0	0	0	1	2	1	2	0	0	0	0	0	0
554	-0.46	312	34	13	36	8	4	42	129	20	0	1	0	0	1	1	2	0	0	0	0	0	0	0	0	0	0	0	0	0
560	-0.52	315	40	10	32	3	8	113	75	9	0	0	0	0	0	1	3	0	0	0	0	0	0	6	0	0	0	0	0	0
563	-0.55	305	53	18	33	7	7	42	104	17	1	0	0	0	0	0	2	0	0	0	1	1	0	2	0	0	0	0	0	0
571	-0.63	318	59	31	41	7	3	28	103	20	0	1	1	0	0	1	3	0	0	0	0	2	0	0	0	0	0	1	0	0
579	-0.71	320	50	27	17	13	1	66	93	18	0	0	0	0	2	4	3	0	1	0	1	1	0	0	0	0	0	0	0	0
594	-0.86	304	51	44	38	11	4	41	60	23	0	0	3	0	1	9	0	0	0	0	1	0	1	0	0	0	0	0	0	0
606	-0.98	306	54	24	40	8	3	34	48	38	1	0	0	0	2	13	6	0	0	0	0	11	0	2	0	0	0	0	0	0
609	-1.01	210	29	26	5	7	0	4	18	7	2	1	23	0	11	14	0	1	1	0	0	26	0	0	0	0	0	0	0	0
613	-1.05	311	45	22	0	4	0	3	20	13	68	1	12	0	11	33	0	0	10	0	0	3	0	0	0	0	0	2	0	0
617	-1.09	312	15	15	41	3	1	20	37	7	23	1	11	0	31	15	5	0	13	4	3	10	0	3	0	1	0	2	0	0
619	-1.11	378	0	2	0	0	0	1	1	0	39	0	0	0	170	1	0	0	4	48	0	0	0	0	0	23	0	57	0	0
621	-1.13	332	2	11	1	0	0	0	0	0	12	0	1	0	266	4	0	0	5	10	1	1	0	0	0	5	0	0	0	0
663	-1.55	209	29	24	34	3	0	4	68	10	2	0	0	0	0	8	1	0	2	0	2	0	1	1	0	0	0	1	0	0
678	-1.70	308	94	44	1	6	0	3	49	67	0	0	2	0	0	14	1	0	3	0	0	0	0	0	0	0	0	0	0	0
686	-1.78	315	116	19	2	8	0	16	80	39	0	1	2	0	1	6	0	0	0	0	0	0	0	0	0	0	0	0	0	0

E.2b continued

Core depth (cm)	Altitude (m OD)	Total number of assigned valves	Paralia sulcata	Podosira stelligera	Thalassiosira eccentrica	Actinoptychus senarius	Campylosira cymbelliformis	Cymatosira belgica	Delphineis surirella	Rhaphoneis amphiceros	Diploneis smithii	Caloneis westii	Diploneis didyma	Navicula eidrigeana	Navicula peregrina	Nitzschia navicularis	Achnanthes delicatula	Rhopalodia operculata	Diploneis interrupta	Nitzschia vitrea	Navicula cari var. cincta	Fragilaria pinnata	Gyrosigma acuminatum	Navicula cryptotenella	Pinnularia obscura	Stauroneis phoenicenteron	Hantzschia amphioxys	Navicula pusilla	Pinnularia lata var. latestriata	Pinnularia appendiculata
695	-1.87	313	93	16	18	4	0	41	65	43	2	0	1	0	0	2	0	0	0	0	0	1	0	0	0	0	0	0	0	0
711	-2.03	304	52	12	16	6	3	36	71	69	1	0	0	0	0	10	0	0	0	0	0	0	0	0	0	0	0	0	0	0
718	-2.10	311	88	27	9	9	1	55	42	37	0	2	3	0	0	5	0	0	0	0	0	1	0	0	0	0	0	0	0	0
726	-2.18	313	79	22	4	6	3	27	70	47	0	0	3	0	2	5	5	0	0	0	0	2	0	0	0	0	0	0	0	0
728	-2.20	305	62	5	23	4	8	47	87	37	0	0	0	0	0	2	5	1	0	0	0	0	0	0	0	0	0	0	0	0
731	-2.23	310	84	25	15	8	0	29	53	46	2	0	0	0	2	5	1	0	0	0	1	1	0	0	0	0	0	0	0	0
735	-2.27	306	58	12	16	6	1	24	82	74	0	0	1	0	0	2	1	0	0	0	0	0	0	0	0	0	0	0	0	0
740	-2.32	206	31	6	5	2	1	20	68	53	0	0	0	0	1	2	3	0	0	0	0	0	0	0	0	0	0	0	0	0
744	-2.36	310	49	7	15	2	2	32	103	68	0	1	0	0	0	2	5	0	0	0	0	2	0	0	0	0	0	0	0	0
757	-2.49	322	83	10	19	3	0	34	77	41	0	0	0	0	1	10	4	0	1	0	3	2	1	0	0	0	0	0	0	0
763	-2.55	333	74	10	19	4	4	30	88	60	1	0	0	0	0	5	5	0	0	0	0	1	0	0	0	0	0	0	0	0
779	-2.71	332	75	14	12	5	4	28	88	67	0	0	1	0	0	5	5	0	0	0	0	1	0	0	0	0	0	0	0	0
795	-2.87	327	61	9	35	4	3	47	82	45	0	0	1	0	1	4	2	0	0	0	0	2	0	0	0	0	0	0	0	0
811	-3.03	355	57	10	48	3	1	41	77	61	1	0	0	0	0	5	4	0	0	0	0	0	20	0	0	0	0	0	0	0
819	-3.11	321	65	11	35	2	3	42	86	43	0	0	0	0	0	5	10	0	0	0	2	2	0	0	0	0	0	0	0	0
827	-3.19	344	70	14	33	3	2	31	103	54	0	0	0	0	0	3	4	0	0	0	0	2	0	0	0	0	0	0	0	0
835	-3.27	346	57	19	28	5	2	18	117	63	0	0	0	0	0	4	4	0	0	0	0	2	0	0	0	0	0	0	0	0
843	-3.35	320	82	12	42	3	4	24	71	34	0	0	0	0	1	3	5	0	0	0	0	0	10	0	0	0	0	0	0	0
847	-3.39	313	86	9	43	9	1	23	73	39	0	0	0	0	0	2	2	0	0	0	0	1	0	0	0	0	0	0	0	0
855	-3.47	310	57	8	72	1	6	26	89	28	0	0	1	0	0	4	0	0	0	0	1	2	0	0	0	0	0	0	0	0

E.2b continued

Core depth (cm)	Altitude (m OD)	Total number of assigned valves	Paralia sulcata	Podosira stelligera	Thalassiosira eccentrica	Actinoptychus senarius	Campylosira cymbelliformis	Cymatosira belgica	Delphineis surirella	Rhaphoneis amphiceros	Diploneis smithii	Caloneis westii	Diploneis didyma	Navicula eidrigeana	Navicula peregrina	Nitzschia navicularis	Achnanthes delicatula	Rhopalodia operculata	Diploneis interrupta	Nitzschia vitrea	Navicula cari var. cincta	Fragilaria pinnata	Gyrosigma acuminatum	Navicula cryptotenella	Pinnularia obscura	Stauroneis phoenicenteron	Hantzschia amphioxys	Navicula pusilla	Pinnularia lata var. latestriata	Pinnularia appendiculata
863	-3.55	387	56	6	72	0	7	29	148	24	0	0	0	0	2	2	6	0	0	0	2	0	2	0	0	0	0	0	0	0
879	-3.71	386	51	7	89	3	7	30	119	34	0	0	1	0	1	5	4	1	0	0	1	1	1	0	0	0	0	0	0	0
887	-3.79	382	46	14	106	1	5	32	123	12	0	0	0	0	0	3	2	0	0	0	0	2	15	0	0	0	0	0	0	0
895	-3.87	304	70	5	71	4	4	13	85	28	0	0	0	0	0	1	7	0	0	0	0	0	0	0	0	0	0	0	0	0
903	-3.95	325	39	3	64	0	15	41	102	15	1	0	0	6	0	6	6	0	0	0	0	2	0	1	0	0	0	0	0	0
911	-4.03	309	25	3	40	2	7	31	148	20	1	0	0	1	0	4	1	0	1	0	0	0	0	0	0	0	0	0	0	0
917	-4.09	305	28	5	49	0	2	30	136	34	2	0	1	0	0	1	3	0	0	0	0	0	0	0	0	0	0	0	0	0
918	-4.10	307	45	12	47	0	7	41	84	33	0	0	1	1	0	4	5	0	0	0	0	0	2	2	0	0	0	0	0	0
923	-4.15	303	24	4	59	0	2	23	117	36	2	0	0	3	0	2	10	0	0	0	0	0	4	0	0	0	0	0	0	0
932	-4.24	368	25	5	74	0	4	35	122	29	2	0	0	12	0	4	12	0	0	0	1	2	0	1	0	0	0	0	0	0
940	-4.32	331	31	6	54	0	8	43	74	25	0	0	1	20	0	1	12	0	0	0	0	0	1	2	0	0	0	0	0	0
944	-4.36	327	27	4	57	0	12	40	111	22	0	0	0	10	0	1	4	0	0	0	0	0	0	0	0	0	0	0	0	0
947	-4.39	319	41	5	72	3	8	40	88	26	0	0	0	4	1	4	5	0	0	0	0	1	1	0	0	0	0	0	0	0
955	-4.47	318	38	12	63	0	37	0	114	19	0	0	2	2	0	5	2	0	0	0	1	0	0	1	0	0	0	0	0	0
963	-5.45	305	18	4	80	0	3	25	104	13	0	0	0	13	1	2	7	0	0	0	0	2	1	0	0	0	0	0	0	0
979	-4.71	313	46	11	66	1	3	19	83	24	0	0	0	3	1	35	3	0	0	0	0	0	0	1	0	3	0	0	0	0
995	-4.87	313	46	12	72	2	7	34	78	10	0	0	0	0	0	23	0	0	0	0	0	0	3	0	0	0	0	0	0	0
1011	-5.03	363	66	10	59	3	7	47	97	23	0	0	0	0	0	8	4	0	0	0	0	1	0	0	0	0	0	1	0	0
1026	-5.18	333	48	8	60	3	4	26	136	11	0	0	0	0	0	5	1	0	0	0	2	0	2	1	0	0	0	0	0	0
1043	-5.35	342	57	11	73	2	4	31	51	22	0	0	0	1	1	36	5	0	0	0	0	1	0	1	0	1	0	1	0	0

E.3a. The relative abundance (%) of diatoms in each ecological group, defined by Vos & De Wolf (1993a), in core Ince 4. Only levels with preserved diatom assemblages are shown.

Core depth (cm)	Altitude (m OD)	Marine plankton	Marine tychoplankton	Brackish plankton	Marine/brackish epipsammon	Marine/brackish epipelon	Marine/brackish aerophilous	Marine/brackish epiphytes	Brackish/freshwater aerophilous	Brackish/freshwater plankton	Brackish/freshwater tychoplankton	Brackish/freshwater epiphytes	Freshwater epiphytes	Freshwater epipelon	Freshwater plankton
93	4.49	0.0	3.4	1.4	5.3	24.5	11.5	0.0	31.2	0.5	0.0	0.0	0.0	22.1	0.0
169	3.73	21.2	30.3	0.0	23.6	19.2	2.4	0.0	1.0	0.0	0.0	0.0	0.0	2.4	0.0
172	3.70	3.1	33.8	9.2	30.3	5.1	3.6	0.0	0.0	0.0	0.0	0.0	0.0	14.9	0.0
177	3.65	9.4	5.7	4.2	13.7	48.6	5.7	0.0	3.3	0.0	0.0	0.0	6.6	2.8	0.0
180	3.62	9.9	1.7	0.0	1.1	51.1	24.6	0.0	8.2	0.0	0.3	0.0	0.0	3.1	0.0
182	3.60	0.4	0.0	0.0	0.0	17.4	8.1	0.0	40.7	0.0	0.0	0.0	0.4	33.0	0.0
184	3.58	2.7	0.0	0.0	0.8	23.6	6.2	0.0	36.8	0.0	0.0	0.0	0.0	29.8	0.0
196	3.46	1.3	0.3	0.0	0.0	80.5	15.4	0.0	2.5	0.0	0.0	0.0	0.0	0.0	0.0
232	3.10	5.1	0.3	0.0	0.3	29.9	5.1	0.0	32.1	0.0	0.8	0.8	2.8	22.8	0.0
236	3.06	0.6	0.0	0.0	0.3	33.4	5.0	0.0	30.9	0.0	0.3	0.0	2.2	27.2	0.0
250	2.92	18.1	25.8	0.0	12.3	40.3	1.3	0.0	2.3	0.0	0.0	0.0	0.0	0.0	0.0
252	2.90	15.7	16.2	0.0	17.6	42.6	0.9	0.0	4.6	0.0	0.0	0.0	0.0	2.3	0.0
255	2.87	16.4	30.3	0.0	32.8	12.9	4.5	0.0	1.5	0.0	0.5	0.0	0.0	1.0	0.0
333	2.09	13.5	0.5	0.0	0.0	84.5	1.5	0.0	0.0	0.0	0.0	0.0	0.0	0.0	0.0
355	1.87	7.0	1.7	0.0	1.3	51.3	7.6	0.0	13.2	0.0	0.0	0.0	1.0	16.9	0.0
366	1.76	5.6	0.3	0.0	0.3	38.4	28.1	0.0	13.9	0.0	0.0	0.3	1.7	11.3	0.0
385	1.57	44.7	28.3	0.0	19.1	7.2	0.0	0.0	0.0	0.0	0.0	0.0	0.0	0.7	0.0
401	1.41	52.0	21.7	0.0	14.0	10.3	0.3	0.0	0.0	0.0	0.0	0.7	0.0	1.0	0.0
417	1.25	47.2	23.3	0.0	16.2	7.8	0.0	0.0	0.3	0.0	1.6	0.3	0.0	3.2	0.0
433	1.09	49.2	21.8	0.0	17.6	8.1	0.0	0.0	0.3	0.0	1.0	0.0	1.3	0.7	0.0
463	0.79	34.4	13.6	0.0	14.9	21.9	1.3	0.0	6.0	0.0	1.7	0.0	0.3	6.0	0.0
479	0.63	25.4	11.0	0.0	11.9	27.5	1.8	0.0	15.3	0.0	1.2	0.3	0.0	5.5	0.0
490	0.52	48.9	22.9	0.0	21.3	5.6	0.0	0.0	0.3	0.0	0.6	0.3	0.0	0.0	0.0
494	0.48	41.8	29.2	0.0	15.7	7.1	0.3	0.0	0.6	0.0	3.7	0.3	0.3	0.9	0.0
497	0.45	54.8	24.9	0.0	14.6	3.7	0.3	0.0	0.0	0.0	1.3	0.0	0.0	0.3	0.0
499	0.43	57.5	16.0	0.0	15.7	6.2	0.3	0.0	0.0	0.0	1.6	0.3	0.3	2.0	0.0
507	0.35	49.7	17.8	0.0	20.6	7.7	0.3	0.0	0.6	0.0	0.9	0.6	1.8	0.0	0.0
511	0.31	40.1	24.8	0.0	21.5	9.5	0.0	0.0	0.0	0.0	2.6	1.1	0.4	0.0	0.0
513	0.29	40.6	24.7	0.0	20.3	8.1	0.0	0.0	0.6	0.0	3.8	0.6	0.3	0.9	0.0
515	0.27	48.2	24.4	0.0	16.4	8.0	0.0	0.0	0.0	0.0	1.7	0.7	0.3	0.3	0.0
527	0.15	45.6	23.2	0.0	17.1	10.3	0.0	0.0	0.0	0.0	1.8	0.0	1.2	0.9	0.0
537	0.05	33.4	13.7	0.0	7.7	29.8	4.3	0.0	7.0	0.0	1.0	0.3	0.0	2.7	0.0
543	-0.01	48.8	26.6	0.0	10.6	8.3	0.0	0.0	0.0	0.0	3.0	2.0	0.3	0.3	0.0
547	-0.05	57.3	24.9	0.0	9.2	5.8	0.0	0.0	0.0	0.0	2.4	0.3	0.0	0.0	0.0

E.3a continued

Core depth (cm)	Altitude (m OD)	Marine plankton	Marine tychoplankton	Brackish plankton	Marine/brackish epipsammon	Marine/brackish epipelon	Marine/brackish aerophilous	Marine/brackish epiphytes	Brackish/freshwater aerophilous	Brackish/freshwater plankton	Brackish/freshwater tychoplankton	Brackish/freshwater epiphytes	Freshwater epiphytes	Freshwater epipelon	Freshwater plankton
553	-0.11	52.5	23.0	0.0	14.4	7.9	0.0	0.0	0.0	0.0	1.0	1.0	0.0	0.3	0.0
557	-0.15	51.0	20.2	0.0	11.3	12.6	1.0	0.3	1.0	0.0	1.7	0.3	0.7	0.0	0.0
582	-0.40	1.5	0.9	0.0	15.4	13.5	0.0	1.5	0.0	0.0	49.8	17.2	0.0	0.0	0.0
584	-0.42	4.5	0.3	0.0	8.6	19.5	0.3	1.7	0.3	0.0	53.4	8.6	0.0	2.7	0.0
587	-0.45	0.4	0.2	0.0	11.6	7.7	0.0	0.0	0.0	0.0	77.8	1.2	1.0	0.0	0.0
600	-0.58	0.1	0.1	0.0	17.8	1.6	0.0	0.0	0.0	0.0	80.3	0.2	0.0	0.0	0.0
603	-0.61	45.0	30.0	0.0	9.7	9.0	0.3	0.3	0.0	0.0	4.3	0.7	0.0	0.7	0.0
604	-0.62	0.0	0.0	0.0	2.8	0.9	0.0	0.0	0.0	0.0	96.4	0.0	0.0	0.0	0.0
606	-0.64	0.0	0.0	0.0	0.3	10.3	0.0	0.0	1.4	0.3	8.6	50.2	2.7	26.1	0.0
645	-1.03	0.0	0.0	0.0	1.7	0.0	0.0	0.0	7.5	0.0	7.5	0.8	59.2	23.3	0.0
647	-1.05	0.8	0.8	0.0	0.0	0.0	0.0	0.0	3.4	0.0	18.6	0.0	55.9	20.3	0.0
649	-1.07	0.0	0.7	0.0	0.0	0.0	0.0	0.0	0.0	0.0	3.3	0.0	75.8	20.3	0.0

E.3b. The relative abundance (%) of diatoms in each ecological group, defined by Vos & De Wolf (1993a), in core Ince 2. Only levels with preserved diatom assemblages are shown.

Corrected core depth (cm)	Altitude (mOD)	Marine plankton	Marine tychoplankton	Brackish plankton	Marine/brackish epipsammon	Marine/brackish epipelon	Marine/brackish aerophilous	Brackish/freshwater aerophilous	Marine/brackish epiphytes	Brackish/freshwater plankton	Brackish/freshwater tychoplankton	Brackish/freshwater epiphytes	Freshwater epiphytes	Freshwater epipelon	Freshwater plankton
30	4.78	3.0	0.0	0.0	0.0	0.0	27.4	35.3	0.0	0.0	0.5	0.5	0.0	33.3	0.0
171	3.37	8.5	4.0	0.0	6.0	80.0	0.0	1.5	0.0	0.0	0.0	0.0	0.0	0.0	0.0
177	3.31	30.1	14.1	0.0	14.1	40.3	0.5	0.0	0.0	0.0	0.0	0.0	0.5	0.5	0.0
183	3.25	45.8	25.0	0.0	23.6	5.2	0.0	0.0	0.0	0.0	0.0	0.0	0.5	0.0	0.0
197	3.11	41.0	8.2	0.0	34.4	12.1	0.3	0.0	0.0	0.0	0.0	1.0	0.3	2.6	0.0
237	2.71	29.8	11.0	0.0	49.3	9.1	0.0	0.0	0.0	0.0	0.0	0.0	0.3	0.5	0.0
245	2.63	36.6	7.2	0.0	45.8	7.5	0.0	0.0	0.0	0.0	0.7	0.7	0.3	1.3	0.0
253	2.55	29.7	5.1	0.0	54.3	10.4	0.0	0.0	0.0	0.0	0.5	0.0	0.0	0.0	0.0
257	2.51	32.9	7.7	0.0	43.1	15.0	1.0	0.0	0.0	0.0	0.0	0.0	0.0	0.3	0.0
259	2.49	37.8	11.9	0.0	24.0	23.1	0.0	0.6	0.0	0.0	1.0	0.0	0.0	1.6	0.0
263	2.45	25.7	9.5	0.0	54.4	8.6	0.3	0.3	0.0	0.0	0.0	0.3	0.3	0.6	0.0
279	2.29	47.0	20.5	0.0	31.2	1.4	0.0	0.0	0.0	0.0	0.0	0.0	0.0	0.0	0.0
283	2.25	35.5	19.4	0.0	35.8	9.0	0.0	0.0	0.0	0.0	0.5	0.0	0.0	0.0	0.0
285	2.23	23.9	10.7	0.0	59.1	5.2	0.3	0.0	0.0	0.0	0.0	0.0	0.0	0.6	0.0
294	2.14	27.7	5.8	0.0	43.8	15.6	0.0	0.3	0.0	0.0	0.3	0.3	0.6	5.8	0.0
310	1.98	25.9	7.0	0.0	53.8	10.0	0.0	0.0	0.0	0.0	0.0	1.7	0.0	1.7	0.0
317	1.91	47.0	8.3	0.0	37.2	6.5	0.0	0.0	0.0	0.0	0.0	0.6	0.0	0.3	0.0
341	1.67	30.1	7.4	0.0	48.2	7.4	0.0	0.3	0.0	0.0	0.0	2.3	2.0	2.3	0.0
349	1.59	24.4	6.7	0.0	41.4	26.4	0.0	0.0	0.0	0.0	0.0	0.0	0.0	1.1	0.0
357	1.51	14.8	4.9	0.0	44.3	35.7	0.0	0.0	0.0	0.0	0.0	0.0	0.0	0.3	0.0
362	1.46	37.5	13.8	0.0	17.2	30.5	0.0	0.0	0.0	0.0	0.6	0.0	0.0	0.3	0.0
364	1.44	35.9	13.8	0.0	42.4	3.8	0.0	0.0	0.0	0.0	0.0	0.0	0.0	3.8	0.0
373	1.35	28.6	9.2	0.0	52.3	6.2	0.3	0.3	0.0	0.0	0.9	0.3	1.2	0.6	0.0
380	1.28	42.1	17.4	3.3	26.3	5.9	0.0	0.3	0.0	0.0	0.3	1.0	1.0	2.0	0.3
385	1.23	41.8	15.2	0.0	33.7	6.5	0.0	0.0	0.0	0.0	0.0	1.5	0.6	0.3	0.3
389	1.19	22.3	12.5	0.0	52.2	10.7	0.0	0.0	0.0	0.0	0.3	1.2	0.9	0.0	0.0
394	1.14	26.1	12.8	0.0	51.4	6.4	0.0	0.5	0.0	0.0	0.0	1.4	0.9	0.5	0.0
408	1.00	40.5	17.0	0.0	24.0	15.5	1.0	0.0	0.0	0.0	0.5	0.5	0.5	0.5	0.0
429	0.79	16.7	3.6	0.0	3.3	65.7	9.8	0.0	0.3	0.0	0.0	0.0	0.0	0.7	0.0
434	0.74	8.3	1.0	0.0	0.0	87.0	3.8	0.0	0.0	0.0	0.0	0.0	0.0	0.0	0.0
452	0.56	12.4	1.6	0.0	4.6	71.3	9.4	0.3	0.0	0.0	0.0	0.3	0.0	0.0	0.0

E.3b continued

Corrected core depth (cm)	Altitude (mOD)	Marine plankton	Marine tychoplankton	Brackish plankton	Marine/brackish epipsammon	Marine/brackish epipelon	Marine/brackish aerophilous	Brackish/freshwater aerophilous	Marine/brackish epiphytes	Brackish/freshwater plankton	Brackish/freshwater tychoplankton	Brackish/freshwater epiphytes	Freshwater epiphytes	Freshwater epipelon	Freshwater plankton
457	0.51	14.1	9.2	0.0	4.9	58.7	7.5	5.6	0.0	0.0	0.0	0.0	0.0	0.0	0.0
462	0.46	6.5	2.3	0.0	2.0	63.7	25.2	0.3	0.0	0.0	0.0	0.0	0.0	0.0	0.0
467	0.41	12.6	4.3	0.0	3.3	54.3	25.5	0.0	0.0	0.0	0.0	0.0	0.0	0.0	0.0
471	0.37	10.9	3.1	0.0	2.4	42.2	41.5	0.0	0.0	0.0	0.0	0.0	0.0	0.0	0.0
474	0.34	10.9	1.7	0.0	8.6	64.9	12.9	0.7	0.0	0.0	0.0	0.3	0.0	0.0	0.0
499	0.09	36.1	30.7	0.0	14.6	15.2	0.0	0.3	0.3	0.0	0.3	0.3	0.0	2.2	0.0
515	-0.07	36.5	25.4	0.0	32.2	4.2	0.0	0.3	0.0	0.0	0.7	0.7	0.0	0.0	0.0
523	-0.15	35.6	28.5	0.0	18.0	5.4	0.0	0.5	0.0	0.0	0.5	0.0	0.0	1.5	0.0
528	-0.20	40.7	25.9	0.0	28.4	4.1	0.0	0.0	0.0	0.0	0.4	0.0	0.0	0.4	0.0
531	-0.23	36.3	34.0	0.0	21.5	3.6	0.0	0.7	0.0	0.0	0.7	0.0	0.0	3.3	0.0
534	-0.26	34.2	29.8	0.0	33.2	2.0	0.0	0.0	0.0	0.0	0.7	1.0	0.0	0.0	0.0
538	-0.30	27.3	30.7	0.0	38.0	3.9	0.0	0.0	0.0	0.0	0.0	0.0	0.0	0.0	0.0
546	-0.38	37.7	28.5	0.0	29.8	2.3	0.0	0.0	0.0	0.0	0.7	0.3	0.0	0.7	0.0
554	-0.46	29.3	24.1	0.0	42.7	3.3	0.0	0.3	0.0	0.0	0.0	0.3	0.0	0.0	0.0
560	-0.52	26.8	42.8	0.0	24.9	3.5	0.0	0.0	0.0	0.0	0.0	0.0	0.0	1.9	0.0
563	-0.55	35.2	24.3	0.0	35.2	3.9	0.0	0.0	0.0	0.0	0.3	0.0	0.3	0.7	0.0
571	-0.63	42.5	18.4	0.0	34.0	3.8	0.0	0.3	0.0	0.0	0.6	0.0	0.3	0.0	0.0
579	-0.71	32.5	30.9	0.0	30.6	5.0	0.3	0.0	0.0	0.0	0.6	0.0	0.0	0.0	0.0
594	-0.86	46.0	26.5	0.0	20.2	6.6	0.0	0.3	0.0	0.0	0.0	0.0	0.0	0.3	0.0
606	-0.98	40.2	27.1	2.0	18.6	7.5	0.0	0.0	0.0	0.0	3.6	0.0	0.3	0.7	0.0
609	-1.01	32.2	8.8	0.0	14.6	29.8	0.5	0.0	1.5	0.0	12.7	0.0	0.0	0.0	0.0
613	-1.05	24.3	7.0	0.0	6.7	55.7	3.3	0.7	1.0	0.0	1.0	0.3	0.0	0.0	0.0
617	-1.09	25.9	10.8	0.0	14.1	31.8	5.6	0.7	0.0	1.0	3.3	0.3	0.0	6.6	0.0
619	-1.11	0.8	0.3	0.0	2.9	56.1	13.8	18.8	0.0	0.0	0.0	0.0	0.0	7.4	0.0
621	-1.13	4.2	0.0	0.0	0.0	86.4	4.5	1.8	0.0	0.3	0.3	0.0	0.0	2.4	0.0
663	-1.55	44.7	9.7	0.0	35.0	8.7	1.0	0.5	0.0	0.0	0.0	0.0	0.0	0.5	0.0
678	-1.70	48.0	26.5	0.0	16.6	7.6	1.0	0.3	0.0	0.0	0.0	0.3	0.0	0.0	0.0
686	-1.78	47.9	20.7	0.0	25.9	5.2	0.0	0.0	0.0	0.0	0.0	0.3	0.0	0.0	0.0
695	-1.87	44.1	28.8	0.0	21.6	5.2	0.0	0.0	0.0	0.0	0.3	0.0	0.0	0.0	0.0
711	-2.03	28.8	37.7	1.3	23.8	7.3	0.0	0.0	0.0	0.0	0.0	0.3	0.3	0.3	0.0
718	-2.10	43.6	34.7	0.0	14.9	6.3	0.0	0.0	0.0	0.0	0.3	0.3	0.0	0.0	0.0
726	-2.18	39.6	29.4	0.0	25.1	5.0	0.0	0.0	0.3	0.0	0.7	0.0	0.0	0.0	0.0
728	-2.20	31.1	31.8	0.0	31.1	5.4	0.0	0.0	0.0	0.0	0.0	0.0	0.3	0.0	0.0
731	-2.23	43.3	27.2	0.0	18.7	9.5	0.0	0.0	1.0	0.0	0.3	0.0	0.0	0.0	0.0
735	-2.27	30.9	34.9	0.0	28.6	5.0	0.0	0.3	0.3	0.0	0.0	0.0	0.0	0.0	0.0
740	-2.32	22.8	37.6	0.0	35.1	4.0	0.0	0.0	0.0	0.0	0.0	0.5	0.0	0.0	0.0

E.3b continued

Corrected core depth (cm)	Altitude (mOD)	Marine plankton	Marine tychoplankton	Brackish plankton	Marine/brackish epipsammon	Marine/brackish epipelon	Marine/brackish aerophilous	Brackish/freshwater aerophilous	Marine/brackish epiphytes	Brackish/freshwater plankton	Brackish/freshwater tychoplankton	Brackish/freshwater epiphytes	Freshwater epiphytes	Freshwater epipelon	Freshwater plankton
744	-2.36	26.3	34.2	0.0	25.9	3.0	0.0	0.0	0.0	0.0	0.7	0.0	0.0	0.0	0.0
757	-2.49	39.4	25.1	0.0	26.1	7.6	0.3	0.3	0.0	0.0	0.6	0.0	0.0	0.0	0.0
763	-2.55	35.2	30.6	0.0	29.3	4.6	0.0	0.0	0.0	0.0	0.3	0.0	0.0	0.0	0.0
779	-2.71	35.1	32.0	0.0	28.9	3.7	0.0	0.0	0.0	0.0	0.3	0.0	0.0	0.0	0.0
795	-2.87	36.1	31.0	0.0	26.6	5.6	0.0	0.0	0.0	0.0	0.6	0.0	0.0	0.0	0.0
811	-3.03	34.9	30.6	0.0	23.1	10.9	0.0	0.0	0.0	0.0	0.0	0.6	0.0	0.0	0.0
819	-3.11	36.1	28.5	0.0	30.4	4.1	0.0	0.0	0.0	0.0	0.6	0.3	0.0	0.0	0.0
827	-3.19	36.8	27.0	0.0	32.3	3.0	0.0	0.0	0.3	0.0	0.6	0.0	0.0	0.0	0.0
835	-3.27	33.5	26.2	0.0	36.5	2.9	0.0	0.0	0.0	0.3	0.6	0.0	0.0	0.0	0.0
843	-3.35	46.7	20.6	0.0	24.1	7.0	0.0	0.0	0.3	0.0	0.0	1.0	0.0	0.3	0.0
847	-3.39	46.9	23.8	0.0	25.7	2.9	0.0	0.0	0.0	0.0	0.3	0.3	0.0	0.0	0.0
855	-3.47	45.3	20.1	0.0	29.1	4.2	0.0	0.0	0.0	0.0	0.6	0.3	0.3	0.0	0.0
863	-3.55	37.8	16.0	0.0	40.4	4.7	0.0	0.3	0.0	0.3	0.0	0.5	0.0	0.0	0.0
879	-3.71	40.6	19.9	0.0	33.8	4.7	0.0	0.0	0.3	0.0	0.5	0.3	0.0	0.0	0.0
887	-3.79	44.9	13.2	0.0	33.8	7.1	0.0	0.0	0.0	0.3	0.5	0.3	0.0	0.0	0.0
895	-3.87	49.7	16.1	0.0	30.3	2.3	0.0	0.0	0.0	0.3	0.0	1.3	0.0	0.0	0.0
903	-3.95	35.5	22.1	0.0	34.6	5.0	0.0	0.0	0.0	0.0	0.6	0.3	0.9	0.9	0.0
911	-4.03	24.3	20.3	0.0	49.2	4.3	0.3	0.3	0.3	0.3	0.0	0.7	0.0	0.0	0.0
917	-4.09	28.1	22.2	0.0	46.4	2.6	0.0	0.0	0.0	0.0	0.0	0.3	0.0	0.3	0.0
918	-4.10	36.0	28.1	0.0	30.0	5.3	0.0	0.0	0.0	0.0	0.0	0.0	0.0	0.7	0.0
923	-4.15	29.6	20.6	0.0	43.2	6.3	0.0	0.0	0.3	0.0	0.0	0.0	0.0	0.0	0.0
932	-4.24	29.2	18.8	0.0	37.6	11.4	0.0	0.0	0.0	0.3	0.5	1.9	0.0	0.3	0.0
940	-4.32	29.5	23.4	0.0	37.7	12.3	0.0	2.2	0.0	0.0	0.0	2.8	0.6	1.5	0.0
944	-4.36	29.6	24.3	0.0	36.8	5.3	0.0	0.0	0.0	0.3	0.0	2.8	0.9	0.0	0.0
947	-4.39	39.5	24.8	0.0	29.9	4.5	0.0	0.0	0.0	0.0	0.3	0.6	0.0	0.0	0.3
955	-4.47	38.0	18.2	0.0	37.4	4.5	0.0	0.0	0.3	0.0	0.0	1.3	0.0	0.3	0.0
963	-5.45	34.7	13.5	0.0	38.0	11.6	0.0	0.0	0.0	0.3	0.7	1.0	0.3	0.0	0.0
979	-4.71	39.6	15.0	0.0	27.5	16.3	0.0	0.0	0.0	0.0	0.0	0.3	0.0	1.3	0.0
995	-4.87	44.2	17.2	0.0	25.6	10.4	0.0	0.3	0.0	0.0	0.0	0.3	1.9	0.0	0.0
1011	-5.03	39.8	22.6	0.0	31.5	5.0	0.0	0.6	0.0	0.0	0.3	0.0	0.3	0.0	0.0
1026	-5.18	39.1	13.5	0.0	42.8	4.0	0.0	0.0	0.0	0.0	0.0	0.3	0.0	0.3	0.0
1043	-5.35	44.2	18.0	0.0	17.7	17.7	0.0	0.3	0.0	0.0	0.3	0.3	0.9	0.6	0.0

Appendix F
$\delta^{13}C$ and C/N composition of cores Ince 4 and Ince 2

F.1a. Core Ince 4 $\delta^{13}C$ ratios, organic carbon content, total nitrogen content and C/N ratios.

Core Depth (cm)	Altitude (m OD)	$\delta^{13}C$ (‰)	$\%C_{organic}$	$\%N_{total}$	C_{org}/N_{tot}
6	5.36	-26.3	2.3	0.3	7.5
13	5.29	-26.3	2.2	0.2	9.9
22	5.20	-26.2	2.6	0.3	8.6
29	5.13	-25.3	1.7	0.2	9.9
38	5.04	-25.9	2.9	0.3	10.6
45	4.97	-25.9	1.6	0.2	8.5
53	4.89	-25.6	0.9	0.1	7.9
57	4.85	-25.2	1.0	0.1	8.3
61	4.81	-25.4	0.5	0.1	9.2
65	4.77	-25.1	0.3	0.0	7.2
73	4.69	-25.5	0.2	0.0	7.2
77	4.65	-25.1	0.4	0.0	7.7
89	4.53	-24.8	0.2	0.0	7.3
93	4.49	-25.3	0.4	0.0	8.6
95	4.47	-25.2	0.1	0.0	7.2
97	4.45	-25.2	0.2	0.0	7.5
103	4.39	-26.5	0.1	0.0	6.4
110	4.32	na	0.1	0.0	7.2
121	4.21	-25.1	0.1	0.0	7.4
126	4.16	na	0.1	0.0	4.5
133	4.09	na	0.1	0.0	6.2
142	4.00	-25.2	0.2	0.0	7.6
151	3.91	-25.3	0.2	0.0	11.5
155	3.87	-24.6	0.5	0.0	14.0
161	3.81	-25.3	0.4	0.0	9.5
169	3.73	-25.1	0.3	0.0	9.1
172	3.70	-24.9	0.6	0.0	13.7
177	3.65	-26.0	1.9	0.2	10.9
180	3.62	-27.7	5.9	0.6	10.3
182	3.61	-28.9	7.7	0.7	11.7
184	3.59	-28.9	6.3	0.5	12.2
186	3.56	-27.8	2.4	0.2	11.5
192	3.50	-27.5	1.5	0.2	9.3
197	3.45	-27.8	1.5	0.1	10.7
202	3.40	-25.8	0.7	0.1	7.3
208	3.34	-25.0	0.6	0.1	5.9
216	3.26	-24.6	0.5	0.1	7.9
224	3.18	-24.8	0.7	8.0	9.1
232	3.10	-25.2	0.7	0.1	8.1

F.1a continued

Core Depth (cm)	Altitude (m OD)	$\delta^{13}C$ (‰)	$\%C_{organic}$	$\%N_{total}$	C_{org}/N_{tot}
236	3.06	-26.5	1.2	0.1	10.1
241	3.01	-28.4	5.7	0.5	12.6
247	2.95	-28.6	7.5	0.5	15.6
252	2.90	-28.6	19.4	1.2	16.2
256	2.86	-28.7	18.0	1.1	16.9
260	2.82	-28.3	23.7	1.2	19.7
263	2.79	-29.1	53.9	2.5	21.7
269	2.73	-28.6	51.1	2.4	20.9
278	2.64	-29.2	54.0	2.5	21.2
286	2.57	-28.3	54.8	1.4	38.9
293	2.49	-28.7	51.6	2.8	18.4
295	2.47	-28.2	na	na	na
301	2.53	-28.3	52.9	2.5	21.5
308	2.47	-29.0	51.7	3.0	17.2
309	2.45	-29.3	27.8	1.3	22.0
322	2.32	-26.6	43.9	2.0	22.0
323	2.31	-26.5	42.5	1.8	23.0
333	2.09	-25.6	2.0	0.2	11.4
336	2.06	-25.6	2.3	0.2	11.6
342	2.00	-25.6	1.4	0.1	10.0
355	1.87	-25.4	1.4	0.1	9.6
360	1.82	-25.2	1.4	0.2	8.9
366	1.76	-25.4	1.1	0.1	9.7
373	1.69	-25.3	0.9	0.1	10.7
377	1.65	-25.8	0.7	0.1	10.7
385	1.57	-25.4	0.4	0.0	10.6
393	1.49	-26.0	0.7	0.1	9.7
401	1.41	-25.2	0.5	0.0	10.4
409	1.33	-25.4	0.6	0.1	12.0
417	1.25	-25.3	0.5	0.0	10.6
425	1.17	-25.2	0.7	0.1	11.5
433	1.09	-25.4	0.4	0.0	11.5
441	1.01	-25.5	0.7	0.1	12.2
450	0.92	na	0.8	0.1	16.5
455	0.87	-27.6	3.0	0.2	16.4
462	0.80	-27.9	2.0	0.1	16.0
471	0.71	-25.5	0.7	0.1	14.9
478	0.64	-27.3	1.0	0.1	13.5
487	0.55	-25.4	0.4	0.1	7.0
490	0.52	-25.2	0.4	0.0	10.3
494	0.48	-25.5	0.3	0.0	10.4
497	0.45	-25.4	0.8	0.1	10.6
499	0.43	-25.6	0.6	0.1	9.9
503	0.39	-25.5	0.6	0.1	13.0
507	0.35	-25.1	0.1	0.0	7.6

F.1a continued

Core Depth (cm)	Altitude (m OD)	$\delta^{13}C$ (‰)	$\%C_{organic}$	$\%N_{total}$	C_{org}/N_{tot}
511	0.31	-25.4	0.2	0.0	10.6
513	0.29	-25.6	0.9	0.1	10.8
515	0.27	-25.5	0.5	0.0	10.3
519	0.23	-25.8	0.6	0.1	11.9
527	0.15	-25.6	0.6	0.1	10.9
533	0.09	-26.0	0.9	0.1	14.1
537	0.05	-28.0	2.2	0.1	15.8
542	0.00	-26.8	1.2	0.1	12.3
546	-0.04	-26.9	1.1	0.1	12.4
549	-0.07	-26.1	0.8	0.1	13.7
552	-0.10	-26.4	1.2	0.1	11.2
556	-0.14	-26.4	1.3	0.1	11.8
565	-0.23	-26.2	1.4	0.2	8.5
572	-0.30	-26.6	1.7	0.2	10.8
577	-0.35	-26.7	2.7	0.3	10.5
581	-0.39	-27.7	11.9	0.8	15.0
584	-0.42	-28.3	13.0	1.0	13.1
595	-0.50	-29.3	14.3	1.1	13.5
596	-0.54	-29.6	12.6	0.9	14.0
599	-0.57	-29.5	22.1	1.6	13.8
602	-0.60	-29.2	28.8	1.9	15.0
607	-0.65	-27.2	41.5	1.6	25.4
611	-0.69	-28.1	51.5	2.3	22.0
621	-0.79	-28.6	51.3	2.5	20.2
628	-0.86	-28.6	51.3	2.5	20.9
636	-0.94	-27.6	51.9	1.8	28.5
637	-0.95	-28.3	46.9	2.5	18.9
644	-1.02	-27.9	39.7	2.1	19.3
645	-1.03	-29.1	46.0	2.6	17.6
647	-1.05	-28.0	33.3	1.7	19.5
648	-1.06	-29.1	38.7	1.5	25.2
651	-1.09	-28.9	0.4	0.0	18.1
661	-1.19	na	0.1	0.0	7.8
670	-1.28	-27.0	0.9	0.1	10.6
684	-1.42	na	0.1	0.0	3.7
699	-1.57	-25.0	0.5	0.0	16.5
707	-1.65	na	0.0	0.0	3.2

F.1b. Core Ince 2 $\delta^{13}C$ ratios, organic carbon content, total nitrogen content and C/N ratios.

Core depth (cm)	Altitude (m OD)	$\delta^{13}C$ (‰)	$\%C_{organic}$	$\%N_{total}$	C_{org}/N_{tot}
15	4.93	-27.6	2.9	0.3	11.3
25	4.83	-25.4	6.4	0.3	19.6
30	4.78	-27.1	2.7	0.2	11.4
33	4.75	-27.3	3.0	0.2	12.0
37	4.71	-25.6	0.7	0.1	8.6
41	4.67	-25.1	0.7	0.1	8.3
45	4.63	-25.3	0.4	0.1	7.1
53	4.55	-24.9	0.3	0.0	7.2
69	4.39	-24.3	0.4	0.0	8.0
77	4.31	-24.2	0.4	0.1	7.7
83	4.25	-24.1	0.3	0.0	8.5
86	4.28	-24.4	0.2	0.0	7.8
94	4.20	-24.2	0.1	0.0	7.9
108	4.06	-24.3	0.3	0.0	9.0
124	3.90	-24.5	0.5	0.1	9.5
140	3.68	-25.0	0.4	0.0	9.5
156	3.52	-24.5	0.4	0.1	8.9
164	3.44	-24.9	0.7	0.1	8.8
171	3.37	-25.2	1.1	0.1	8.9
173	3.35	-24.8	0.7	0.1	8.7
177	3.31	-24.7	0.8	0.1	8.2
183	3.25	-25.1	0.7	0.1	8.4
189	3.19	-25.5	1.3	0.1	9.8
197	3.11	-25.1	1.5	0.2	9.4
205	3.03	-25.2	1.4	0.2	9.4
213	2.95	-25.2	1.4	0.1	9.3
221	2.87	-25.4	1.3	0.1	9.6
229	2.79	-25.5	1.2	0.1	9.7
237	2.71	-25.5	1.2	0.1	10.4
245	2.63	-26.0	1.6	0.1	10.6
253	2.55	-25.3	1.6	0.2	9.8
257	2.51	-25.5	1.5	0.1	10.4
259	2.49	-25.1	1.2	0.1	9.7
263	2.45	-25.1	1.3	0.1	9.6
271	2.37	-25.3	1.1	0.1	9.4
279	2.29	-24.5	0.5	0.1	8.7
283	2.25	-24.5	0.6	0.1	8.3
285	2.23	-25.5	1.5	0.1	10.4
293	2.14	-25.6	1.5	0.1	10.7
309	1.98	-25.4	1.4	0.1	10.2
317	1.91	-25.1	1.6	0.2	8.7
333	1.75	-25.1	1.4	0.2	8.3
341	1.67	-25.5	1.6	0.2	9.6
357	1.51	-25.3	1.2	0.1	9.5

F.1b continued

Core depth (cm)	Altitude (m OD)	$\delta^{13}C$ (‰)	$\%C_{organic}$	$\%N_{total}$	C_{org}/N_{tot}
362	1.46	-25.1	1.3	0.2	8.6
364	1.44	-25.1	1.1	0.1	9.6
372	1.35	-24.8	0.6	0.0	13.3
380	1.28	-25.1	0.5	0.0	10.4
385	1.23	-25.2	1.1	0.1	9.9
389	1.19	-25.3	0.9	0.1	10.0
394	1.14	-25.3	0.6	0.1	9.6
396	1.12	-24.6	0.4	0.0	9.5
400	1.07	-25.0	0.3	0.0	8.4
408	1.00	-25.2	0.4	0.1	8.0
420	0.88	-25.0	0.5	0.1	8.5
427	0.81	-24.2	0.4	0.0	8.6
429	0.79	-26.0	1.5	0.2	9.7
433	0.74	-25.5	0.9	0.1	9.2
441	0.66	-25.8	1.0	0.1	9.4
453	0.55	-25.9	1.3	0.1	9.6
457	0.51	-26.6	1.9	0.2	11.2
459	0.49	-27.8	6.8	0.4	18.6
461	0.47	-28.1	18.9	0.7	28.4
462	0.46	-27.4	6.4	0.3	24.1
466	0.41	-26.0	1.1	0.1	10.6
470	0.37	-25.8	1.1	0.1	9.6
474	0.34	-26.6	2.4	0.1	15.8
476	0.32	-27.4	12.4	0.4	32.3
478	0.30	-27.4	29.9	0.8	35.8
480	0.28	-27.2	32.2	0.8	40.9
482	0.26	-27.2	18.4	0.5	38.0
484	0.24	-26.0	1.8	0.1	12.3
486	0.21	-25.4	0.6	0.1	10.2
490	0.17	-25.0	0.4	0.0	12.0
498	0.09	-25.0	0.4	0.0	10.4
514	-0.06	-25.3	0.4	0.0	11.3
522	-0.14	-20.4	0.6	0.0	13.6
527	-0.19	-24.9	0.4	0.0	10.0
531	-0.23	-25.5	0.6	0.0	12.5
533	-0.25	-24.8	0.2	0.0	9.3
537	-0.29	-24.6	0.2	0.0	10.7
545	-0.37	-24.3	0.2	0.0	9.6
553	-0.45	-24.8	0.2	0.0	10.3
560	-0.52	-24.7	0.3	0.0	10.2
563	-0.55	-25.3	0.4	0.0	11.5
571	-0.63	-19.8	0.4	0.0	10.1
579	-0.71	-24.9	0.3	0.0	9.9
594	-0.86	-25.4	0.4	0.0	11.4
602	-0.94	-25.0	0.3	0.0	10.0

F/1b continued

Core depth (cm)	Altitude (m OD)	$\delta^{13}C$ (‰)	$\%C_{organic}$	$\%N_{total}$	C_{org}/N_{tot}
606	-0.98	-23.9	0.6	0.0	12.3
609	-1.01	-27.0	3.0	0.2	13.7
613	-1.05	-27.0	2.7	0.2	14.7
615	-1.07	-27.1	6.9	na	na
617	-1.09	-27.3	12.9	0.9	14.1
619	-1.11	-26.9	6.6	0.5	13.2
621	-1.13	-27.0	4.6	0.4	13.2
625	-1.17	-26.2	1.1	0.1	14.7
628	-1.20	-26.5	0.4	0.0	12.1
637	-1.29	-25.8	0.2	0.0	9.3
644	-1.36	-25.6	0.2	0.0	10.4
652	-1.44	-25.2	0.2	0.0	10.6
656	-1.48	-24.9	0.2	0.0	9.6
662	-1.54	-25.3	0.3	0.0	10.7
671	-1.63	na	0.4	0.0	13.8
673	-1.65	-26.0	0.8	0.1	11.7
678	-1.70	-24.9	0.3	0.0	8.7
695	-1.87	-24.7	0.2	0.0	9.8
703	-1.95	-24.4	0.3	0.0	12.0
711	-2.03	-24.8	0.3	0.0	10.8
718	-2.10	-25.0	0.4	0.0	11.1
725	-2.18	-24.9	0.3	0.0	12.5
728	-2.20	-25.0	0.3	0.0	11.8
731	-2.23	-25.0	0.3	0.0	11.4
735	-2.27	na	0.5	0.0	25.8
740	-2.32	na	0.2	0.0	17.2
744	-2.36	na	0.2	0.0	9.2
757	-2.49	-24.8	0.2	0.0	9.4
763	-2.55	na	0.2	0.0	9.8
778	-2.70	-23.1	0.2	0.0	11.1
795	-2.87	-25.0	0.2	0.0	10.8
810	-3.02	-24.8	0.2	0.0	12.4
818	-3.10	na	0.2	0.0	11.6
826	-3.18	-24.4	0.2	0.0	10.5
834	-3.26	na	0.3	0.0	15.7
842	-3.34	-24.7	0.4	0.0	12.3
846	-3.38	-24.7	0.5	0.0	11.1
854	-3.46	-21.9	0.4	0.0	12.6
863	-3.55	-24.8	0.5	0.1	10.7
878	-3.70	-25.2	0.3	0.0	10.3
886	-3.78	-24.9	0.6	0.1	10.6
894	-3.86	-25.0	0.5	0.0	10.1
902	-3.94	-24.5	0.2	0.0	8.9
910	-4.02	-24.5	0.2	0.0	11.0
916	-4.08	-25.0	0.2	0.0	11.7

F.1b continued

Core depth (cm)	Altitude (m OD)	$\delta^{13}C$ (‰)	$\%C_{organic}$	$\%N_{total}$	C_{org}/N_{tot}
918	-4.10	-24.6	0.2	0.0	11.2
923	-4.15	-24.9	0.3	0.0	12.4
931	-4.23	-24.2	0.2	0.0	11.5
940	-4.32	-24.9	0.3	0.0	10.1
944	-4.36	-25.0	0.3	0.0	10.6
946	-4.38	-25.5	0.3	0.0	12.2
954	-4.46	-25.0	0.4	0.0	10.5
963	-4.55	-25.7	0.7	0.1	13.7
978	-4.70	-25.2	0.6	0.1	10.3
994	-4.86	-25.0	0.7	0.1	10.3
1010	-5.02	-25.0	0.5	0.1	10.3
1026	-5.18	-25.1	0.5	0.0	10.8
1042	-5.34	-25.3	0.9	0.1	10.2